Tropical Cyclones in the Australian/Southwest Pacific Region

by
Greg J. Holland

P.I. William Gray

Department of Atmospheric Science
Colorado State University
Fort Collins, Colorado

NSF #ATM-7923591
NOAA/NHRL #NA 81 RAH-00001
Australian Government

Colorado State University

Department of Atmospheric Science

Paper No. 363

TROPICAL CYCLONES IN THE AUSTRALIAN/SOUTHWEST PACIFIC REGION

By

Greg J. Holland

Atmospheric Science Department

Colorado State University

Fort Collins, Colorado

March, 1983

Atmospheric Science Paper No. 363

ABSTRACT

Some results are presented from the completed first stage of a collaborative Colorado State University/Australian Bureau of Meteorology project to investigate various aspects of tropical cyclones in the Australian/southwest Pacific region. We begin with a brief description of the major environmental and geographical features of this region, together with an overview of previous research work. We then discuss the distinguishing climatological and structural features of tropical storms, hurricanes and major hurricanes throughout the region, and highlight the effects of the prevailing flow patterns and the Australian continent. Finally, we present a theoretical and observational examination of the mechanisms leading to development, intensification and motion of these cyclones.

DEDICATION

TO

Christine
Gary, Daryl and Sarah

Home is wherever they are

TABLE OF CONTENTS

TABLE OF CONTENTS (cont'd)

TABLE OF CONTENTS (cont'd)

I. INTRODUCTION

Between the landmark 1956 Brisbane Tropical Cyclone Symposium (Bureau of Meteorology, 1956) and the mid 1970's considerable effort was devoted to examining and documenting various features of tropical cyclones in the Australian/southwest Pacific region. As we briefly outline in section 1.3, diverse characteristics ranging from storm surge to rainfall observations, and from small severe hurricanes to vortex pairs across the equator were described by a number of authors. In addition the Australian Bureau of Meteorology has published annual case history summaries after 1962, together with occasional more extensive and detailed investigations into tropical cyclones which had a severe impact on coastal communities.

Despite such efforts, our knowledge of the important features of, and processes in these cyclones has remained quite patchy. This has largely been due to lack of adequate data in the cyclone vicinity. In all cases, chance observations have provided tantalizing glimpses of different characteristics but insufficient data were available for an adequate description of the entire cyclone. The deficiency is especially evident in the Australian Tropical Cyclone Forecasting Manual (Bureau of Meteorology, 1978) in which we had to adapt Northern Hemispheric results to a Southern Hemisphere perspective on the assumption that the basic characteristics were similar.

We have, however, seen substantial progress since 1978: the Australian Bureau of Meteorology has placed a high priority on tropical cyclone research and encouraged collaboration with external institutions; and the data coverage and usage has improved with the development of rawinsonde compositing techniques, the use of recorded radar data, instrumented tower boundary layer data, the Japanese Geostationary Meteorological Satellite (GMS), and the first reconnaissance by an instrumental research aircraft (Sheets and Holland, 1981).

In this paper we present the results to date from one component of this increased activity; that is, an examination of the general features of tropical cyclones in the Australian/southwest Pacific region, their climatology, structure, energetics, environmental interactions and diurnal modulation. This is a collaborative project between Colorado State University and the Australian Bureau of Meteorology and has involved the collation of all available tropical cyclone and synoptic data in the Australian/southwest Pacific region, together with the adaption of Professor Gray's compositing methodology to a Southern Hemisphere perspective. These data collations and new compositing procedures are described in Chapters 2 and 3; in Chapters 4 and 5 we discuss the climatology, structure and energetics of tropical storms and hurricanes; in Chapter 6 we attempt to isolate the major intensification mechanisms, and relate these to the development of the major hurricane; and in Chapter 7 we discuss the physics of tropical cyclone motion.

Before proceeding, however, we shall first introduce some basic concepts and definitions, describe the regional geography and meteorology, and give a brief background on previous research work. A full list of symbols and acronyms is provided in appendix 1 and a summary of all composite stratifications is in appendix 2.

1.1 Definitions and Terminology

Following Lourensz (1977, 1981), Kerr (1976) and Revelle (1981), the Australian/southwest Pacific region is defined as that area from 95°E to 150°W and the equator to 30°S. This region, which is shown in Fig. 1.1, extends from the western edge of Lourensz' data set to the eastern extremity of tropical cyclone occurrence in the South Pacific Ocean. Three subsets of this large region will also be used. These are: the Australian region, which encompasses the Australian and Papua New Guinea areas of tropical cyclone warning responsibility, from 105 to 165°E; the southwest Pacific region, which extends east of 145°E; and the north/west Australian region which extends west of 145°E.

After Bureau of Meteorology (1978), the following terminology is adopted:

Tropical Disturbance (TD): a synoptic scale weather system of tropical origin which may or may not be detectable as a wind field perturbation.

Monsoonal Trough (MT): the trough of low pressure into which the monsoons converge.

Monsoonal Depression (MD): a cyclone on the monsoon trough.

Tropical Cyclone (TC): a non-frontal synoptic scale, cyclonic rotational low pressure system of tropical origin, in which 10 minute mean winds of at least 17 m s^{-1} occur, the belt of maximum winds being in the vicinity of the system's center. In the absence of wind data, a central pressure of less than 995 mb is used.

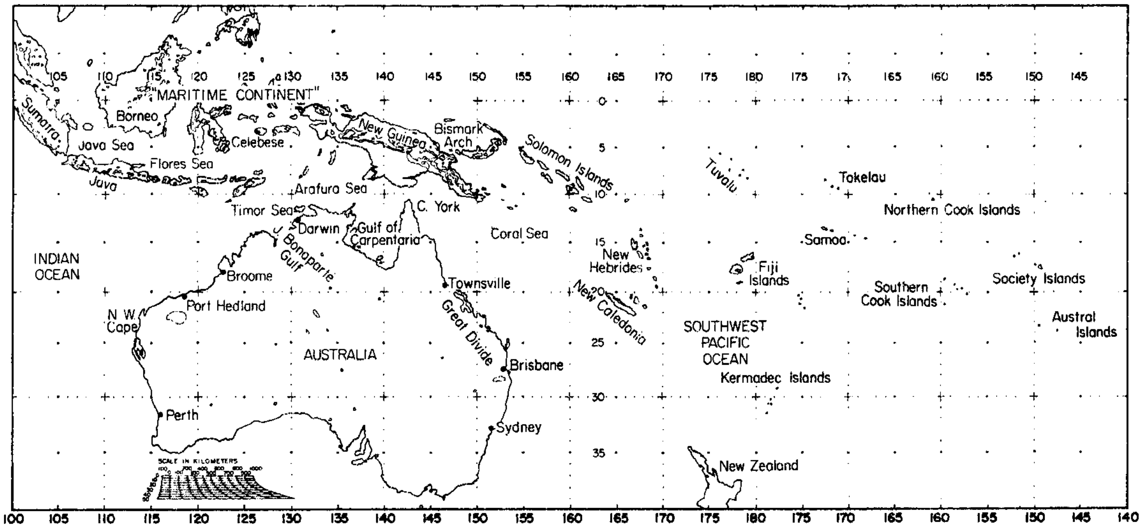

Fig. 1.1. The Australian/southwest Pacific region showing major geographical features.

Tropical Storm (TS): a tropical cyclone in which the maximum wind speeds are in the range 17-33 m s^{-1}, or the central pressure lies between 995 and 980 mb.

Hurricane or Typhoon: a tropical cyclone in which the maximum wind speeds exceed 33 m s^{-1}, or the central pressure is less than 980 mb.

Major Hurricane: a tropical cyclone in which the maximum wind speeds exceed 45 m s^{-1}, or the central pressure falls below 960 mb. This corresponds to class 4,5 hurricanes on the Saffir-Simpson code (Simpson, 1974) and to the major hurricane classification in Revelle (1981).

Core Region: the region within 200 km of the cyclone center.

Inner Circulation: the region within 300 km of the cyclone center.

Outer Circulation: the region 300-800 km from the cyclone center.

Following the suggestion by Gray (personal communication 1982) and Merrill (1982), we separated tropical cyclone "intensity" into three modes: inner core intensity (which we shall simply refer to as intensity), strength and size. These are illustrated in Fig. 1.2 as changes from an initial profile. Intensity is defined by the maximum wind, or by the central pressure if no maximum wind data are available. Strength is defined by the average relative angular momentum of the low level inner circulation. Size is defined by the axisymmetric extent of gale force winds, or by the outer closed isobar.

This is a physically and energetically consistent separation. Merrill (1982) has shown that there is a poor correlation between intensity and size, and our experience is that intensity and strength are also only weakly correlated. However, as we shall discuss in Chapter 6, strength changes are almost certainly associated with, and follow, size changes. Energetically, intensity change is usually, if not always, associated with an inward contraction of the radius of maximum winds and a quasi-conservation of angular momentum as the inflowing air penetrates closer to the cyclone axis. However, because of the small radius, even very large intensity changes are only associated with relatively small angular momentum changes on the entire storm scale. This angular momentum can be easily provided by a slight rearrangement of the inner circulation without any import from the environment. By comparison, strength and size changes (or the maintenance of a strong or large system against surface friction) require substantial angular momentum imports.

We believe that many previous studies of the environmental influences on tropical cyclone intensity have been, in reality, examining strength changes. The distinction between tropical cyclone intensity, strength and size is also especially important in the Australian/southwest Pacific region. As we shall show in later chapters, tropical cyclones in this region are in the mean larger and stronger than those in the northwest Pacific or north Atlantic regions. They are, however, no more intense.

The terms origin, maximum intensity, and decay also have special meanings. Origin and decay are used to describe the first and last points on a cyclone track as defined by Lourensz (1981), Kerr (1976) or Revelle (1981) with the following exceptions: 1) a cyclone which moves polewards of 30°S, or over land, is considered to have decayed; 2) should a cyclone move over land, decay to a monsoonal depression, then move back over water and reintensify, it is given a new origin point at the coast. Cyclones poleward of 30°S are removed to prevent contamination of the data by extratropical systems, a policy which is consistent with that adopted by Lourensz (1981). The new land to sea 'origins' correspond to the regeneration points defined by McBride and Keenan (1982). Maximum intensity is that achieved by the cyclone throughout its entire lifetime as a distinct system (i.e., regardless of movement over land).

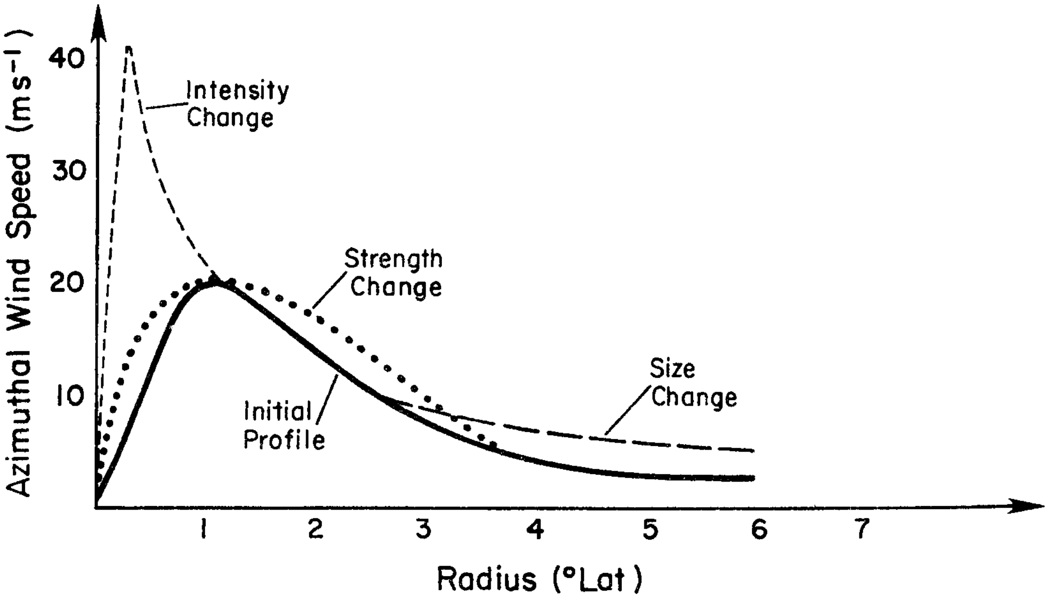

Fig. 1.2. A schematic of the effects of intensity, strength and size change on the radial profile of azimuthal winds in a tropical cyclone.

Following Holland (1981) we also place tropical cyclone tracks into five categories: <u>westward</u>, <u>southward</u> and <u>eastward</u> moving, <u>recurving</u> and <u>erratic</u>. The first three describe cyclones which move continuously towards the west to southwest, southwest to southeast, and southeast to east throughout their lifetime, with no major track perturbations. To be classified as recurving a cyclone must have moved steadily to the west or southwest for at least two days, recurved in an anticlockwise manner then moved steadily east to southeast for another two days (or crossed the coast). All cyclones which do not fit the above classification are placed in the erratic category.

1.2 Regional Geography and Meteorology

The Australian/southwest Pacific region has several geographical and meteorological peculiarities which not only distinguish it from the well documented North Atlantic and northwest Pacific basins, but, as we shall presently see, produce cyclones with quite different structures and physical characteristics. We shall highlight some of these peculiarities in the following paragraphs. However, the discussion is kept to a brief and introductory nature; interested readers might consult Bureau of Meteorology (1978), Sadler (1975), Atkinson (1971), Ramage (1970), Newell <u>et al</u>., (1972), or Gray (1968, 1979) for further information on some of the fascinating meteorological details of this region.

The broad geographical features of the region may be seen in Fig. 1.1. In the northwest, the long, high Indonesian island chain stretches from Sumatra to the Arafura Sea. This zonally orientated barrier averages over 1000 m in height, with peaks exceeding 3000 m, and separates the Indian Ocean from the 'maritime continent' (Ramage, 1968). On the northeastern side of the Arafura Sea rises the New Guinea massif, a formidable orographic barrier with average heights around 3000 m and peaks exceeding 5000 m. Further polewards, but right in the center of the tropical cyclone activity, lies the arid Australian continent. Much of the western and northern Australian regions are orographically featureless and semi-desert. A wide continental shelf is found off the northwest coast and in the northeast lies the warm, shallow Gulf of Carpentaria. The major orographic feature is found along the east coast. This mountain chain, the Great Divide, is typically 1-2000 m in height and rises sharply from a generally narrow coastal plain.

In a counterpoint to these large orographic and continental features, the southwest Pacific region consists of a myriad of coral cays and tropical islands, many of which are of volcanic origin.

The Australian/southwest Pacific tropical cyclone season typically begins in October or November and ends in May through June (Bureau of Meteorology, 1978; Revelle, 1981). The major meteorological features of the region during this season, as shown in Figs. 1.3, 1.4 and 1.5, include the monsoonal regime over northern Australia, the orographic controls on convective activity, and the southwest Pacific cloud band and associated zonal Walker circulation along the equatorial Pacific.

The advance and retreat of the monsoonal westerlies over the Indonesian and northern Australian area are clearly seen in Fig. 1.3. In October, trade wind easterlies extend from the subtropical ridge over southern Australia and across the equator (though a substantial heat trough has developed over western Australia). By January a monsoonal

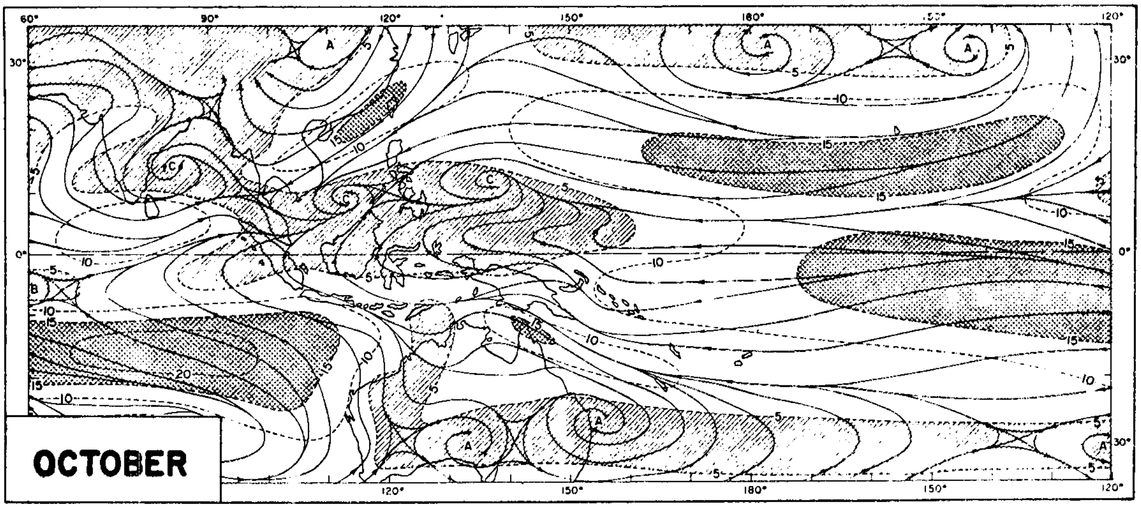

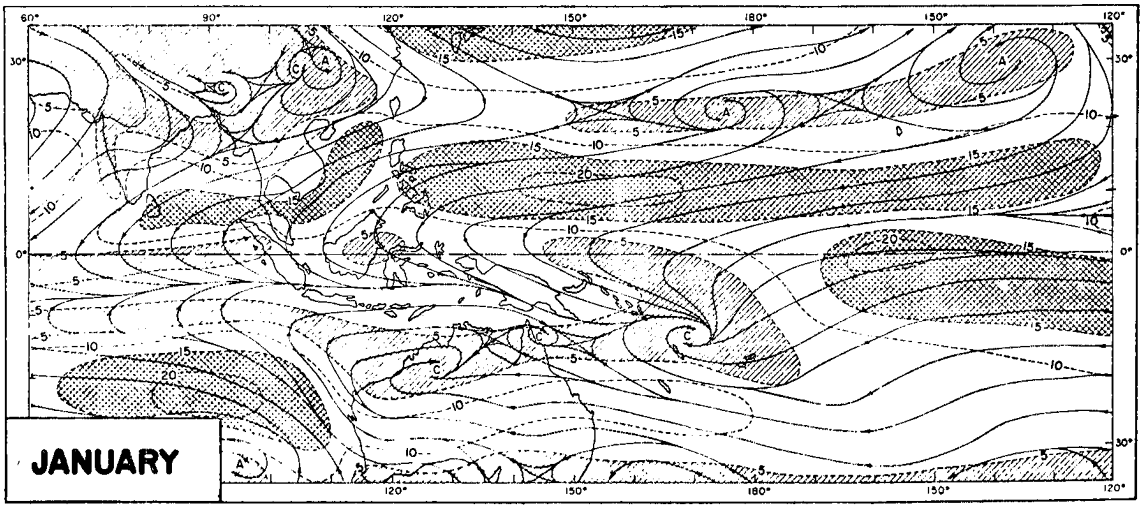

Fig. 1.3. Mean gradient level streamline/isotach for October, January, and April (after Atkinson, 1971).

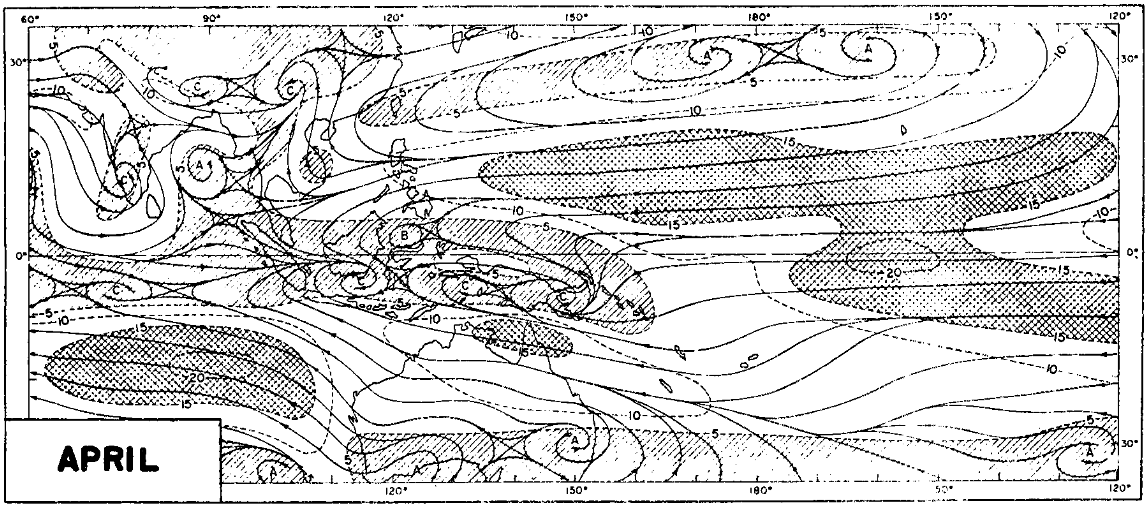

Fig. 1.3. Continued.

trough has developed in the Southern Hemisphere and advanced down over northern Australia and eastwards to the New Hebrides. This trough reaches its maximum southward extent in February then begins to retreat, as may be seen in the April analysis of Fig. 1.3. Of course, these are only mean movements; on occasions the monsoonal trough may extend over southern Australia or out into the central South Pacific.

The upper level flow features also evolve in association with the complete monsoonal circulatiion. As may be seen in Fig. 1.4, between October and January the subtropical ridge moves southward over northern Australia, breaks into two cells, and develops a distinct cross-equatorial flow into the Northern Hemisphere (the return branch of the monsoon). The subtropical ridge then moves back to the north between January and April and the cross-equatorial flow weakens. Note, however, that the ridge remains quasi-stationary over the southwest Pacific and westerly winds extend to quite low latitudes there, even in January. We shall presently see that this feature, together with the monsoonal

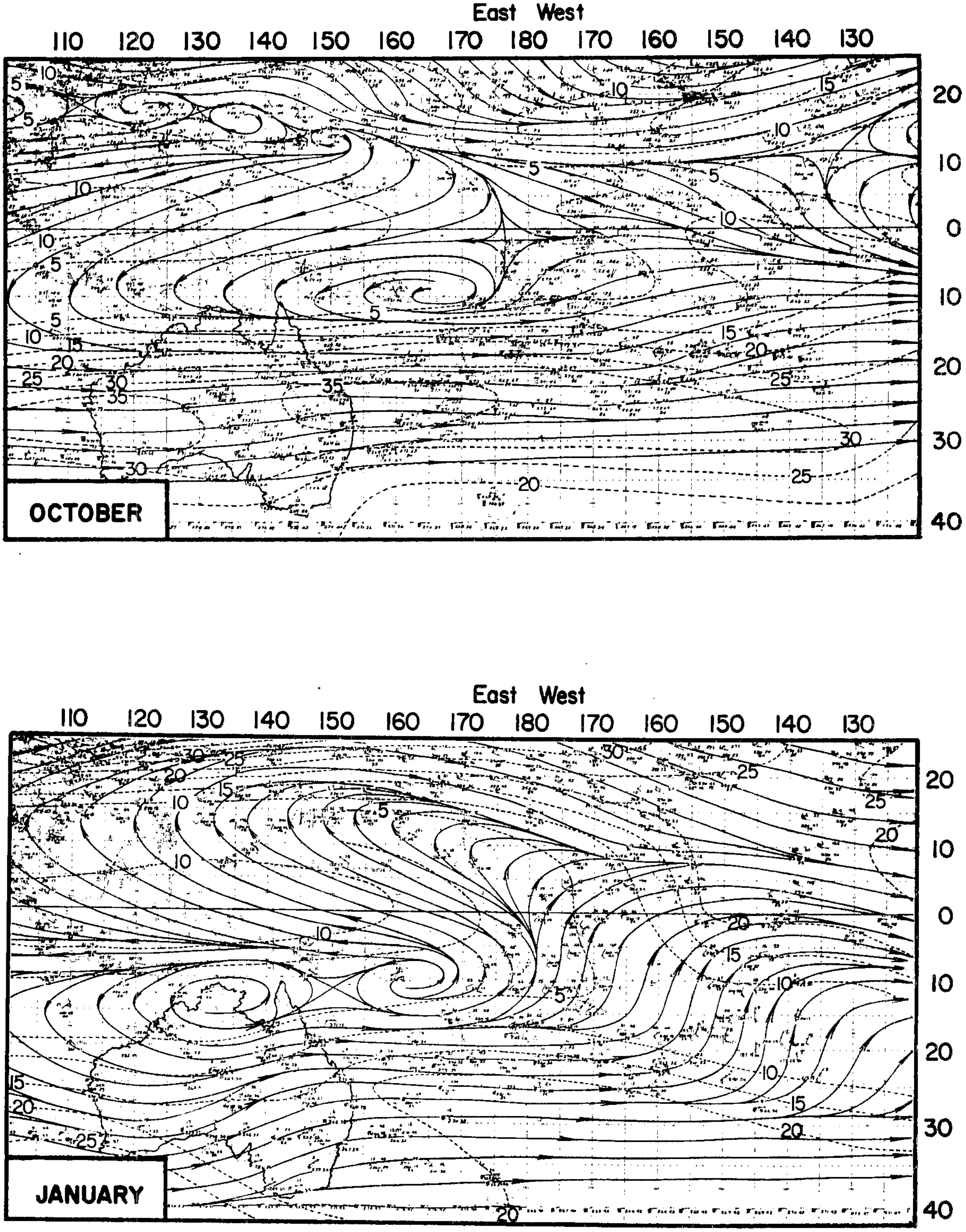

Fig. 1.4. Mean 200 mb level streamline/isotach analyses for October, January, and April (after Sadler, 1975).

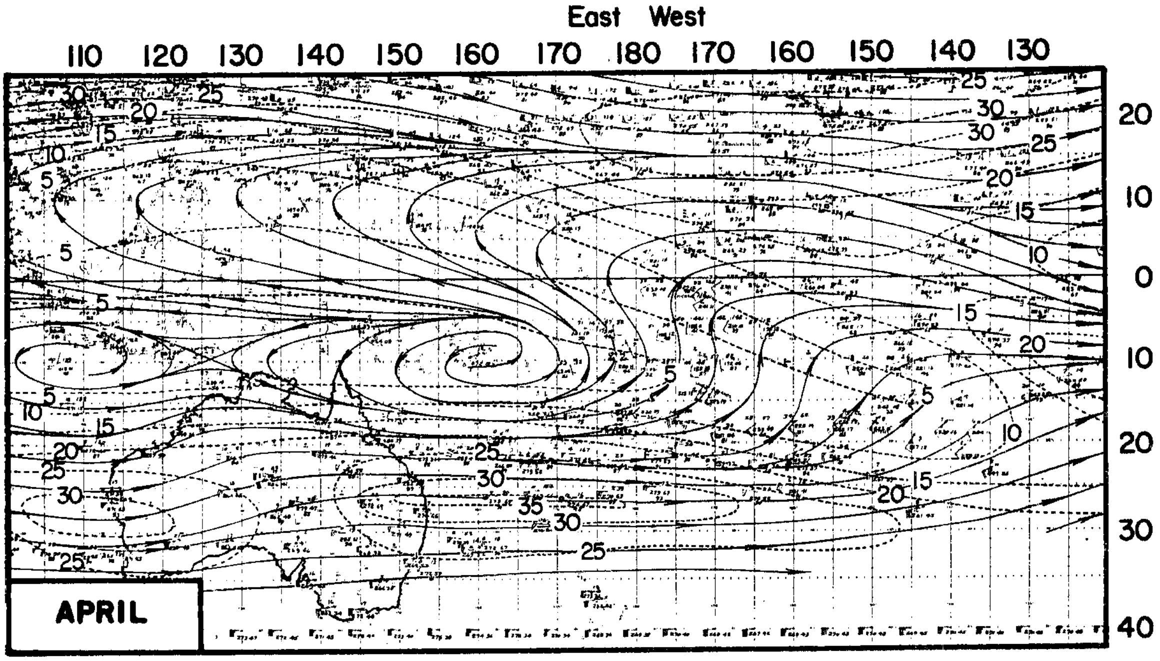

Fig. 1.4. Continued.

climate over northern Australia, has a distinct effect on tropical cyclones across the region.

Associated with, and providing the connection between these upper and lower features are the regions of deep tropical convection, whose general distribution may be seen in Fig. 1.5. (To be pedantic, Fig. 1.5 is comprised more of extensive stratiform clouds. But such stratiform clouds are generally preceded, or maintained by deep convective activity.) Comparing Fig. 1.5 with Fig. 1.3 we see that the cloud maximum lies along the tropical convergence zone on the equatorward side of the monsoonal trough. There is, in addition, a distinct orographic association, particularly over the maritime continent (see e.g., Holland and Keenan, 1980) and around New Guinea. A distinctive cloud band may also be seen extending southeast from New Guinea. This is the 'South

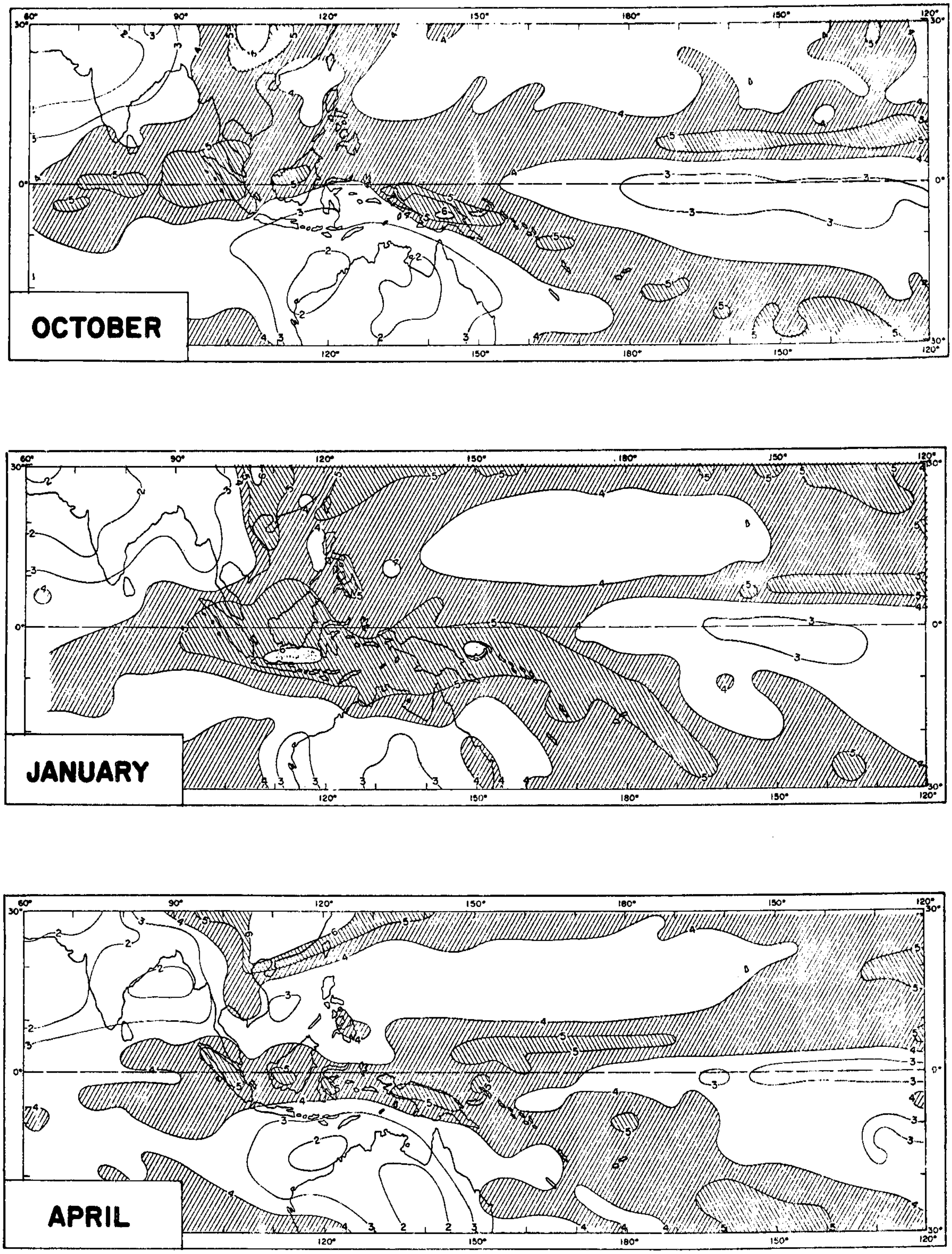

Fig. 1.5. Mean cloud cover (oktas) for October, January, and April (after Atkinson, 1971).

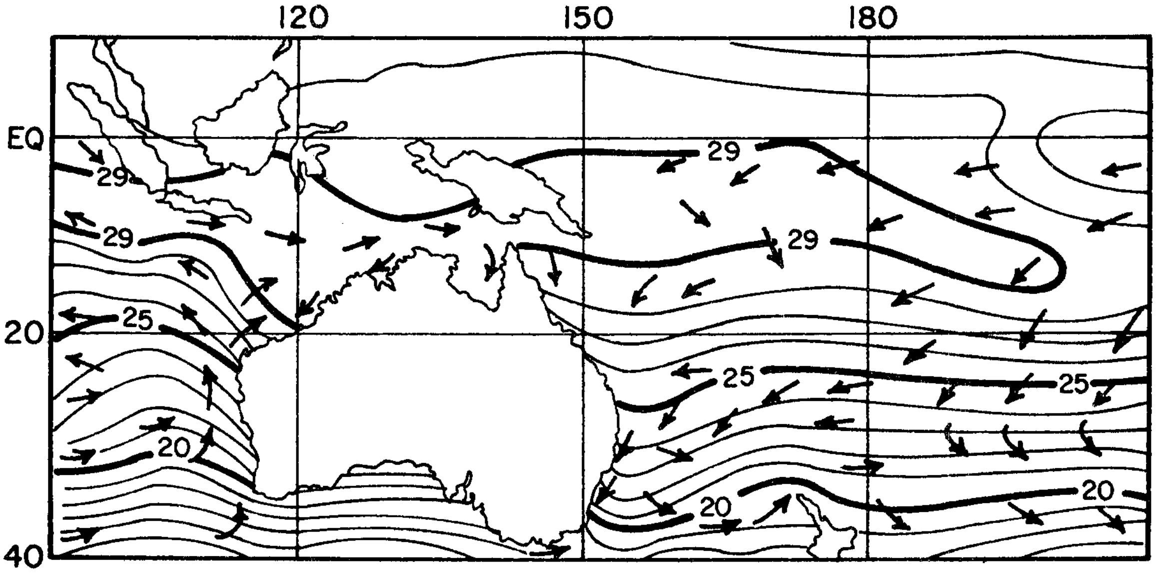

Fig. 1.6. Mean sea surface temperatures for January with superimposed prevailing ocean currents (after Gorshkov, 1976).

Pacific cloud band' (Streten, 1970), which lies along the intersection of the mean Hadley circulation over eastern Australia and the zonal Walker circulation (Bjerknes, 1966) along the equatorial Pacific.

The final meteorological feature in this brief description is the mean sea surface temperature fields in Fig. 1.6. An east Australian current brings warm water over the southern Coral Sea and a cool west Australian current, combined with upwelling slightly cools the waters off southwest Australia. But note the warm pool off the northwest coast. Wyrtki (quoted in Ramage, 1971) suggested that upwelling water in this region is replaced by warmer subsurface water drifting polewards over the continental shelf and around northwest Cape. Thus, we have a unique situation in that the waters off parts of the west coast are warmer than those off the east coast at the same latitude.

1.3 Overview of Previous Research

The earliest known reports on tropical cyclones in the Australian/southwest Pacific region may be found in Reid (1838), Dobson (1853), Piddington (1855), and Fitz Roy (1863), and the first complete climatology in Visher (1925) and Visher and Hodge (1925). Since that time climatological information on various tropical cyclone aspects has been included in H.M. Hydrographic Department (1938), Meteorologisch Instituut (1949), Giovanelli (1952), Hutchings (1953), Brunt and Hogan (1956), Gabites (1956), Giovanelli and Robert (1964), Gray (1968, 1975), Brunt (1969), Ramage (1970), Atkinson (1971), Gentilli (1971), Crutcher and Quale (1974), Crutcher and Hoxit (1974), Oliver (1974), Dobson and Stewart (1974), Chong et al. (1980), Dexter (1981), and Holland and Pan (1981). Seasonal summaries of tropical cyclones in the Australian region have also been compiled by the Australian Bureau of Meteorology since 1962.

The most recent, comprehensive climatological information on tropical cyclones may be found in Bureau of Meteorology (1978), Holland (1981), Lourensz (1981), and McBride and Keenan (1981) for the Australian region, and in Kerr (1976) and Revelle (1981) for the southwest Pacific region. Lourensz (1981) is an update of earlier publications by Coleman (1972) and Lourensz (1977) (from which much of our data are derived). He presents track and maximum intensity information on all cyclones in the Australian region from 1909-1980, together with some statistics on, among other things, occurrence, motion and coastal crossings. Kerr (1976) and Revelle (1981) contain similar information for cyclones in the southwest Pacific region for the periods 1939-1969 (Kerr) and 1969-1979 (Revelle), and Revelle provides further statistics on gale, storm, hurricane and major hurricane classes. Bureau of Meteorology (1978, Chapter 4) present a wide range of statistics on Australian region tropical cyclones from the periods 1909-1975 and 1949-1975; they discuss the data problems before 1949 and examine some relations between tropical cyclones and the general meteorological features of the region. A further analysis of the quality of the Australian cyclone data is contained in Holland (1981); in that paper we examined the period 1909-1979 and concluded that only since 1959 are the data of research quality. McBride and Keenan (1982) also extend the analysis in Bureau of Meteorology (1978) to present a detailed climatology of the modes of cyclogenesis in the Australian region and their relation to environmental parameters.

Since the Brisbane Tropical Cyclone Symposium (Bureau of Meteorology, 1956) a number of authors have also examined various aspects of tropical cyclones in the Australian/southwest Pacific region, including structure, storm surge, rainfall, motion mechanisms and unusual or interesting phenomena. A number of structural features have been examined by Bond and Rainbird (1956), Whittingham (1960, 1964), Whittingham and Swan (1960), Falls (1970), Neal and Wilkie (1970), Barclay (1972), Gomes and Vickery (1976), Holland (1980), Sheets and Holland (1981), and McBride and Keenan (1982). Cyclone genesis and intensification mechanisms have been documented by Gibbs (1955, 1956), McRae (1956), Southern and Scott (1976), McBride and Keenan (1982), and Love (1982), while some motion relationships are described in Lajoie and Nicholls (1974), Lajoie (1976a,b, 1977) and Holland and Pan (1981). Case studied of specific cyclones may be found in Bath (1957), Whittingham (1963, 1964), Whittingham and Aubrey (1967), Director of

Meteorology (1970, 1972, 1977, 1979), Wilkie and Gourlay (1971), a report by staff members of the Australian Bureau of Meteorology (1975), Lajoie (1981), Sheets and Holland (1981), Love (1982), Holland and Black (1983) and Black _et al_. (1983). Extensive information on cyclone rainfall is contained in Brunt (1958a, b, 1966, 1968), Wilkie (1960), and Milton (1978), and on storm surge in papers by Mackey and Whittingham (1956), Whittingham (1958, 1959), James Cook University of Northern Queensland (1972), Dexter and Watson (1975) and Spillane and Dexter (1976). Specific, unusual features of, or results from tropical cyclones in the region may be found in Pisharoti and Kulkarni (1956), Neumann and Upton (1958), Leigh (1969), Gourlay (1970), Maragos _et al_. (1973), Holland (1978), and Holland _et al_. (1983) and general surveys of tropical cyclone socioeconomic effects are given by Oliver (1974) and Southern (1981).

For a more comprehensive survey of the results of these research efforts, the reader is referred to the Australian Tropical Cyclone Forecasting Manual (Bureau of Meteorology, 1978).

2. DATA

2.1 Tropical Cyclone Data

Even though tropical cyclone data are readily available back to the 1909 in the Australian region and to 1939 in the southwest Pacific, much of the earlier data are of intermittent quality. Hence, following our recommendation in Holland (1981), we chose the period 1958-1979 as containing the optimum length of research quality data. Cyclone data for this period were then obtained from four sources: 1) a magnetic tape, prepared by R. Lourensz of the Australian Bureau of Meteorology, containing Australian region track data corresponding to that in Lourensz (1977); 2) hard copy of post analyzed Australian region track data from 1975-1979 (Lourensz, private communication 1980; Neal, private communication, 1980); 3) Kerr (1976), which contained tracks for southwest Pacific cyclones up to 1969; and hard copy tracks provided by C. Revelle of the New Zealand Meteorological Service and which were used in preparing Revelle (1981).

The Australian sources provided positions, central pressures and flags to indicate coastal crossings, over-water or over-land trajectories, and times of minimum central pressures. Revelle provided positions together with estimated times of transition to and from tropical depression, tropical storm, and hurricane. With few exceptions, only position data and a rough separation of hurricanes and tropical storms could be obtained from Kerr (1976).

These data were then melded into a common format and linearly interpolated, where necessary, to the standard synoptic times of 05, 11, 17, 23 GMT. On occasions when tracks from two sources overlapped, the Australian data were used because of their greater detail. Any extra New Zealand data were then smoothly fitted to the ends of the Australian tracks. Cyclone velocities were calculated using centered differences, or one sided differences at the track extremities. Following the Australian convention, flags were set to denote coastal crossings, over-water or over-land trajectories, interpolated data, times of minimum central pressure, and to delineate Australian and New Zealand data.

After a careful examination of the whole data set, a few atypical systems were deleted; these atypical systems included a couple of short lived tropical depressions which never intensified below 1000 mb, extremely short lived systems on the coast or at the western edge of the Australian region, and a couple of high latitude, late season, and seemingly extratropical systems. In a post-examination of the completed data set we also noted that Hurricane Kerry (1979) and Hurricane Hazel (1979) were inadvertantly omitted and the last couple of days of track were left off two cyclones in the southwest Pacific. The final data set then contained 363 cyclones of which 140 were estimated to have reached hurricane intensity. The spatial and temporal distributions of these cyclones will be presented in Chapters 4, 5 and 6.

Because of the lack of regular aircraft reconnaissance these Australian/southwest Pacific cyclone data are not of comparable quality to those from the northwest Pacific or Atlantic regions. It is also difficult to provide an objective estimate of the underlying cyclone intensity and positioning errors. In Holland (1981) we examined the basic observing systems over the Australian region, incorporated the known radar, satellite etc. errors from other regions, and used some simple tests to arrive at a best guess at these errors. To summarize, our estimates were that: cyclones within 500 km of the Australian coast are accurately located to within 20-50 km; cyclone positions more than 500 km from the coast are generally in error by 50-100 km and occasionally moreso; maximum wind estimates have virtually no skill; and central pressure estimates are generally quite poor and may be biased on the weaker side by about 10 mb in the Coral Sea region. These results are consistent with comparisons of "best track" positions of northwest Pacific cyclones from different agencies (Bell, 1981).

Fortunately, we also concluded that the position errors are considerably reduced whenever observations are available in the cyclone core region. Hence the inner circulation of the composites presented in this study are probably only rarely effected by the larger errors. And, as Frank (1976) has noted, random position errors of up to 100 km will have little effect on the composite outside 4-500 km. Uncertainties in the central pressure data are potentially much more serious, particularly if the intensity trends are wrong. We have made every effort to minimize the impact of these errors in deriving the composite stratifications used in this paper.

2.2 Environmental Data

All available archived wind and thermal data for the period 1958-1979 were obtained from the Australian Bureau of Meteorology, the New Zealand Meteorological Service, the Malaysian Meteorological Service, and the U.S. National Center for Atmospheric Research. Unfortunately, data from the Indonesian Islands, the French Pacific trust territories, and Papua New Guinea since 1972 were not available in such an accessible form. Some of these data were, however, obtained from the Australian Bureau of Meteorology, who have kept a real time archive of all traffic over the World Meteorological Organization's Global Telecommunication System since 1972.

Except for some extra consistency checks on the Australian data, all archived data were accepted as being sufficiently accurate for our purposes. Their quality control typically proceeds as follows: after recording in the field the soundings are manually recalculated and checked; they are then placed on magnetic tape and subjected to a number of standard meteorological tests before archival. These tests vary from simple checks of superadiabatic lapse rates etc. to long term checks on station bias.

The real time data were not so easily accepted. Aside from possible field errors they contained considerable coding errors and transmission line noise. By devising a series of automated tests we were able to recover about 70% of these soundings. Another 20% were corrected manually and 10% were beyond hope. Thus, we were able to archive about 90% of the soundings, though many have been truncated or have levels missing.

A valuable feature of these Australian/southwest Pacific data is that most stations make wind flights four times daily, though thermal observations are only made once daily. Hence we have compiled separate wind-only and thermal data sets. The wind-only set contains some 3 million flights from the 155 stations shown in Fig. 2.1. These flights

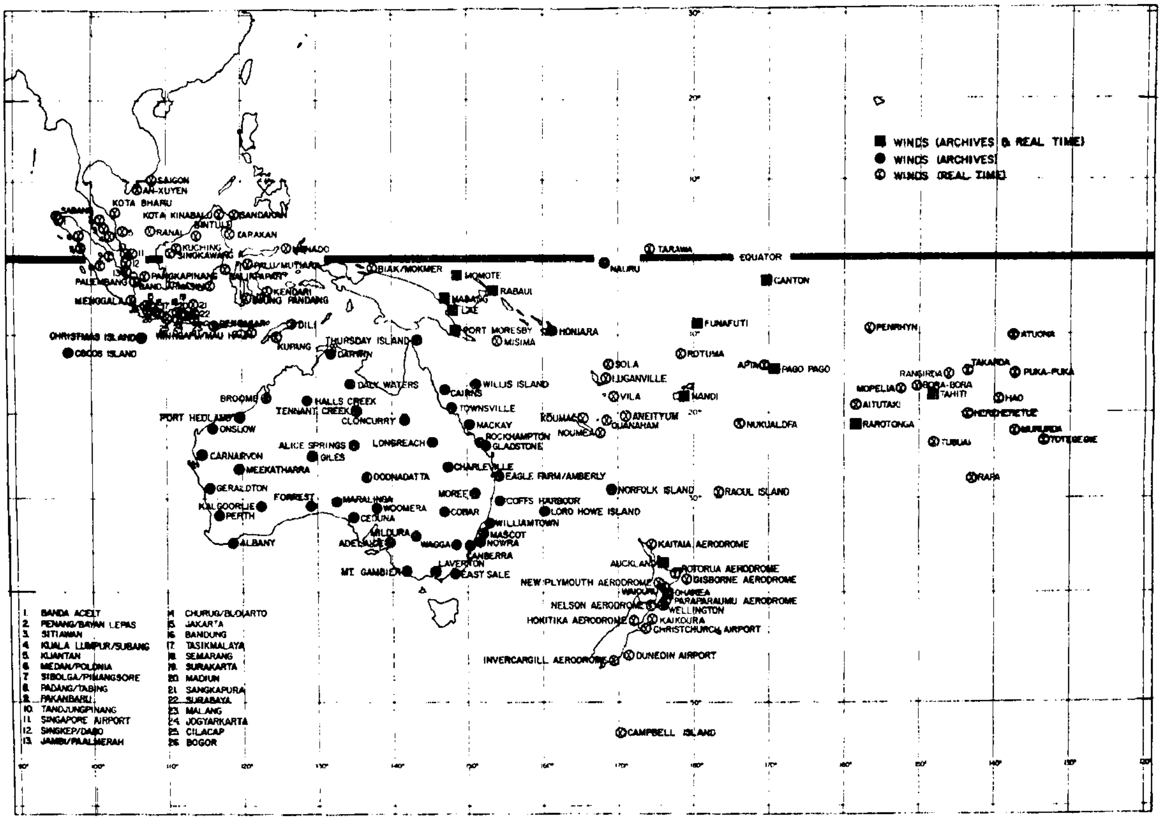

Fig. 2.1. The distribution of stations contained in the Australian/southwest Pacific wind-only data set.

were generally made at or near 05, 11, 17, 23Z (23Z varies from 06 to 14 LST across the region) and contained wind velocities for 18 pressure levels: surface, 950, 900, 850, 750, 700, 600, 500, 400, 300, 250, 200, 150, 100, 80, 70, 60, 50 mb. The thermal set contains 300,000 radiosonde soundings for the stations in Fig. 2.2. These soundings, which were generally taken at 23Z, contain temperature, moisture, height and wind velocity data at the same 18 pressure levels as the wind-only set.

A complete listing of all stations and summary of the procedures used in building the data sets may be found in Gray et al. (1982).

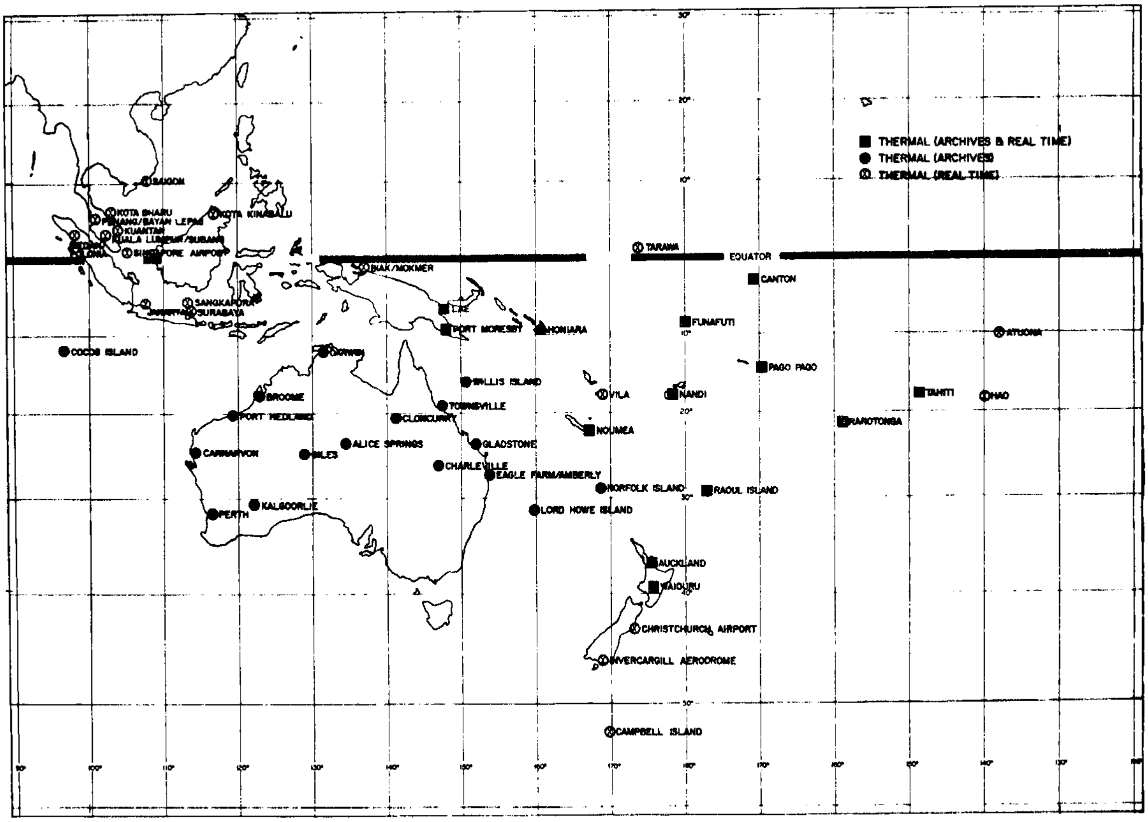

Fig. 2.2. The distribution of stations contained in the Australian/southwest Pacific thermal data set.

3. COMPOSITING TECHNIQUE

Our basic philosophy is to composite observations from a number of similar systems to increase the data density to a level sufficient for detailed analyses and budget calculations. The general technique follows that described by Williams and Gray (1973), Frank (1976) and Gray et al. (1982). We have, however, introduced a number of refinements and modifications based on the collective experience obtained over the past few years.

3.1 Coordinate System and Sign Convention

As shown in Fig. 3.1, a cylindrical coordinate system is used. The coordinates and sign convention are: radius, r, measured along the curved earth's surface and positive outwards; azimuth, θ, measured counterclockwise from either due north or the direction of storm motion; and pressure, p, in the local vertical. Four coordinate system perspectives have been adopted:

a) NAT system: as in Fig. 3.1

b) MOT system: as in Fig. 3.1 but with cyclone motion subtracted from all wind observations

c) ROT system: as in Fig. 3.1 but with azimuth measured counterclockwise from the direction of cyclone motion

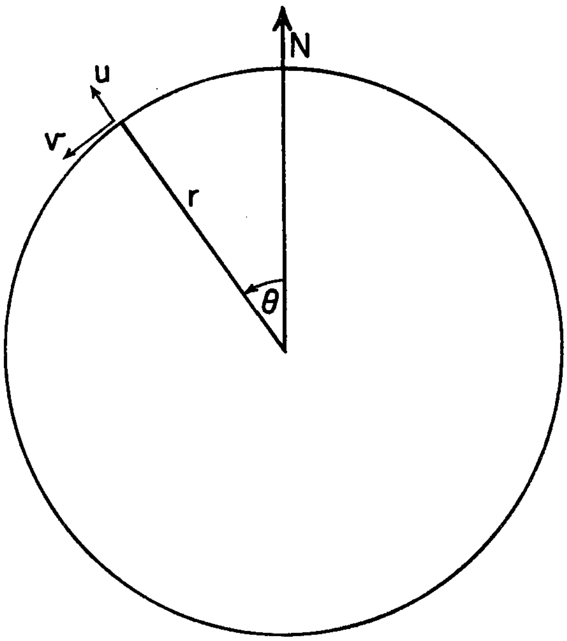

Fig. 3.1. The cylindrical coordinate system used in compositing studies, shown in the NAT system perspective.

d) MOTROT system: the same perspective as the ROT system but with the cyclone motion subtracted from all wind observations.

3.2 General Technique

Full details on the general composite technique may be found in Gray et al. (1982). To summarize, the relevant coordinate system is located at the cyclone center at each time period and the positions of all observations within 15° latitude radius are derived. The effect of balloon and cyclone motion during ascent are accounted for. As shown in Fig. 3.2 the cyclone is then divided into octants and into a nested radial grid at each pressure level. The average of all observations in each grid box is then assigned to a grid-point at the box center. Outside 6° latitude radius a 2° latitude resolution is maintained, with sampling across the mean spatial and seasonal gradients in such absolute parameters as temperature, height and moisture. As an example, in examining the effects of such asymmetries we deliberately made an indiscriminant composite of all cyclones in the Gulf of Carpentaria and Western Australian region (Fig. 1.1). The mean position of the resulting cyclone was near 20°S. But, because of the data void Indian Ocean, the southwest quadrant came from observations over northern Australia and the northwest quadrant from observations along the Indonesian Islands. Thus, the southwest quadrant was anomalously warm and dry and the northwest quadrant was anomalously warm and moist. Cyclone size and intensity differences across the region and the proximity of the subtropical jet stream produced further biases.

Robert Merrill (much personal communication 1981, 1982) has proposed a technique for removing this bias. He suggested a separate composite of the absolute value, squares and covariances of latitude, longitude and Julian day number. These data may then be combined with the mean spatial and temporal distribution of each parameter to remove much of the observational system bias. Following this suggested approach, we routinely composite the latitude, longitude and day number. Should these indicate a large degree of bias, the composite is discarded. In normal circumstances, however, a few biased grid points are indicated and are treated as suspect at the analysis stage.

Our experience thus far is that wind composites (which are a measure of height gradients) are quite robust and insensitive to minor observational asymmetries. The hot, dry Australian continent, however, places a strong limitation on the thermal composites that may be made.

Thus, in some cases we are able to derive very good wind composites but cannot provide corresponding thermal information.

Statistical Techniques: Two types of statistical techniques are employed. Following Merrill (1982) we routinely produce statistics on the distribution and standard deviation of observations at each grid point, together with pooled distributions and standard deviations of each radial band for the 850, 500 and 250 mb levels. Other levels are derived as necessary. These statistics provide a valuable tool in the hand analysis of the various parameter fields. Multi Response Permutation Procedure (MRPP) statistics (Mielke et al., 1976) may also be employed in special cases to examine the internal consistency of some composites and to test the significance of observed parameter differences.

3.4 Summary

The complete composite procedure is summarized in the flow diagram in Fig. 3.3.

We must emphasize that the composite cyclones produced by this procedure have a specific purpose. Considerable care is taken to retain certain features in a stable configuration. But this is occasionally at the cost of other features. For example, composite AUS04 (Appendix 2) delineates the effect of the Australian continent on east-coast hurricanes only, and would be useless for almost all other applications. A re-examination of the relevant data is required before the composites listed in Appendix 2 can be used for any other than their designated purposes.

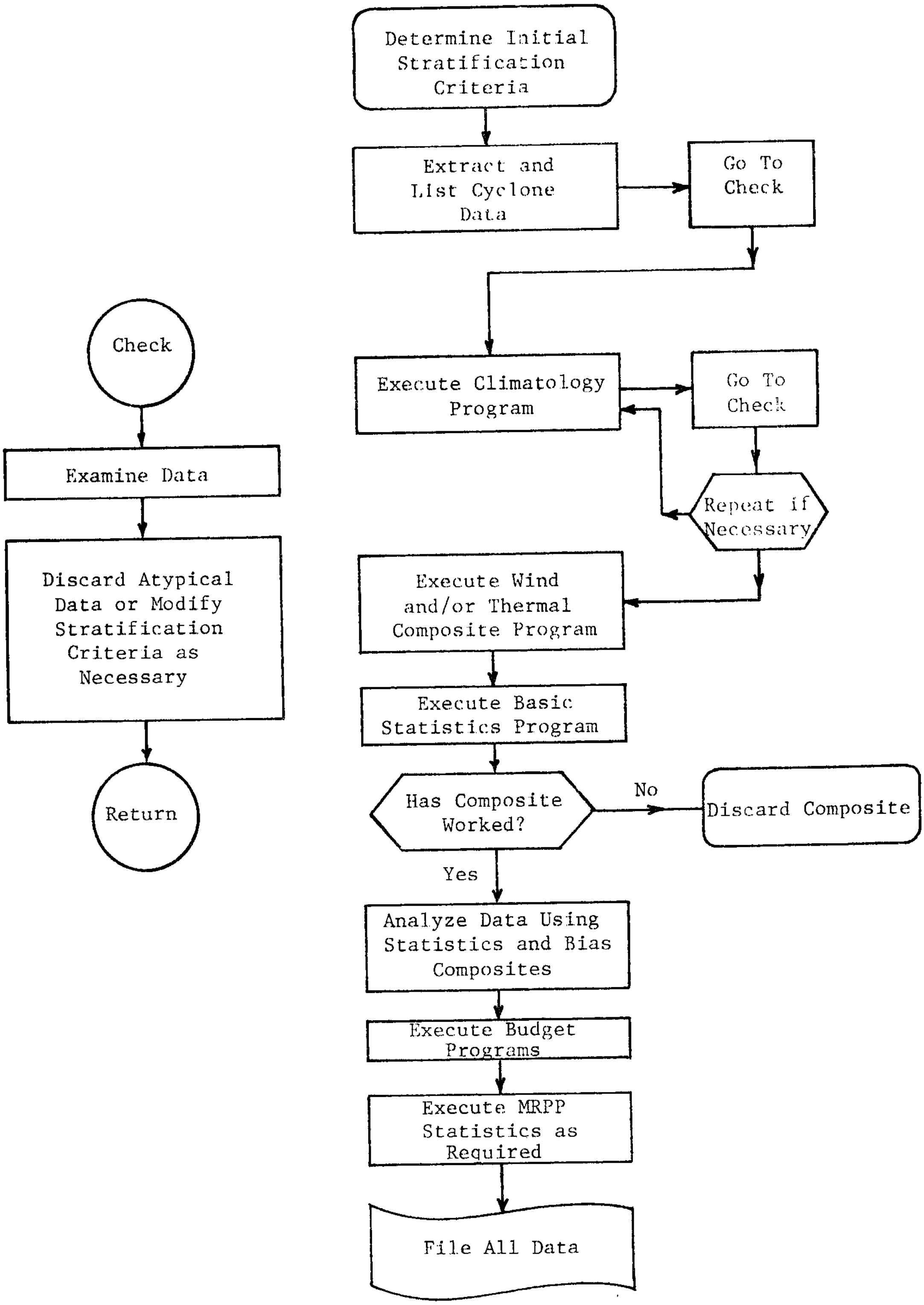

Fig. 3.3. A flow diagram illustrating the procedure used in deriving a tropical cyclone composite.

4. TROPICAL STORMS

As we have noted in Chapter 2 there are no adequate data on maximum sustained winds in Australian/southwest Pacific tropical cyclones; and those east of 165^{o}E do not even have central pressure data. Hence, Australian region tropical storms were selected as all cyclones with minimum central pressures higher than 980 mb. East of 165^{o}E we placed all cyclones not defined as hurricanes by Kerr (1976) and Revelle (1981) in the tropical storm category. This is not a precise separation and it almost certainly has left a number of hurricanes in the tropical storm category. But it is the best we can do with the available data.

The hot, dry Australian continent also has a marked effect on the thermal characteristics of tropical cyclones in its vicinity (Chapter 3). Hence only very limited thermal composites can be made for much of the Australian region. In the next chapter we describe two such limited composites, the east and west coast Australian hurricanes, and give a quantitative description of these continental effects. Here we present a complete climatology of tropical storms throughout the region. But we shall limit our discussion of the composite structure and energetics to developing and non-developing tropical storms over the southwest Pacific at least 1000 km from the Australian coast.

4.1 Tropical Storm Climatology

Spatial Distribution: These are given in Fig. 4.1 in terms of the number of days in which a tropical storm was present within a five degree latitude/longitude Marsden square centered on each point (the spatial grid resolution is one degree latitude/longitude). In terms of tropical cyclone days, then, the highest frequency of tropical storms occurs in the Gulf of Carpentaria with secondary maxima in the Coral Sea and off the northwestern Australian coast.

These distribution features arise from a variety of mechanisms of which the continent is a major factor. Three mechanisms contribute to the strong peak in the Gulf of Carpentaria. Firstly, as we have shown in section 1.2, the monsoonal trough extends across northern Australia for much of the cyclone season. The warm Gulf waters are thus in an optimum position to allow monsoonal depressions to develop. Secondly, the proximity of land on three sides ensures a relatively high proportion of tropical storms, since most intensifying tropical cyclones cross the coast before reaching hurricane intensity. And, thirdly, as we will show in Fig. 4.8, these Gulf storms are also moving quite slowly (and erratically); they thus affect a given place for a longer time. The maximum off the northwest coast is a reflection of the large proportion of cyclones which track to the west/southwest, parallel to and just off the coast in this region. We shall show in our discussion of the West Coast Hurricane in section 5.3 that the Australian continent indirectly forces this preferred motion. The maxima in the Coral Sea arise from the regular annual occurrence over these tropical waters, particularly in the vicinity of the South Pacific cloud band (Streten, 1970; section 1.2) which extends southeastward from New Guinea. The

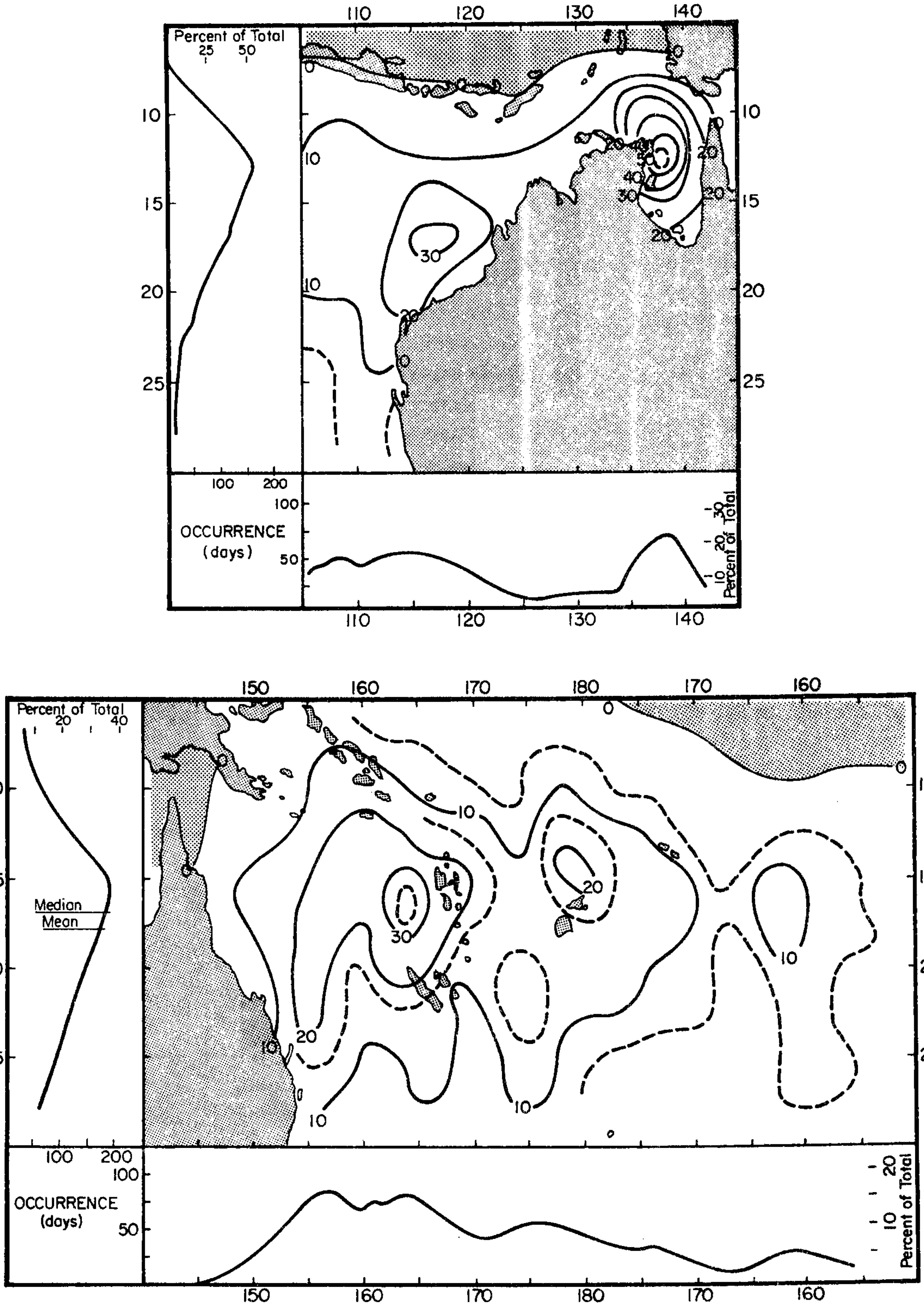

Fig. 4.1. Tropical storm occurrence (days per 5° Marsden square for the 1959-1979 period) for the north/west Australian and southwest Pacific regions. Stippling indicates regions of no occurrence and dashed lines indicating intermediate 5 day isochrones are use for extra detail.

eastward spread is more a result of intermittent years in which large numbers of cyclones form over the central South Pacific.

The origin, maximum intensity, and decay point distributions, given in Fig. 4.2, show the major regulating effect of the Australian continent. As Bureau of Meteorology (1978) and McBride and Keenan (1982) have noted, most tropical storms in the western region originate on the monsoonal trough, which is located over northern Australia (Fig. 1.3). One third of these systems also originate from over land depressions. This provides the sharp maximum between 15-20^{o}S, and also the peaks in the longitudinal distribution over the southeast Timor Sea, warm Joseph Bonapart Gulf (southwest of Darwin) and Gulf of Carpentaria. By comparison, no well defined mean monsoonal trough or continental effect extends over the southwest Pacific. There, almost all tropical storm origins are over the ocean and are spread over a broad latitudinal range. However, in both regions very few tropical storms keep intensifying on moving past 20^{o}S. This is undoubtedly due to the combined effects of strong upper tropospheric westerlies (Fig. 1.4) and cold sea surface temperatures (Fig. 1.6) poleward of this latitude.

Fifty five percent of western region tropical storms decay over land, 40% decay over tropical waters, and less than 5% become extratropical poleward of 30^{o}S. Thus, there are relatively sharp latitudinal peaks in the distributions of maximum intensity and decay points, and these are nearly coincident with the origin maximum. No such coincidence occurs in the southwest Pacific. There the tropical storms generally reach maximum intensity well poleward of their origin latitude and decay at high latitude over the ocean. Only 10% of these

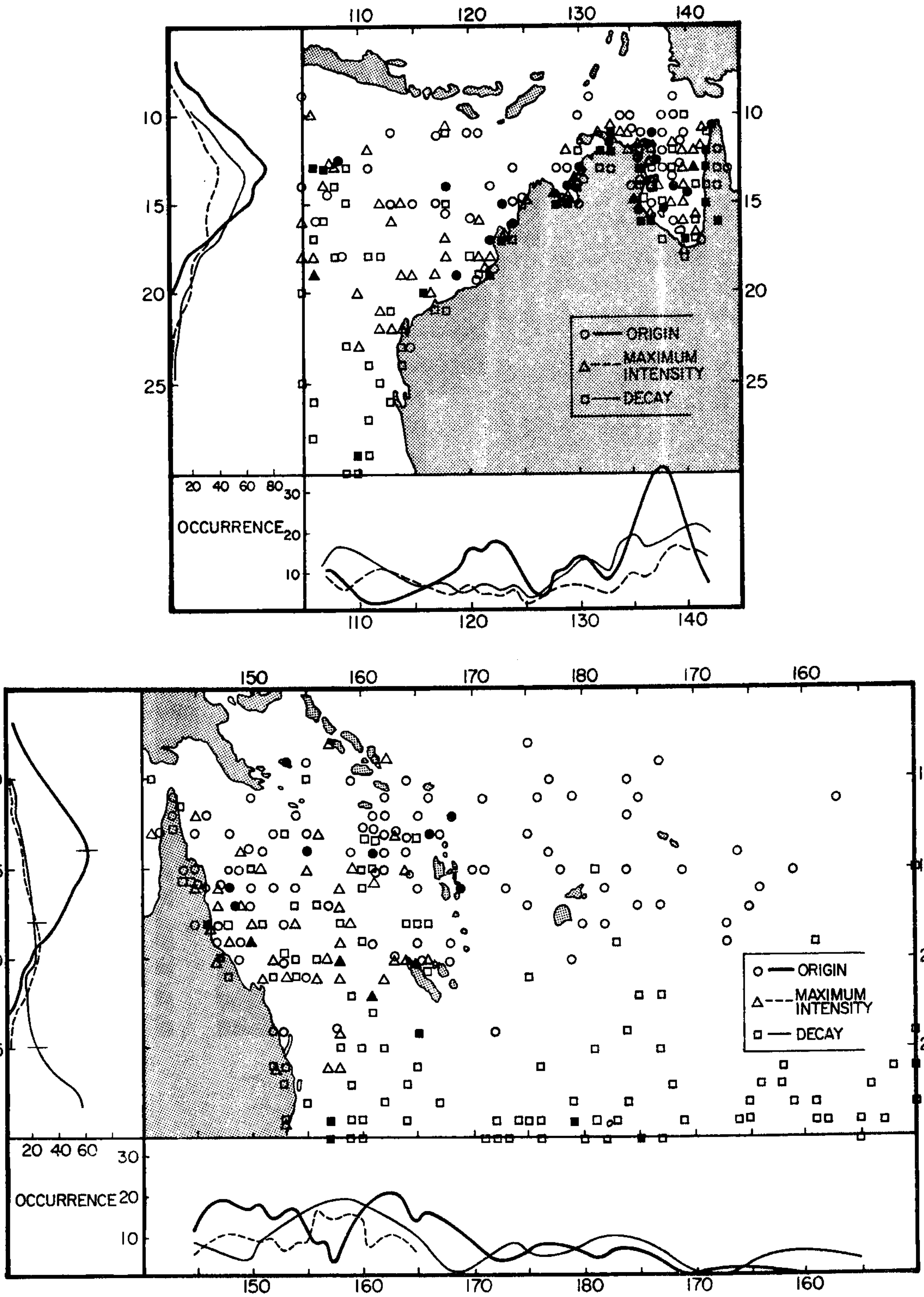

Fig. 4.2. Tropical Storm origin, maximum intensity and decay point distributions for the north/west Australian and southwest Pacific regions during the period 1959-1979. Tic marks indicate median latitudes and filled in symbols indicate multiple occurrence.

storms decayed over land, while 57% decayed over the ocean equatorward of $30^{o}S$ and 33% moved poleward as extratropical depressions.

Intraseasonal Distributions: The intraseasonal distributions of tropical storm occurrence are shown in Fig. 4.3. In both regions the season extends from late October to May and the southwest Pacific has occasional late season storms. Both regions also have an early season peak in storm activity followed by a gradual rise to a maximum in January/February. A sharp decline occurs in late February. This is followed in March and April by an increase in the north/west Australian region, and an essentially constant occurrence frequency in the southwest Pacific. The sharp late February drop in the north/west Australian region is associated with a rapid increase in hurricane occurrence (c.f. Fig. 5.3). This is because more systems are able to reach hurricane intensity as the monsoonal trough migrates equatorward away from the Australian continent.

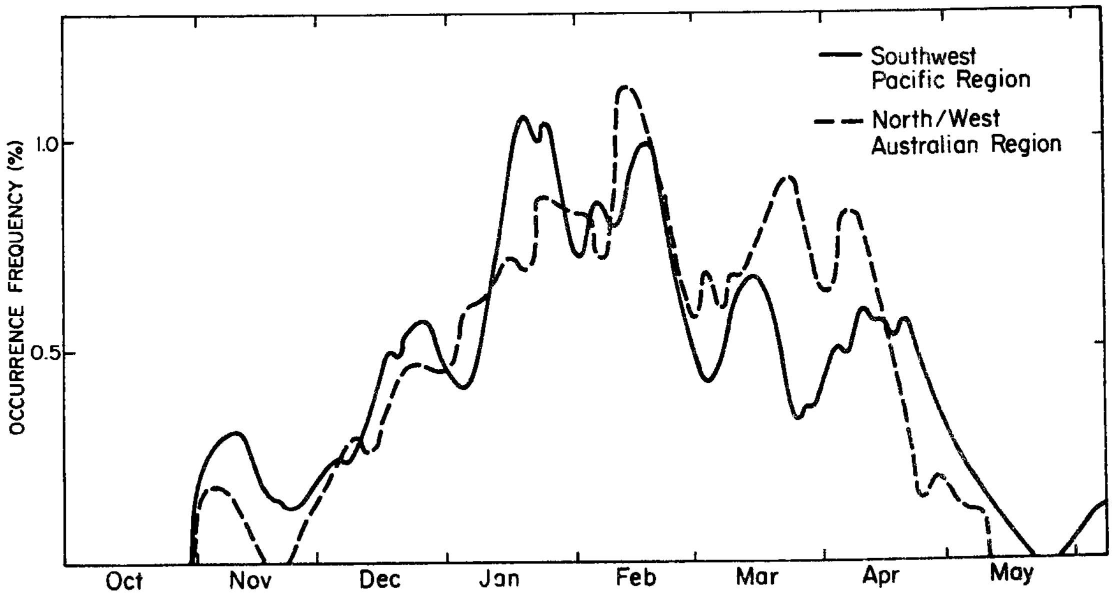

Fig. 4.3. Tropical storm intraseasonal distribution for the northwest Australian and southwest Pacific regions. Except for the extremities the curves have been smoothed by a running 15 day mean.

The tropical storm distributions for the north/west Australian region are different to those for all tropical cyclones (including hurricanes). As we have shown in Bureau of Meteorology (1978), the distribution of all tropical cyclones in this region has a distinct minimum in January and February. We shall see in Chapter 5, that this minimum is entirely due to a marked decrease in hurricane occurrence.

Motion: In the southwest Pacific region, tropical storm (and hurricane) motion is characteristically quite different to that observed in other ocean basins around the world. As may be seen in Fig. 4.4, tropical storms in this region consistently track towards the east/southeast at a high median speed of around 8 m s^{-1}. Only a small proportion move in the westward direction common to other basins. This propensity for eastward motion has previously been described by Bureau of Meteorology (1978), Holland and Pan (1981), Holland (1981), Revelle (1981) and Gray (1982), who note that it arises from the large proportion (around 40%) of cyclones which continually move eastward throughout their lifetime. This is well illustrated by Fig. 4.5, which shows the spatial distribution of the zonal component of tropical cyclone motion. We see that westward motion dominates only in very low latitudes and is nonexistent in the far east of the region.

By comparison, the majority of tropical storms in the north/west Australian region track to the west or southwest (Fig. 4.4); though a significant proportion also move towards the east. As may be seen in Fig. 4.5, the westward motion dominance arises from storms tracking nearly parallel to the northwest Australian coast. The smaller proportion of eastward moving storms are a combination of high latitude recurving cyclones, a few eastward moving storms just south of Java and

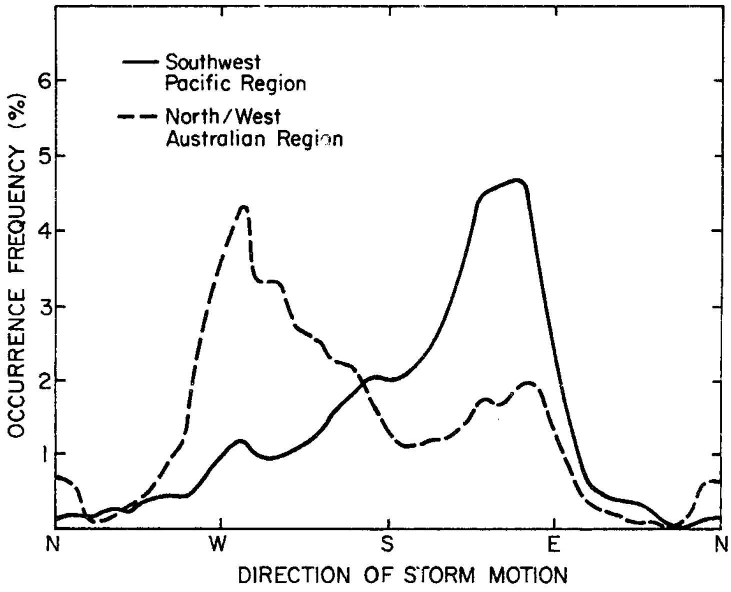

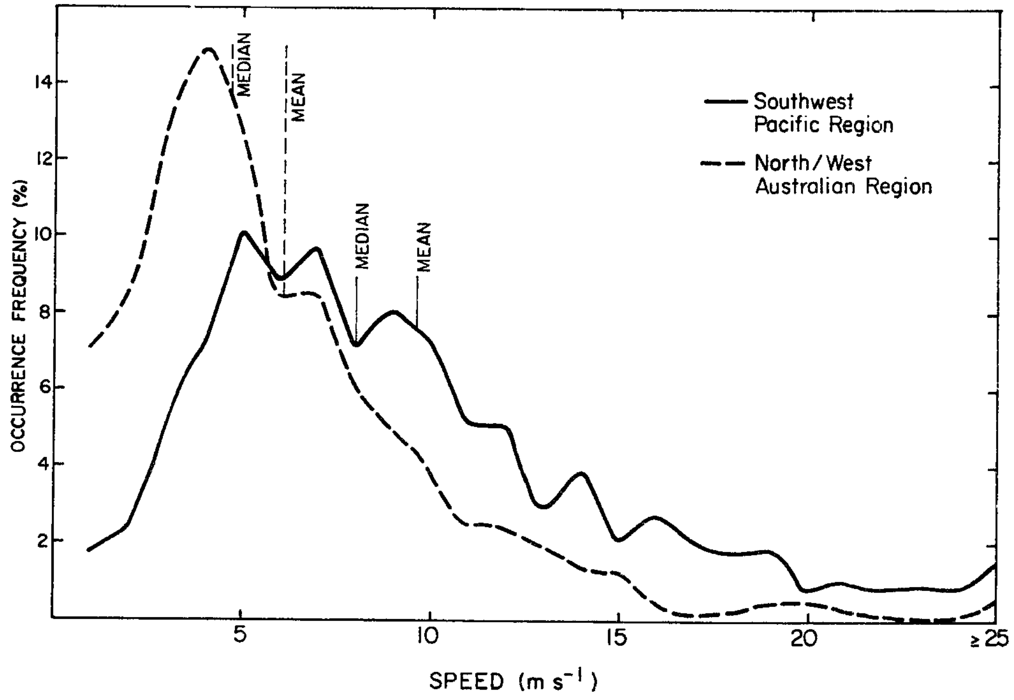

Fig. 4.4. Tropical storm direction and speed distributions for the north/west Australian and southwest Pacific regions. The curves have been smoothed by five point running means.

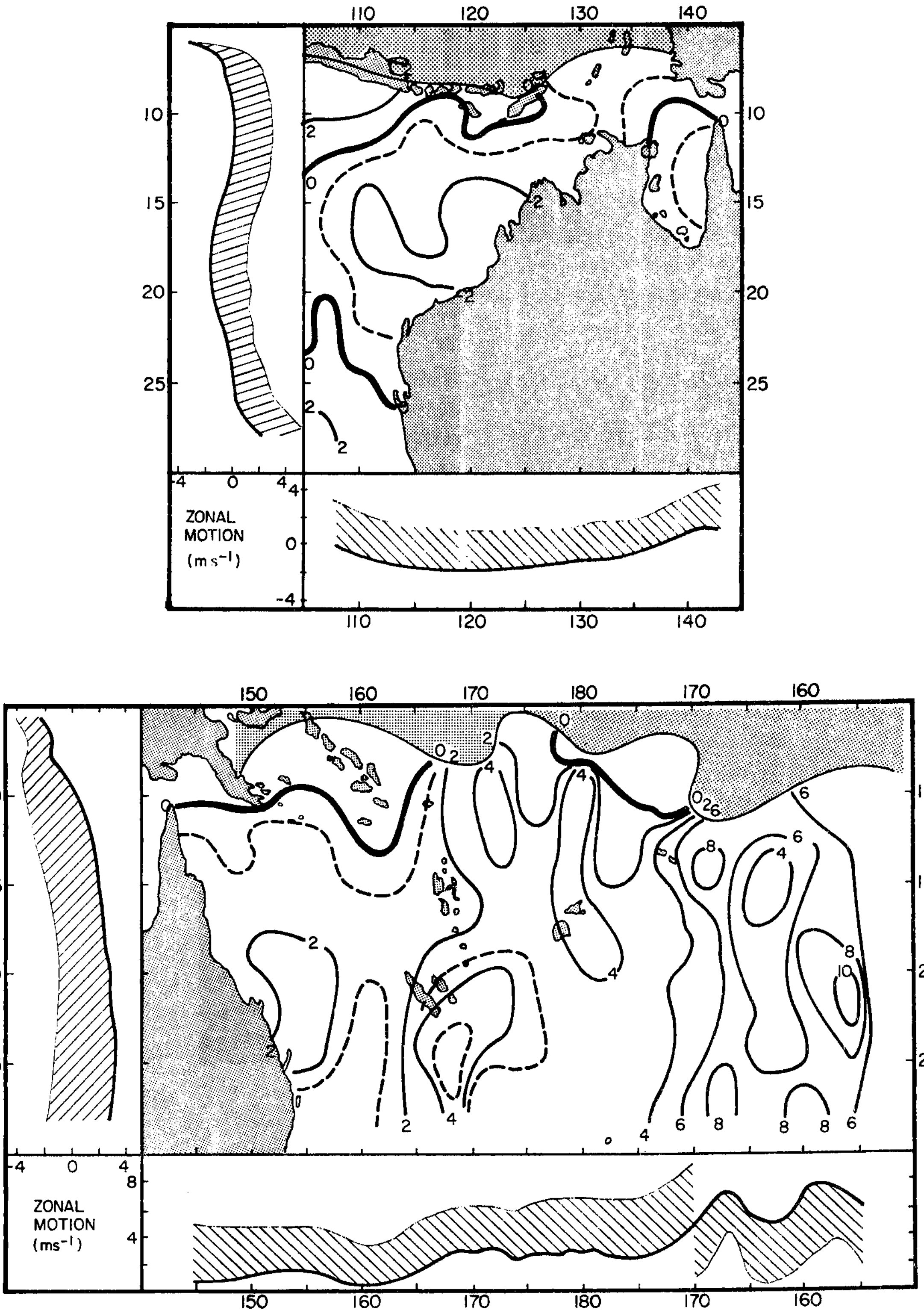

Fig. 4.5. Tropical storm zonal motion distribution (averaged over 5° Marsden squares) for the north/west Australian and southwest Pacific regions. Stippling indicates regions of no occurrence and hatching indicates one standard deviation.

a slight preference for eastward motion amongst the highly erratic storms in the Gulf of Carpentaria. These erratic, slow moving Gulf storms, combined with the effective removal of most rapidly moving high latitude storms by the Australian continent, also result in a relatively low median speed of around 5 m s^{-1}.

4.2 Tropical Storm Structure

We shall use the AUS08 and AUS09 composites to describe the general structure of oceanic tropical storms in the southwest Pacific region. A complete description of these composites is contained in Appendix 2. They consist of intensifying tropical storms between 10 and 25°S and at least 1000 km from the Australian Coast. (We shall describe the effects of the Australian continent on east and west coast cyclones in Chapter 5.) AUS08, the Non-developing Tropical Storm, represents the intensifying phase of tropical storms which never reach hurricane intensity. AUS09, the Pre-hurricane Tropical Storm consists of the intensifying tropical storm phase of those systems used in the AUS06 and AUS07 hurricane composites in the next chapter.

4.2.1 Dynamical Structure

The axisymmetric cross-sections of azimuthal winds in Fig. 4.6 indicate that the two storms have a similar overall size, with a cyclonic circulation extending beyond 14° latitude radius. However, the Pre-hurricane Tropical Storm is slightly stronger and more intense; has a much weaker lower tropospheric vertical shear; a stronger vertical shear near 300-200 mb; and a better developed anticyclone, with anticyclonic winds closer to the center.

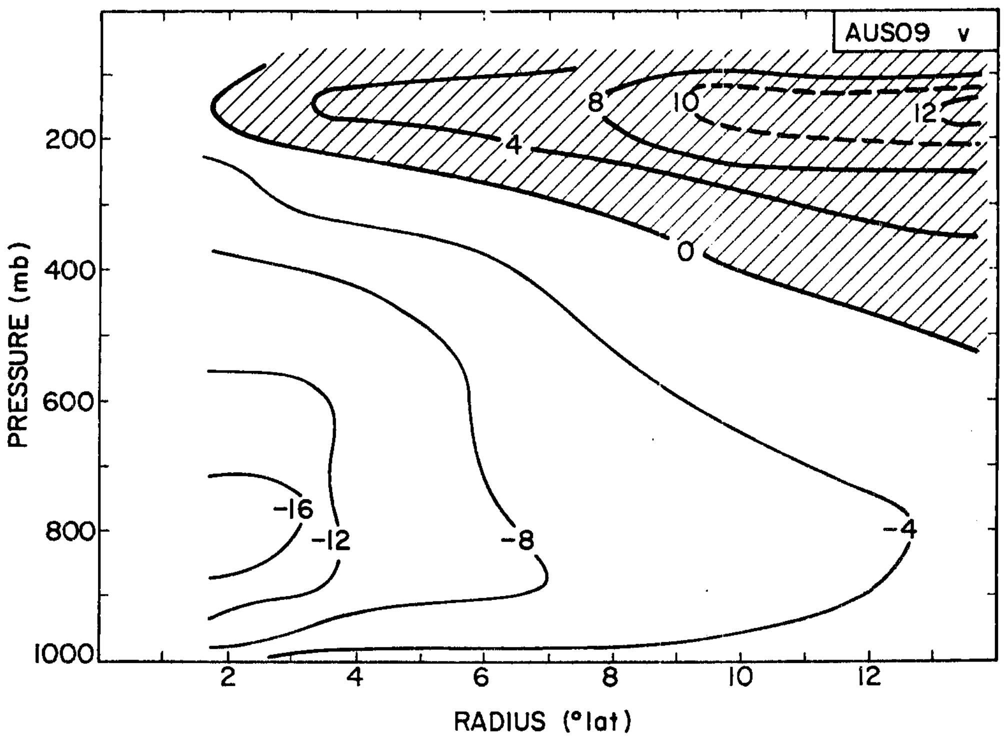

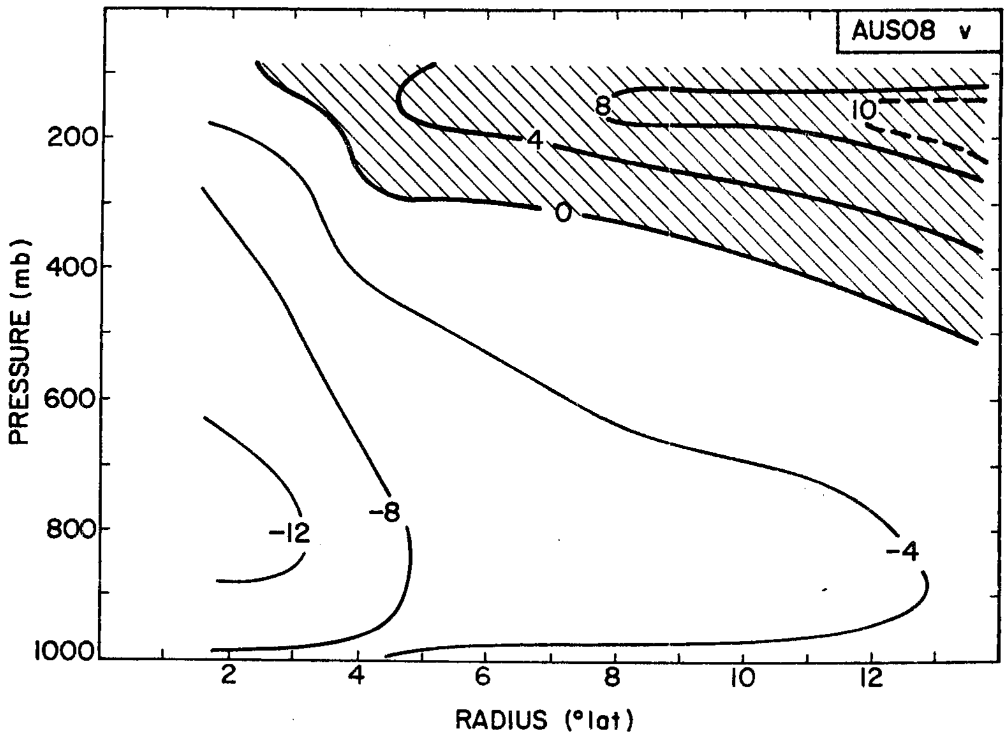

Fig. 4.6. Axisymmetric azimuthal wind (m s^{-1}) cross-sections for the Pre-hurricane (AUS09) and Non-developing (AUS08) Tropical Storms. Hatching indicates anticyclonic circulation.

The processes acting to maintain, or develop, these azimuthal wind features may be seen in the axisymmetric radial wind cross-sections in Fig. 4.7. The Pre-hurricane Tropical Storm has a well developed upper outflow from the core region, thus maintaining the anticyclonic circulation in Fig. 4.6. It also has a strong inflow between 400-300 mb which extends to 8° latitude radius and, by an increased import of cyclonic angular momentum, ensures a concentration of vertical wind shear in the upper troposphere. This, in turn, helps maintain and develop the necessary warm core near 300 mb. The outer region, low level inflow into the pre-hurricane system is also importing substantial amounts of angular momentum and accelerating the cyclone winds there. As Love (1982) has recently noted, and as we show in section 6.4, this increases the overall size of the system and provides an enhanced environment for further intensification.

The lower stratospheric inflow into the Pre-hurricane Tropical Storm may also contribute to its continued intensification. As we shall show in section 6.4, we believe that this results from the same processes which maintain the long outflow and upper inflow regimes. Such low stratospheric inflow can provide subsidence warming, and hence surface pressure falls, in the nascent eye region.

The flow field asymmetries, and the impact of the environment, for the Pre-hurricane Tropical Storm can be seen in the streamline/isotach fields in Fig. 4.8. (The location of this,and all subsequent composite plan views, on a geographical grid is defined by the mean latitude and longitude of all systems in the composite stratification.) This developing system has a quasi-symmetric cyclonic circulation to at least 500 mb, is overlain by an anticyclonic outflow regime at 150 mb and has

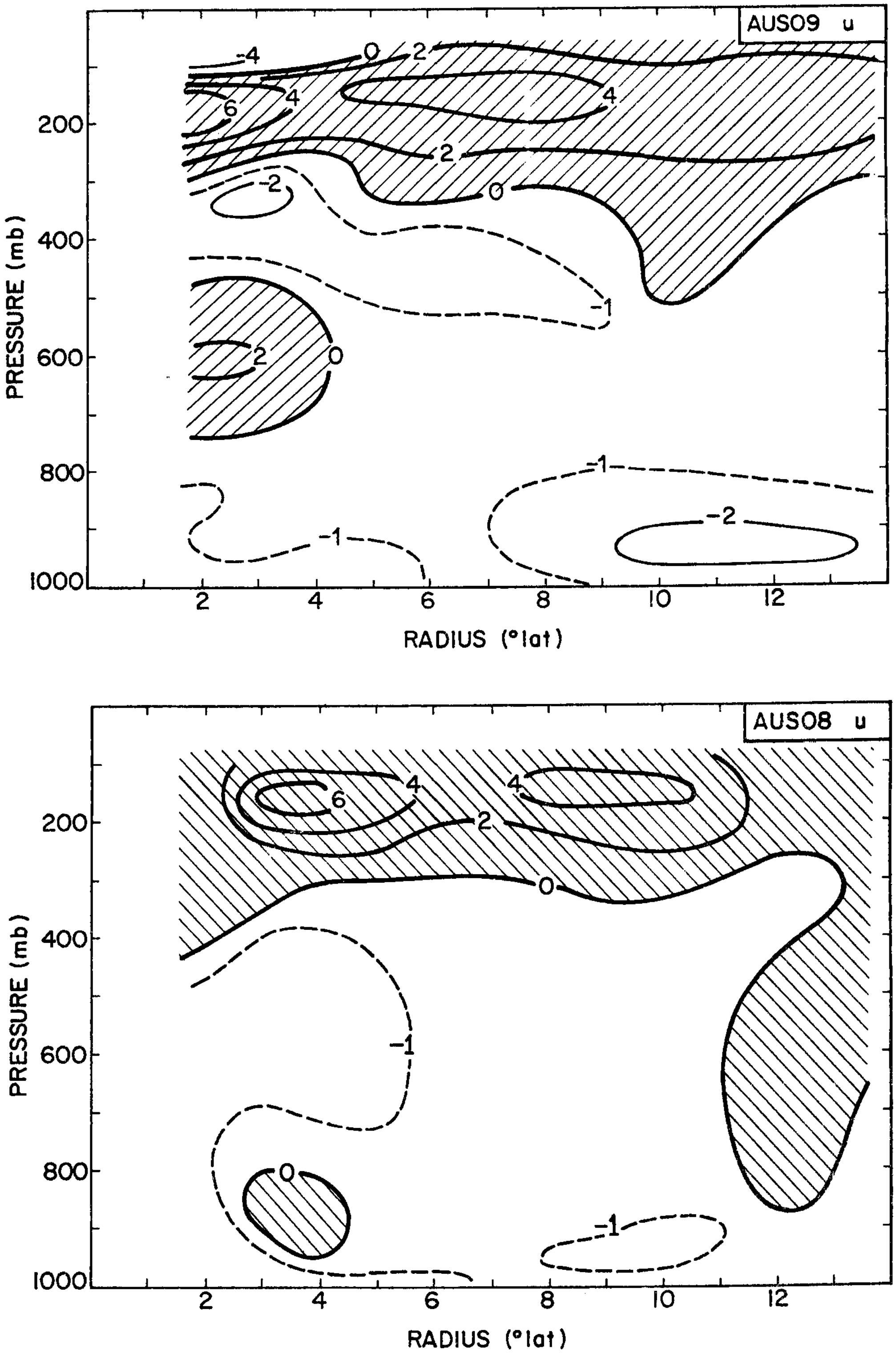

Fig. 4.7. Axisymmetric radial wind (m s^{-1}) cross-sections for the Pre-hurricane (AUS09) and Non-developing (AUS08) Tropical Storms. Hatching indicates outflow. Radial winds of less than 1 m s^{-1} are not significantly different from zero.

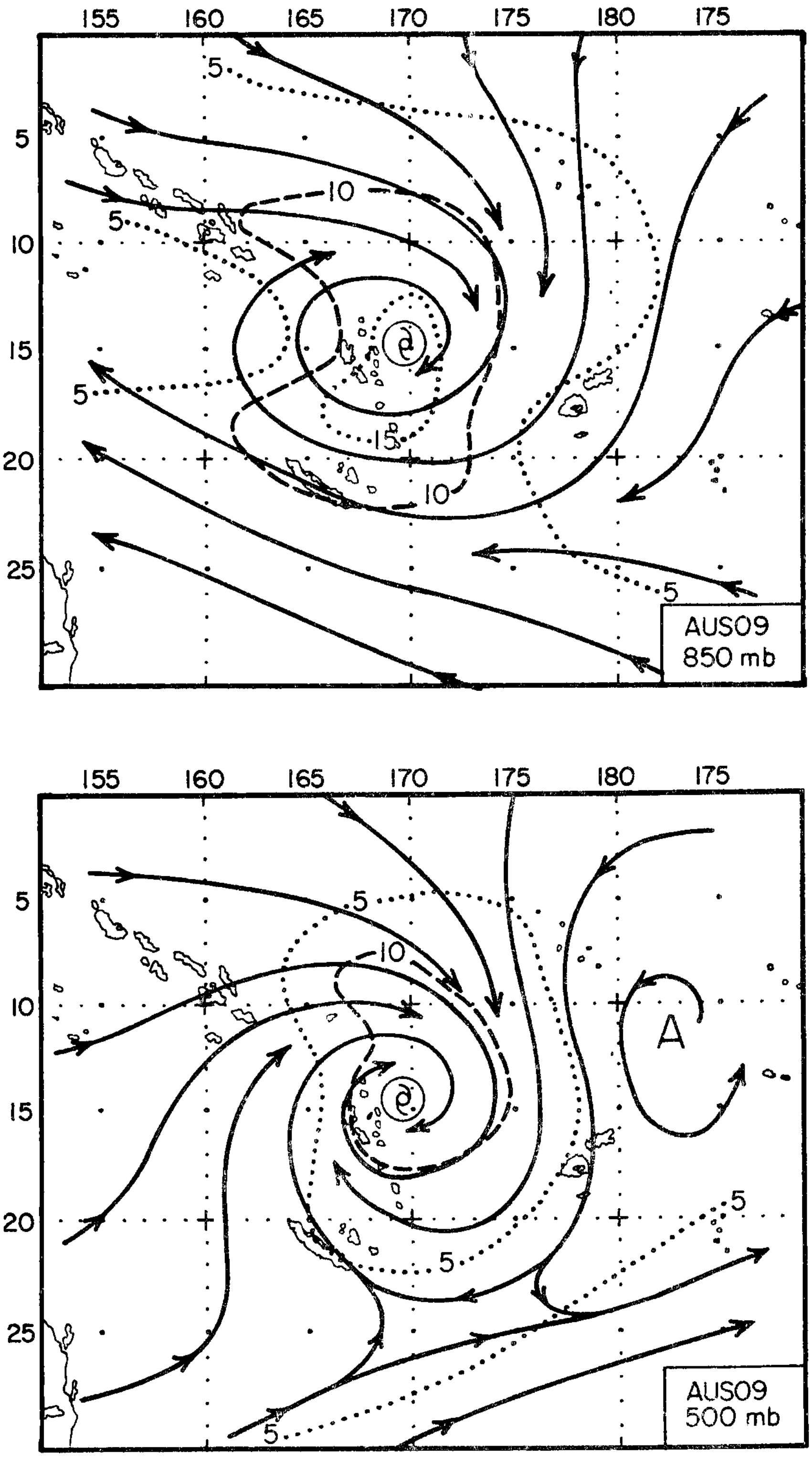

Fig. 4.8a. Plan view streamline/isotach (m s^{-1}) fields for the Pre-hurricane Tropical Storm at 850 and 500 mb.

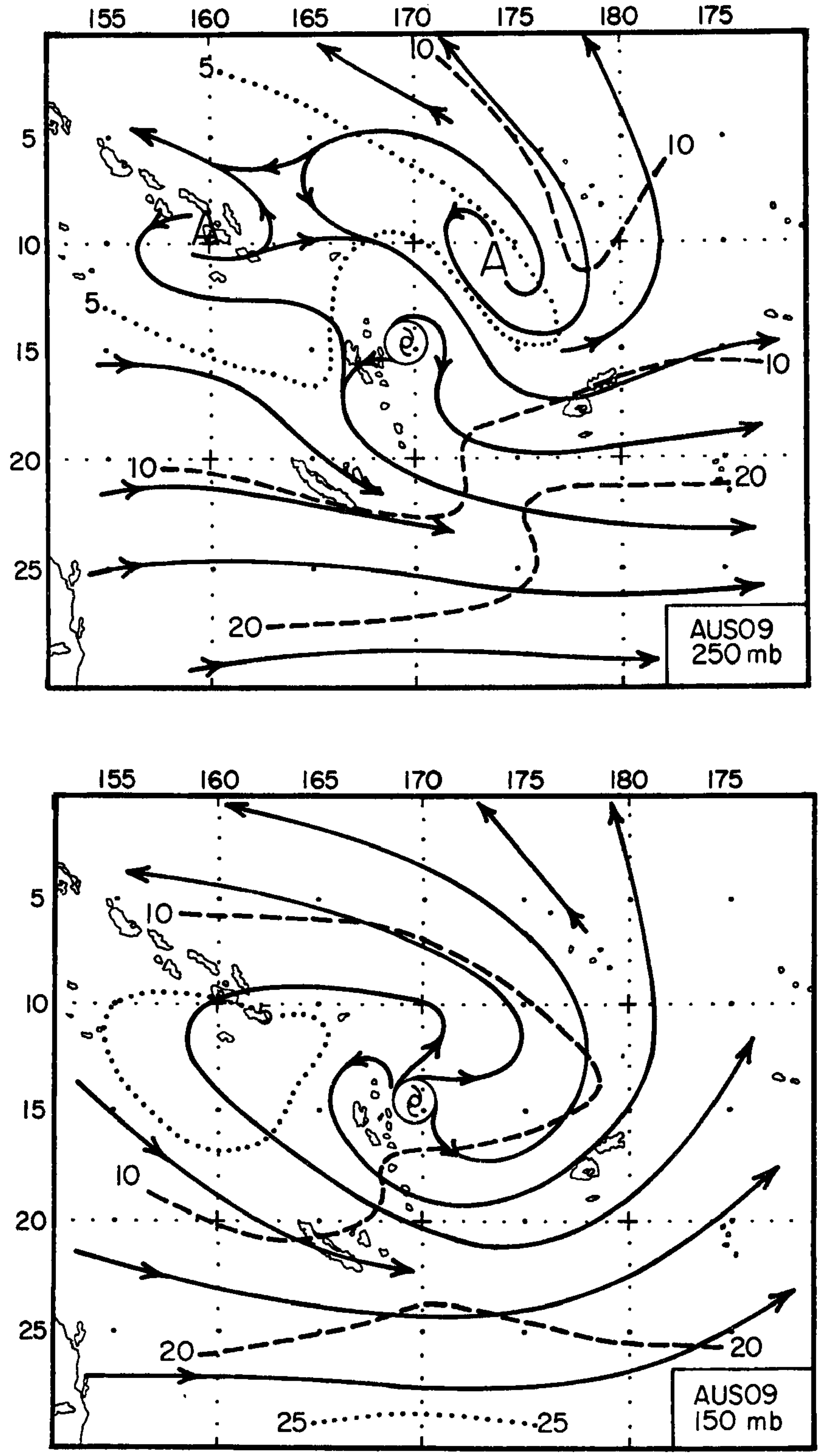

Fig. 4.8b. Plan view streamline/isotach (m s^{-1}) fields for the Pre-hurricane Tropical Storm at 250 and 150 mb.

outflow channels to both the equatorial easterlies and subtropical westerlies.

The major low to mid-level asymmetry arises from a strong inflow jet from the equatorial westerlies. This convergent jet imports high enthalpy tropical air. It is also associated with a characteristic cloud 'feeder band'; an example of which is shown in Fig. 4.9. A similar equatorial inflow has been noted by Love (1982) for the pre-tropical storm environment, and Simpson (1971) has associated the concomitant cloud band with sustained intensification of tropical cyclones in the Atlantic

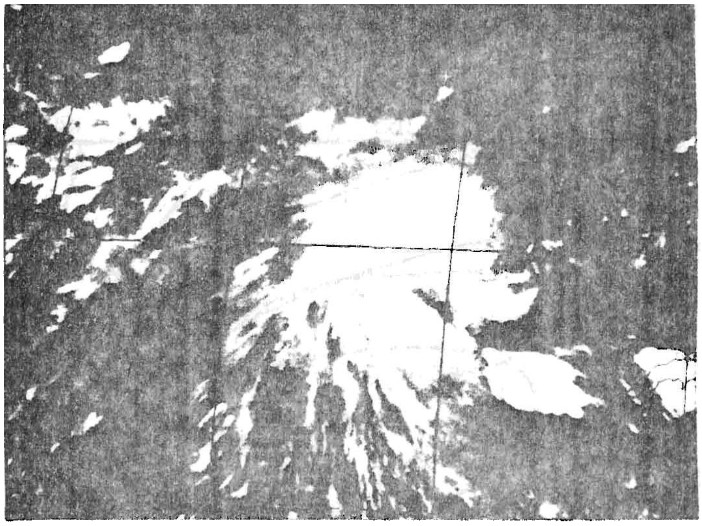

Fig. 4.9. GMS visible satellite imagery of tropical storm Kerry at 0600Z on 15 February 1979.

A second, 850 mb trade wind maximum occurs on the poleward side of the Pre-hurricane Tropical Storm and appears to overshoot, with a low level outflow to the southwest. This basic 850 mb pattern of anticyclonic flow well to the east, convergence immediately to the east, and divergence and cyclonic flow to the west, will be seen in all composites presented in this thesis. As Anthes and Hoke (1975) have noted and as we shall describe fully in Chapter 7, this distortion is largely a non-linear result of advection of earth vorticity by the cyclonic circulation, or a beta effect.

Returning to Fig. 4.8b, we note that the subtropical westerlies impinge on the southwest sector at 250 and 150 mb. But they do not penetrate the core region. Rather, they provide a long outflow channel to the southeast in addition to the weaker equatorward channel at 150 mb. A similar poleward outflow channel has been described by Ramage (1959, 1974) and Sadler (1978) as being associated with sustained intensification of tropical cyclones in the northwest Pacific. It is also similar to the 'jet on the ridge' configuration, which McRae (1956) and Wilkie (1964) have described as the most common situation for cyclogenesis and subsequent intensification in the Australian region.

The wind fields for the Non-developing Tropical Storm are shown in Fig. 4.10. All of the processes which we described as being conducive to further intensification in the pre-hurricane system are weaker or absent. the low-level jet from the equatorial westerlies is weaker and shallower, and a strong, deep subtropical westerly flow extends over the center at 500 mb and above. Though there is a resulting very strong 'outflow channel' to the southeast, the westerlies are literally ripping the system apart. Thus, this composite is typical of the characteristic 'shearing off process' which is responsible for most of the instances of premature decay over tropical waters in the Australian/southwest Pacific region (c.f., Rooney, 1981).

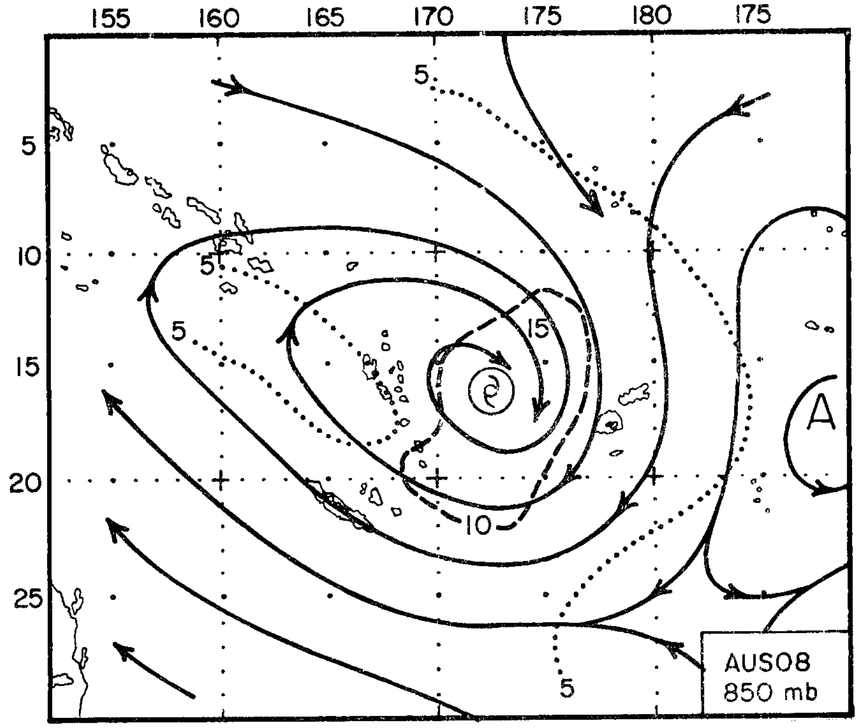

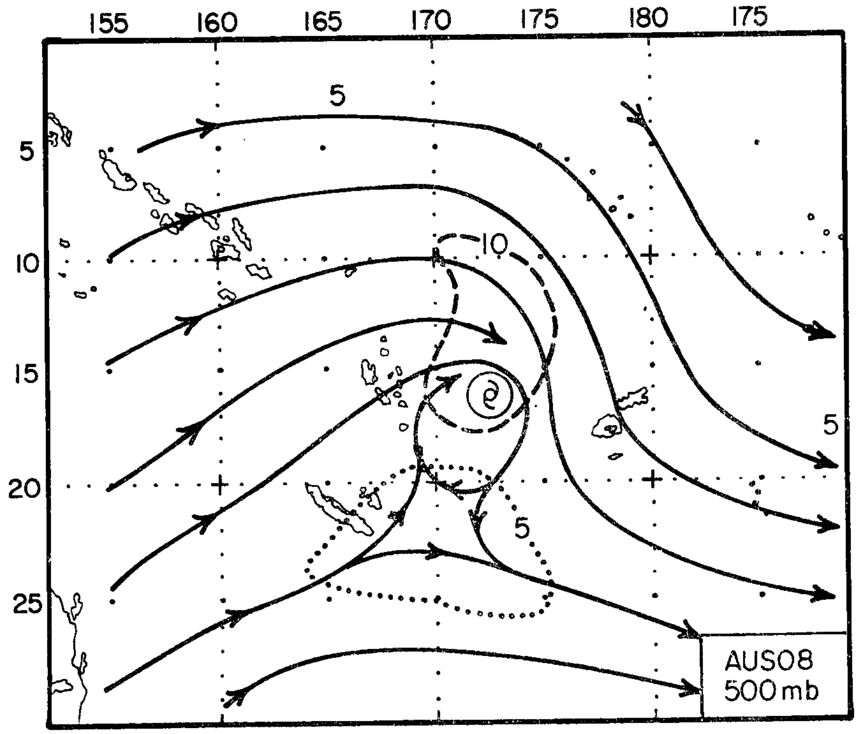

Fig. 4.10a. Plan view streamline/isotach (m s^{-1}) fields for the Non-developing Tropical Storm at 850 and 500 mb.

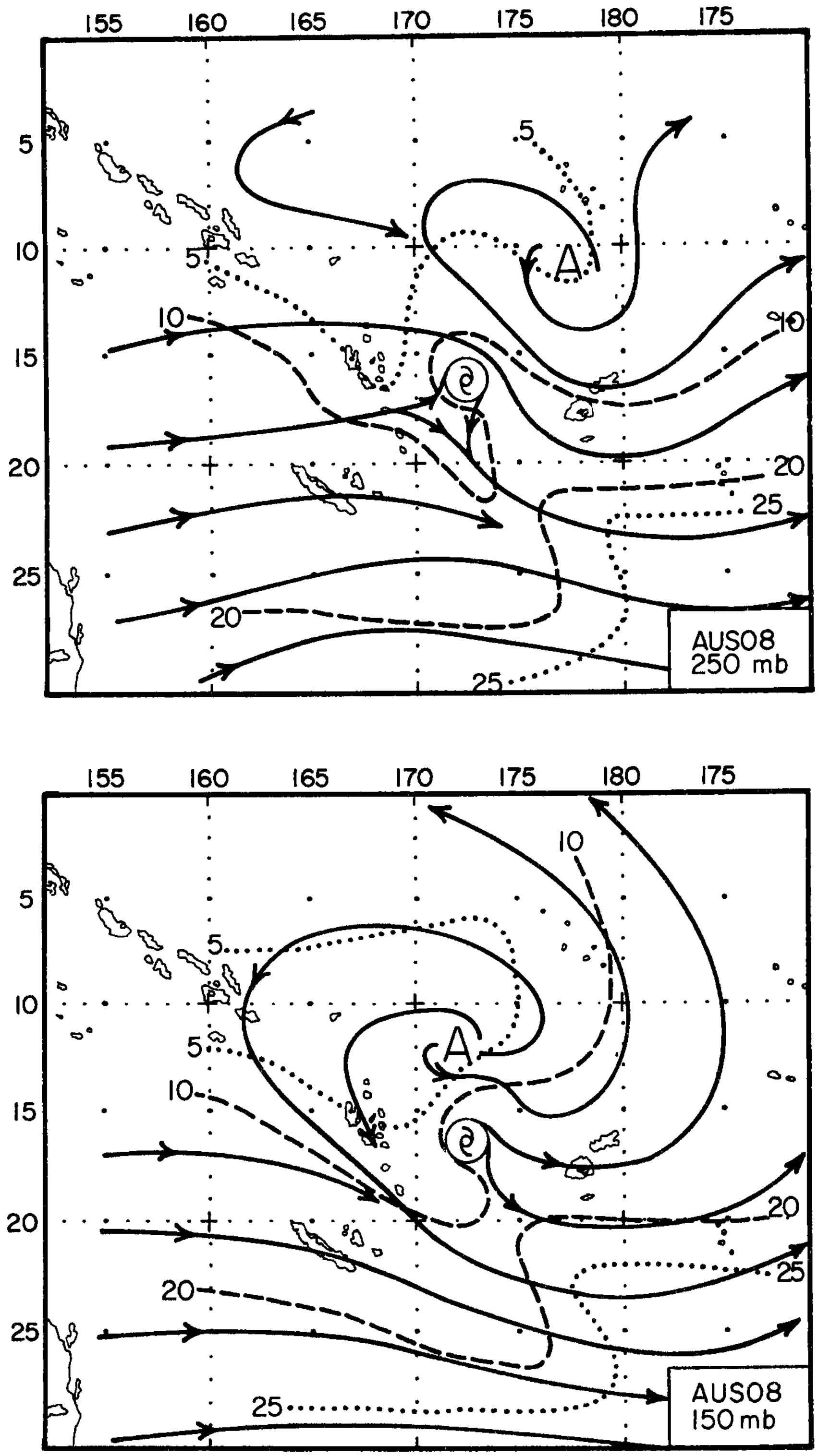

Fig. 4.10b. Plan view streamline/isotach (m s^{-1}) fields for the Non-developing Tropical Storm at 250 and 150 mb.

4.2.2 Thermal Structure

The Pre-hurricane Tropical Storm moisture and upper level potential temperature fields are shown in Figs. 4.11 and 4.12. The double banded moisture maxima to the north and east of the system clearly support the wind field indications of an influx of equatorial air and deep convection in these regions (Figs. 4.8 and 4.9). The moisture extends completely around the core to embed this pre-hurricane system in a deep, moist tropical air mass.

Notice also in Fig. 4.11 the deep dry slot which extends from the west and around the equatorward perimeter of the cyclone core. This will be seen to be a consistent feature of intensifying cyclones in the Australian/southwest Pacific region. We believe that this is partially a beta effect, in which distinct spiral bands of alternating moist convection and dry subsidence are preferentially arranged by the cyclone's interaction with the earth vorticity field (Anthes, 1972); and partially a result of advection of dry subtropical air around the cyclone on the poleward side of the moist equatorial inflow jet (c.f., Fig. 4.8). We shall provide a complete description of the underlying processes in Chapter 7.

The upper level potential temperature fields in Fig. 4.12 show that the Pre-hurricane Storm is indeed warm-cored. Interestingly, however, secondary warm regions also occur to the northeast and southwest of the center. The warm region to the northeast lies over the lower level moist 'cloud band' in Fig. 4.11. It is probably a result of vertical recycling in the vicinity of the unresolved cloud bands which constitute this composite mean. The warm band to the southwest lies along the

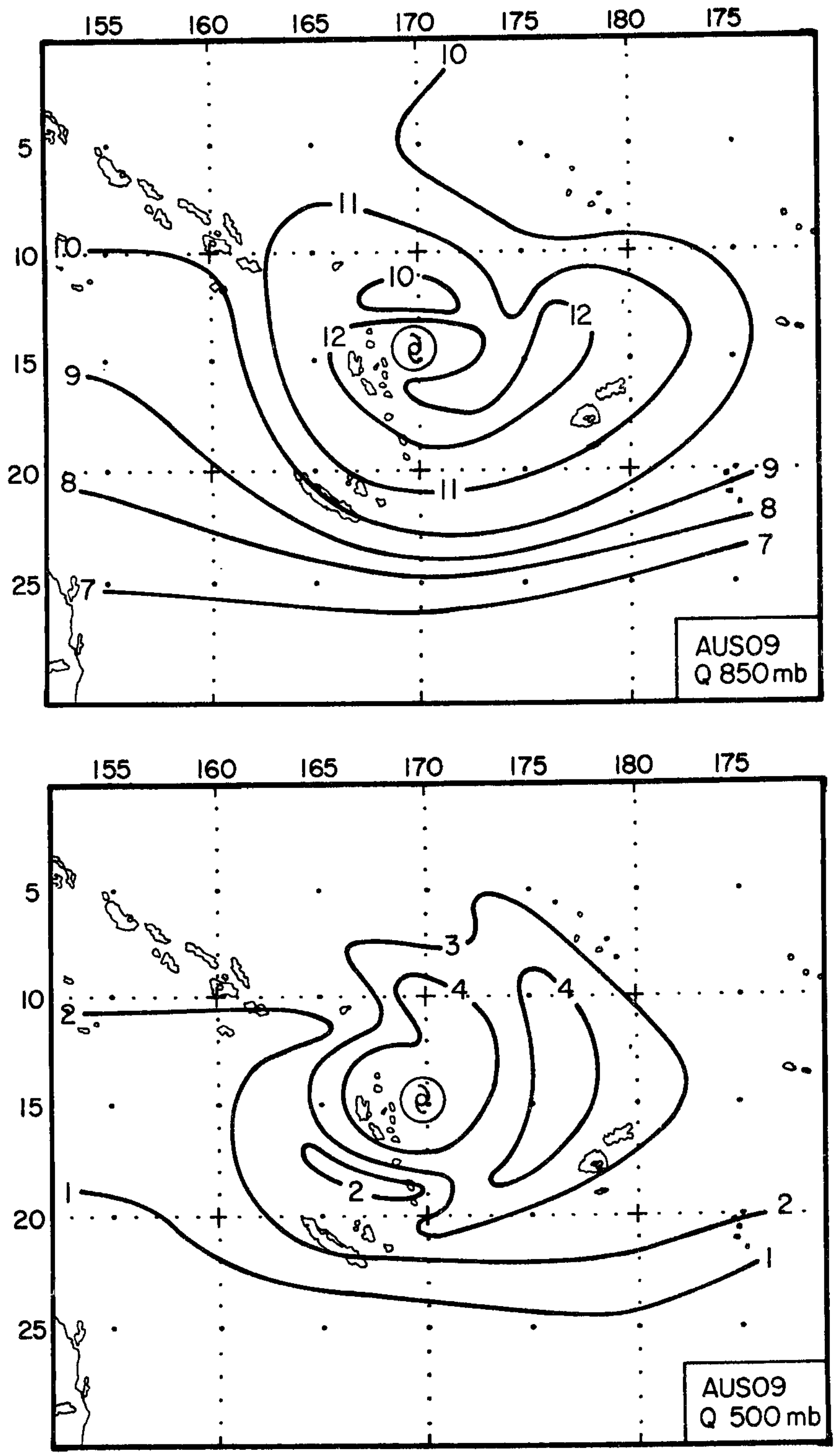

Fig. 4.11. Plan view moisture mixing ratio (g/kg) fields for the Pre-hurricane Tropical Storm at 850 and 500 mb.

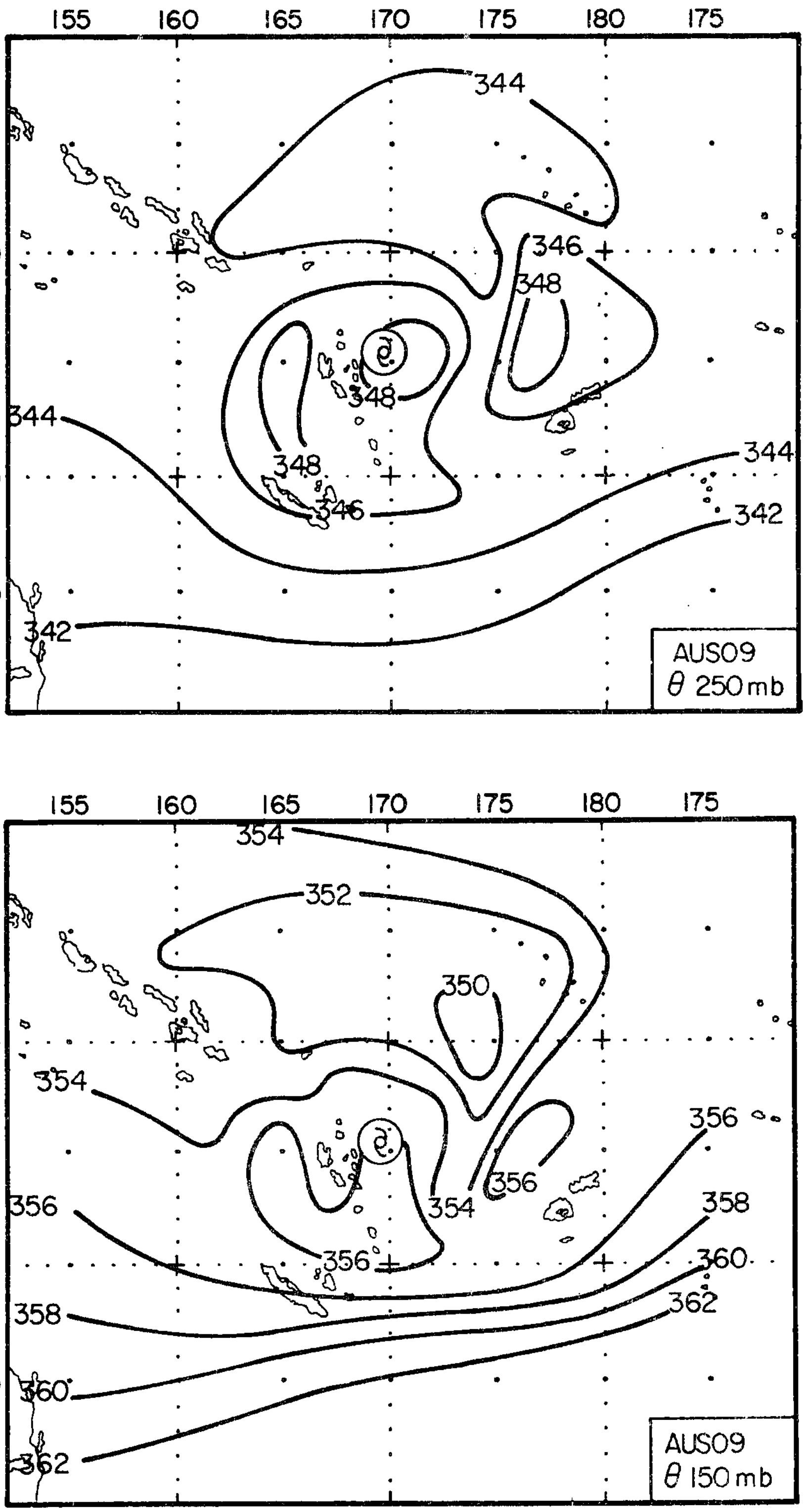

Fig. 4.12. Plan view potential temperature (K) fields for the Pre-hurricane Tropical Storm at 250 and 150 mb.

confluence between the subtropical westerlies and storm outflow (Fig. 4.8b) and also extends into the, presumably weakly subsident, right entrance region of the outflow jet. The lower level dry slot in Fig. 4.11 indicates that this subsidence extends downwards to at least the 500 mb level.

The moisture and upper level potential temperature fields for the Non-developing Tropical Storm are shown in Figs. 4.13 and 4.14. They are quite different to those for the pre-hurricane system. At 500 mb much of the moisture is constrained to the eastern sector; a dry slot is found just west of the core and a strong moisture gradient exists over the storm center. This results from the previously described shearing off effect of the subtropical westerlies (Fig. 4.10). Deep convection cannot be maintained in the western sector and is also shifted eastward away from the core region. Thus, there is an eastern sector moisture maximum at 500 mb, and the radial outflow maximum in Fig. 4.7 occurs some 400 km from the center.

The upper level potential temperature fields in Fig. 4.14 show that the Non-developing Tropical Storm is still warm cored, despite the intrusion of subtropical air. (Recall that this composite is made up of intensifying systems that are destroyed before reaching hurricane intensity.) A remarkable warm band also occurs on the poleward side. As with the similar, but much weaker feature in the pre-hurricane system, this band lies along the confluence zone of the cyclone circulation and westerly environmental flow. It is thus almost certainly just poleward of the often observe sharp edge of the anticyclonically curved cirrus band which extends polewards and eastwards of such systems.

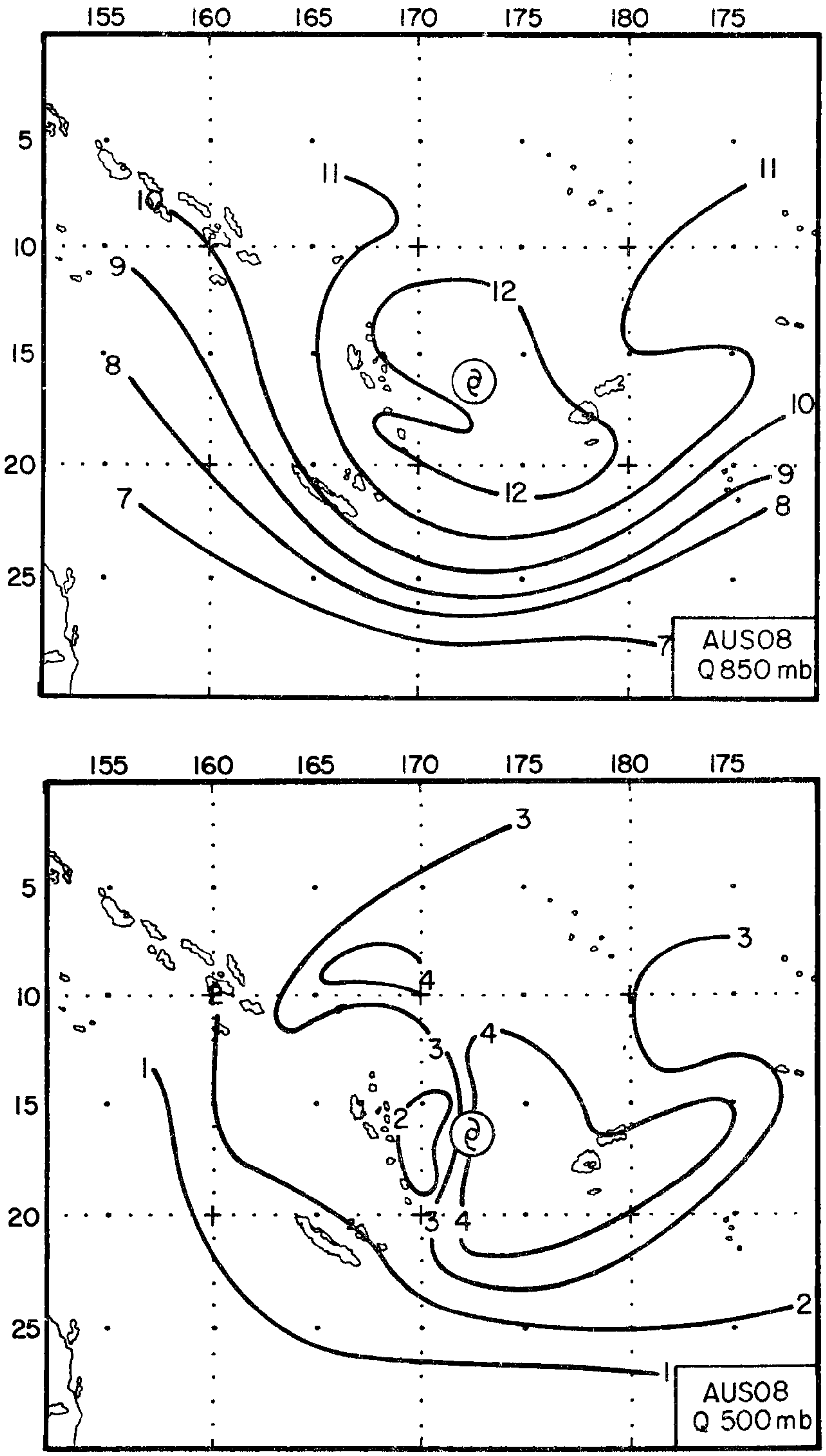

Fig. 4.13. Plan view moisture mixing ratio (g/kg) fields for the Non-developing Tropical Storm at 850 and 500 mb.

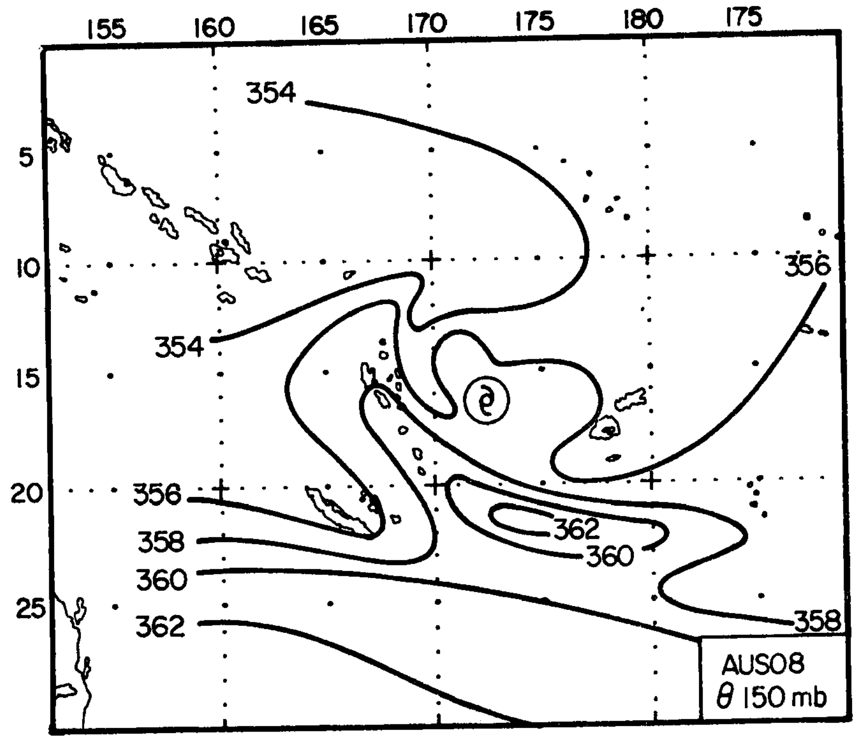

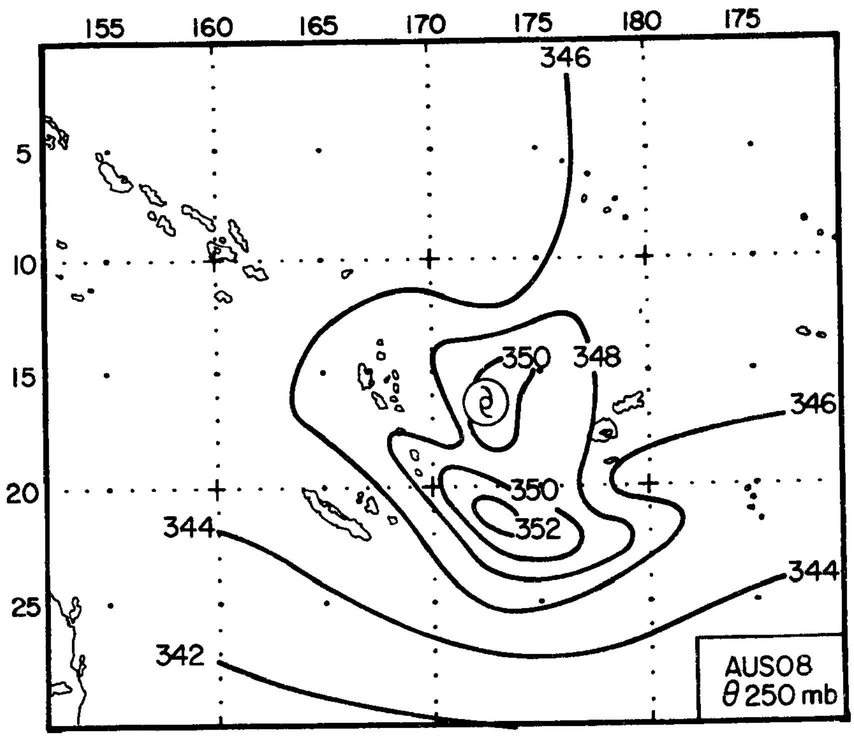

Fig. 4.14. Plan view potential temperature (K) fields for the Non-developing Tropical Storm at 250 and 150 mb.

Since the maximum amplitude occurs in the right entrance of the strong 'outflow' jet in Fig. 4.10b, this band is probably largely maintained by the toroidal circulation around the jet streak. Indeed, as may be seen in the meridional cross-section in Fig. 4.15, it has a number of similarities to the temperature field usually observed in association with the subtropical jet (c.f., Palmen and Newton, 1969, p. 226). However, Holland et al. (1983) have presented aircraft observations of a phenomenal warming of 18 K above ambient near 230 mb in this region for tropical cyclone Kerry (1979). By using a combination of physical reasoning and observations, they concluded that this warming required stratospheric subsidence in which the potential energy gain was derived from the kinetic energies of the opposing subtropical westerlies, the easterlies around the poleward side of the cyclone, and downward advection of easterly momentum from the stratosphere. The observed warm band in Figs. 4.14 and 4.15 probably arises from a combination of these processes.

4.3 Summary

In this chapter we have described a number of features of tropical storms in the Australian/southwest Pacific region.

We have shown that these systems occur almost exclusively between November and May with a peak frequency in January or February. Their highest frequency is in the Gulf of Carpentaria, and secondary maxima are found in the Coral Sea and just off the northwestern Australian coast. The Australian continent appears to predominate in determining these distributions. Many storms form in its coastal waters and decay

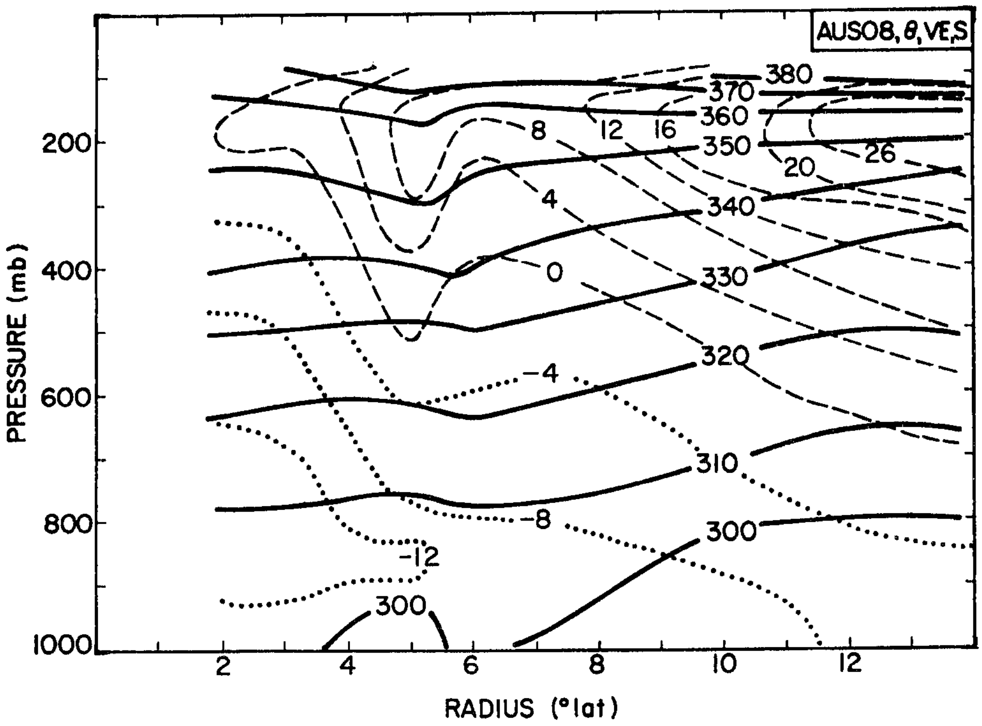

Fig. 4.15. Meridional cross-sections of potential temperature (K, solid lines) and zonal wind component (m s^{-1}, dashed lines for westerlies, dotted lines for easterlies) poleward of the Non-developing Tropical Storm.

soon after by making landfall. Further, since the continent has a role in the determination of the large scale wind fields (section 1.2), it also has an indirect influence on tropical storms over the open ocean.

Perhaps the most notable result of this indirect influence is seen in the preferred eastward movement and decay over tropical waters of tropical storms over the southwest Pacific Ocean. We have shown that these storms lie under a strongly sheared mid to upper level subtropical westerly flow. They thus move consistently eastward (and often erratically). They also suffer a considerable vertical shearing, with the major convective region pushed to the southeast and a strong thermal and moisture gradient over the core, and thus prematurely decay over tropical waters.

Paradoxically, those oceanic tropical storms which subsequently develop into hurricanes seem to benefit from the same upper level westerly flow. In these latter systems the subtropical westerlies do not extend over the core region, but are close enough to provide a distinct, strong outflow channel on the poleward side. Thus, we have shown that the interaction with the upper level flow can either destroy or sustain the storm intensification.

We have also seen a distinctive low level signature in both tropical storm composites. Both storms are very large and the developing system has a strong secondary inflow at large radii. This secondary inflow arises from a combination of subtropical, trade wind inflow to the southeast and a tropical, monsoonal inflow to the northeast. Further, both storms have a divergent flow and extension of the cyclone to the west, a deep equatorward inflow, convergence to the east and an anticyclone well to the east.

We shall discuss the processes behind, and importance of these features in Chapters 6 and 7. But first we shall examine the climatology and structure of hurricanes throughout the region.

5. HURRICANES

Following our discussion on tropical storm classification in the first paragraph of Chapter 4 and our definitions in section 1.1, we classify hurricanes as: 1) all cyclones in the Australian region in which the central pressures fell below 980 mb; and 2) all systems east of 165°E which were classified as hurricanes by Kerr (1976) or Revelle (1981). An additional, major hurricane classification contains all cyclones in the Australian region which attained minimum central pressures of less than 960 mb. In this chapter we present a complete hurricane climatology for the Australian/southwest Pacific region, and compare this to the tropical storm climatology in Chapter 4. We also examine and compare the structure of the intensification and decaying phases of oceanic hurricanes in the southwest Pacific region, and describe the continental influence on hurricanes just off the east and west Australian coasts.

Unfortunately, we do not have sufficient information in the region east of 165°E to differentiate major hurricanes for the whole period. Hence, our major hurricane climatology is limited to the Australian region. Some additional climatological information on major hurricanes in the southwest Pacific may be found in Revelle (1981). We are also unable to present any information on the oceanic structure of the major hurricane, though we shall discuss some dynamic features of major recurving hurricanes in section 5.4

5.1 Hurricane Climatology

Spatial Distribution: By comparing Fig. 5.1 to Fig. 4.1 we see that the spatial distribution of hurricanes is qualitatively similar to that for tropical storms in the southwest Pacific, but there are marked differences in the north/west Australian region. Intensifying tropical storms in the landlocked Gulf of Carpentaria tend to cross the coast before, or soon after reaching hurricane intensity. Hence, we observe a much lower frequency of Gulf hurricanes (Fig. 5.1) compared to tropical storms (Fig. 4.1). By comparison there is a remarkable peak in hurricane occurrence off the northwest Australian coast. Hurricanes in this area typically track along and parallel to the coast and either continue to the southwest or suddenly recurve and make landfall anywhere between Broome and Geraldton (Fig. 5.1). Thus, a town such as Port Hedland is in the outer fringes of, and under direct threat from, a hurricane on an average of 2-3 days every year!

The hurricane origin, maximum intensity and decay point distributions are shown in Fig. 5.2. For the southwest Pacific region these are qualitatively similar to those for tropical storms in Fig. 4.2. However, the hurricanes display a trend towards lower latitude origins and higher latitude maximum intensity and decay points. By comparison, in the north/west Australian region the median storm and hurricane origin latitudes are similar but most hurricanes originate in the Timor Sea, reach maximum intensity off the northwest Australian coast and decay by crossing that coast. As with tropical storms, the detrimental environmental winds and cold ocean poleward of 20^{o}S has a strong limiting effect on the distribution of intensifying hurricanes.

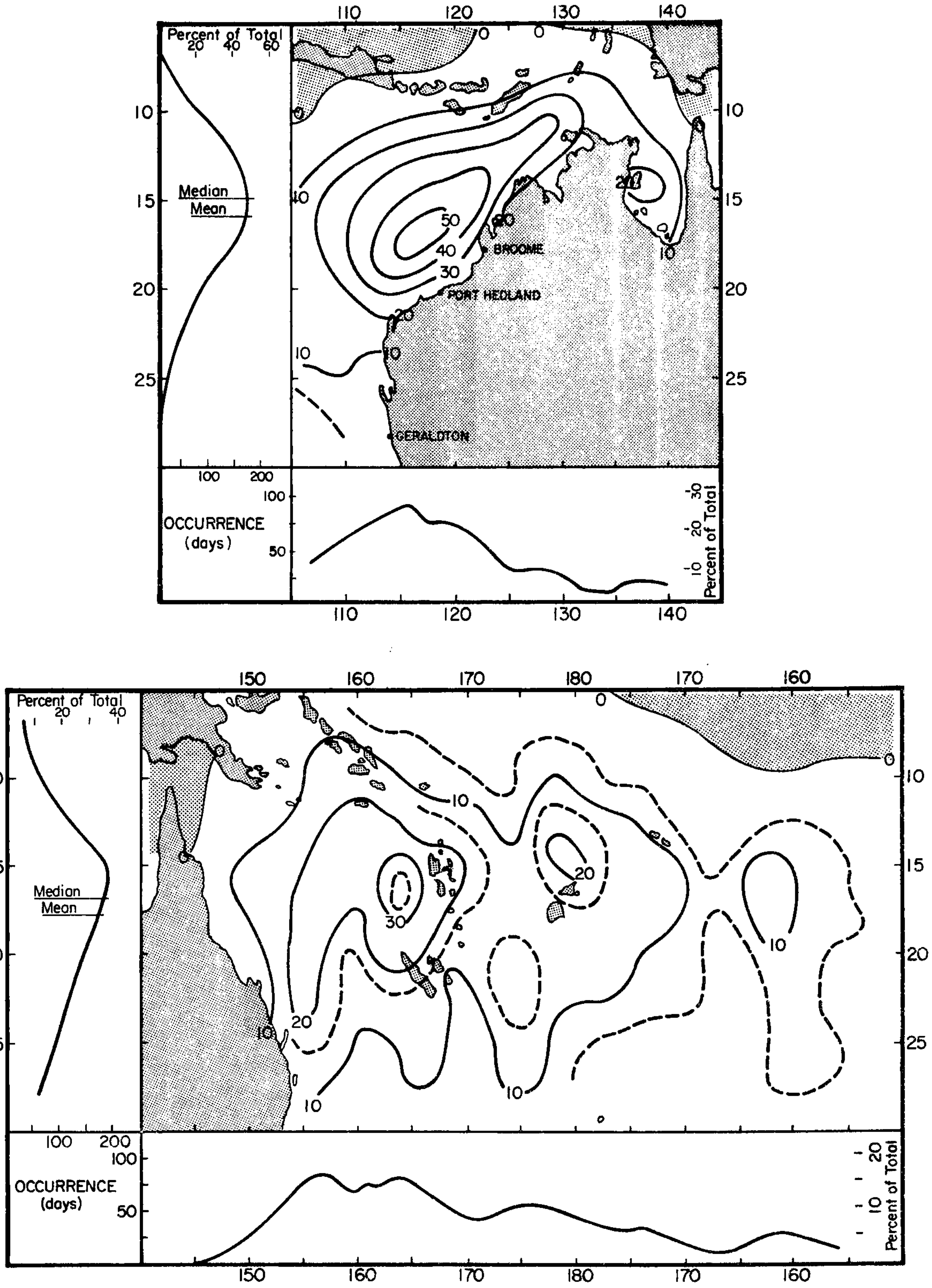

Fig. 5.1. Hurricane occurrence (days per 5^{o} Marsden square for the 1959-1979 period) for the northwest Australian and southwest Pacific regions. Stippling indicates regions of no occurrence and dashed lines, indicating intermediate 5 day isochrones, are used for extra detail.

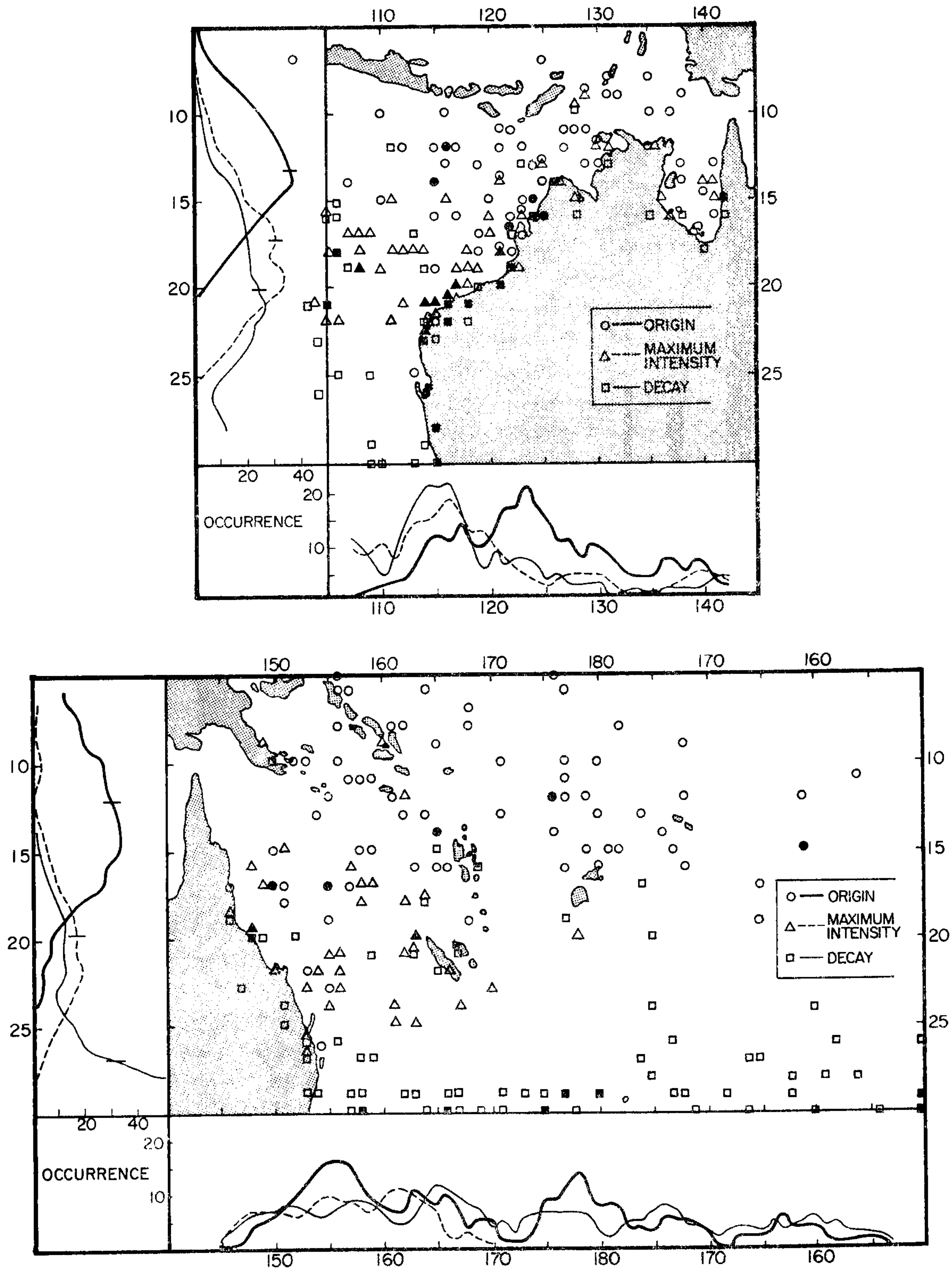

Fig. 5.2. Hurricane origin, maximum intensity and decay point distributions for the north/west Australian and southwest Pacific regions during the period 1959-1979. Tic marks indicate median latitudes and filled in symbols indicate multiple occurrences.

<u>Intraseasonal Distributions</u>: The intraseasonal distributions in Fig. 5.3 indicate that both regions have an early season hurricane maximum, whereas the tropical storms (Fig. 4.3) rise to a late season peak. This is due to a tendency for the early season systems, which form along the fledgeling monsoonal trough (Bureau of Meteorology, 1978; McBride and Keenan, 1982) at low latitudes, to become hurricanes and also have longer lifetimes. Hurricanes in the north/west Australian region also exhibit a distinct mid-season minimum, which we believe is caused by the Australian continent. During the mid-season the monsoonal trough lies over northern Australia (Fig. 1.3) and the oceanic area over which cyclones can form is considerably reduced. Further, those cyclones which form, generally do so close to the coast and subsequently make landfall, or are otherwise adversely affected. Thus, there is very

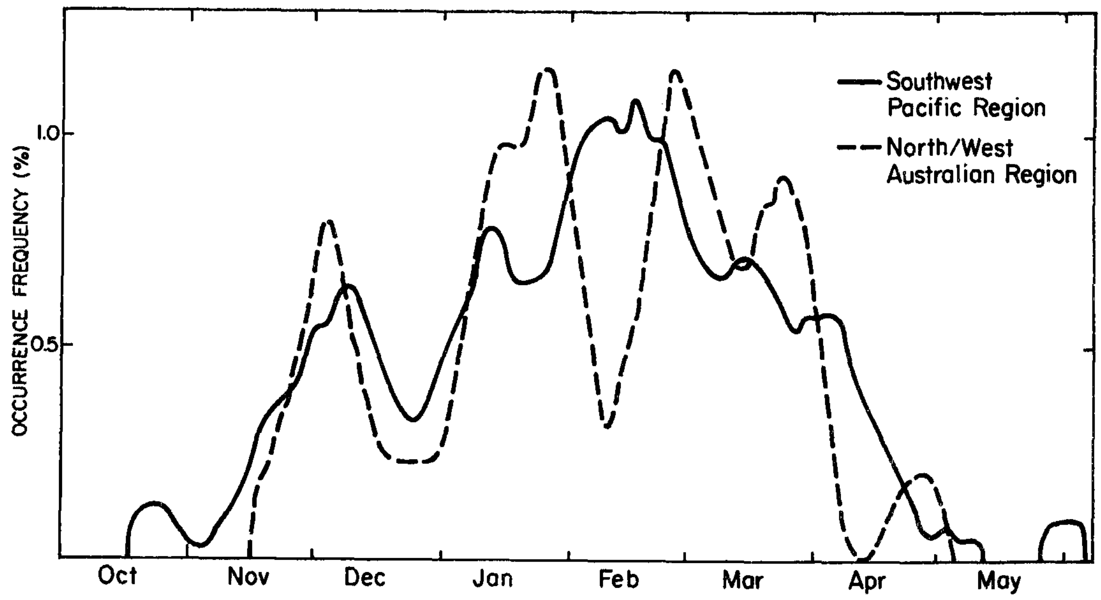

Fig. 5.3. Hurricane intraseasonal distribution for the north/west Australian and southwest Pacific regions. Except for the extremities, the curves have been smoothed by a running 15 day mean.

little reduction in the frequency of tropical storms (Fig. 4.2) but a distinct reduction in hurricane occurrence. As the monsoonal trough moves equatorwards off the continent in late February the hurricane occurrence increases sharply (Fig. 5.3) whereas, as we have already noted in Fig. 4.3 the tropical storm occurrence decreases.

Motion: Westward moving systems comprise a much larger proportion of hurricanes (Fig. 5.4) than tropical storms (Fig. 4.4). A similar feature has been noted by Revelle (1981) for the southwest Pacific region. However, the southwest Pacific hurricanes still have an eastward motion maximum and move faster on an average than those in the north/west Australian region. The zonal motion distributions in Fig. 5.5, indicate that these features are largely a result of high latitude, decaying systems (which are removed from the north/west Australian region by the Australian continent). The majority of low latitude hurricanes are moving westward in both regions.

5.2 Major Hurricane Climatology:

Spatial Distribution: The major hurricanes form a subset of the hurricanes, and, as shown in Fig. 5.6 have a very similar spatial distribution to that for all hurricanes in Fig. 5.1. The origin, maximum intensity and decay point distributions, shown in Fig. 5.7, are also qualitatively similar to those for the hurricane. Note, however, the concentration of coastal crossings along the north/west Australian coast. Eighty six percent of major hurricanes in the north/west Australian region made landfall compared to only 38% of non-major hurricanes and 55% of tropical storms. Further, 41% of the major

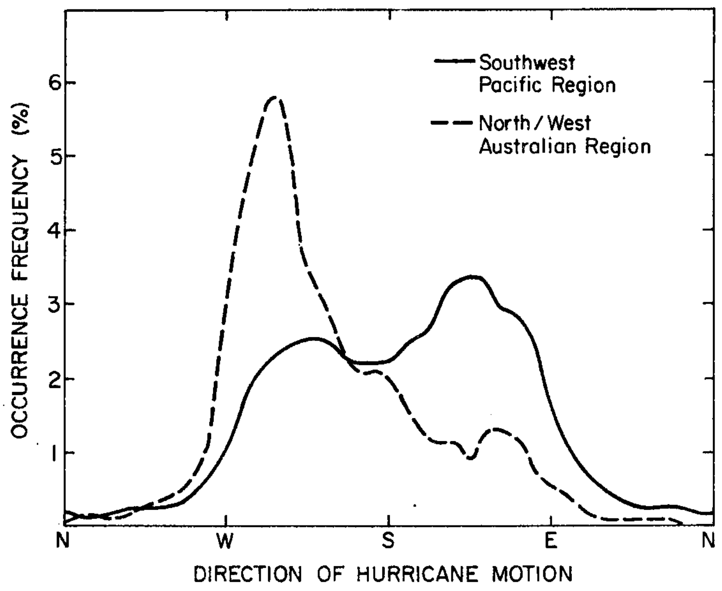

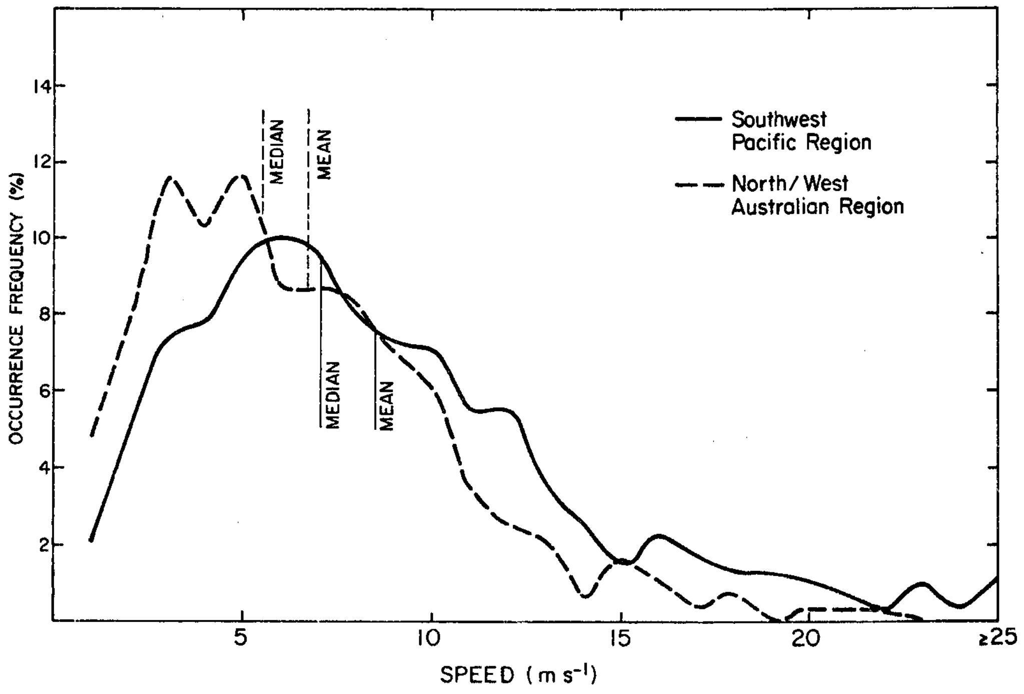

Fig. 5.4. Hurricane direction and speed distributions for the north/ west Australian and southwest Pacific regions.

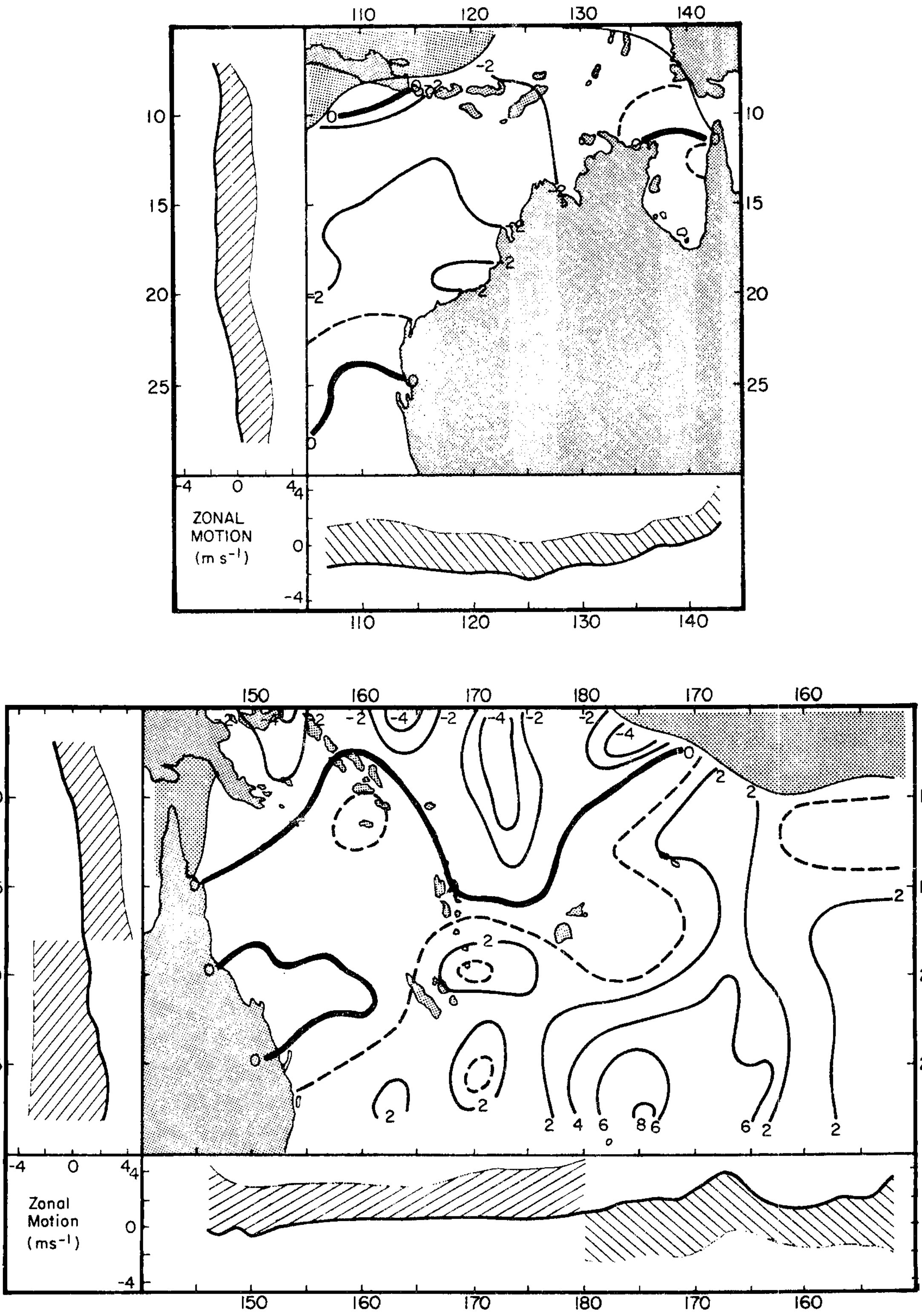

Fig. 5.5. Hurricane zonal motion distribution (averaged over 5° Marsden squares) for the north/west Australian and southwest Pacific regions. Stippling indicates regions of no occurrence and hatching indicates one standard deviation.

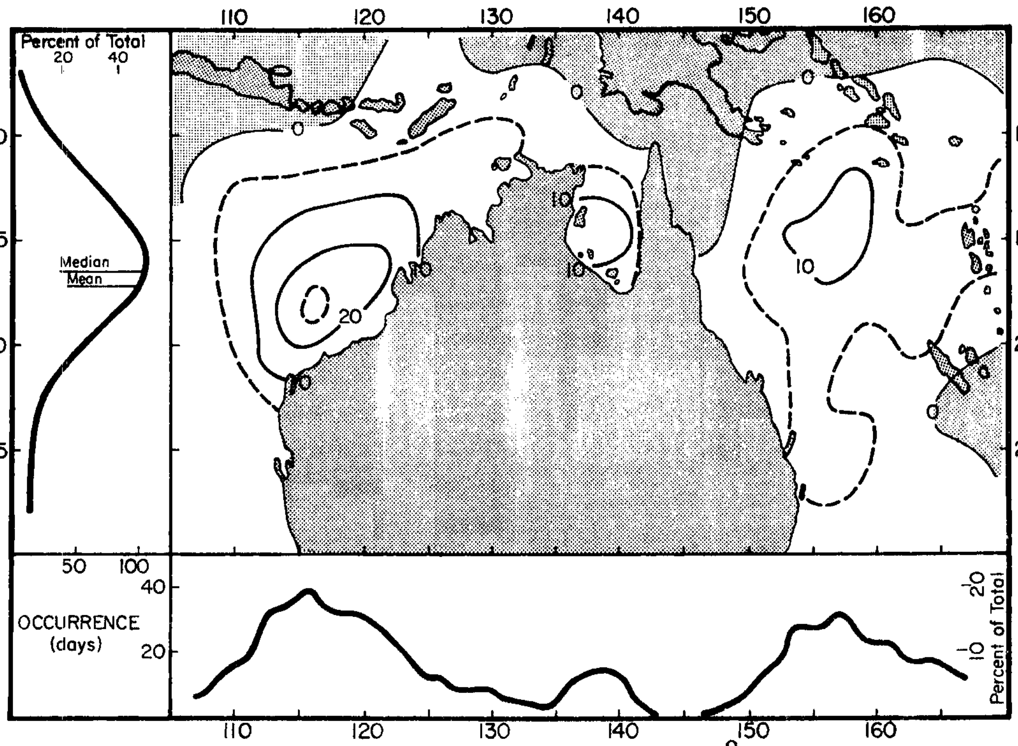

Fig. 5.6. Major hurricane occurrence (days per 5° Marsden square for the period 1959-1979) for the Australian region. Stippling indicates regions of no occurrence, and dashed lines indicate intermediate isochrones.

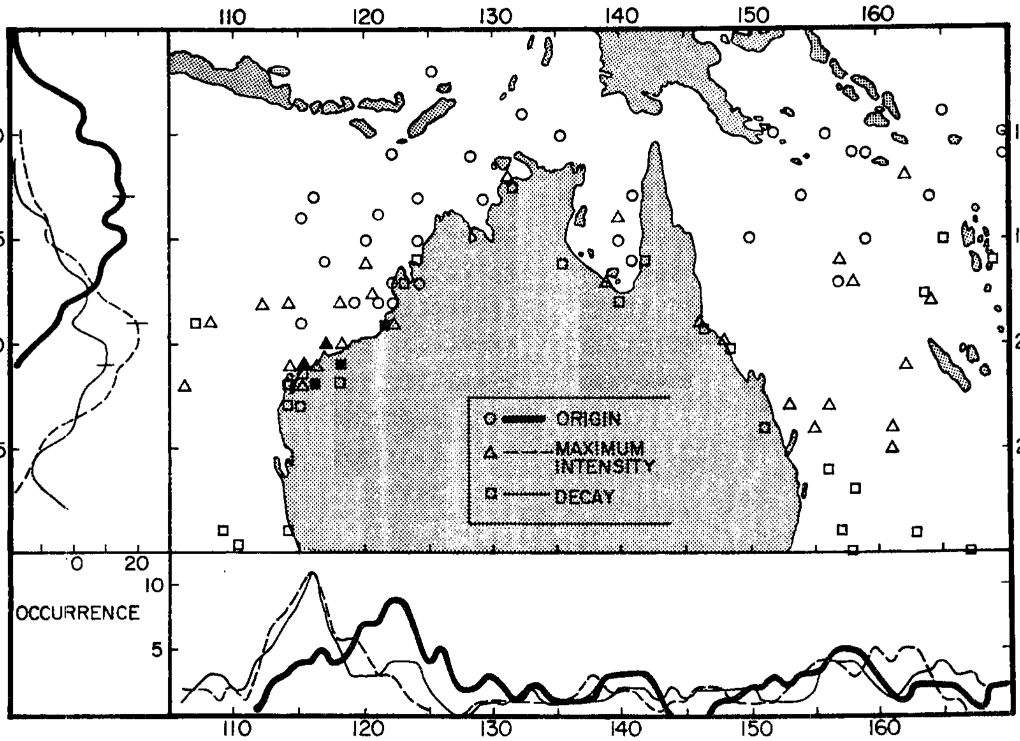

Fig. 5.7. Major hurricane origin, maximum intensity and decay point distributions for the Australian region. Tic marks indicate median latitudes and filled in symbols indicate multiple occurrences.

hurricanes in the entire Australian region made landfall on the north/west Australian coast at or very near maximum intensity. As we shall show in section 5.3 and Chapter 6, these statistics are largely due to the generally benevolant environment for west coast hurricanes.

Intraseasonal Distribution: The intraseasonal distribution of major hurricanes, shown in Fig. 5.8 contains the same early season maximum as the hurricane distributions in Fig. 5.3, but no mid-season minimum. The lack of a mid-season minimum arises partly from the mixing of Coral Sea hurricanes with the north/west Australian systems. But there is also tentative evidence that a higher proportion of hurricanes become major in this mid-season period. The sharp March reduction is somewhat of a mystery and is to be investigated further.

Motion: The trend for hurricanes to move more consistently westward than tropical storms (Figs. 4.4, 5.4) is continued in the major hurricane classification. As Fig. 5.9 shows, major hurricanes in the

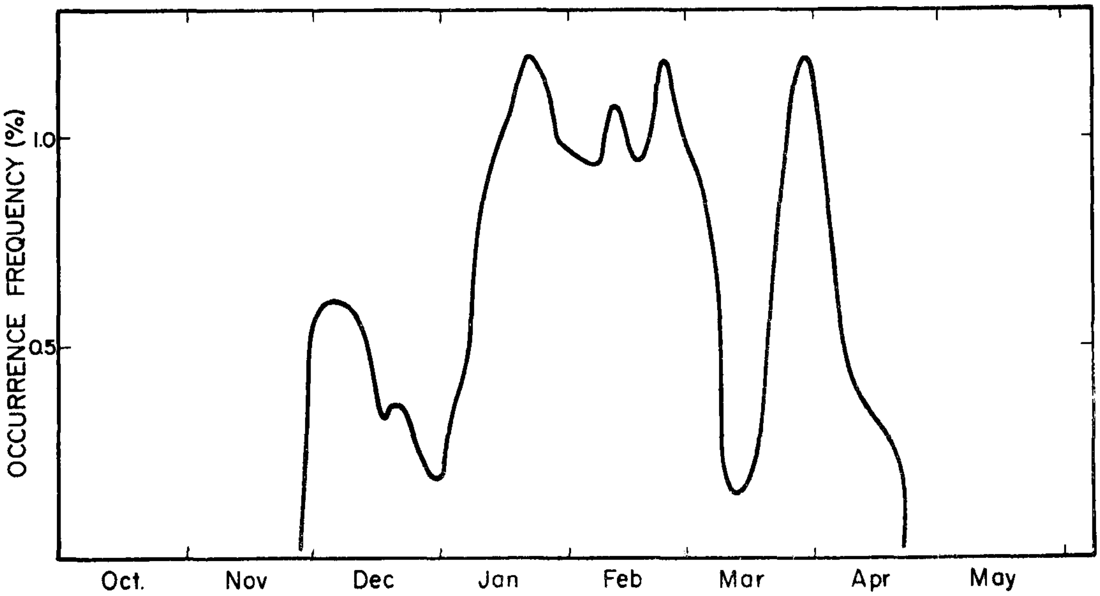

Fig. 5.8. Major hurricane intraseasonal distribution for the Australian region. Except for the extremities, the curves have been smoothed by a running 15 day mean.

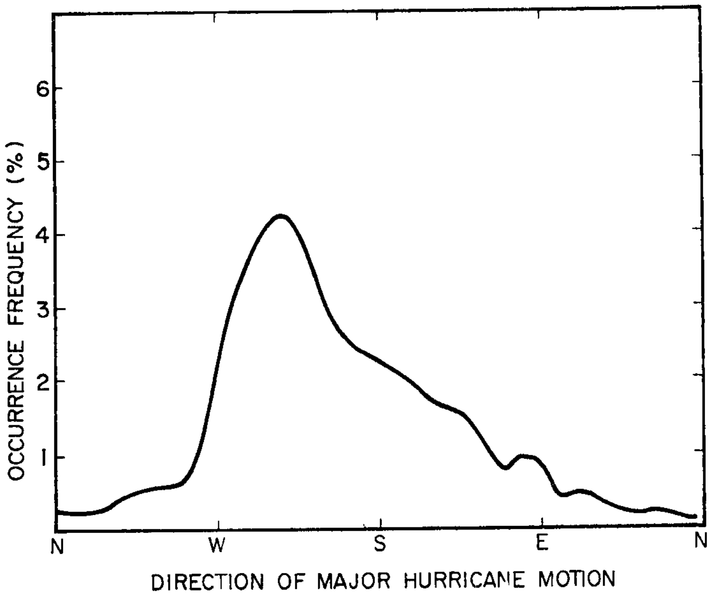

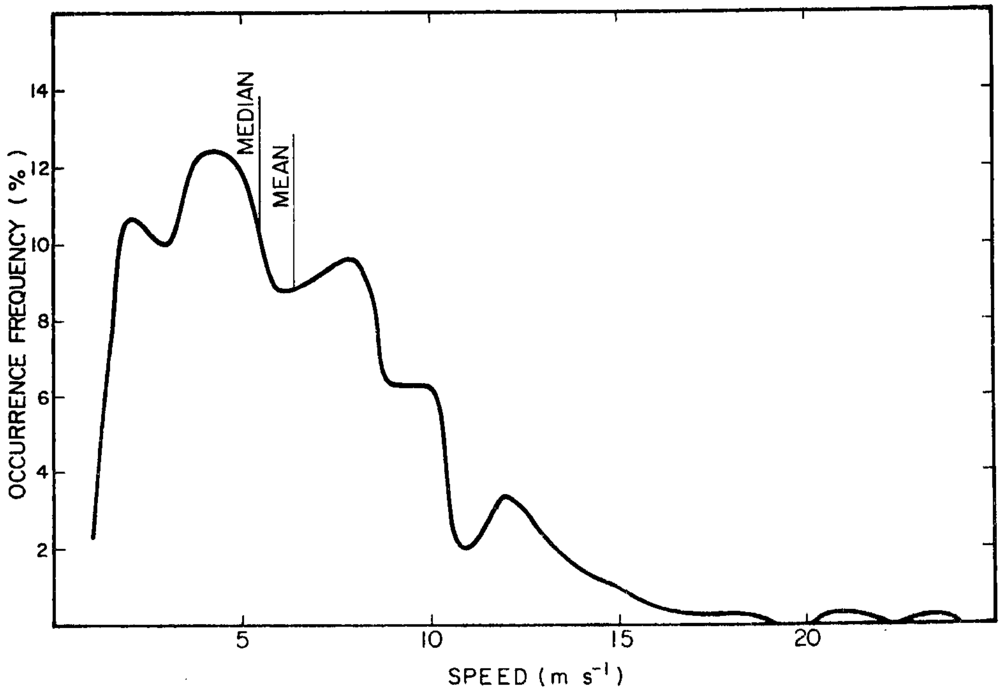

Fig. 5.9. Major hurricane direction and speed distributions for the Australian region. The curves have been smoothed by 5 point running means.

Australian region are dominated by westward moving systems. A similar finding has been made for the southwest Pacific by Revelle (1981). We shall, however, show in Chapter 6 that these major hurricanes are comprised mainly of recurving cyclones which cross the Australian coast after recurvature. Cyclones which move continuously westward rarely become major hurricanes. This is quite different to other ocean basins where westward moving systems, which can move for long periods over warm tropical waters with no detrimental upper tropospheric shearing effects, may become very intense.

5.3 The Structure of the Oceanic Hurricane

We shall use the AUS06 and AUS07 composites in this section to describe the general features of deepening and decaying oceanic hurricanes in the southwest Pacific. These composites are described fully in Appendix 2, but briefly, they are both comprised of hurricanes in the southwest Pacific between 15 and 25^{o}S and at least 1000 km from the Australian coast and contain the hurricane portion of those systems in the AUS09, Pre-hurricane Tropical Storm composites; AUS06 represents the developing phase and AUS07 represents the decaying phase of these hurricanes.

5.3.1 Dynamical Structure

As may be seen in the axisymmetric cross-sections in Figs. 5.10 and 5.11 the oceanic hurricane is quite large. In both the developing and decaying phase it has a deep cyclonic circulation extending beyond 14^{o} latitude radius, and is overlain by an extensive anticyclone. In this

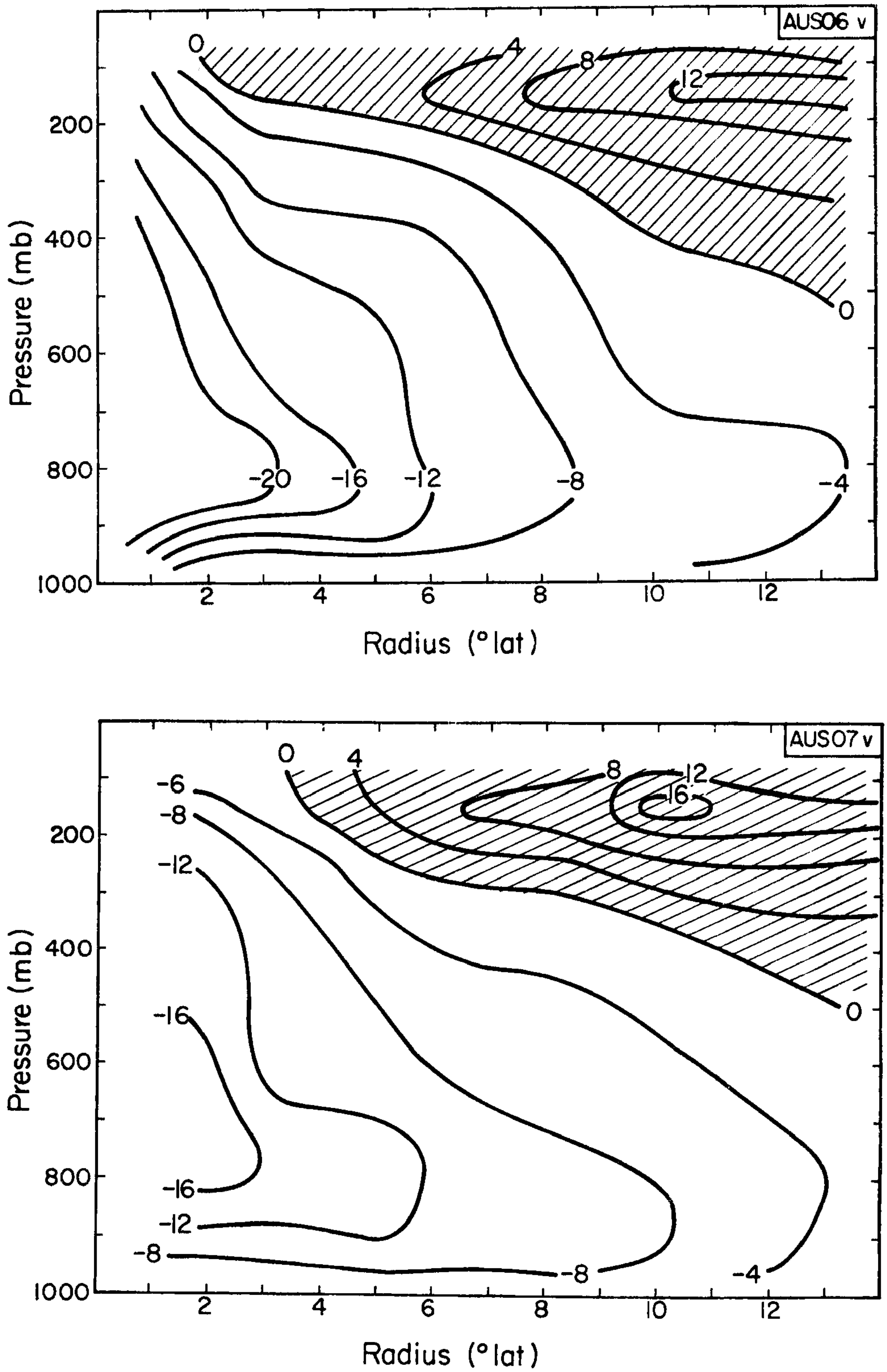

Fig. 5.10. Axisymmetric azimuthal wind (m s^{-1}) cross-sections for the Developing (AUS06), and the Decaying (AUS07) Oceanic Hurricane. Hatching indicates anticyclonic circulation.

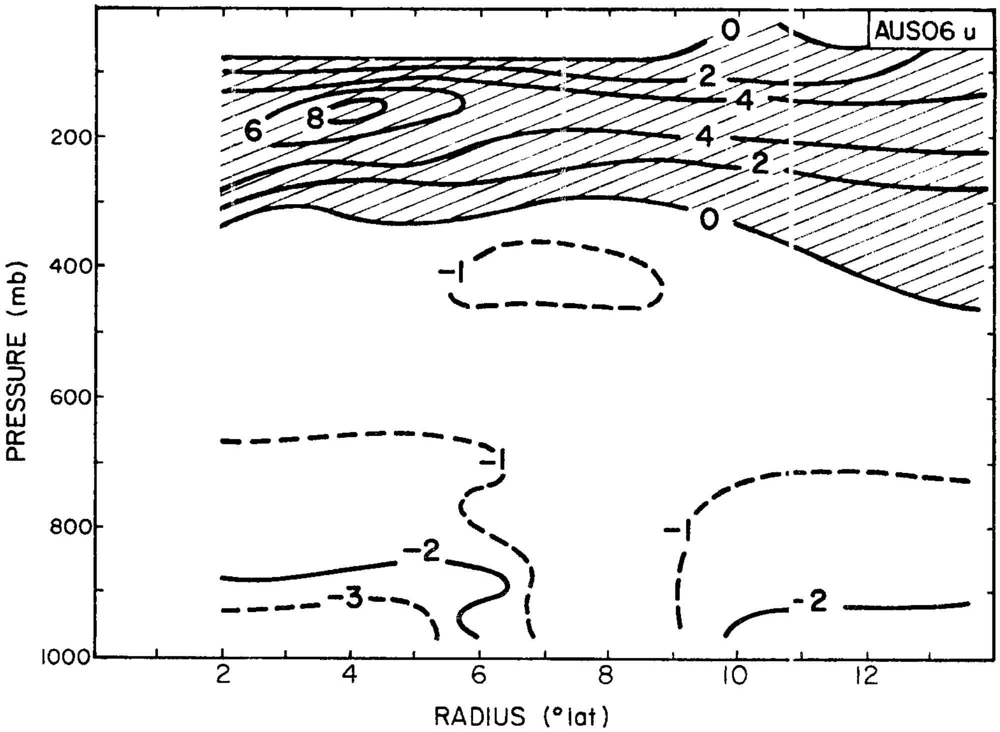

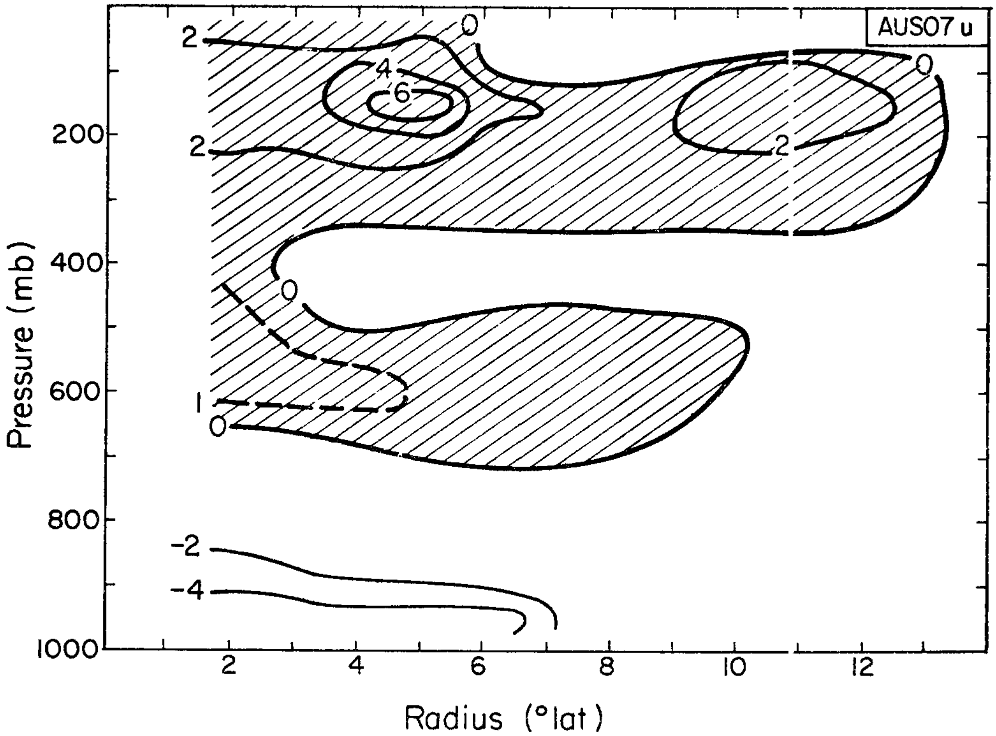

Fig. 5.11. Axisymmetric radial wind (m s^{-1}) cross-sections for the Developing (AUS06), and the Decaying (AUS07) Oceanic Hurhuricane. Outflow regions are hatched. Radial winds of less than 1 m s^{-1} are not significantly different from zero.

regard the oceanic hurricane is quite similar to the steady state typhoon described by Frank (1977a). However, the developing and decaying phases do have some interesting additional features.

The developing hurricane in Figs. 5.10 and 5.11 is similar to the Pre-hurricane Tropical Storm in Figs. 4.6 and 4.7. It exhibits a strong, deep cyclonic circulation out to a radius of 8° latitude with weak vertical wind shear between 850 and 400 mb. A low level wind maximum also extends beyond 10° latitude radius and is associated with a secondary maximum in radial inflow (Fig. 5.11); we shall presently see (Fig. 5.12) that this is a result of sustained northwesterly environmental winds equatorward, and southeasterly environmental winds poleward of the hurricane. The developing hurricane further contains a deep low level inflow, with the remnants of the secondary maximum near 400 mb which were noted in the pre-hurricane phase. An extensive upper tropospheric outflow is also present, with a maximum between $2-6^{\circ}$ latitude radius and a constant radial wind from $6-14^{\circ}$. This outflow is associated with an increasing anticyclonic circulation with radius and is overlain by a lower stratospheric inflow.

By comparison, the decaying hurricane in Figs. 5.10 and 5.11 has a stronger upper level anticyclone, a weaker low level cyclone, and considerable vertical wind shear between 700 and 400 mb. The radial flow is also quite different: the stratospheric inflow has ceased inside 6° latitude radius; the upper troposphere outflow and lower tropospheric inflow are weaker and cease at $12-14^{\circ}$ latitude radius; and a distinct outflow has developed near 600 mb, though a residual inflow remains near 400 mb.

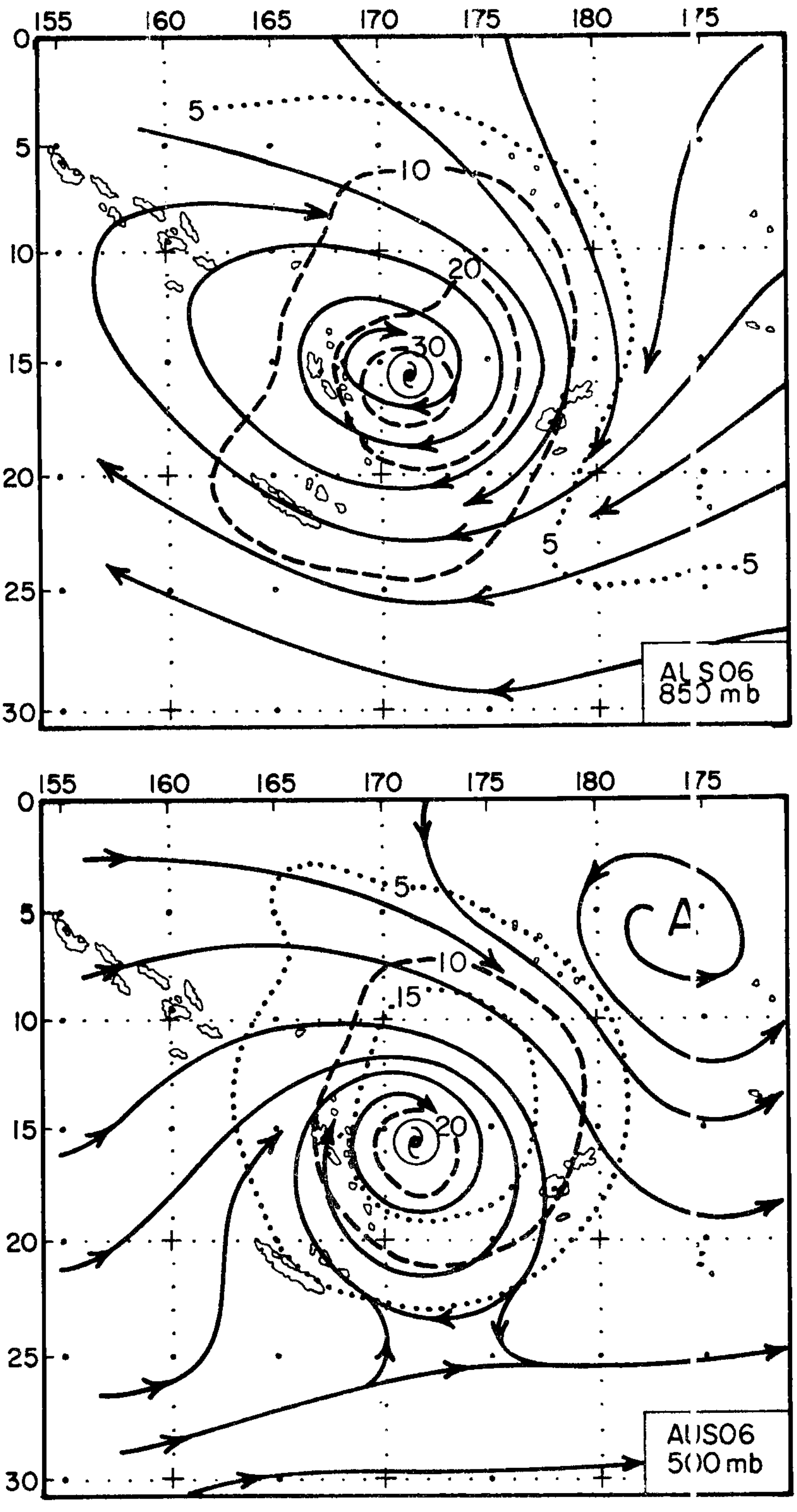

Fig. 5.12a. Plan view streamline/isotach (m s^{-1}) fie.ds for the Developing Oceanic Hurricane at 850 and 500 mb.

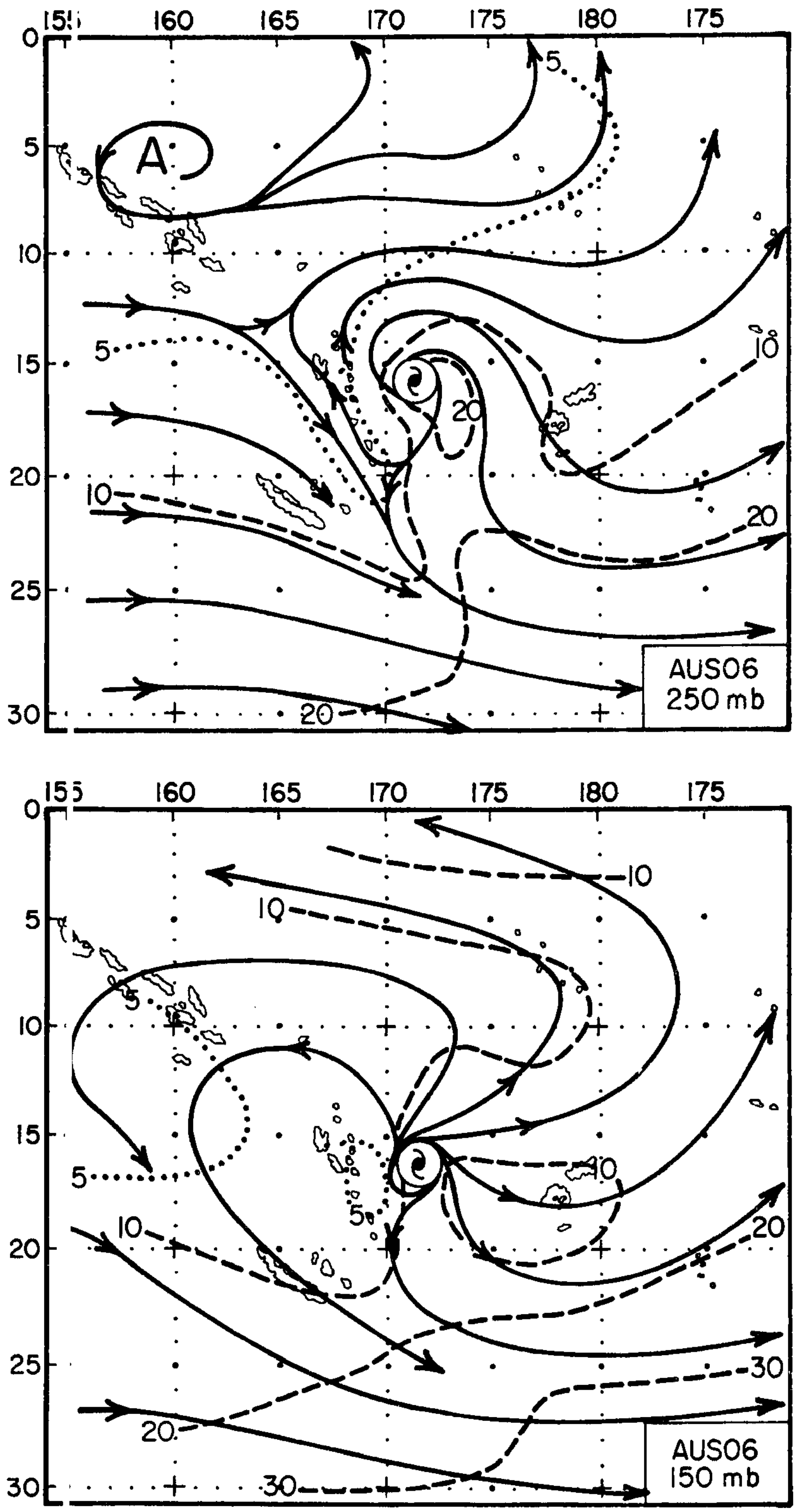

Fig. 5.12b. Plan view streamline/isotach (m s^{-1}) fields for the Developing Oceanic Hurricane at 250 and 150 mb.

The plan view wind fields for the Developing Oceanic Hurricane, contained in Fig. 5.12, show a stronger, but otherwise similar structure to the tropical storm phase in Fig. 4.8. In the low to mid-levels the composite hurricane has a large extent and is nearly symmetric. The strong, deep tropical inflow jet is still being maintained and the beta effect distortion is clearly evident at 850 mb. At 250 mb, the upstream trough now extends equatorward of the hurricane, but the confluence zone between the subtropical westerlies and the hurricane outflow has remained some 6^{o} latitude from the center. The subtropical outflow jet has also strengthened considerably with average radial winds exceeding 15 m s^{-1}.

The westerly winds have less effect at the 150 mb level. There is, however, still evidence of the strong outflow jet to the southeast. As with the tropical storm phase, this jet is complemented by a second equatorward jet to the northeast.

The streamline/isotach fields for the decaying hurricane are shown in Fig. 5.13. By comparison to the developing stage the 850 mb circulation is less extensive and weaker, and the deep tropical inflow has ceased. Indeed, the 500 mb flow contains a distinct subtropical inflow, and has become considerably distorted. The upper level westerlies now extend well over the hurricane with only the remnants of an outflow regime at either 250 or 150 mb. While the southeastward outflow jet is still weakly present, its equatorward counterpart at 150 mb has largely ceased. In these regards the Decaying Oceanic Hurricane is quite similar to the Non-developing Tropical Storm in Fig. 4.10.

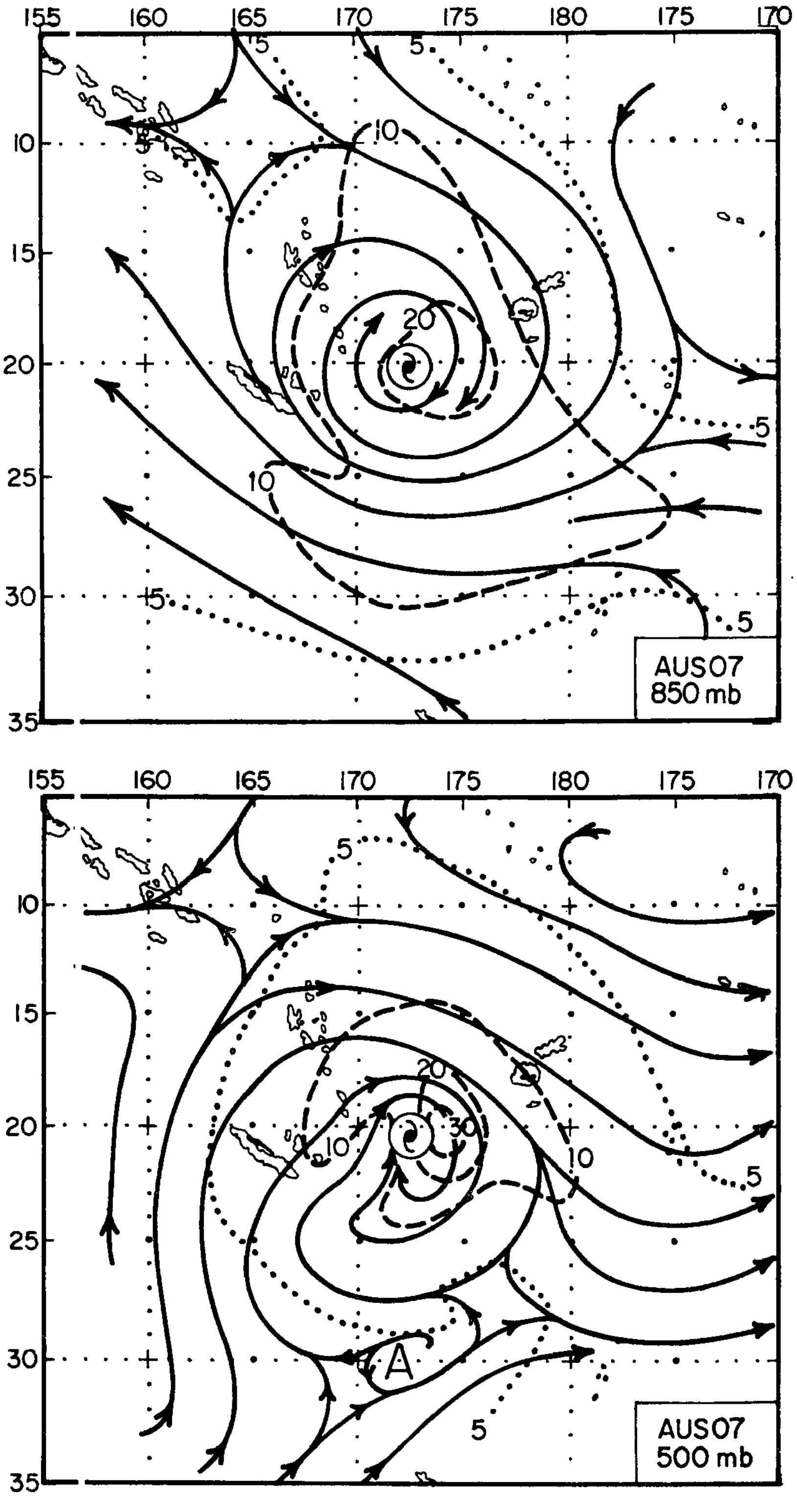

Fig. 5.13a. Plan view streamline/isotach (m s^{-1}) fields for the Decaying Oceanic Hurricane at 850 and 500 mb.

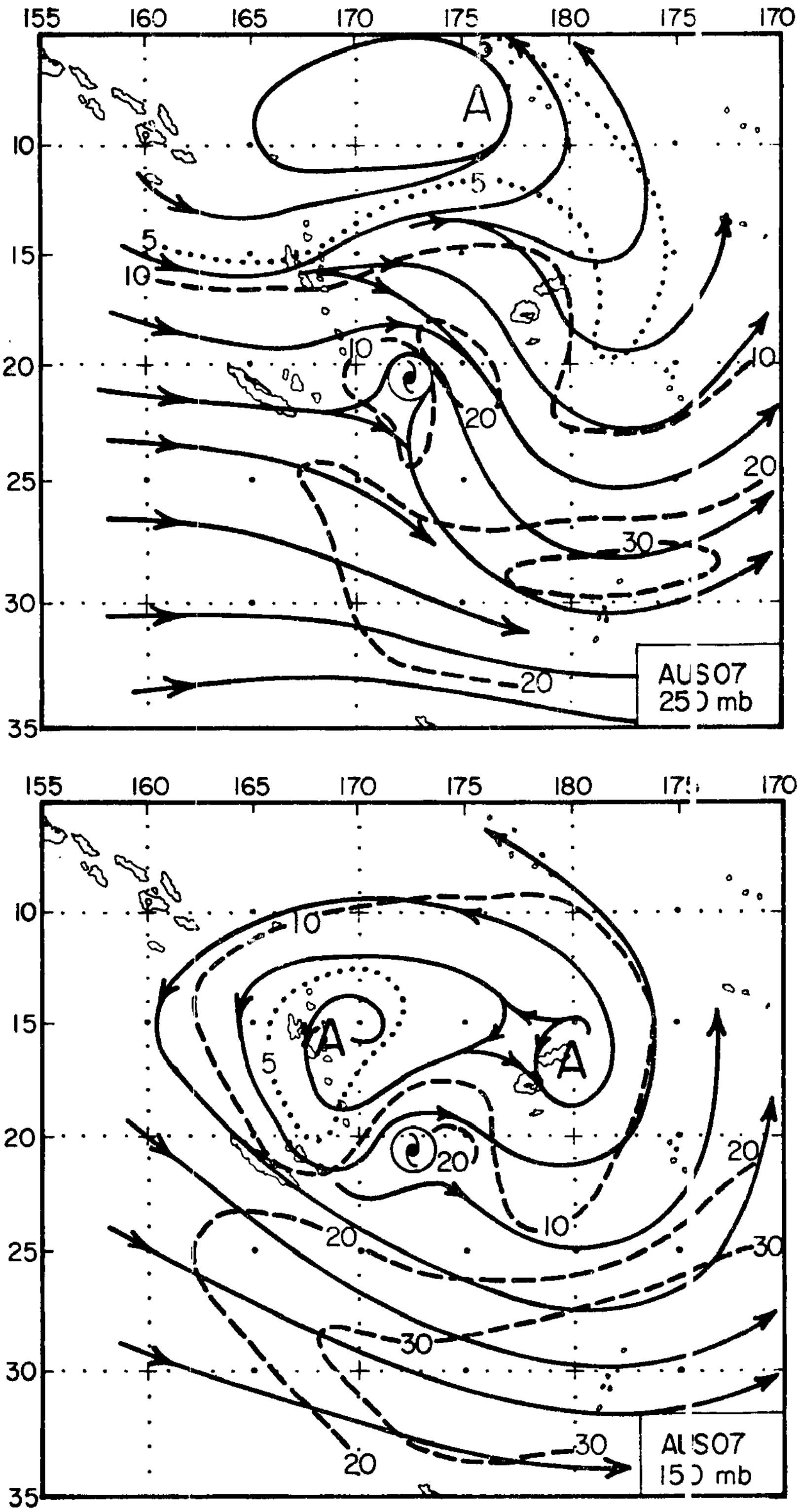

Fig. 5.13b. Plan view streamline/isotach (m s^{-1}) fields for the Decaying Oceanic Hurricane at 250 and 150 mb.

5.3.2 Thermal Structure

The axisymmetric cross-sections of temperature anomalies in the developing and decaying hurricanes are shown in Fig. 5.14. The well documented mid to upper tropospheric warm core (e.g., Shea and Gray, 1973; Hawkins and Rubsam, 1968; Frank, 1977a) may be clearly seen. In the developing hurricane the warm anomaly is quite strong and concentrated near 300 mb (the actual maximum anomaly in the eye cannot possibly be resolved by our larger scale compositing procedure). In the decaying hurricane the warm core is weaker and vertically more diffuse. These observations are consistent with our vertical wind shear observations in Fig. 5.10. Though not completely shown due to lack of resolution, a cold band of up to $5^{\circ}C$ is also present in the lower stratosphere, surrounding an apparently warmer center. In the developing phase this band extends from $1-3^{\circ}$ latitude radius; in the decaying phase it is further from the center and covers $3-5^{\circ}$ latitude radius. Frank (1977a) also observed a stratospheric cooling over the typhoon, but this extended over the core region. Even though there are only a few observations, the lower stratosphere of both phases of the southwest Pacific hurricane is warmer in the core region than at $2-6^{\circ}$ latitude radius. We also note that the cool bands in Fig. 5.14 correspond closely to the outflow maxima in Fig. 5.11, which must be associated with sustained vertical motion. These observations support the speculation by Frank (1977a) that the lower stratospheric cooling results from overshooting cumulonimbus clouds.

A notable feature is the lower level cool band at 2° latitude radius in the developing phase and at 3° latitude radius in the decaying

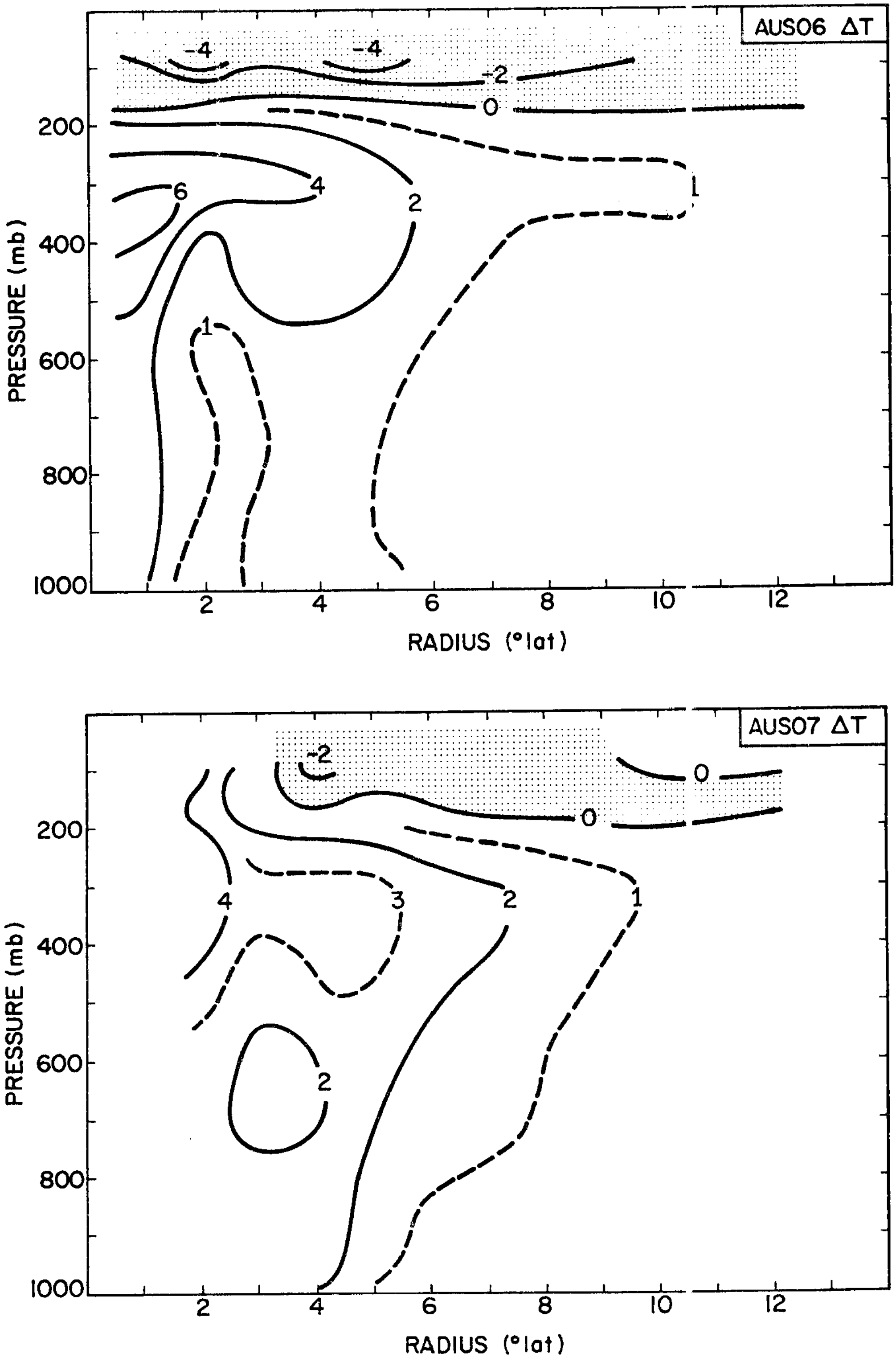

Fig. 5.14. Axisymmetric cross-section of temperature anomaly (°C) (taken as the difference from the 14° latitude radius value at the same level) for the Developing (AUS06) and the Decaying (AUS07) Oceanic Hurricanes. Stippling indicates cold regions.

phase. The mixing ratio cross-sections in Fig. 5.15 indicate that these cool bands are also quite dry. They thus show distinctively in the equivalent potential temperature cross-sections of Fig. 5.16. These are an axisymmetric indication of the distinctive banded structure of all tropical storm and hurricane composites presented in this study. As we have noted in Chapter 4, and as we shall describe fully in Chapter 7, we believe that this banded structure arises from: 1) an interaction between the cyclone and earth's vorticity field; and 2) differential advection of potentially warm tropical, and cold subtropical air.

The plan view equivalent potential temperature fields for the developing hurricane are shown in Fig. 5.17. The variations in equivalent potential temperature below 500 mb are largely due to moisture variations; at 250 mb they are entirely due to temperature variations. We can see that a deep tongue of warm, moist tropical air occurs on the northeast side. As with the Pre-hurricane Tropical Storm, this tropical air extends around and to the poleward side of the hurricane core. Cool, dry subtropical air is starting to flow equatorwards at large radii to the west of the hurricane; and a distinct low level dry slot, corresponding to that in the axisymmetric cross-section of Fig. 5.14, extends from west through north and east of the core region.

Notice also the rapid fall in equivalent potential temperature to the southwest of the core at both 500 and 250 mb. This gradient lies along the confluence zone between the potentially warm hurricane outflow and cool upper level environmental westerlies (Fig. 5.12). Unlike the pre-hurricane phase in Fig. 4.12, there is no evidence of strong upper level subsidence along this confluence zone. This agrees with the

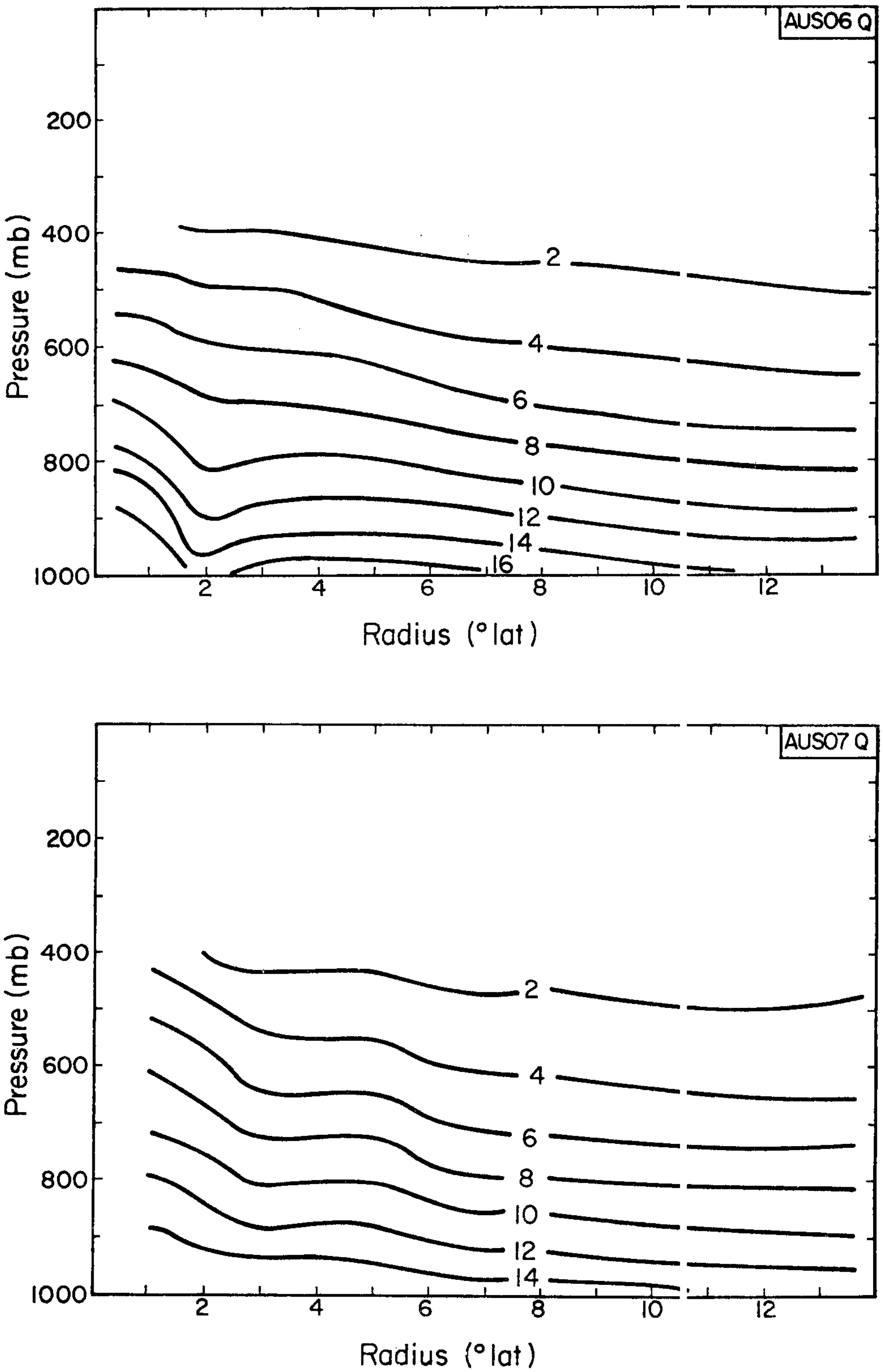

Fig. 5.15. Axisymmetric cross-section of moisture m xing ratio (g/kg) for the Developing (AUS06) and the Decay ng (AUS07) Oceanic Hurricane.

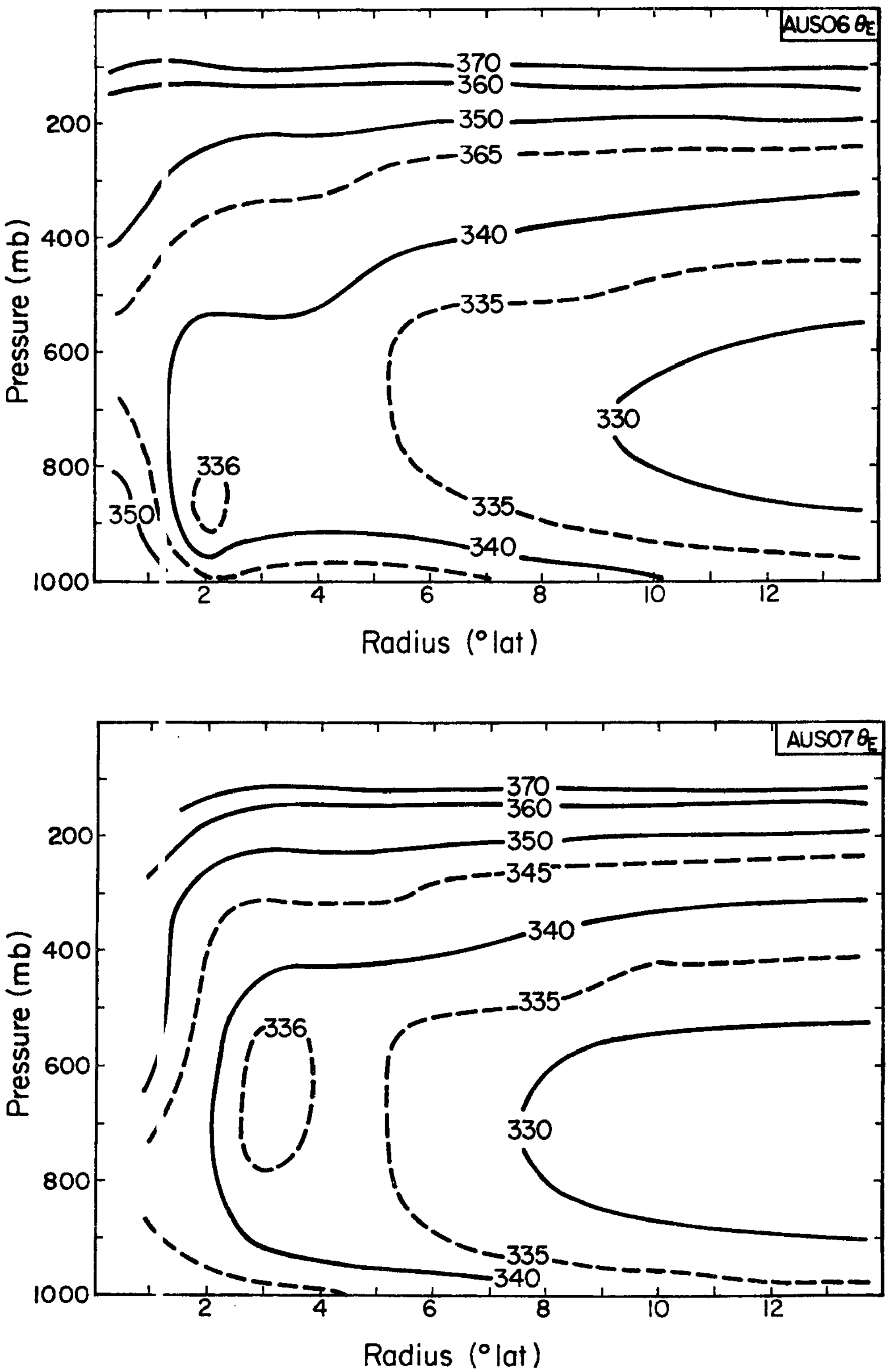

Fig. 5.16. Axisymmetric cross-section of equivalent potential temperature (K) for the Developing (AUS06) and the Decaying (AUS07) Oceanic Hurricane. Dashed lines denote intermediate isotherms used to provide detail.

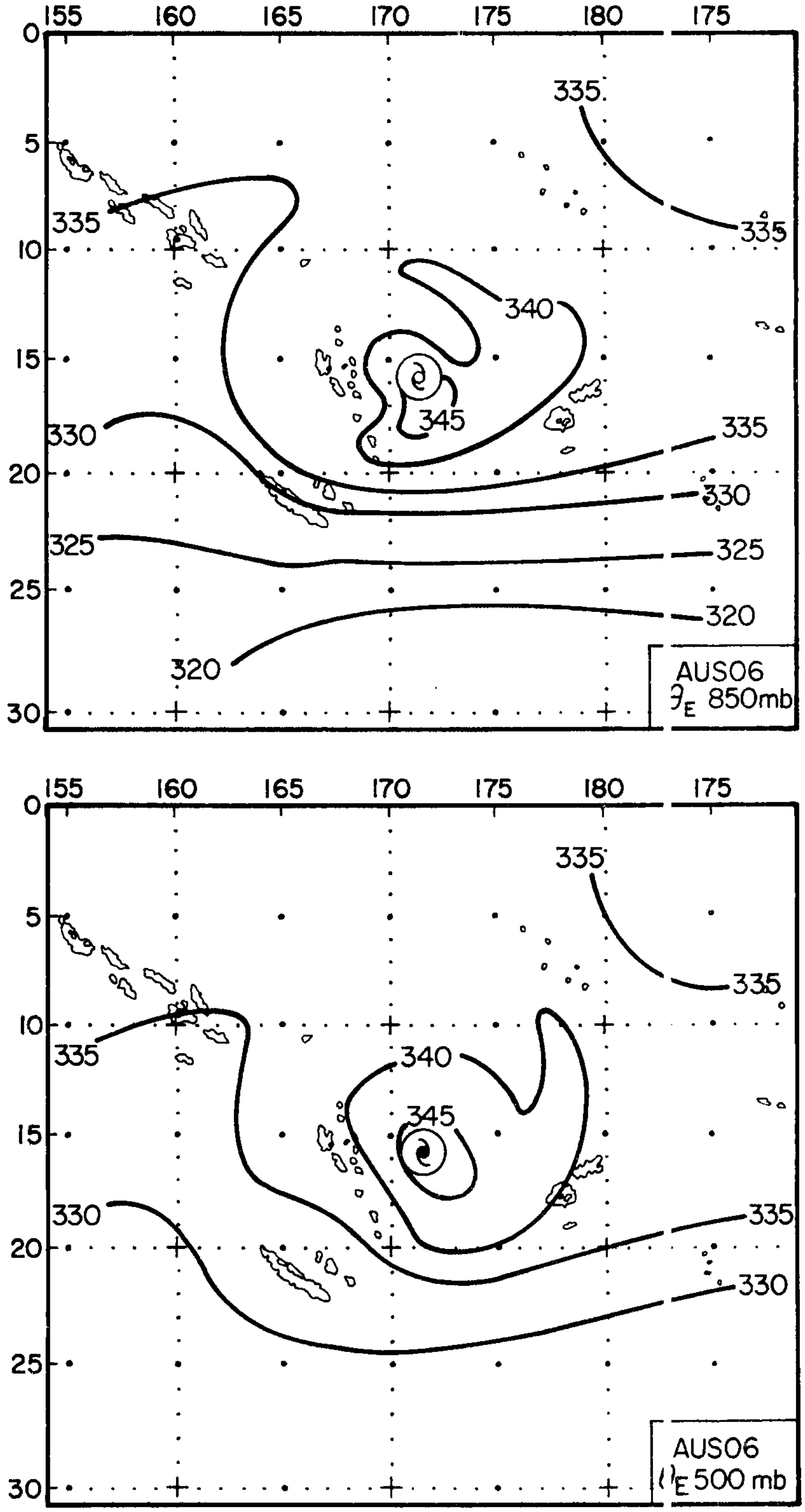

Fig. 5.17a. Plan view equivalent potential temperature (K) fields for the Developing Oceanic Hurricane at 850 and 500 mb.

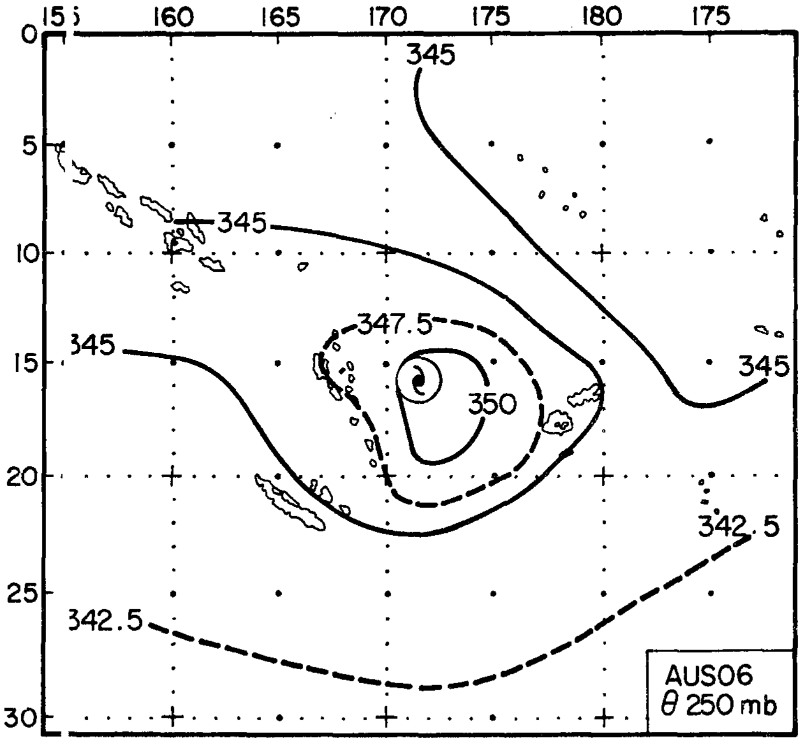

Fig. 5.17b. Plan view equivalent potential temperature (K) field for the Developing Oceanic Hurricane at 250 mb.

qualitative wind field observations in Fig. 5.12b that there is also much weaker confluence, and less concentrated upper level convergence in this region. However, the continued presence of a dry slot in the 500 mb moisture field of Fig. 5.18 indicates that some middle level subsidence is being maintained in this confluence region.

The higher latitude, subtropical effects on the thermal structure of the decaying hurricane are clearly shown in Fig. 5.19. Only a residual of the warm moist tropical tongue (Fig. 5.17a) remains to the northeast. This tongue is cut off from the core and no longer wraps around the poleward side. Rather, a strong equivalent potential temperature gradient has developed to the southeast as the hurricane comes under the influence of the westerly subtropical airstream.

Note, however, that the impinging westerly airstream has a less adverse affect on the stronger hurricane circulation than was evident in

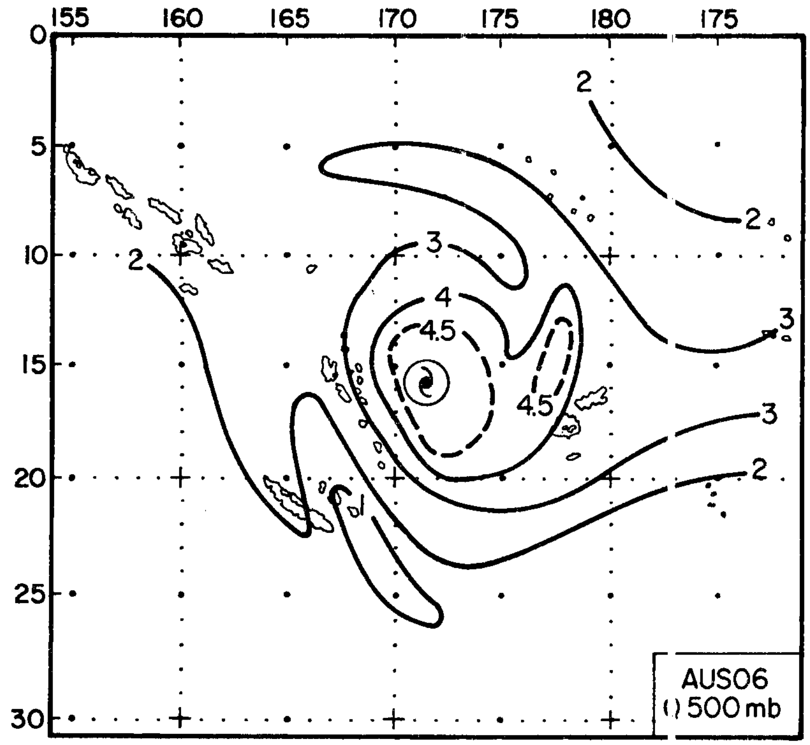

Fig. 5.18. Plan view moisture mixing ratio (g/kg) f.eld at 500 mb in the Developing Oceanic Hurricane.

the Non-developing Tropical Storm (Figs. 4.13 and 4.:4). We shall summarize these effects in section 5.7.

5.4 The Continental Influence on Hurricanes off the East and West Australian Coast.

As we have seen in sections 4.1 and 5.1, many t:opical cyclones complete their entire life cycle within a few hundred kilometers of the Australian coast. They are thus affected in varying degrees by the close proximity of this large, dry landmass. In the extreme, a number of these cyclones are destroyed in their formative or intensification stages by crossing the coast. But even those which remain out to sea have a substantial proportion of their circulation over land. Australian forecasters have long been aware of the debilitating effect of dry continental air being entrained into these coastal cyclones. Further, aside from these direct influences, the continent may

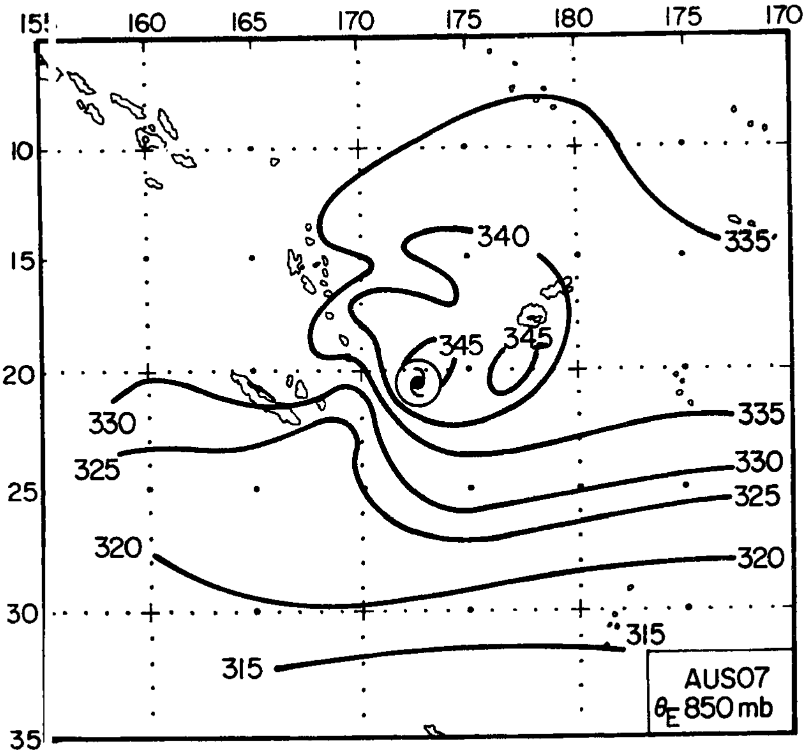

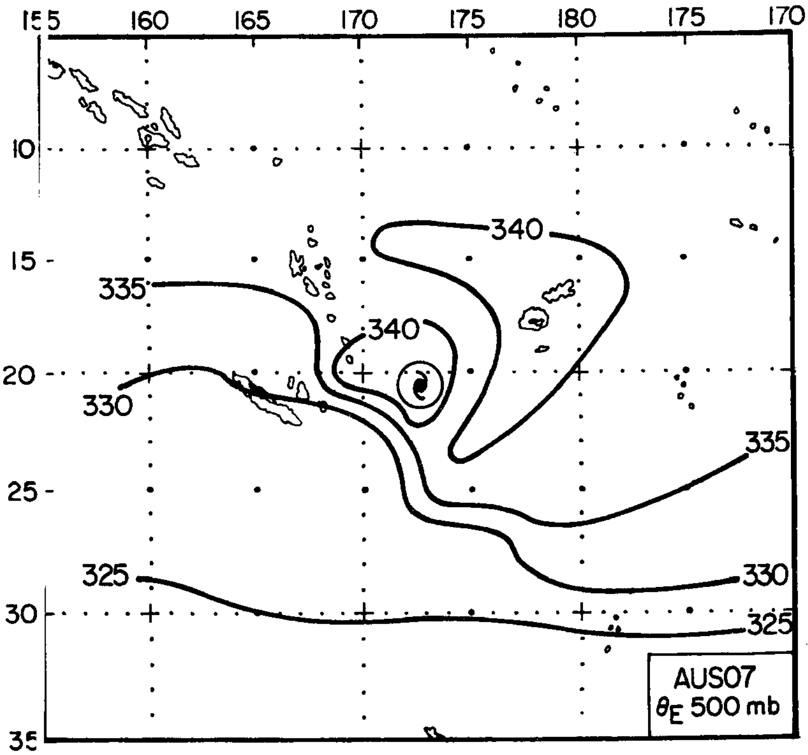

Fig. 5.19a. P:an view equivalent potential temperature (K) fields for tl.e Decaying Oceanic Hurricane at 850 and 500 mb.

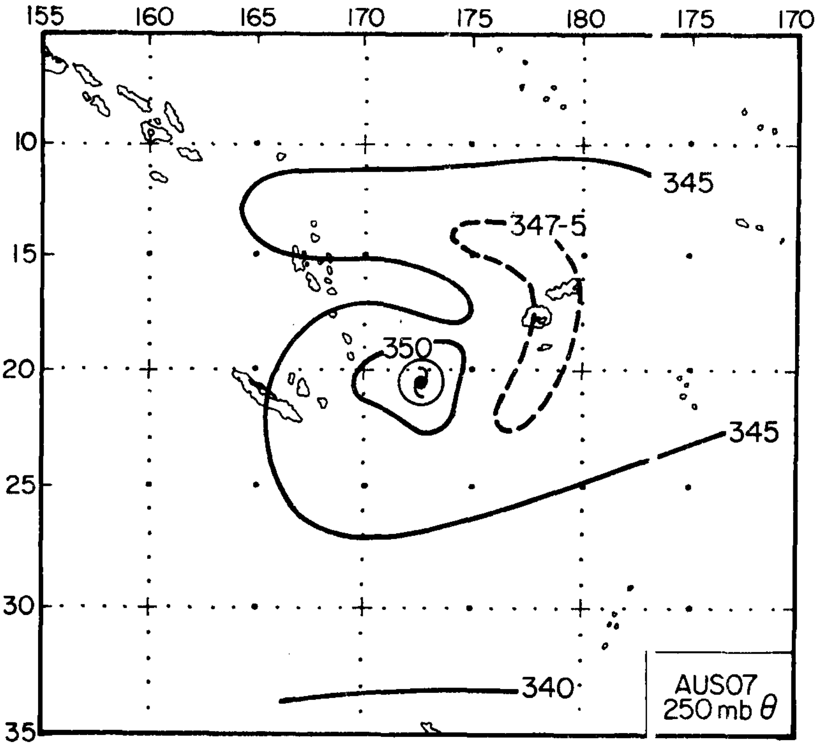

Fig. 5.19b. Plan view equivalent potential temperature (K) field for the Decaying Oceanic Hurricane at 250 mb.

indirectly affect coastal cyclones by the modifying effect that it has on the larger scale flow fields.

In this section we shall discuss some of these influences by using the AUS04 and AUS10 composites. These are described fully in Appendix 2, but briefly: AUS04, the East Coast Hurricane, contains all tropical cyclones within about 500 km of the east Australian coast between 15 and 25°S, and with central pressures less than 990 mb; AUS10, the West Coast Hurricane, contains a similar cyclone set for the west Australian coast. In order to obtain sufficient observations for a detailed analysis, both deepening and decaying phases were included. However, the regional peculiarities resulted in the East Coast Hurricane being, on average, decaying, while the West Coast Hurricane is deepening.

5.4.1 The East Coast Hurricane

The 850 mb and 500 mb moisture fields for the East Coast Hurricane are shown in Fig. 5.20, together with the 850, 500, 250, 150 mb wind fields in Fig. 5.21. At 850 mb the monsoonal trough extends west/northwest across Cape York Peninsula and a strong jet in the monsoonal westerlies provides the major influx of mass and moisture into the hurricane. The characteristic beta effect distortion and elongation to the west, which we noted in our discussion of the oceanic cyclones, appears to be modified by the Great Dividing Range. Considerable orographic funnelling of these low level winds is evident. Thus, even though a distinct moisture band extends from the monsoonal westerlies around the hurricane, the inland regions are relatively unaffected (the encircled stations are not significantly different from their January mean from Maher and Lee, 1977). Some advection of dry continental air is, however, evident from the west through north of the hurricane.

At 500 mb the coastal funnelling has disappeared. Instead, the hurricane appears to lie poleward of the subtropical ridge and is being influenced by a subtropical southwesterly flow. Thus, even though there is a deep monsoonal flow to the north, very dry continental air is being advected into the cyclone and is tending to cut off the tropical moisture supply. The poleward extent of tropical air around the hurricane, and the efflux of dry air from the continent, may be seen more clearly in the moisture cross-section of Fig. 5.22. This cross-section extends northwest and due south of the cyclone and approximately parallels the coastline. We see that moist tropical air extends

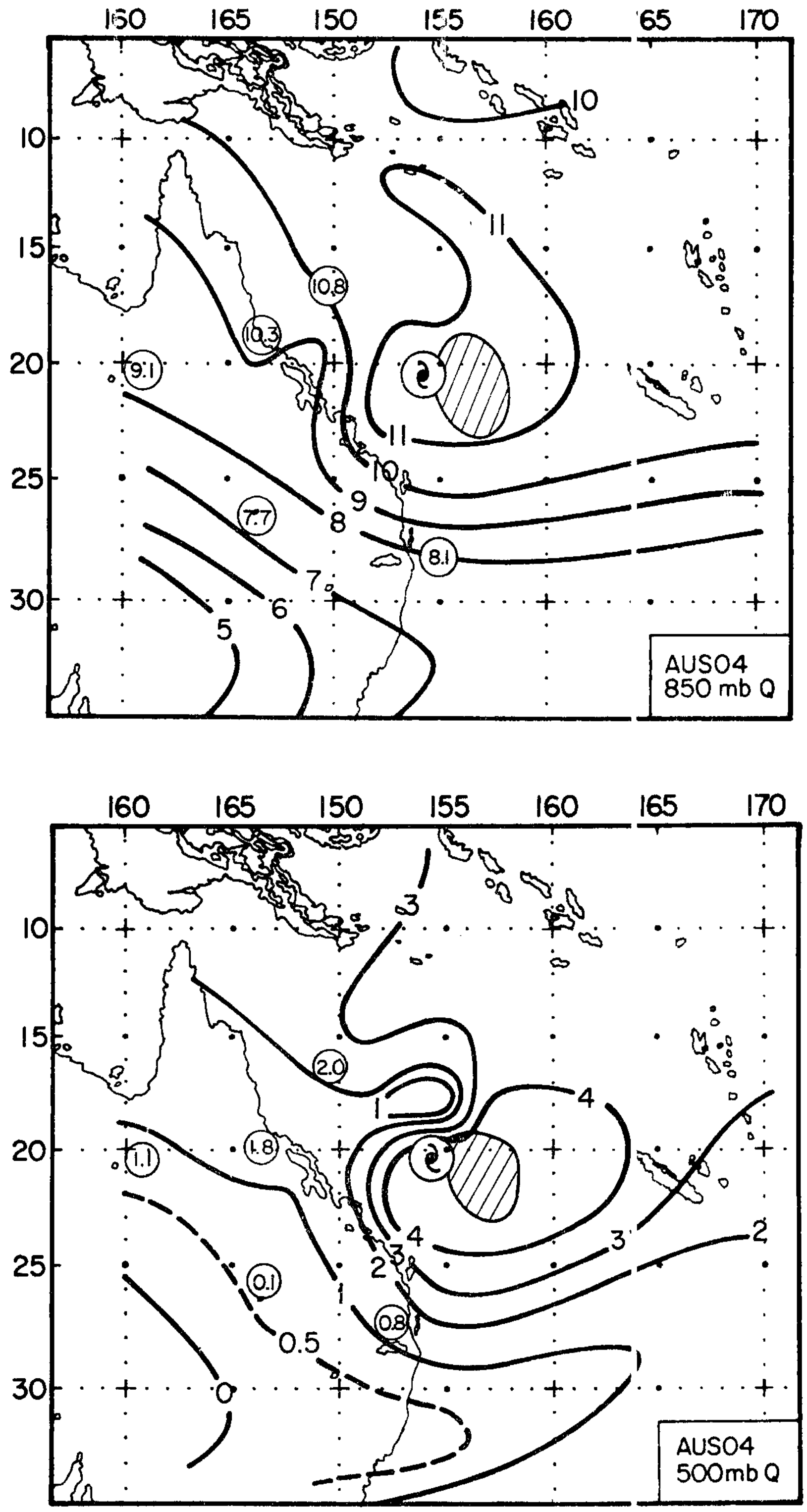

Fig. 5.20. Plan view moisture mixing ratio (g/kg) fields for the East Coast Hurricane at 850 and 500 mb. Also shown in circles are mean January mixing ratios for a selection of stations from Maher and Lee (1977). No data were available for the hatched regions.

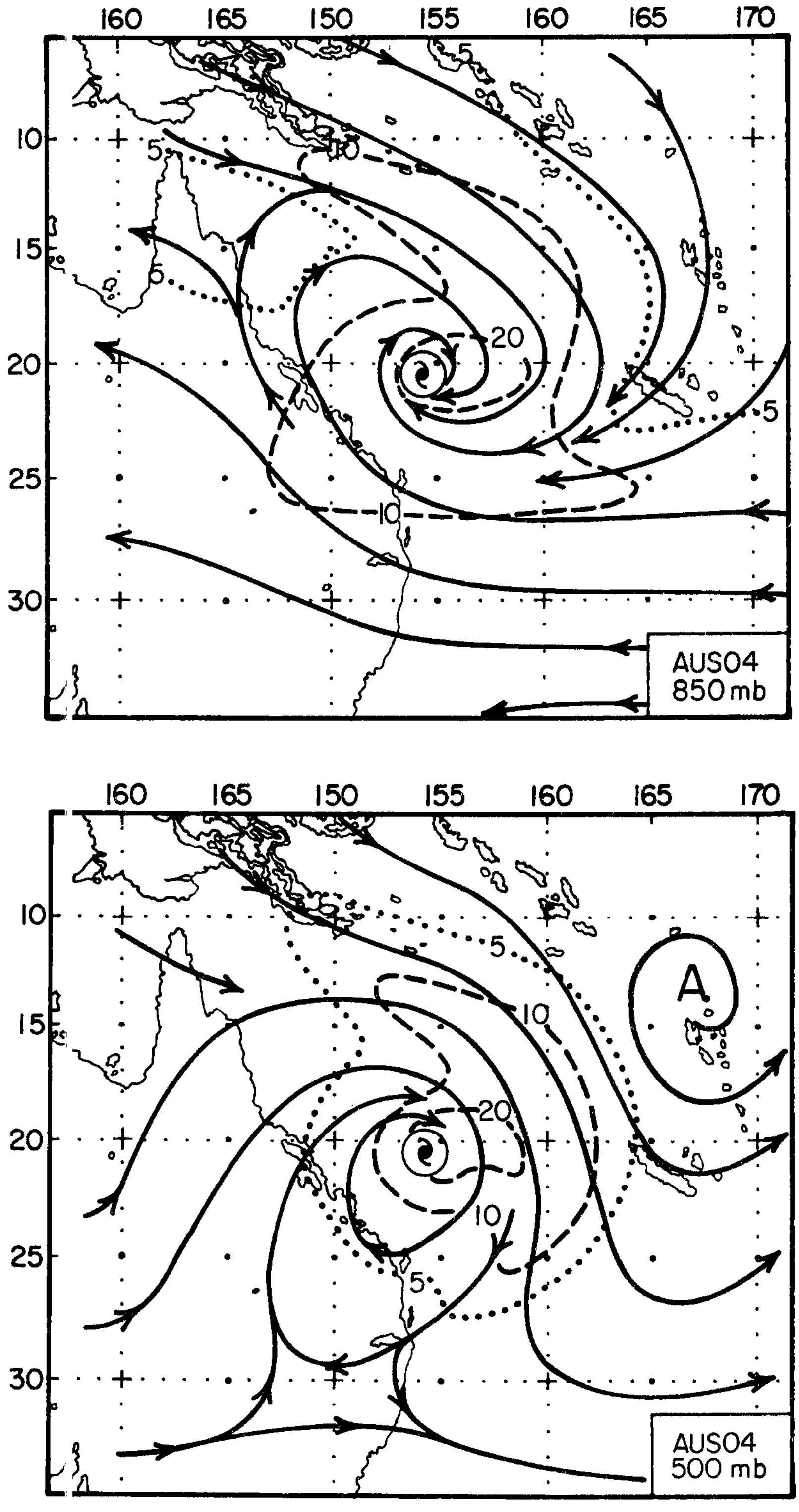

Fig. 5.21a. Plan view streamline/isotach (m s^{-1}) fields for the East Coast Hurricane at 850 and 500 mb.

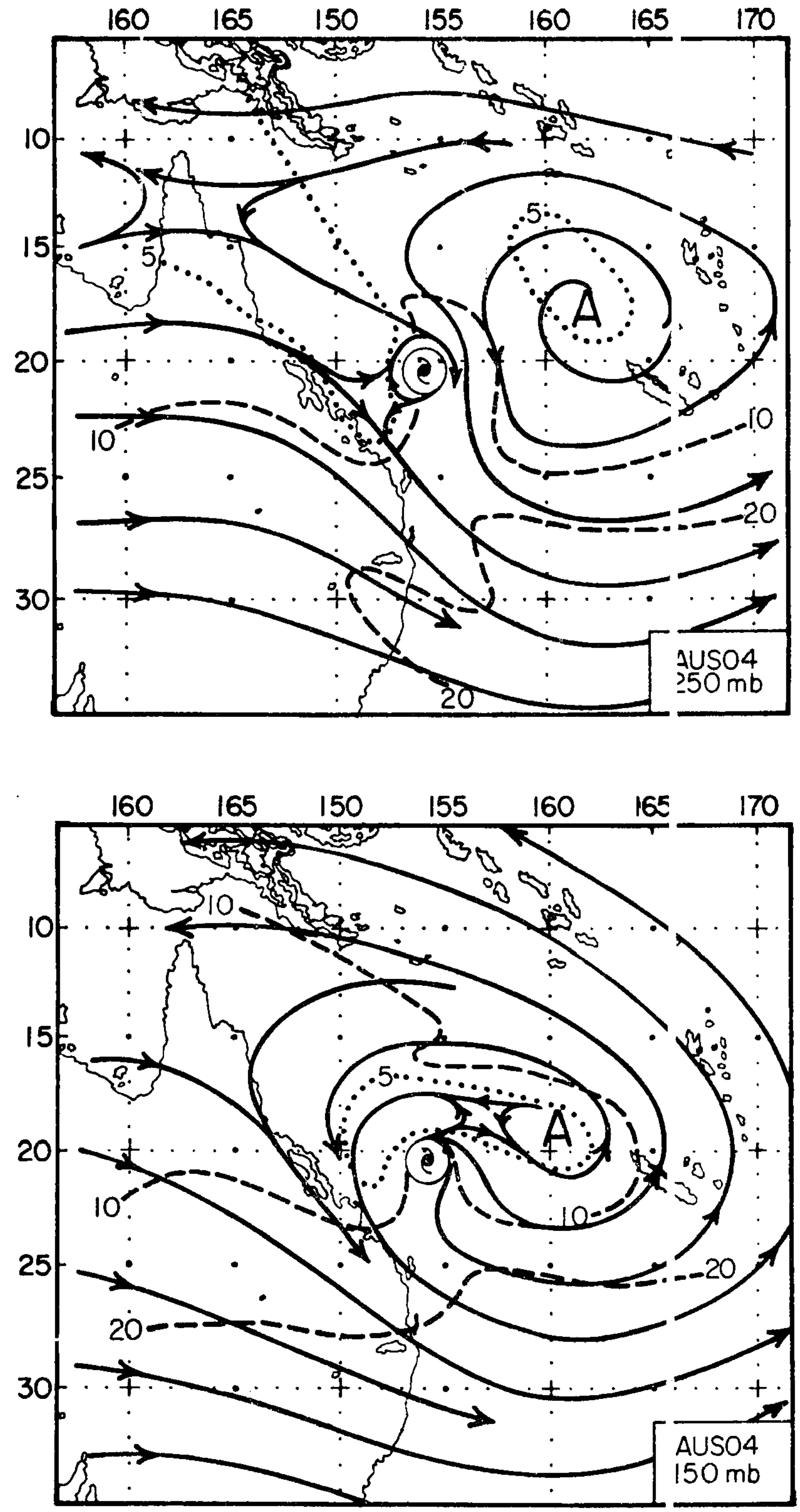

Fig. 5.21b. Plan view streamline/isotach (m s^{-1}) fi ılds for the East Coast Hurricane at 250 and 150 mb.

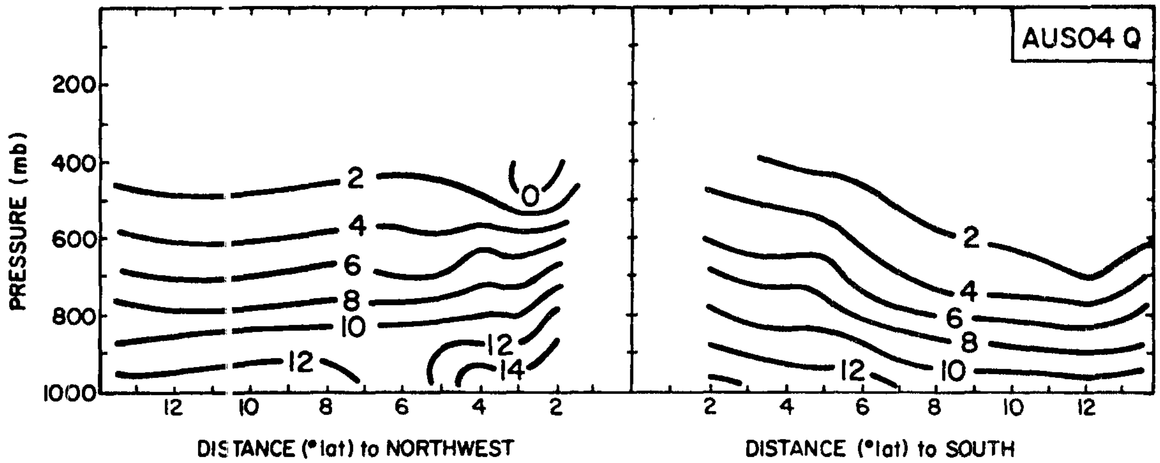

Fig. 5.22. Vertical moisture mixing ratio (g/kg) cross-section through the East Coast Hurricane and approximately parallel to the Australian coastline.

polewards some 700 km at the surface and slightly less at higher levels. The low level coastal funnelling also prevents the dryer continental air below 850 mb from moving over the ocean within 600 km to the northwest. But this effect is lost above 800 mb, and dry air penetrates close to the center under the influence of the impinging subtropical westerlies.

The associated characteristic convective signature for East Coast Hurricanes is illustrated by two infamous hurricanes, Ada (1970) and Althea (1971) in Fig. 5.23. Note: 1) the large convective region to the south and southeast which ends along the coast and is curved anticyclonically by the interaction with the upper level westerlies (c.f. the 250 mb level in Fig. 5.21); 2) the dry slot around the northern perimeter of the cloud masses; and 3) the convective band lying along the approximate position of the low level monsoonal jet and moist band in Figs. 5.20 and 5.21. It is also now evident that the large 500 mb moist region encompassed by the 4 g/kg isohyet in Fig. 5.20 arises more from in situ convective activity than from horizontal advection.

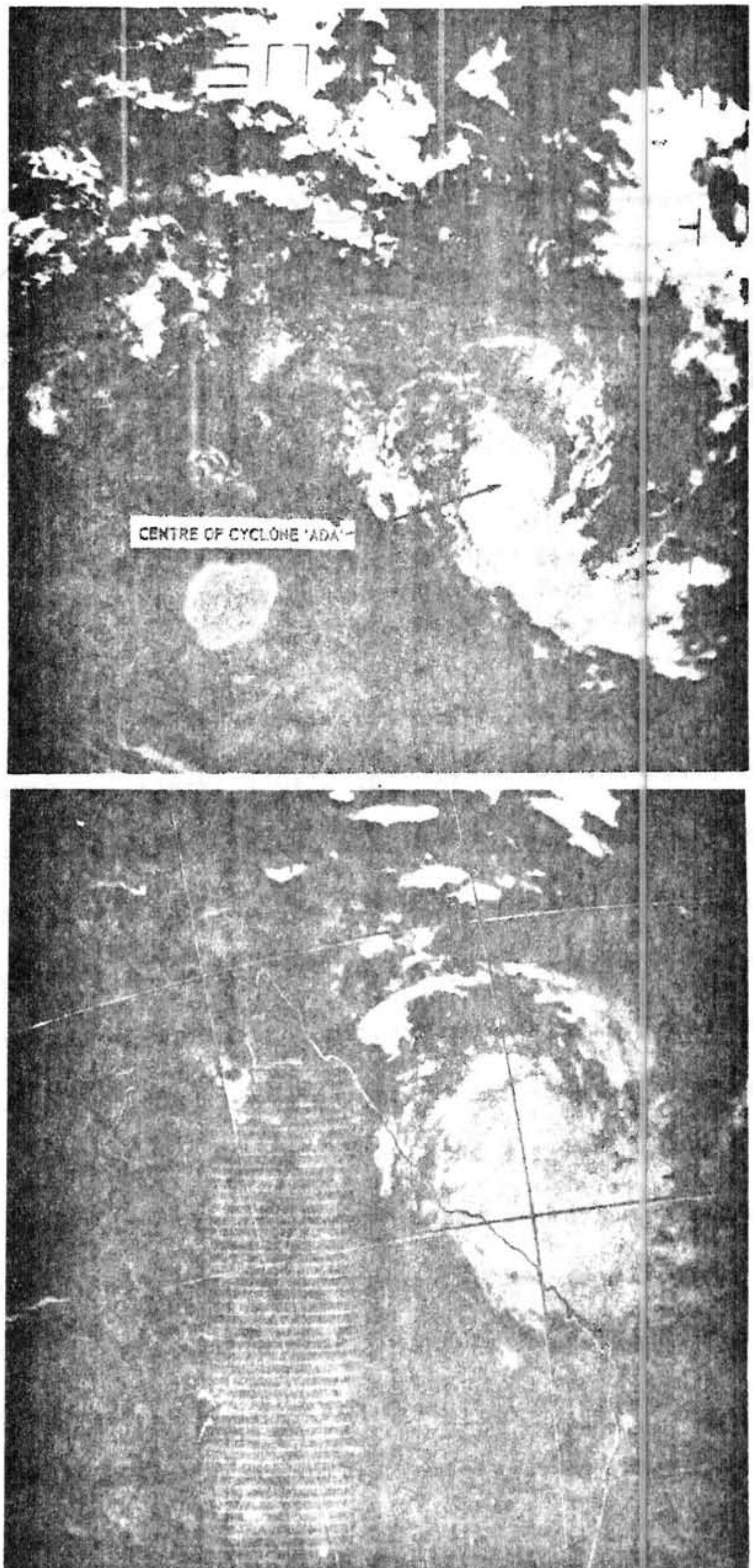

Fig. 5.23. ESSA 8 visible satellite imagery of hurricanes Ada (from Director of Meteorology, 1970) and Althea (from Director of Meteorology, 1972) off the east Australian coast.

There is, however, some advection of moisture out of this region over the continent.

The flow fields at 250 and 150 mb (Fig. 5.21) and the upper level thermal fields (not shown) are not directly influenced by the Australian continent. They, and the lower level fields, are, however, under a considerable indirect influence. As we have briefly discussed in Chapter 1, the poleward extension of the monsoonal trough and convective activity over northern Australia produces a concomitant poleward extension of the upper tropospheric subtropical ridge. A downstream trough then forms over the Coral Sea region (Fig. 1.4), with subtropical westerlies extending to very low latitudes. Holland and Pan (1981) have shown, using a series of monthly mean charts, that this Coral Sea trough extends downward to the 500 mb level. Below this level a sharp poleward shift of the subtropical ridge was observed with trade wind easterlies over the southern Coral Sea (Fig. 1.3). Thus, the generally destructive effect of the upper level subtropical westerlies, shown in Figs. 5.20 to 5.23 may be attributed to an indirect continental influence.

5.4.2 The West Coast Hurricane

The 850 mb and 500 mb moisture fields for the West Coast Hurricane are shown in Fig. 5.24 together with the 850, 500, 250 and 150 mb flow fields in Fig. 5.25. At 850 mb the monsoonal trough extends northeastward over northern Australia. The now familiar jet from the monsoonal westerlies extends into the hurricane and there appears to be a secondary monsoonal surge equatorward of the Indonesian Islands (though this feature could be a result of data bias). Extensive trade wind easterlies lie poleward of the hurricane, and the superpositioning

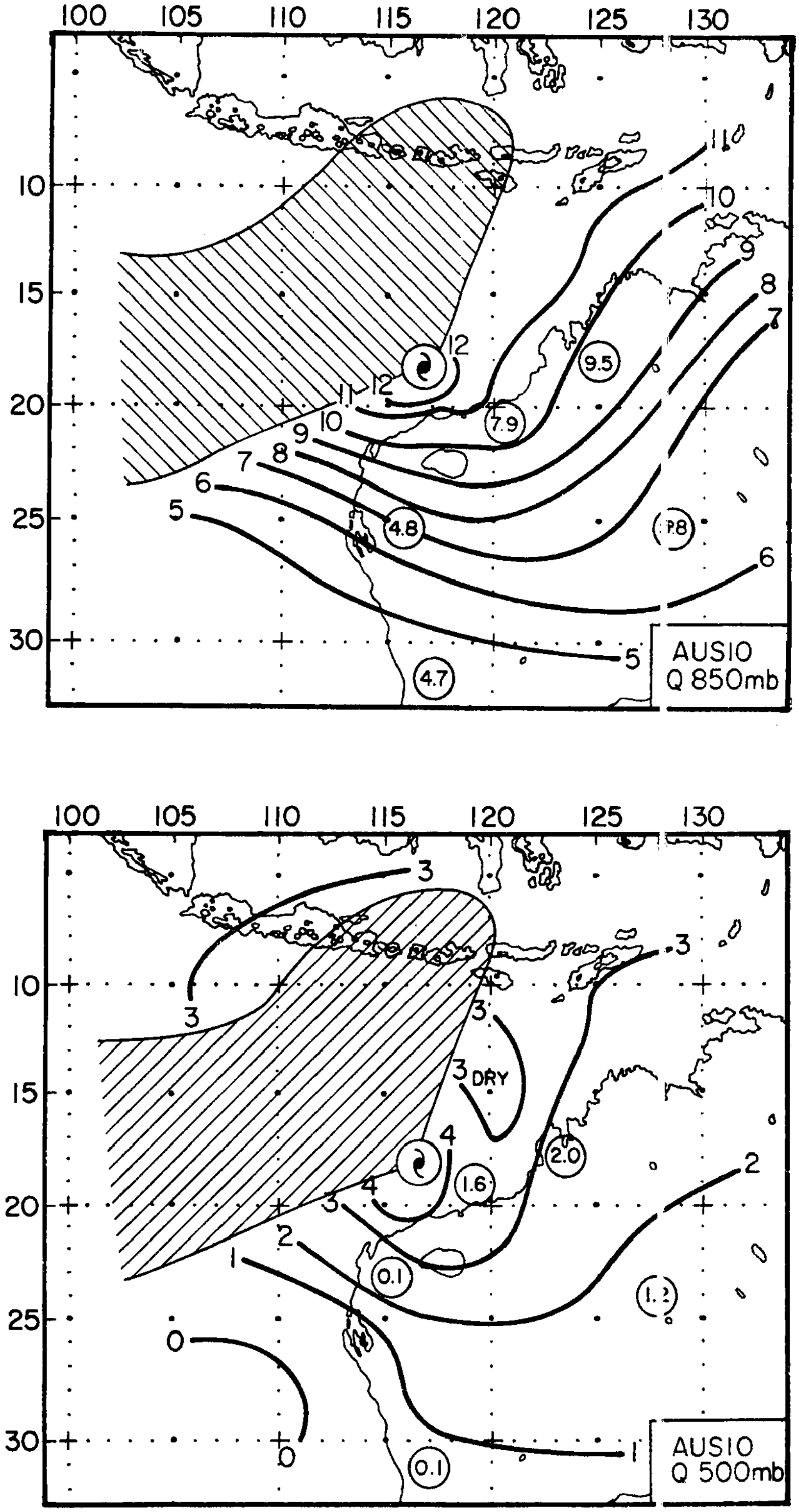

Fig. 5.24. Plan view moisture mixing ratio (g/kg) fields for the West Coast Hurricane at 850 and 500 mb. Also shown in circles are mean January mixing ratios for a selection of stations from Maher and Lee (1977). No data were available for the hatched region.

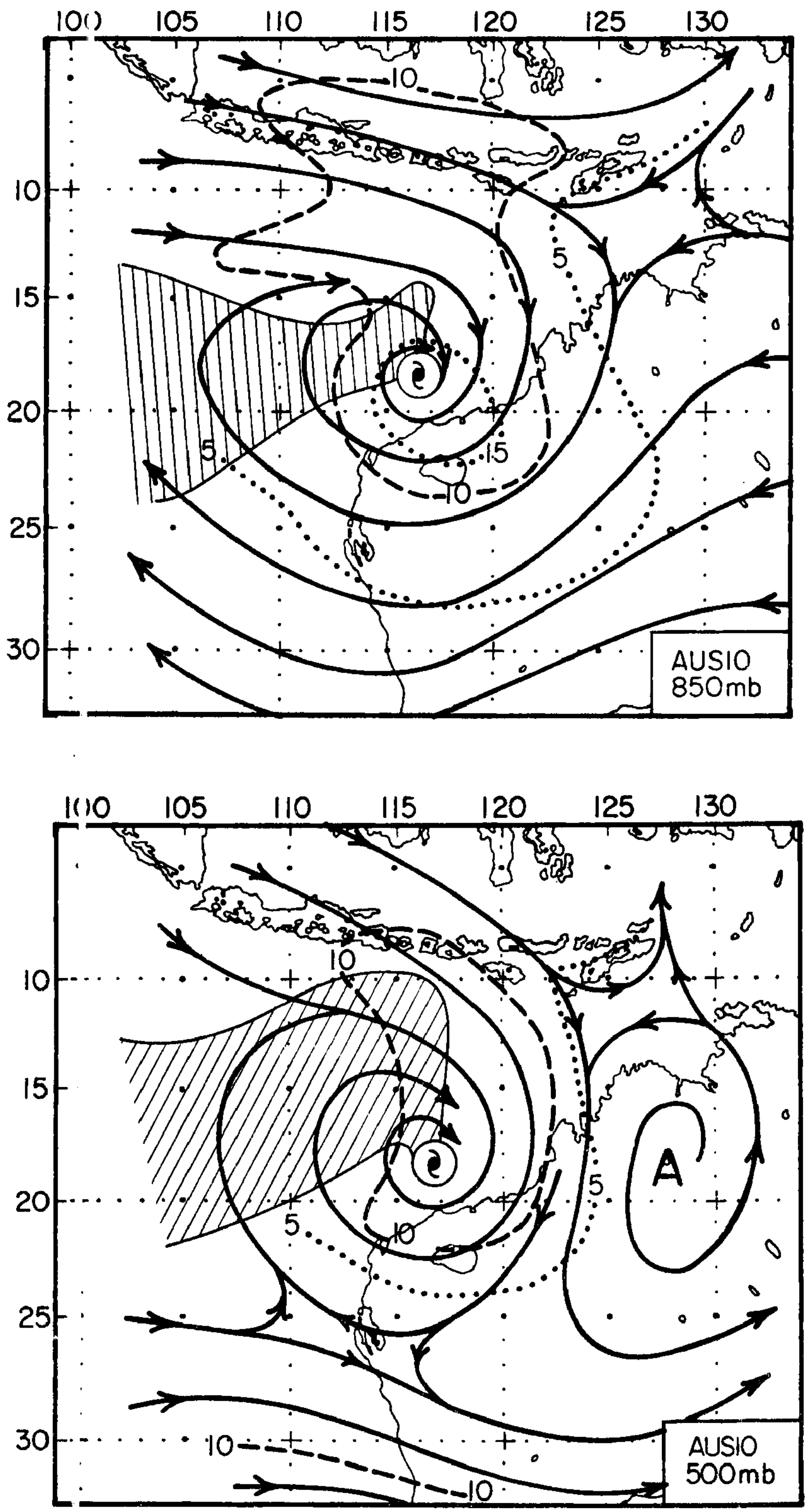

Fig. 5.25a. Plan view streamline/isotach (m s^{-1}) fields for the West Coast Hurricane at 850 and 500 mb. No data were available for the hatched regions.

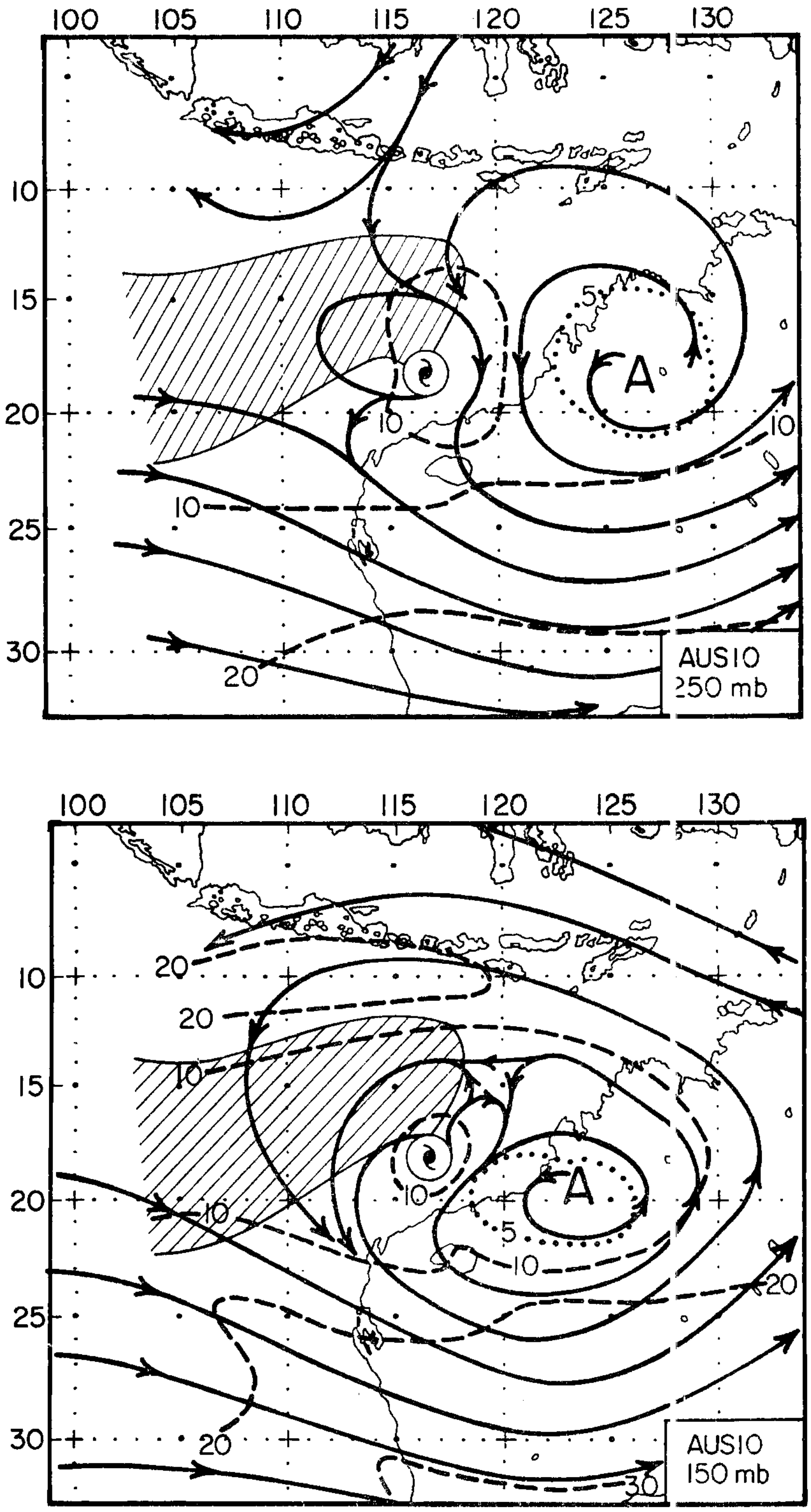

Fig. 5.25b. Plan view streamline/isotach (m s^{-1}) fields for the West Coast Hurricane at 250 and 150 mb. No data were available for the hatched regions.

of the Western Australian Coastal Trough (Fig. 1.3) and the cyclone circulation is clearly evident at 850 mb. Unfortunately, we have no thermal data, and very little wind data, to the west and northwest of the hurricane. However, to the east and southeast the hurricane circulation is advecting a considerable amount of tropical moisture over the normally dry northwestern deserts. This is in direct contrast to the East Coast Hurricane where orographic funnelling prevented an inland penetration of tropical air. This flux of moisture around the eastern side also protects the hurricane from incursions of dry continental air. Instead, mixing between the continental and maritime air produces a strong moisture gradient to the south. Any continental air reaching the core region will have been considerably modified by a long trajectory over warm tropical oceans.

A similar situation exists at 500 mb. This shows the depth of the monsoonal influx and the protection of the core region from dry continental air. The hurricane also lies just equatorward of the subtropical ridge at this level and is well removed from the subtropical westerlies. There is, however, evidence of the now familiar dry tongue extending around the northern perimeter; this is probably enhanced by dry continental air extending around the hurricane.

These features may be more completely seen in the moisture cross-section of Fig. 5.26 and the satellite mosaic of hurricane Joan (1975) in Fig. 5.27. The moisture cross-section runs northeast to southwest through the composite cyclone, however, it has been derived almost entirely from coastal stations and is thus representative of a mean coastal cross-section. On the poleward side, then, we see that the moist maritime air extends some 700 km near the surface and nearly 1000 km

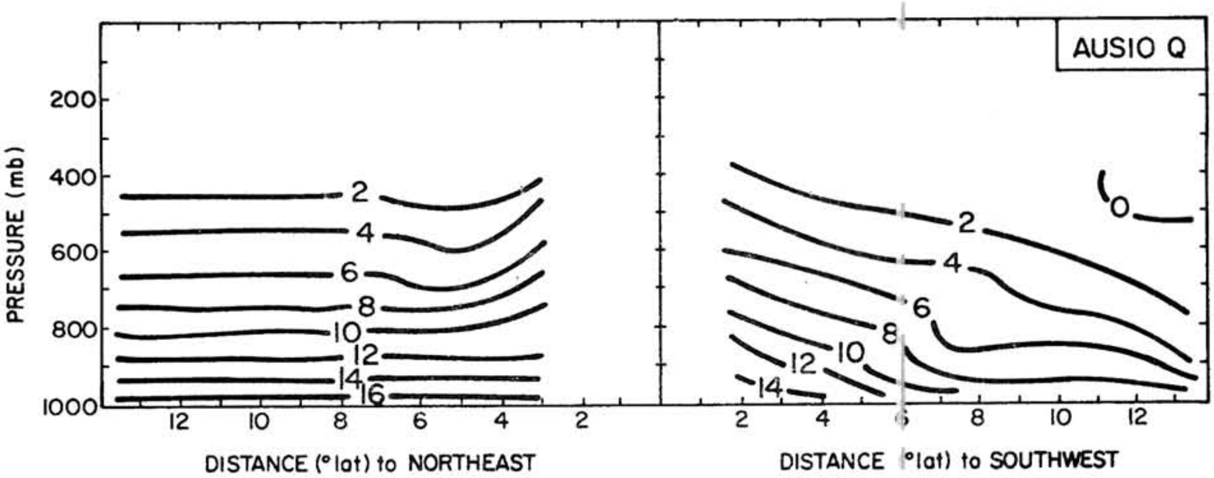

Fig. 5.26. Vertical moisture mixing ratio (g/kg) cross-section through the West Coast Hurricane and approximately along the Australian coastline.

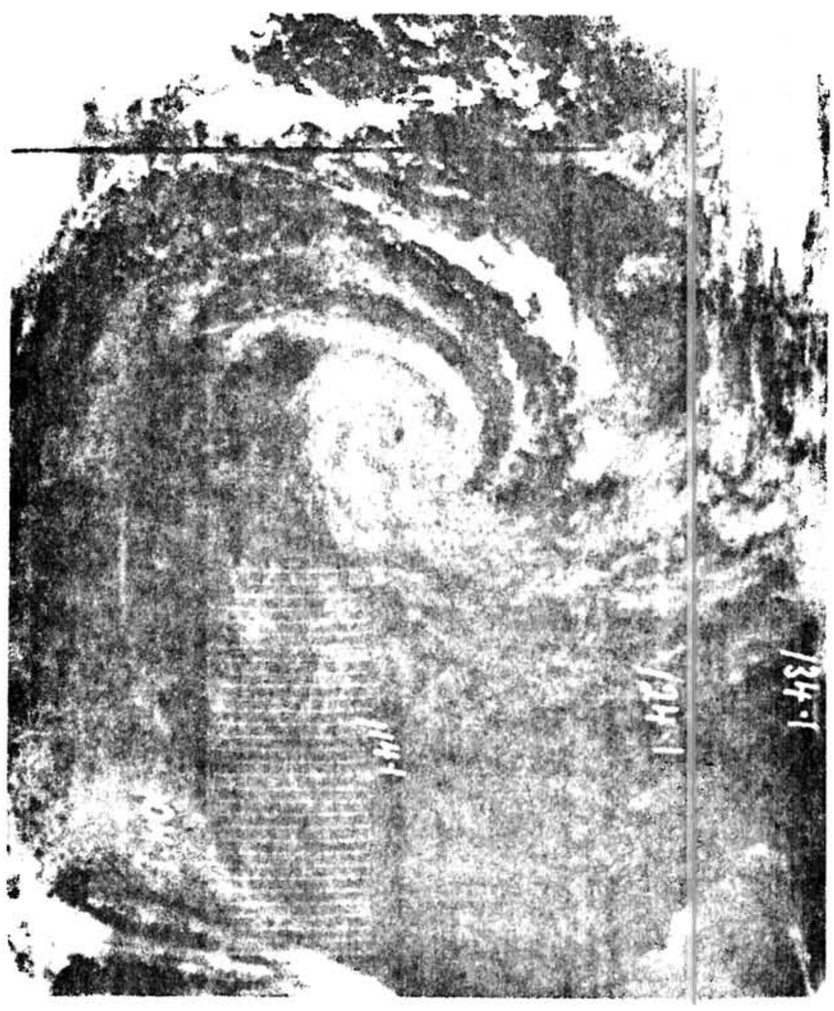

Fig. 5.27. ESSA 8 visible satellite mosaic of hurricane Joan (from Director of Meteorology, 1979) off the west Australian coast.

at higher levels. Presumably this increased extent with height is due to the stronger flux of dryer continental air in the low level trade winds. To the northeast lies an extensive region of tropical maritime air, interrupted only by the 400-600 km dry tongue above 750 mb. The cloud patterns for hurricane Joan further illustrate the flux of tropical moisture over the continent; the protected core region; the efflux of dry continental air off the southwest coast, and its advection around the western periphery of the storm; and the dry tongue to the north and northeast.

Some quite interesting examples of the continental effect on the West Coast Hurricane may be seen in Fig. 5.28. This figure gives a coastal cross-section of the temperature deviations from the Port Hedland January mean. We can see the usual mid-to upper tropospheric warm core and the lower stratospheric cold band. The weakly sloping tropopause and absence of colder subtropical air within 1200 km also confirm that the cyclone is well within the tropics. Of most interest, however, is the reversal of the normal meridional temperature gradient, and the extremely cold core (by tropical standards) below 700 mb. The advection of hot tropical continental air around the poleward side of the hurricane, with colder tropical maritime air on the equatorward side, produces an equatorward directed temperature gradient. From thermal wind considerations, this results in an easterly vertical wind shear over the hurricane (c.f., the zonal wind observations in Fig. 5.28). These easterly winds, in turn, tend to advect the hurricane towards the west. As may be seen in Fig. 5.25, the deep subtropical

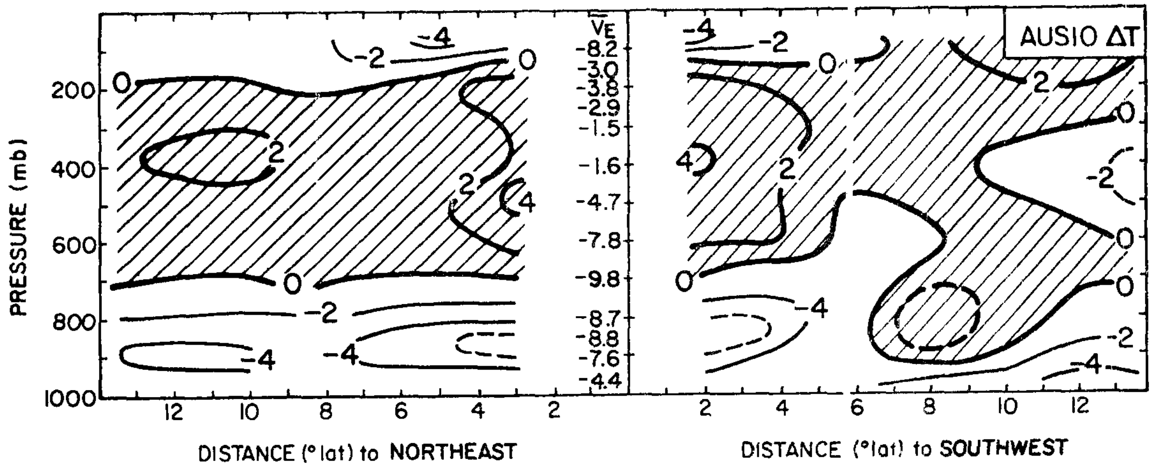

Fig. 5.28. Vertical cross-section of temperature deviations from the Port Hedland January mean (Maher and Lee, 1977) through the West Coast Hurricane and approximately parallel to the west Australian coastline. Also shown are the mean zonal wind components in the hurricane core.

ridge, which is anchored over the monsoonal trough across northern Australia (c.f., section 1.2), also protects the West Coast Hurricane from the subtropical westerlies. Thus, the Australian Continent appears to be largely responsible for the remarkably consistent southwestward trajectory, and peak occurrence frequency, of hurricanes just off the northwest coast (c.f., Figs. 5.1 and 5.5).

The poleward advection of tropical maritime air around the cyclone further produces a considerable low level cooling from the climatological norm; 900 mb temperatures within 600 km of the hurricane are 1-2 standard deviations below the January mean at Port Hedland. Combined with the hot tropical continental air at larger radii, this produces a strong cold core below 700 mb. (However, the unresolved eye region is almost certainly warm cored at these levels.) The resulting thermal wind effect on the azimuthal winds is shown in Fig. 5.29. Instead of the normally observed 850 mb wind maximum, the cyclonic winds increase in the vertical with a maximum near 700 mb. This cold cored feature has also been observed by McBride and Keenan (1982).

In the upper levels (Fig. 5.25b) we find an anticyclone due east of the hurricane, which overlies, and is probably partially supported by the deep overland convective activity in this region (c.f., Fig. 5.27). The hurricane is still protected from the full impact of the subtropical westerlies, but is close enough to be able to maintain an outflow channel in the divergent flow to the southwest of the anticyclone. We shall show in Chapter 6 that this is a favorable situation for continued intensification.

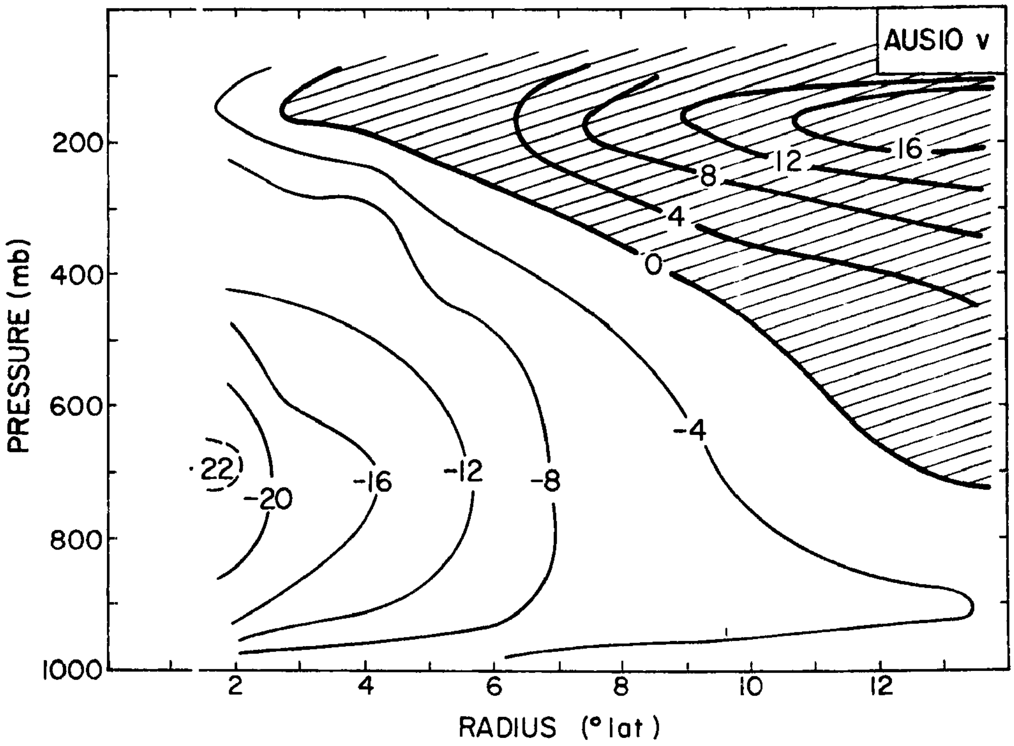

Fig. 5.29. Axisymmetric azimuthal wind cross-section for the West Coast Hurricane. Hatching indicates anticyclonic circulation.

5.5 The Structure of the Major Recurving Hurricane

As we have previously noted, the lack of major hurricane information in the southwest Pacific east of 165°E means that we are unable to derive any composites for the major oceanic hurricane. Fortunately, however, as we shall show in Chapter 6 most major hurricanes also recurve. This not only implies that a consistent environmental influence is responsible for their development, it also allows us to produce a dynamic composite of most major hurricanes in the Australian region, while minimizing any bias problems. To do this, we selected all major Australian hurricanes (minimum central pressure less than 960 mb) which recurved and which reached maximum intensity at or within one day of recurvature. These were separated into three phases: the developing tropical storm phase, with central pressure between 995 and 980 mb (AUS01); the intensifying hurricane phase, with central pressure less than 980 mb (AUS02); and the decaying hurricane phase, again central pressure less than 980 mb, no land falls, and at most two days after maximum intensity was reached (AUS03). Further details on the resulting composites, AUS01, AUS02 and AUS03, are contained in Appendix 2.

We note that the major hurricanes which comprise this composite come from both eastern and western Australia. We have assumed that the narrow stratification criteria imply a consistent environmental wind field, and thus minimize any wind bias. However, the wide longitudinal range of the observations, with the presence of the Australian continent, stop us from also producing an acceptable thermal composite.

For comparison purposes a similar set of rawinsonde composites were produced for recurving northwest Pacific supertyphoons. These include: the developing tropical storm stage, NWPRI1 (995-980 mb); the initial typhoon development phase, NWPRI2 (980-960 mb); the intensifying super typhoon stage NWPRI3 (<960 mb and reaches maximum intensity within one day of recurvature); and the filling typhoon stage NWPRF (<980 mb and at most two days after maximum intensity). Further details on these composites may also be found in Appendix 2. Note that in the northwest Pacific we were able to produce an extra intensifying typhoon composite (NWPRI2). While this is slightly noisy it provides valuable information on the initial typhoon intensification phase. Unfortunately we had insufficient data to produce a similar, stable composite in the Australian region.

Azimuthal Winds: The axisymmetric cross-sections of azimuthal winds for the Australian and northwest Pacific composites are shown in Figs. 5.30 and 5.31. The tropical storm phase of the major hurricane is almost identical to the Pre-hurricane Tropical Storm in Fig. 4.6. The storm is very large and strong, has a weak vertical wind shear in the lower troposphere and is overlain by an extensive anticyclone. It does, however, have a slightly more extensive cyclonic circulation in the lower stratosphere. By comparison, the northwest Pacific tropical storm stage (NWPRI1) has a similar vertical structure but is slightly weaker and smaller.

At the hurricane, or typhoon stage, the Australian system is still stronger and larger than its northern hemispheric counterpart. It also strengthens slightly in the decaying stage, but becomes smaller and develops a low level vertical wind shear, indicating the rapid

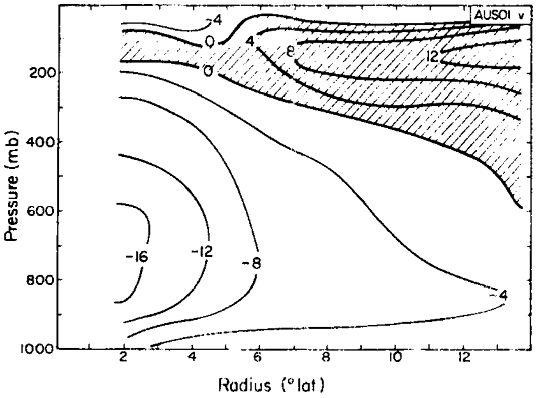

Fig. 5.30. Axisymmetric cross-section of azimuthal winds for the Australian region major recurving hurricane at the intensifying tropical storm stage AUS01, the intensifying hurricane stage AUS02 and the decaying hurricane stage AUS03. Regions of anticylonic circulation are hatched.

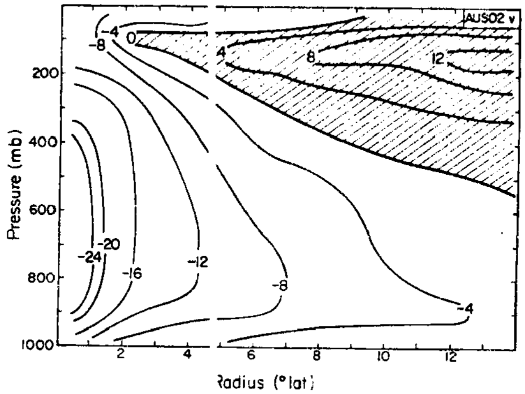

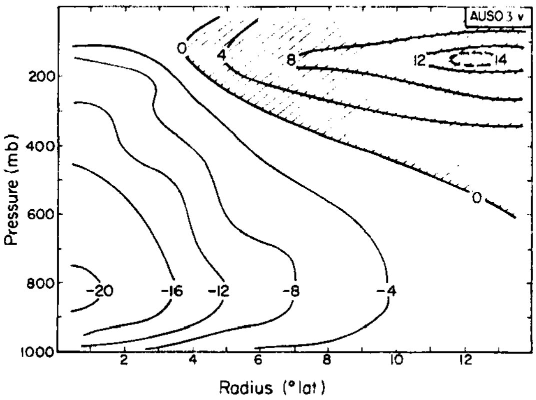

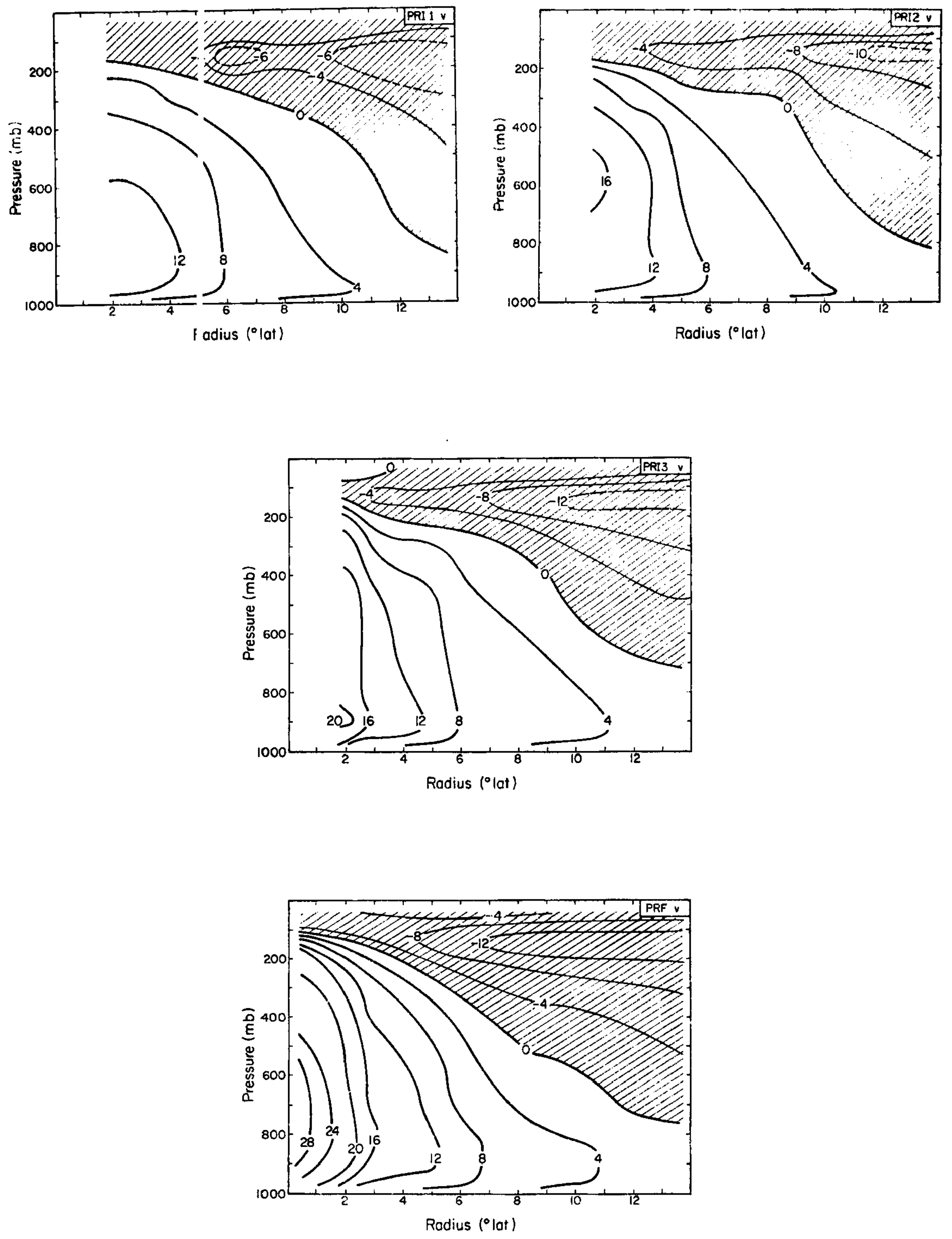

Fig. 5.31. Axisymmetric cross-section of azimuthal winds for the northwest Pacific region recurving supertyphoon at the intensifying tropical storm stage PRI1, the initial typhoon intensification stage PRI2, the intensifying supertyphoon stage PRI3, and the decaying typhoon stage PRF. Hatching indicates anticyclonic circulation.

destruction by the strongly sheared environmental flow. By comparison, the typhoon becomes stronger and larger after recurvature.

The size difference between the two regions is provided by their large scale environment. Australian region tropical cyclones form in a well developed monsoonal trough. They typically have 10-20^{o} latitude of westerly monsoonal flow on their equatorward side and a similar extent of easterly trade wind flow on their poleward side. Thus, they form with a very large size. As these Australian region cyclones track polewards they move out of this favorable region and contract slightly. Cyclones in the northwest Pacific, however, have extensive trade wind easterlies on their poleward side but do not typically form with an extensive westerly monsoonal flow on their equatorward side. Hence, they start out smaller than their Southern Hemisphere counterparts. As these cyclones move into the far west Pacific or South China Sea, the equatorial westerlies increase in extent. This, together with subtropical surges off the Asian mainland (Merrill, 1982; Pan Chien-shang, personal communication, 1982), generally causes northwest Pacific cyclones to grow during the latter stages of their lifecycle.

It is also notable that the intensity of the upper level anticyclone remains essentially constant throughout the recurving major hurricane's lifetime. By comparison, the intensity of the upper anticyclone over the supertyphoon increases considerably. Again, this is an environmental effect. The Australian system spends its entire lifetime near the upper level subtropical ridge and just on the equatorward side of strong subtropical westerlies. These maintain the strong axisymmetric upper level anticyclone from formation through decay. The northwest Pacific system, however, forms in the deep tropics. It then moves under the upper level subtropical ridge and close to the subtropical westerlies.

Radial Winds: The axisymmetric radial wind cross-sections for the Australian and northwest Pacific systems are shown in Figs. 5.32 and 5.33. If we recall that radial winds of less than 1 m s^{-1} are not significantly different from zero, then the tropical storm phases are almost identical. The major difference lies in the stratospheric and low level outer region inflow maxima in the Australian storm.

Considerable regional differences emerge, however, in the hurricane/typhoon stages. In the developing stage the stronger Australian system produces a stronger low level radial flow. But, it is also being directly affected by the upper level westerly flow. Thus, we see a strong deep upper outflow. This outflow becomes deeper and more extensive at the decaying stage as the strongly sheared environmental flow tears the hurricane apart. The supertyphoon develops a strong 300-400 mb inflow layer during intensification. This weakens and a very strong low level inflow, a result of the stronger circulation in Fig. 5.31, develops during the decaying stage.

The plan view wind fields are not shown since they are very similar to the Pre-hurricane Tropical Storm and Developing and Decaying Oceanic Hurricane described earlier.

5.6 Hurricane Kerry: A Case Study

Throughout Chapters 4 and 5 we have made extensive use of compositing to determine the major features of different types of tropical cyclones. We have, wherever possible used very restrictive

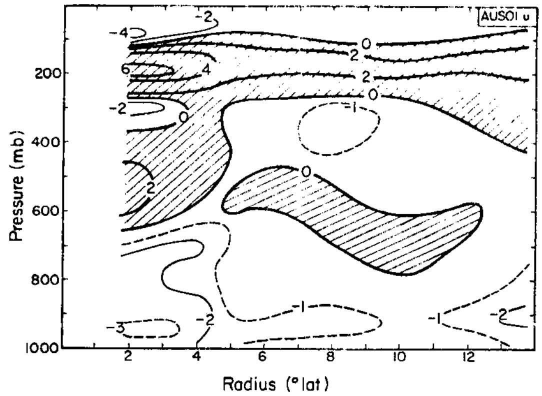

Fig. 5.32. Axisymmetric cross-section of radial winds for the Australian region major recurving hurricane at the intensifying tropical storm stage AUS01, the intensifying hurricane stage AUS02 and the decaying hurricane stage AUS03. Outflow regions are hatched. Radial winds less than 1 m s^{-1} are not significantly different from zero.

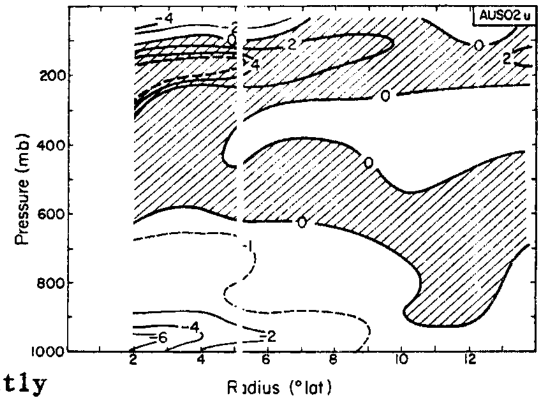

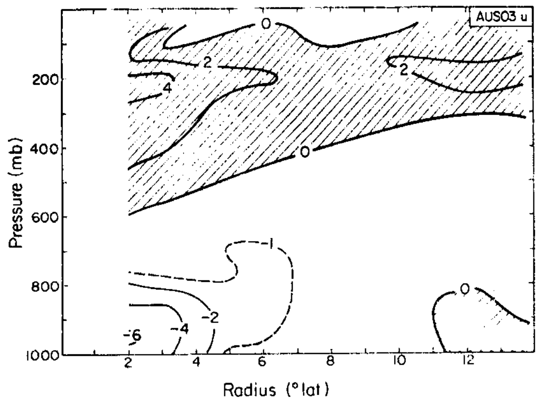

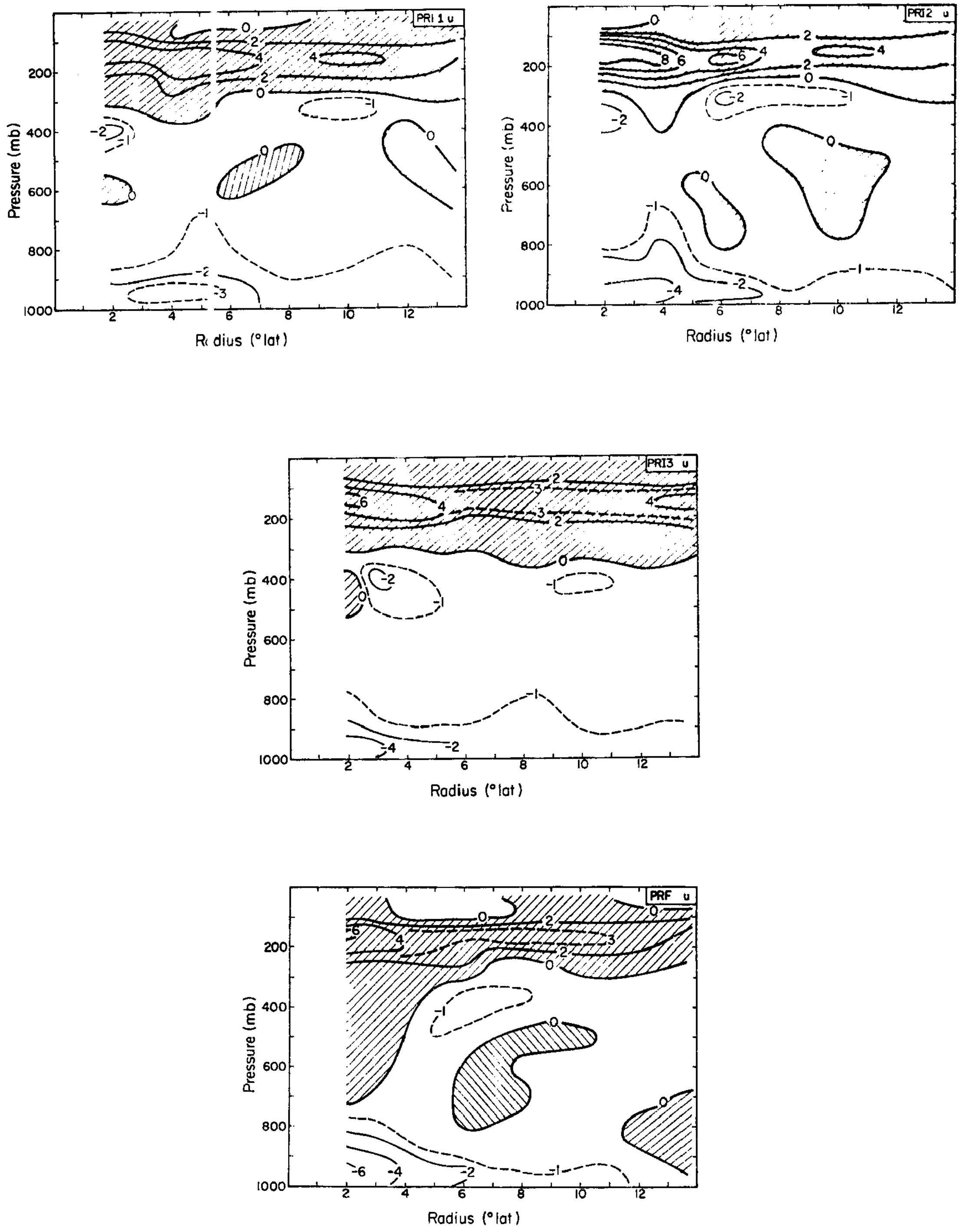

Fig. 5.33. Axisymmetric cross-section of radial winds for the northwest Pacific region recurving supertyphoon at the intensifying tropical storm stage PRI1, the initial typhoon intensification stage PRI2, the intensifying supertyphoon stage PRI3, and the decaying typhoon stage PRF. Outflow regions are hatched. Radial winds less than 1 m s^{-1} are nct significantly different from zero.

selection criteria in and attempt to keep smoothing to a minimum and retain salient details while still providing sufficient observations for an objective analysis. But how representative are the resulting composites? This and other questions can only be answered by a detailed analysis of many cyclones, which, though an item for future research, is far beyond the scope of the present study. However, we can show that at least one tropical cyclone, Hurricane Kerry, is quite similar to the Oceanic Hurricane composite described in section 5.2. Kerry was the first southwest Pacific hurricane to be reconnoitred by a fully instrumented research aircraft (Sheets and Holland, 1981) and has also been extensively analyzed (Lajoie and Butterworth, 1982; Lajoie, 1981; Holland _et al_., 1983; Holland and Black, 1983; Black _et al_., 1983). Since it was also not included in the Oceanic Hurricane composite it provides an excellent example for comparison.

As shown in Fig. 5.34, Hurricane Kerry formed at low latitude over the southwest Pacific Ocean and moved generally westward. It intensified to minimal hurricane strength on February 15, weakened while crossing the Solomon Islands, and subsequently reintensified in the Coral Sea. Maximum intensity of 954 mb was achieved on February 19 (Broadbrige, 1981) following distinct evidence of a missed recurvature. Kerry subsequently decayed gradually while following a long, erratic path across the Coral Sea.

The general synoptic scale structure of the cyclone during the intensification period are illustrated by the gradient level and 200 mb analyses in Fig. 5.35, the GMS satellite imagery in Fig. 5.36, and the sequential outflow layer analyses in Fig. 5.37. A more complete sequence of analyses may be found in Sheets and Holland (1981).

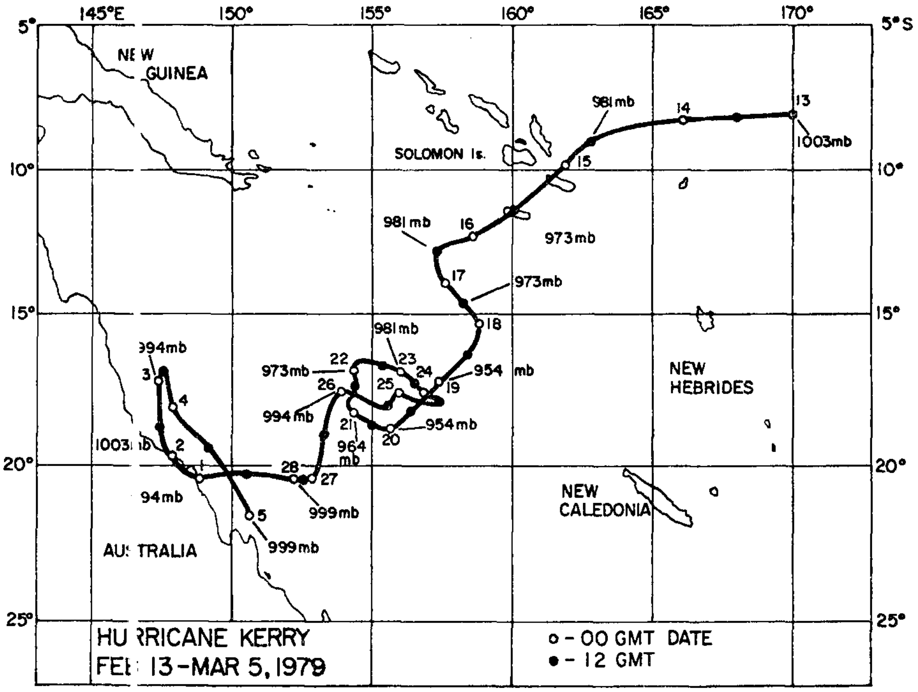

Fig. 5.34. Track of Hurricane Kerry showing dates (open circles 00 GMT) and selected central pressure estimates. (From Sheets and Holland, 1981).

On February 15th, Kerry was at minimal hurricane strength and the operational analyses in Fig. 5.35 compare very favorably to the tropical storm composite wind fields in Fig. 4.11, and to the intensifying hurricane composites in Fig. 5.12. At the gradient level we see the same equatorial inflow jet, the outer region trade wind inflow from the southeast, the distinct convergence to the east and cyclonic distortion to the west. At this stage at 200 mb, however, Kerry was slightly different to the composite wind fields. It lay slightly equatorward of the subtropical ridge, with a weak westerly trough to the south, and displayed a stronger equatorward and weaker poleward outflow channel configuration.

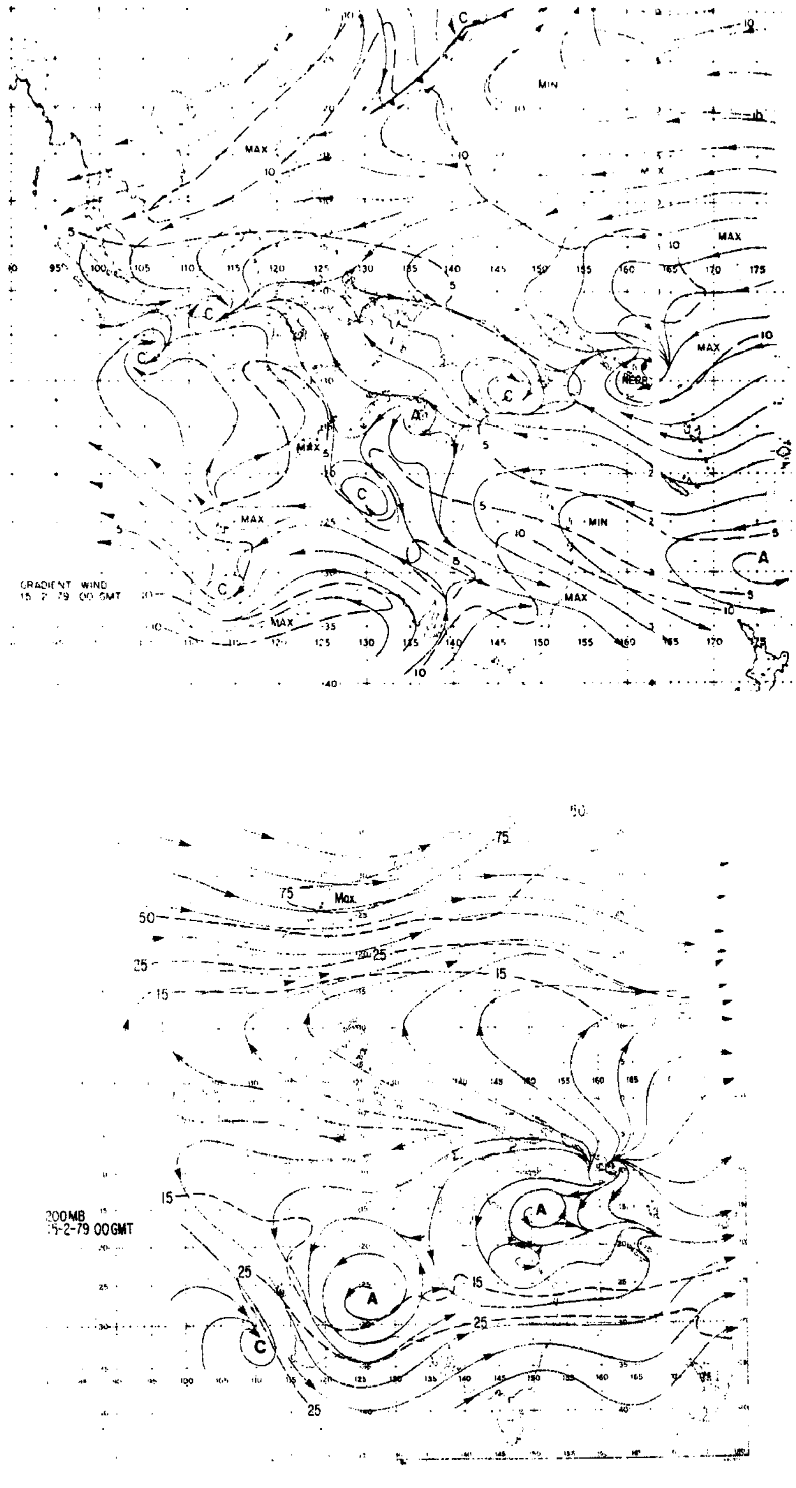

Fig. 5.35. Operational gradient and 200 mb streamline/isotach (m s^{-1}) analyses for 00 GMT on February 15, 1979 from the Darwin Tropical Analysis Centre.

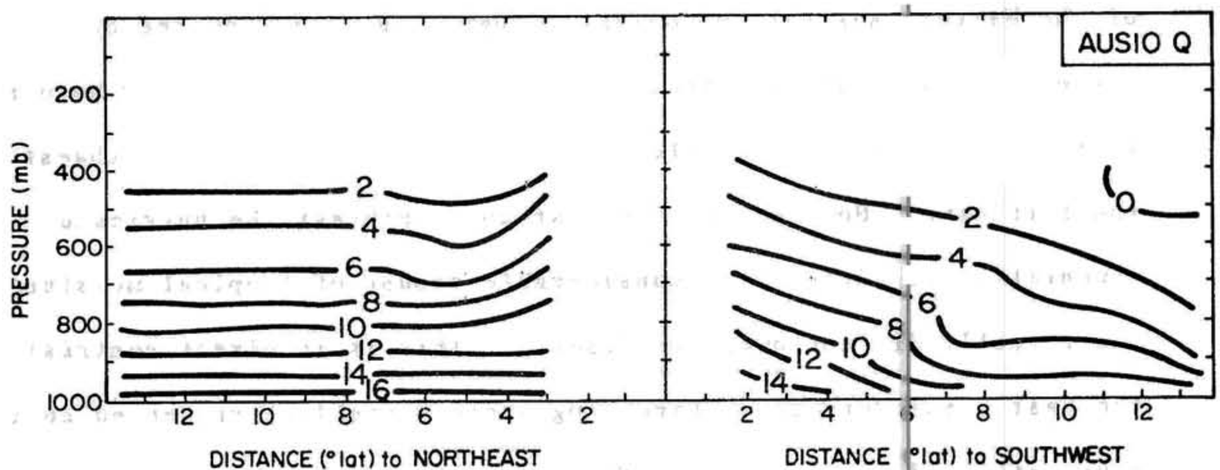

Fig. 5.26. Vertical moisture mixing ratio (g/kg) cross-section through the West Coast Hurricane and approximately along the Australian coastline.

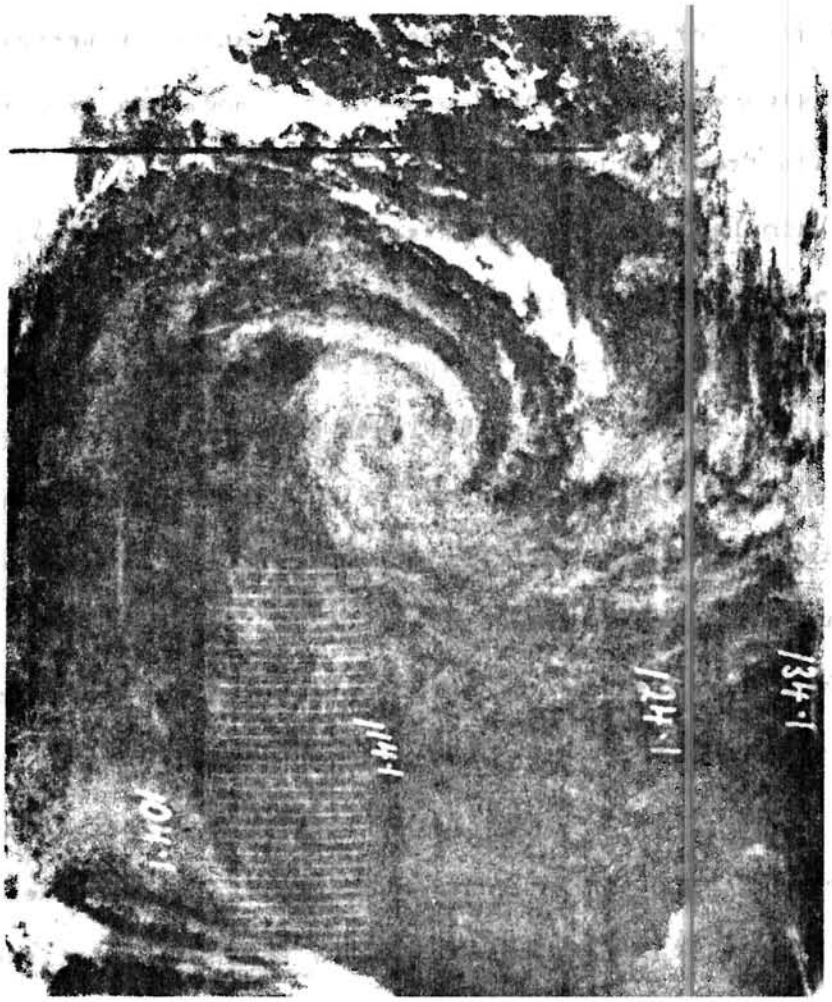

Fig. 5.27. ESSA 8 visible satellite mosaic of hurricane Joan (from Director of Meteorology, 1979) off the west Australian coast.

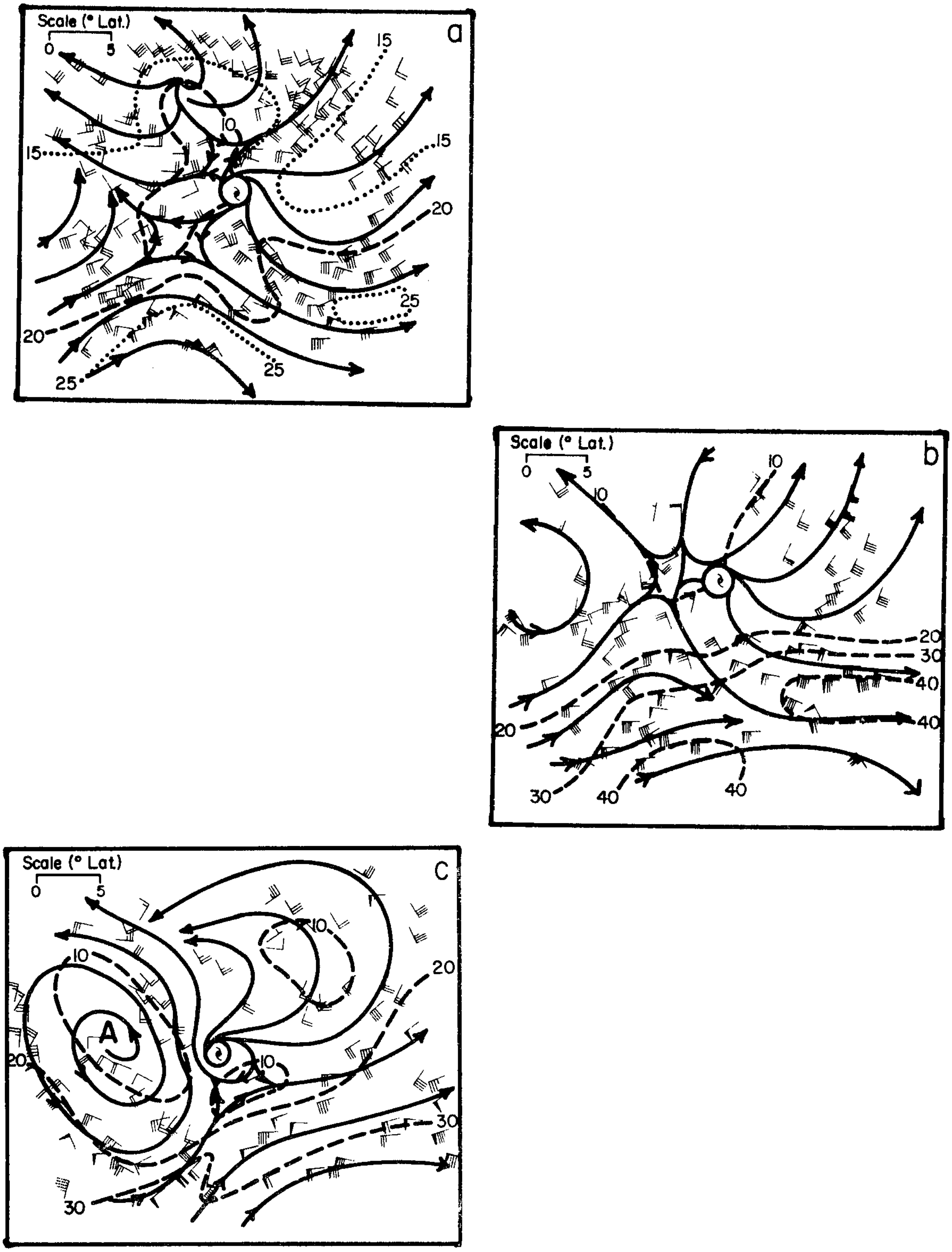

Fig. 5.37. Composite outflow layer structure of Hurricane Kerry for: a) 16/00-17/12Z, b) 18/00-19/12Z, and c) 20/00-21/12Z. (After Lajoie, personal communication 1982). Isotachs are in m s^{-1}.

The convective signatures for February 15 and 19 (Fig. 5.36) show a major cloud band from north through east; a cloud free region, or dry slot; and a sharp end to the convection in the southwest sector. These features are quite similar to our observations and deductions from the composite moisture and thermal fields in sections 4.2 and 5.2.

The outflow regime variations during the intensification and decay phases are more clearly seen in Fig. 5.37, which has been provided by F. Lojoie (personal communication, 1982). It contains three short term composites of all available upper level aircraft, satellite wind and rawinds for the first part of the intensification period (Fig. 5.37a), during which the central pressure fell 12 mb; the second part of the intensification period (Fig. 5.37b), during which the central pressure fell 15 mb; and the initial decay period (Fig. 5.37c), during which central pressure rose 13 mb. Also, shown in Fig. 5.38 are the corresponding divergence patterns on the poleward side of Hurricane Kerry. At the commencement of reintensification, then, a weak equatorward outflow is present. But the dominant feature is the strong poleward outflow into the divergent region ahead of an approaching westerly trough. Intensification continues as the westerly trough amplifies, the subtropical jet moves past the cyclone, and the outflow strengthens considerably. By February 20, however, the upper level trough has moved past the cyclone. Convergent southwesterly flow has cut off the poleward outflow channel. Hurricane Kerry begins to decay.

No comparable low level circulation variations were observed during this time (apart from a general increase in the cyclonic winds). Thus, these case study results provide good support to our composite conclusions that interactions with the subtropical jet stream dominate

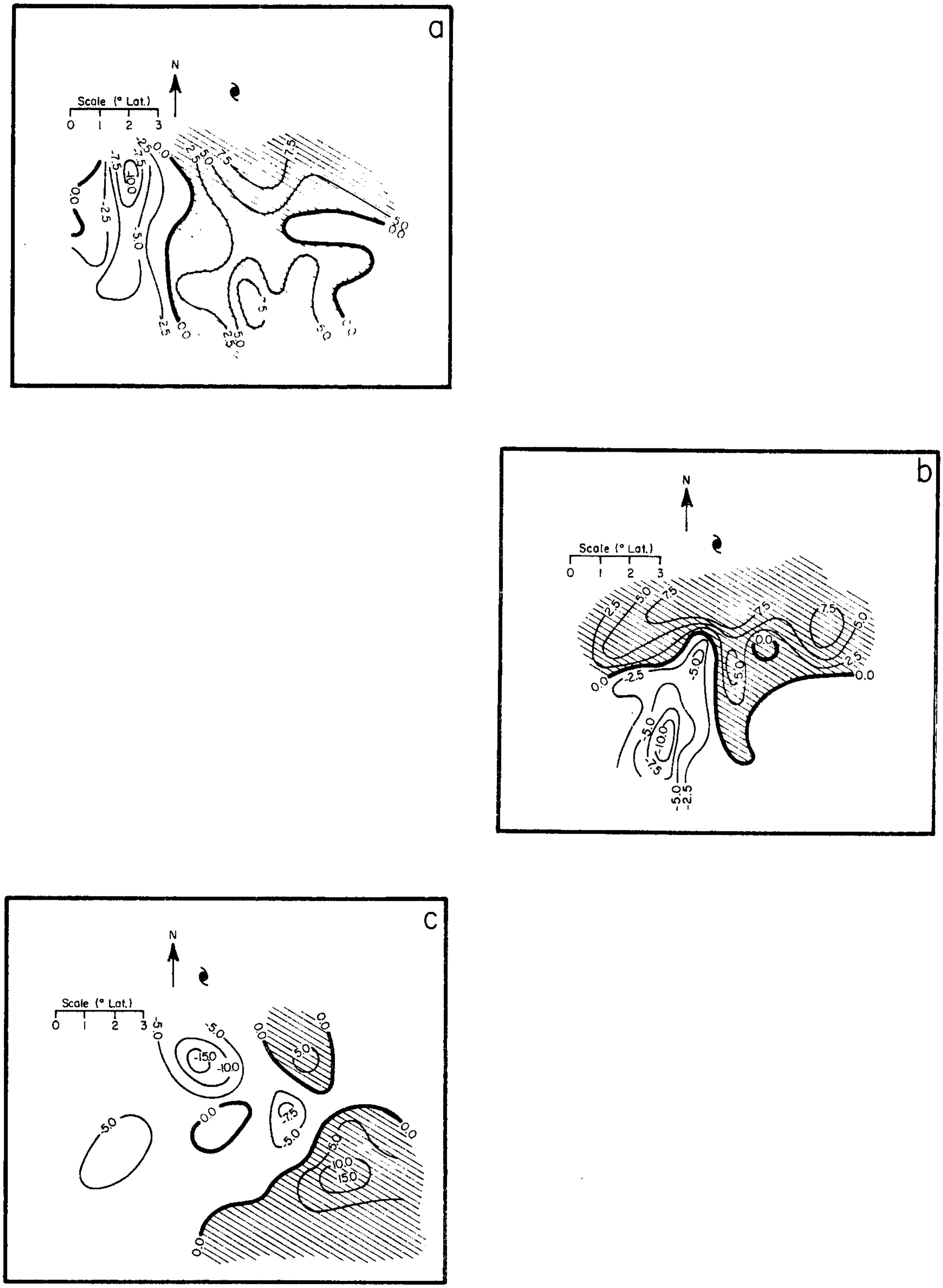

Fig. 5.38. Divergence patterns derived from the Hurricane Kerry from the Hurricane Kerry composite outflow layer wind fields in Fig. 5.37: a) 16/00-17/12Z, b) 18/00-19/12Z, and c) 20/00-21/12Z. (After Lajoie, personal communication 1982).

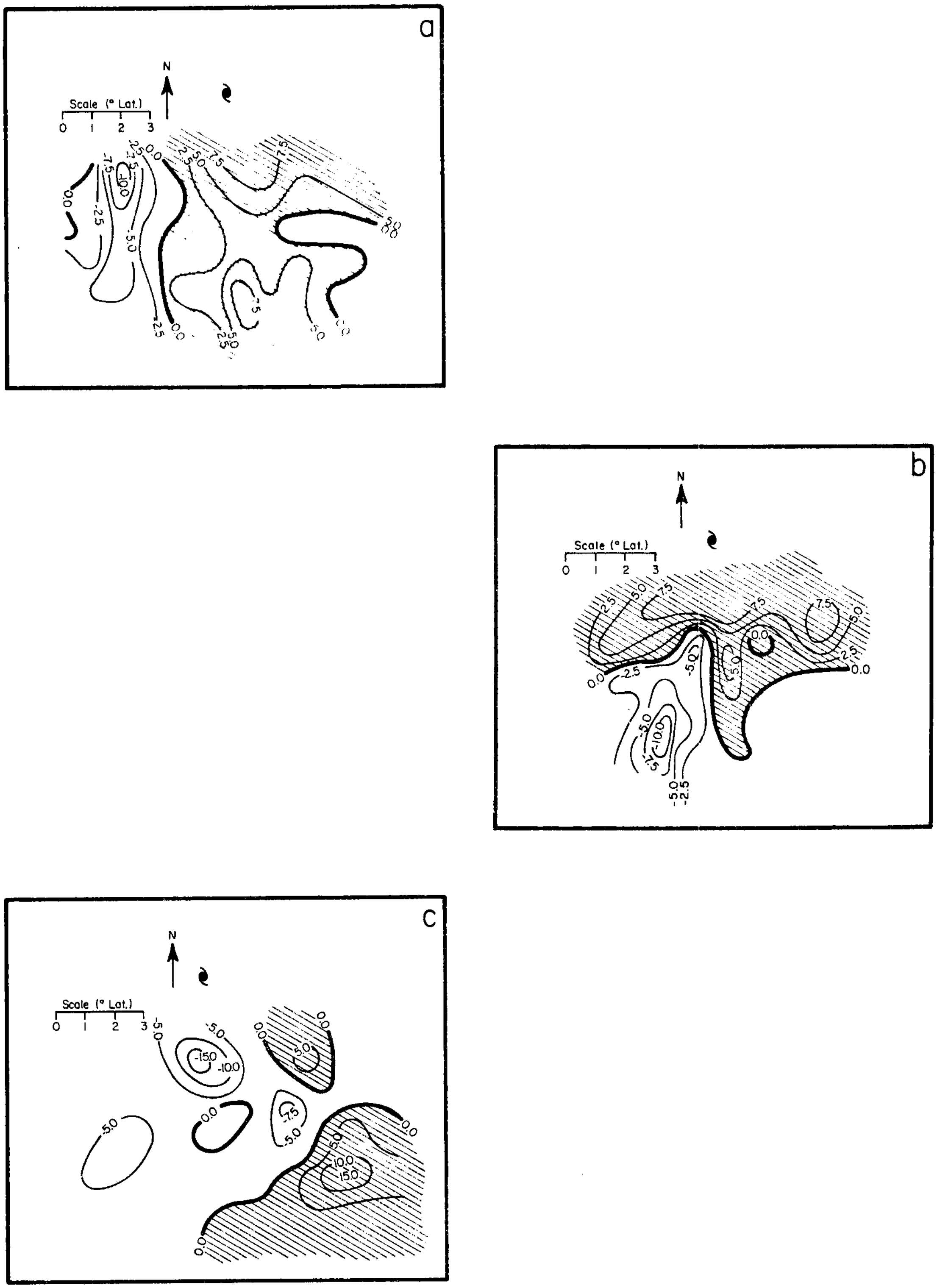

Fig. 5.38. Divergence patterns derived from the Hurricane Kerry from the Hurricane Kerry composite outflow layer wind fields in Fig. 5.37: a) 16/00-17/12Z, b) 18/00-19/12Z, and c) 20/00-21/12Z. (After Lajoie, personal communication 1982).

The convective signatures for February 15 and 19 (Fig. 5.36) show a major cloud band from north through east; a cloud free region, or dry slot; and a sharp end to the convection in the southwest sector. These features are quite similar to our observations and deductions from the composite moisture and thermal fields in sections 4.2 and 5.2.

The outflow regime variations during the intensification and decay phases are more clearly seen in Fig. 5.37, which has been provided by F. Lojoie (personal communication, 1982). It contains three short term composites of all available upper level aircraft, satellite wind and rawinds for the first part of the intensification period (Fig. 5.37a), during which the central pressure fell 12 mb; the second part of the intensification period (Fig. 5.37b), during which the central pressure fell 15 mb; and the initial decay period (Fig. 5.37c), during which central pressure rose 13 mb. Also, shown in Fig. 5.38 are the corresponding divergence patterns on the poleward side of Hurricane Kerry. At the commencement of reintensification, then, a weak equatorward outflow is present. But the dominant feature is the strong poleward outflow into the divergent region ahead of an approaching westerly trough. Intensification continues as the westerly trough amplifies, the subtropical jet moves past the cyclone, and the outflow strengthens considerably. By February 20, however, the upper level trough has moved past the cyclone. Convergent southwesterly flow has cut off the poleward outflow channel. Hurricane Kerry begins to decay.

No comparable low level circulation variations were observed during this time (apart from a general increase in the cyclonic winds). Thus, these case study results provide good support to our composite conclusions that interactions with the subtropical jet stream dominate in determining intensity changes for tropical cyclones in the southwest Pacific region. It is also notable that following this sequence of events Kerry spent a further 10 days over tropical waters (Fig. 5.34) and continued to decay. After crossing the coast, Kerry moved back over the ocean just ahead of an approaching westerly trough and rapidly intensified for a brief period before being destroyed as the trough impinged upon it.

5.7 Summary

In this chapter we have described a number of features of hurricanes in the Australian/southwest Pacific region.

We have shown that hurricanes occur almost exclusively between November and May, with an early season peak occurrence in December. Hurricanes in the southwest Pacific region then reach a second peak in February. Those in the northwest Australian region occur most frequently in January and March with a distinct minimum in February. The overwhelmingly preferred location is just off the northwestern Australian coast with a secondary maximum in the southeastern Coral Sea. Major hurricanes display similar characteristics to the overall hurricane classification. But, notably, nearly half the major hurricanes in the entire Australian region are found just off the northwestern Australian coast and make landfall on that coast at or near maximum intensity.

Hurricanes in the northwest Australian region move almost exclusively westward. This is partially due to the general easterly environmental winds there, and partially a result of higher latitude, eastward moving systems being removed by the Australian continent.

Those hurricanes in the southwest Pacific region have a slight preference for eastward movement, but the low latitude, intensifying systems generally move westward.

We have separately examined the structure of intensifying and decaying oceanic hurricanes (at least 1000 km from the Australian coast); of hurricanes just off the east and west Australian coasts; and of recurving major hurricanes and supertyphoons.

As with the tropical storms in Chapter 4, all composite hurricanes throughout the region, and Hurricane Kerry, are very large, have a deep equatorial inflow, and display a characteristic beta effect distortion. This is, however, modified by coastal funnelling in the East Coast Hurricane.

A comparison of intensifying and decaying oceanic hurricanes also showed the dominating influence of the subtropical jet. In the intensifying hurricane, the upper westerlies impinge to within 6^{o} latitude of the center. Thus, they do not affect the core region directly but provide an intense outflow channel to the southeast. When the westerlies move over the hurricane (or the hurricane moves under the westerlies) it is sheared off and rapidly decays. These composite conclusions are supported by our case study of Hurricane Kerry. In addition, the composite intensifying hurricane is distinguished by a marked inflow near 400 mb, a stratospheric inflow and a very weak vertical wind shear in the lower troposphere.

Hurricanes just off the west and east Australian coasts are affected considerably by the continent. The climatological upper level westerly trough over the Coral Sea (section 1.2) tends to weaken east coast cyclones and move them away from the coast. And an advection of dry continental air around the northern perimeter tends to cut off the tropical moisture supply to these systems. In general, the dryness of the continental air has little, if any, direct affect on west coast hurricanes. Rather, these systems protect themselves by maintaining a strong influx of tropical moisture over much of northern Western Australia. It is the hot temperature of the air over the northwestern deserts that has the major influence. We have shown that this produces a distinctly cold cored structure below 700 mb. Further, as west coast hurricanes advect the hot desert air off the coast, the normal meridional temperature gradient is reversed, and a deep easterly flow is maintained across the hurricane core. Thus, the observed consistent westward trajectory in this region is at least partially due to the cyclone/continent interaction.

Our comparison of the dynamic features of recurving major hurricanes and supertyphoons showed a lot of similarities and some interesting differences. The Australian system is larger and stronger during intensification. But it shrinks to the decaying stage whereas the typhoon grows and strengthens further. The large initial size of the Australian system appears to be due to angular momentum imports by a strong outer region low level inflow on both poleward an equatorward sides during the pre-storm (Love, 1982) and storm stage. The developing major hurricane is also in close proximity to the subtropical jet at all stages.

6. TROPICAL CYCLONE INTENSIFICATION

Having established some of the major structural and climatological differences between intensifying and decaying systems in the Australian/southwest Pacific region, and between tropical storms, hurricanes, and major hurricanes, we proceed naturally to the question of how and why such differences are established. In Chapter 1 we defined three separate "intensity" modes: intensity (maximum wind speed or central pressure); strength (average relative angular momentum inside 300 km radius); and size (extent of gale force winds or outer closed isobar). In this chapter we shall first review the current knowledge of mechanisms leading to intensification, strength and size changes. We shall then describe the ways in which cyclones can interact with their environment to produce these changes. Finally, we shall discuss the applicability of these conclusions to cyclone evolution in the Australian/southwest Pacific region, and propose a tentative model of the major intensification process.

6.1. Background

6.1.1 The Role of Moist Convection.

> "the spirit of CISK as the cooperative intensification theory is valid and alive' : Ooyama (1982).

The intensification and maintenance of the high energy core of a tropical cyclone is a very complex process, involving interactions between many scales. One mechanism, which has been summarized by Ooyama (1982) and forms the basis of extensive numerical modelling work, is the non-linear cooperative interaction between the cyclone and cumulus scales. Basically, the clouds are arranged into consistent and organized patterns by the relative vorticity and inertial stability (rotational stiffness) associated with the vortex. Entrainment into the clouds drives a secondary circulation with a deep inflow layer in the low to middle troposphere and a shallow, upper level outflow. Conservation of angular momentum then results in a strengthening of the lower and middle tropospheric cyclone and upper anticyclone. Note, however, that the portion of the secondary circulation driven by boundary layer friction does not contribute directly to intensification – it provides at best sufficient angular momentum to offset surface dissipation. It does, however, indirectly aid the intensification process by supplying some of the moisture convergence required to maintain the convection.

The clouds themselves are crucial to the whole process; they not only provide the release of latent heat which drives the secondary circulation, but also they support a local recycling of mass. This recycling serves two functions: the first is to provide warming which, for a given vortex structure, forces a sufficient secondary circulation to maintain a thermal balance; and the second is to help the system preserve energetic balance against the secondary circulation export of moist static energy. Gray (1979, 1982) has noted that oceanic evaporation and sensible heat flux associated with the primary circulation alone are unable to balance the observed export. Gray then suggested that cloud induced recycling provides the required extra energy flux. In essence, he believes that the anticyclonic vertical wind shear organizes mesoscale cumulonimbus cloud lines; these in turn extract high enthalpy air from the boundary layer, replace it with low enthalpy mid-tropospheric air, and thus locally enhance the sea surface evaporation above that available from the steady primary circulation. Holland and Black (1983) and Black et al. (1983) have shown that such recycling occurred in Hurricane Kerry. However, though this is a necessary ingredient of the intensification process it is probably not a primary cause.

The character and effectiveness of the cumulus-cyclone interaction also changes as the cyclone develops. During the initial stages of cyclone development, the rotational Froude number (a measure of the ratio of the characteristic scale of the system to the Rossby radius of deformation) is much less than unity. Any perturbations in the mass field are largely dispersed by gravity-inertia waves. Recycling occurs locally and only a very weak secondary circulation can be maintained on the cyclone scale. During the tropical storm stage, the Froude number approaches unity, the convection becomes more organized, and the increasing inertial stability restricts the secondary circulation and rapidly increases the efficiency of heating in the nascent eye region, as shown by Schubert and Hack (1982a,b). Schubert and Hack also showed that, once formed, the eye and maximum wind region act to stabilize the cyclone.

Shapiro and Willoughby (1982) have demonstrated the non-linearlity of the interaction. They used Eliassen's balanced vortex model (Eliassen, 1951) to show that a localized heat source (or convective band) outside the radius of maximum winds may cause a secondary eyewall and belt of maximum winds to form. This secondary eye wall dissipates the primary eye wall and maximum wind region and temporarily causes a decrease in the intensity of the cyclone. The cyclone then re-intensifies as the new band of maximum winds contracts inwards as a result of acceleration of the wind just inside the radius of maximum winds - a process described by Gray and Shea (1973) and Pearce (1981). Recent observations of this process occurring in tropical cyclones are provided by Willoughby et al. (1982).

6.1.2 The Role of the Environment.

> "all things considered, the most important factors appear to be: a) the area influenced by the initial convergence of very humid air determining in part the amount of air evicted upward; b) the temperature of the environment, influencing the upward convection velocity; and c) the facilities for disposal of air aloft": Depperman (1947).

Cyclone Formation: Even though the cyclone intensification is driven by moist convection and its non-linear interaction with the vortex, the rate and extent of this intensification is regulated by the environment. As Gray (1968, 1975) has summarized, certain minimum requirements must be met for genesis and subsequent intensification. These include an initial surface disturbance; a sea surface temperature of at least 26°C and a deep thermocline to prevent cooling should upwelling occur; a minimum latitude of 5° and an environment with cyclonic vorticity to provide the required background absolute vorticity; a conditionally unstable and moist environment to allow convection to occur; and a weak vertical wind shear at the disturbance center to enable the deep convection to provide a coupling between the lower and upper troposphere. Such conditions allow an accumulation of enthalpy to occur over the surface disturbance.

However, while these provide the usual minimum conditions, they are by no means sufficient. McBride and Zehr (1981) compared composite developing and non-developing weather systems over the tropical Atlantic and northwest Pacific. They concluded that the only significant difference was that, in the mean, developing cyclones are immersed in a region of stronger low level cyclonic vorticity and stronger upper level anticyclonic vorticity. McBride and Keenan (1982), however, found that little confidence could be placed in this differential on a case by case basis in the Australian region. Love (1982) in a combined observational and modelling study found that tropical cyclone formation in the western Pacific Ocean was associated with more vigorous Hadley circulations in both hemispheres. An important component was provided by a cold surge moving equatorwards in the winter hemisphere. This produced high pressures on the equator upstream of the development region, followed by a down-the-pressure-gradient acceleration of the monsoonal westerlies prior to cyclone formation. Forecasters in both hemispheres have also developed a rule of thumb that anticyclogenesis poleward of an existing disturbance, with an accompanying trade wind surge, was very favorable for development (Norton, 1947; Wilkie, 1964).

The low level import, and upper level export of angular momentum by these processes can provide a rapid development of the type of formation environment described by McBride and Zehr (see, e.g. Holland, 1983a; Lee, 1982). But the important question of how often such surges occur without subsequent formation of a tropical cyclone has yet to be resolved.

Hurricanes, or very good facsimiles thereof, also occasionally form in far more adverse conditions than those prescribed by Gray. Since the advent of satellites a number of hybrid systems have been observed forming at high latitudes, in baroclinic environments, and with cold sea surface temperatures (see, eg, Erickson, 1967). Though direct observations are lacking, these systems develop many of the characteristic cloud features of hurricanes in the deep tropics (Hebert and Poteat, 1975). Rasmussen (1979) also indicates that some polar lows, which form within outbreaks of arctic air, are very similar to tropical hurricanes in structure and energetics. Yet they form in highly baroclinic environments and over oceans with sea surface temperatures as low as 10^{o}C!

The major mechanisms leading to the formation of these hybrid and polar low systems appears to be a marked upper level divergence (usually associated with strong cyclonic vorticity advection) and the advection of cold air over a warmer (though still quite cold by normal standards) ocean surface. Thus, the air/sea temperature difference still maintains a conditionally unstable atmosphere and sufficient sea surface enthalpy flux for a convectively active system. The east coast 'bomb' or rapidly deepening cyclone (e.g. Sanders and Gyakum, 1980) is a good example of the importance of these sea to air fluxes in such circumstances.

<u>Sea Surface Temperatures and Intensity Change</u>: The air/sea temperature difference will also be a major factor in determining the ultimate possible intensity of the tropical cyclone. As has been discussed by Miller (1958) and Ooyama (1969), the upper level warm core in the developing cyclone stabilizes the inner convective region. Thus, for a given air/sea temperature difference and conditional instability

of the environment, a cyclone will reach an intensity at which the core region is neutrally stable to moist processes. Any convective forcing will then stop. Of course, the actual intensity of the cyclone at this stage is a function of both the horizontal dimension and magnitude of the upper tropospheric warm core. Thus, cyclones of different size, strength and ultimate intensity are possible for the same air/sea temperature difference.

The interdependence of intensity and air/sea temperature difference has led a number of people to suggest that mesoscale changes in sea surface temperature may cause concomitant changes in tropical cyclone intensity (see e.g., Perlroth, 1967, 1969). However, Ramage (1974) strongly disputed this and provided examples of continued, or even commencement of, intensification as typhoons moved over cooler waters. This is supported by our observations of occasional cyclones in the Autralian region which move hundreds of kilometers inland while still maintaining a mid- to upper tropospheric hurricane structure. (McBride and Keenan, 1982, include an example of cyclone Madge which traversed the entire continent while still maintaining organized convective bands and an eye.) As Ooyama (1982) has suggested, it is reasonable to expect a mature cyclone, which has reached its ultimate intensity for the current conditions, to change rapidly in response to sea surface temperature variations. But it is unlikely that a developing cyclone, and especially one subject to other strong external forcing mechanisms, will be so effected.

<u>Upper Tropospheric Environment/Cyclone Interactions and Cyclone Intensity Change</u>: Holland (1983a) described Lagrangian (moving with the cyclone) angular momentum budgets for a number of composite northwest

Pacific cyclones of different intensities. This research supported the findings of a number of previous authors that the major environmental interaction was provided by eddy fluxes in the upper troposphere. We also showed that the relative positions and movement of the cyclone and environmental features was important in determining the result of this interaction.

This upper tropospheric cyclone/environment interaction during intensification is by far the most observed and discussed process in the literature. A synthesis of the many papers on this topic indicates that the three synoptic models, two of which are shown in Fig. 6.1, are the most important for rapid intensification and/or the development of very intense systems. We shall only mention each briefly here and reserve a complete discussion of the underlying physics to sections 6.4 and 6.5.

In the first model, which seems to mainly occur in the north Atlantic, a cold upper tropospheric low and the cyclone come into close proximity. This may occur from any combination of development or relative movement. A sudden filling of the cold low, with strong outflow from the cyclone into its center is often associated with rapid development of an intense hurricane. Riehl (1959, 1979) suggested that this is due to a spontaneous collapse of the cold low. A solenoidal circulation is then generated with subsiding cold air in the low and rising warm air in the cyclone. The original potential energy is converted to kinetic energy of the overturning solenoid, or secondary circulation. The cyclone then "intensifies" by a low level import and upper level export of angular momentum (depending on the scale involved a strength or size change may be the more likely outcome).

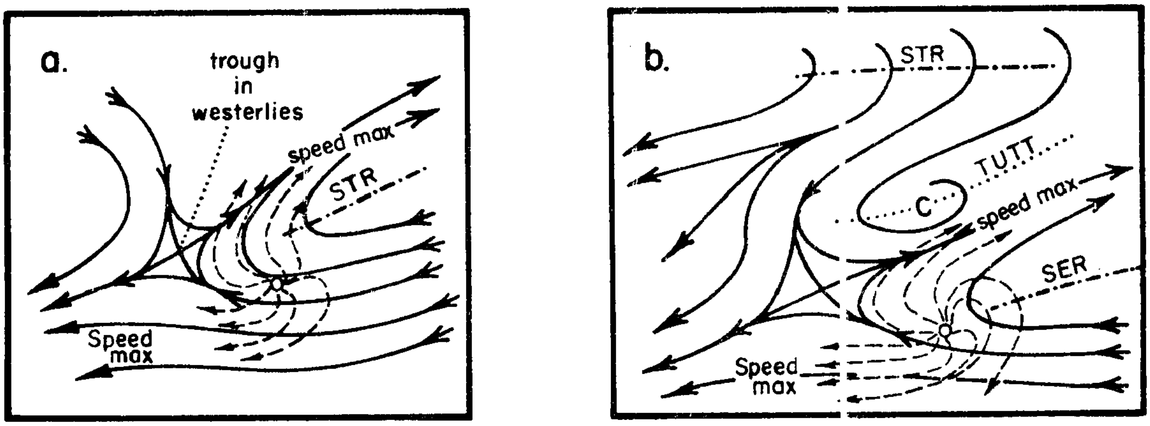

Fig. 6.1. Two synoptic models of favorable subtropical upper level flow patterns for tropical cyclone intensification (after Sadler, 1978). STR is the SubTropical Ridge, SER the SubEquatorial Ridge, and TUTT the Tropical Upper Tropospheric Trough.

The second model (Fig. 6.1a) involves the development of a strong outflow channel to the westerlies as an upper level, subtropical jet type, trough approaches or develops to the west of the cyclone. We have already seen that this is the predominant mechanism in the Australian/southwest Pacific region. McRae (1956) and Ramage (1959) (see also Tsui et al., 1977) proposed that cyclonic vorticity advection downstream of this developing, or approaching trough provides mass divergence over the cyclone. They hypothesized that as a result the surface pressures fall and the cyclone intensifies. However, no observations that the upper divergence actually exceeded lower compensating convergence have been provided. Ramage (1974) further suggested that the accompanying poleward streaming cirrus cloud is indicative of a ventilation of excess heat away from the cyclone. This presumably allows further intensification by reducing the inner circulation subsidence warming (Riehl, 1954), though Ramage did not elaborate on the underlying mechanisms. We shall examine this interaction further in later sections.

As a corollary to this second model, should the cyclone move under the high speed westeries around this upper trough, its vertical structure and upper warm core will be disrupted. A rapid decay to a weak, shallow depression will then occur. We have seen this effect in the non-developing tropical storm and decaying hurricane composites of Chapters 4 and 5.

The third model (Fig. 6.1b) is largely a northwest Pacific phenomenon in which the cyclone moves into an advantageous position relative to the Tropical Upper Tropospheric Trough, or TUTT, (Sadler, 1967). Sadler (1967, 1978) noted that this is normally associated with intensification of the typhoon. Sadler also suggested that the underlying mechanism was an establishment of two outflow channels, one to the easterlies and a second to the westerlies. These supposedly provide enhanced ventilation of excess heat from the cyclone. But, as with Ramage (1974), no supporting discussion of how this leads to intensification was given.

Chen (1983) has conducted a detailed global study of outflow configurations for all intensifying tropical cyclones during the FGGE year. His observation is that most of the intense and rapidly deepening systems conform to the above three synoptic models. But the weaker tropical storms and minimal hurricanes tend to be associated with a variety of other upper level flow patterns and generally constrained outflow configurations.

<u>Dynamic Instability and Cyclone Intensification</u>: In addition to these synoptic models, the possible development of regions of dynamic instability have been investigated by Sawyer (1947), Kleinschmidt (1951), Alaka (1962), Yanai (1964), and Black and Anthes (1971). In the

absence of any external forcing mechanisms or sources, conservation of angular momentum in the outflowing air will produce regions of strong anticyclonic vorticity. If this anticyclonic vorticity exceeds the cyclonic Coriolis component, the outflowing air will become dynamically unstable (see section 6.4 for a more complete discussion) and tend to spontaneously accelerate outward. The consequential mass divergence may cause surface pressure falls and cyclone intensification. Dynamic instability occurs consistently in numerical models (e.g., Ooyama, 1969; Anthes, 1972; Kurihara, 1975; Kitade, 1980). But extensive areas of dynamic instability have not been observed, despite careful analyses by Alaka (1962) and Black and Anthes (1971).

Summary: In summary, then, we have shown that previous studies on the role of the environment in intensity change clearly indicate the importance of interactions in the upper tropospheric outflow layer. The consensus is that the 'necessary' climatological conditions summarized by Gray (1968), once satisfied, do not differentiate between weak and intense hurricanes; indeed in some cases hurricanes may form under far more adverse conditions. Further, except for the special case of a hurricane at its ultimate intensity, sea surface temperature variations of a few degrees are probably not a major factor in determining intensity change.

To our knowledge, no one has explicitly described the physical processes behind strength and strength change; though a number of papers on "intensity change" may have actually been describing strengthening. However, Merrill (1982) has recently examined the size change process. His preliminary conclusions were that size change results from a sustained environmental interaction in the lower troposphere.

We shall discuss this topic further from separate climatologial, observational and theoretical viewpoint in the following sections.

6.2 Climatology

At this stage of our investigation we have not been able to develop a climatology of tropical cyclone size or strength change in the Australian region. Further, as we have previously noted in section 2, data deficiencies prevent an adequate documentation of cyclone intensities over the southwest Pacific region east of 165°E. Thus, we limit our presentation here to a clinical description of the intensity and intensity change features of tropical cyclones in the Australian region (west of 165°E). A discussion of possible physical processes behind these features will be given in sections 6.3 and 6.4.

6.2.1 Intensity and Intensity Change.

The maximum intensity distribution for tropical cyclones over the Australian region is shown in Fig. 6.2. The distribution curve gives the number of cyclones with minimum central pressures lying in overlapping 5 mb bands (1 mb resolution), and has also been smoothed by a running 5 point mean. We see that over the entire region 45% of tropical cyclones reached hurricane intensity and 15% became major hurricanes. The proportions for the north/west Australian region and the southwest Pacific taken separately are similar. However, in the north/west Australian region most tropical storms are found in the Gulf of Carpentaria and most hurricanes off the northwest Australian coast. Hurricanes with central pressures less than 940 mb also occurred exclusively off the northwest Australian coast; the corresponding lack

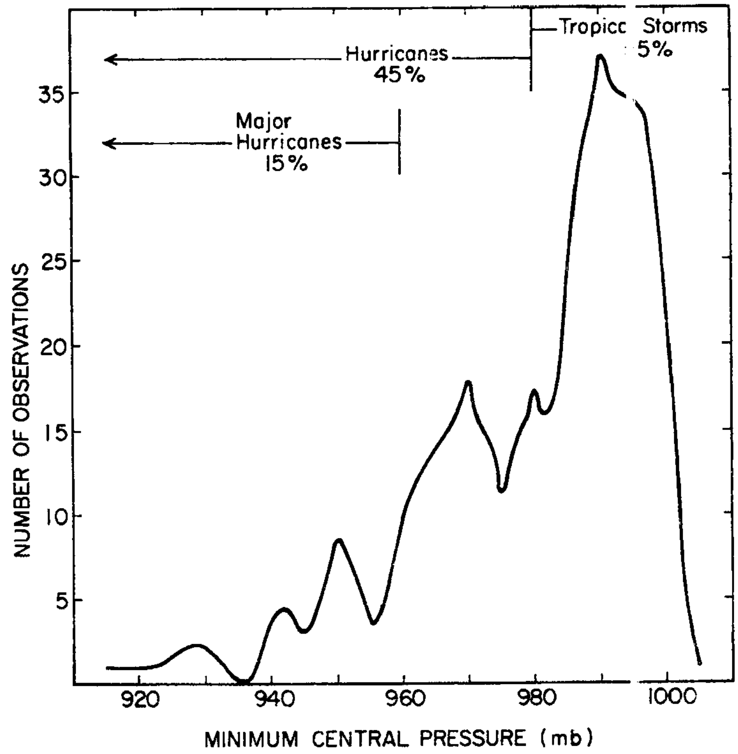

Fig. 6.2. Maximum intensity distribution of tropical cyclones in the Australian region. The ordinate gives the number of observations in 5 mb bands and the curve has been smoothed by a 5 point running mean.

of very severe cyclones over the Coral Sea may be real or it may be a result of the possible data bias in this region described by Holland (1981).

Of particular interest in Fig. 6.2 is the presence of three distinct peaks at 990, 970 and 950 mb. The location of these peaks precisely at the ten millibar values is probably due to a propensity for analysts to round off the maximum intensity values (note, for example, the small peak at 980 mb). Nevertheless, we consider that the general increase in occurrence near 970 and 950 mb is meteorologically significant and shall consider this feature further in section 6.5.

Figure 6.3 contains the maximum intensity distribution of origin latitude. No trend can be discerned in the north/west Australian region, and in the Coral Sea region the wide scatter and small number of

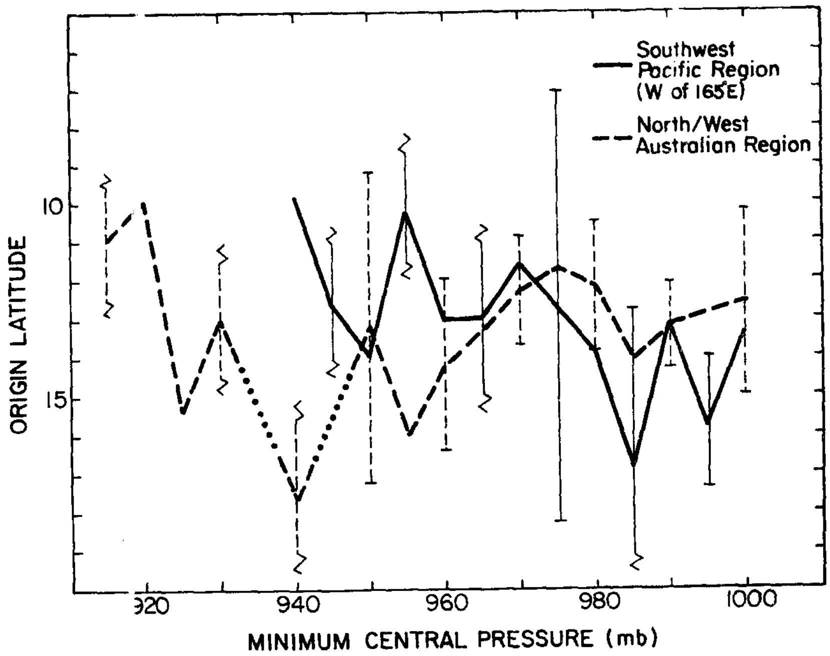

Fig. 6.3. Maximum intensity distribution of origin latitude for tropical cyclones in the Australian region. 95% confidence intervals are shown by cross bars; cross bars with open ends that indicate no statistical confidence can be placed in the observation.

data points prevent us from attaching any statistical significance to the trend for more intense cyclones to originate at lower latitudes. However, significant trends emerge if we separate tropical storms from hurricanes and plot minimum central pressure against origin latitude. As may be seen in Fig. 6.4, the most intense hurricanes tend to originate around 10°S in the Coral Sea region and at a higher latitude of 15-18°S in the north/west Australian region. Notably, in both regions cyclones which originate at very low latitudes do not become as intense as those which originate at higher latitudes.

As shown in Fig. 6.5 there are also significant trends in the maximum intensity distribution of intensification period and mean intensification rate (from origin to maximum intensity). Comparing tropical storms (980-995 mb) to major hurricanes (< 960 mb), we see that

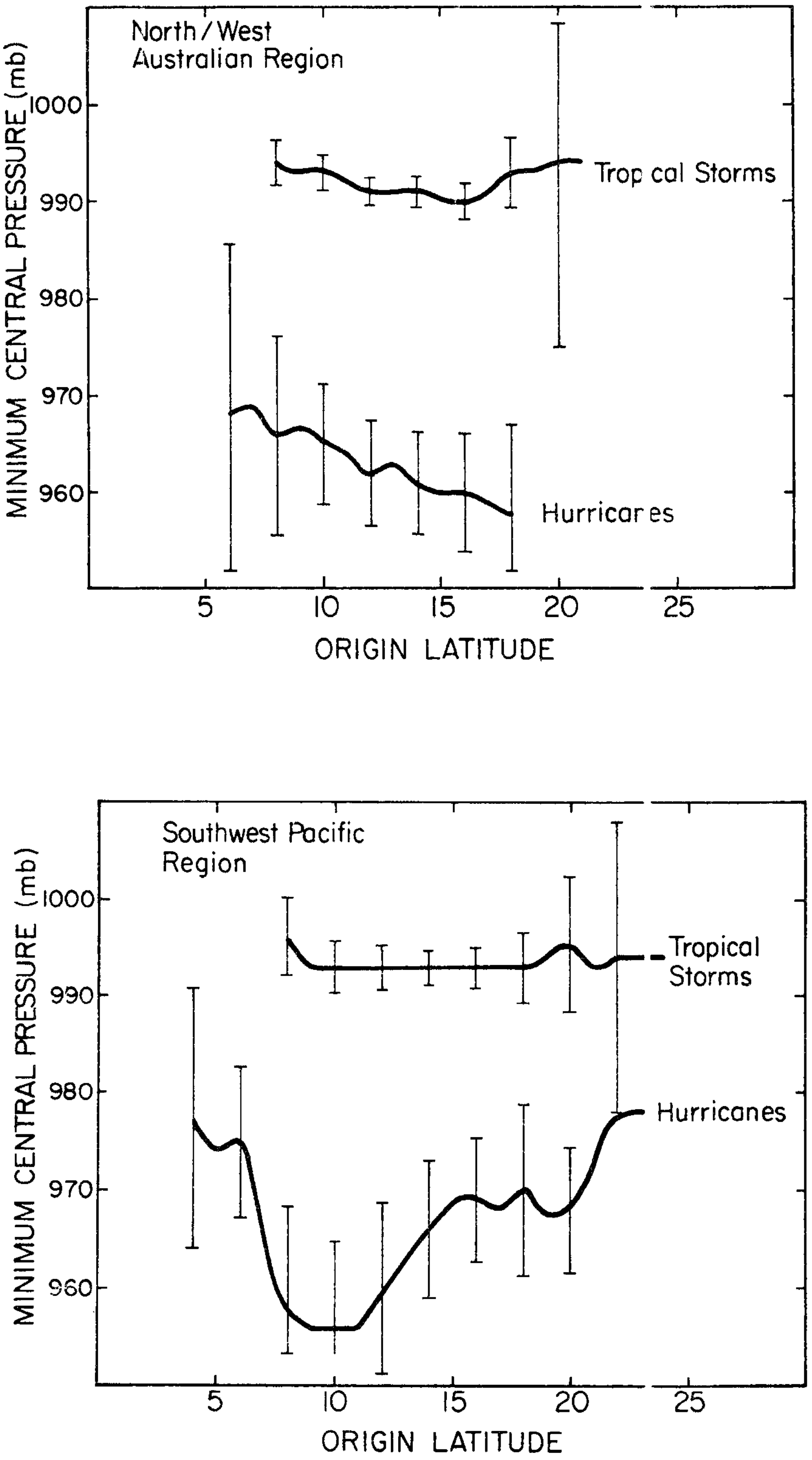

Fig. 6.4. Origin latitude distribution of minimum c ntral pressures for tropical storms and hurricanes in the Australian region. 95% confidence intervals are also shown.

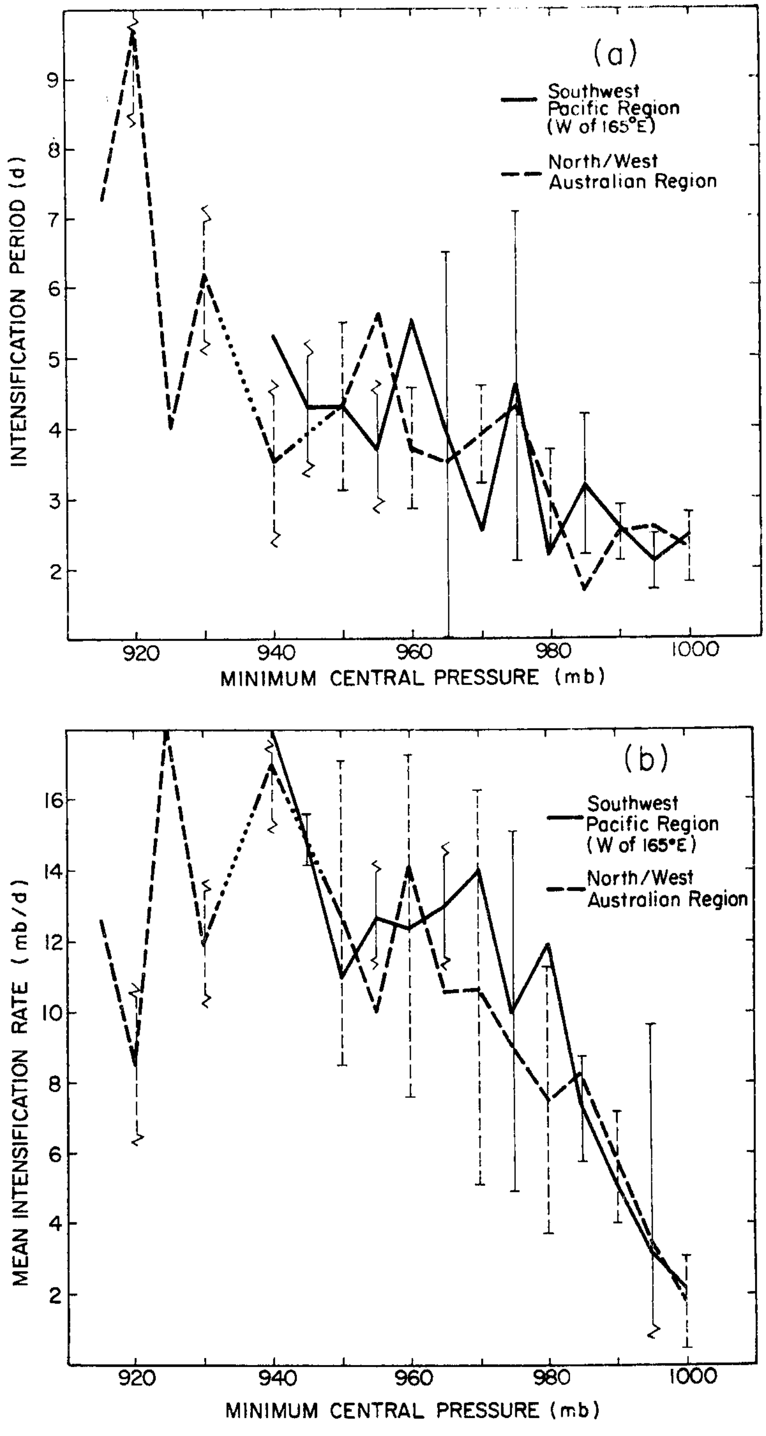

Fig. 6.5. Maximum intensity distribution of: a) Intensification Period in days; and b) Mean Intensification Rate for tropical cyclones in the Australian region. 95% confidence intervals are also shown by cross bars; cross bars with open ends indicate that no statistical confidence can be placed in the observation.

the major hurricanes typically take twice as long to reach maximum intensity and also intensify at three times the rate of tropical storms. Because of the limited data points, no statistical significance can be placed on the trends below 940 mb; yet it is interesting that below 970 mb the time to maximum intensity, and the intensification rate curves are distinctly out of phase. This implies that either the ultimate intensity of each cyclone was somehow predetermined (regardless of intensification rate), or that whatever processes cause rapid intensification also hasten the eventual destruction of the cyclone. We shall return to this important point in section 6.4.

The latitudinal distribution of the local rates of intensification (6 hour resolution and exclusive of landfalling storms) of those cyclones which became hurricanes is shown in Fig. 6.6. In both regions decaying systems dominate polewards of 22°S. In the Coral Sea region the average intensification rate is essentially constant equatorwards of 20°S, whereas in the north/west Australian region a significant maximum occurs between 15-20°S. By comparison, tropical storms (not shown) also have a preponderance of decaying systems polewards of 20°S. But equatorward of this latitude they exhibit an almost zero net intensification rate, a result of deepening and filling systems occurring in nearly equal proportions. Thus, while hurricanes typically decay in the subtropics, a large proportion of tropical storms decay over the tropical oceans.

The mean meridional and zonal motion for tropical storms and hurricanes is contained in Table 6.1. In both regions hurricanes move more rapidly westward than tropical storms, and in the southwest Pacific tropical storms tend to move eastward during intensification.

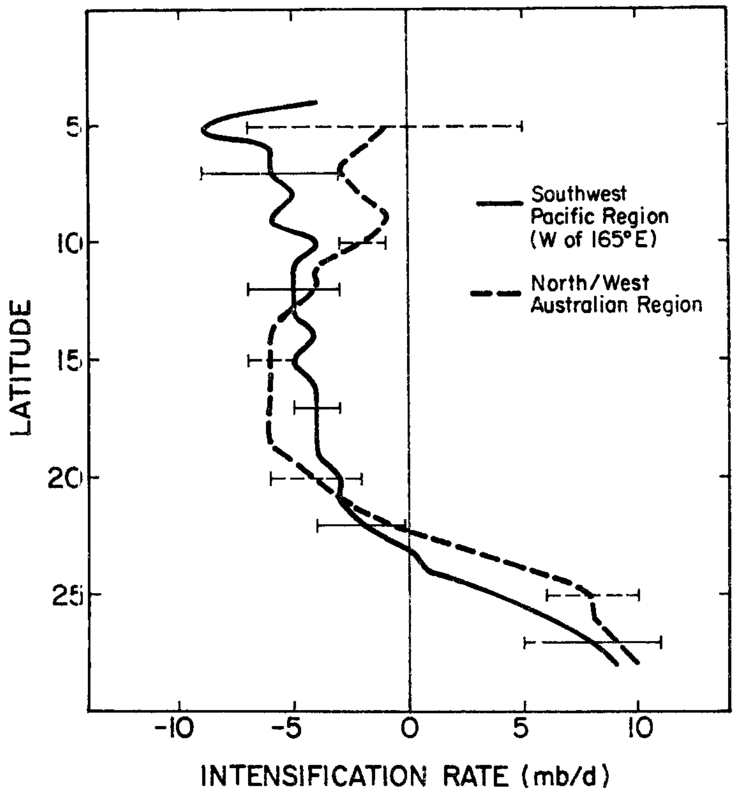

Fig. 6.6. Latitudinal distribution of local intensification rates for the complete life cycle of hurricanes in the Australian region. 95% confidence intervals are also shown.

Surprisingly, hurricanes in both regions move poleward faster on an average than tropical storms. Revelle (1981) obtained different results for the entire southwest Pacific from 1969-1979. He found that tropical storms (which he defines as being greater than 25 ms^{-1} maximum wind speed) moved eastward at 3.6 ms^{-1} and poleward at 2.6 ms^{-1} while hurricanes move westward at 0.8 ms^{-1} and poleward at 1.9 ms^{-1}. As we have already shown in section 4.1, this difference is due to the distinct increase in poleward and eastward motion for tropical storms east of 165^{o}E.

TABLE 6.1

Mean zonal (V_E) and meridional (V_N) motion (m s^{-1}) during the intensification period of tropical storms and hurricanes in the north/west Australian region and southwest Pacific region west of 165^oE.

REGION	INTENSITY	MOTION	
		V_E	V_N
North/west Australian Region	Tropical Storms	-1.1	-1.0
	Hurricanes	-2.0	-1.5
Southwest Pacific Region West of 165^oE	Tropical Storms	0.5	-2.0
	Hurricanes	-0.6	-2.4

A quite important finding of this study is the distinction between track types and cyclone intensity shown in Fig. 6.7. This figure contains the maximum intensity distribution of four of the five track types defined in section 1.1. The southward moving cyclones were very few in number and thus not included. We also required that the recurvature point for recurving cyclones be near the point of maximum intensity (if not the cyclone was placed in one of the other categories, i.e. a recurving cyclone in which recurvature occurred three days after maximum intensity would be classified in Fig. 6.7 as a westward moving cyclone). We see that tropical storms are comprised of roughly equal numbers of recurving, westward and eastward moving, and erratic cyclones. But most of the hurricanes, and almost all the major ones, came from the recurving category. In addition, many of the westward moving hurricanes displayed evidence of missed recurvature during intensification. This provides further confirmation of our composite

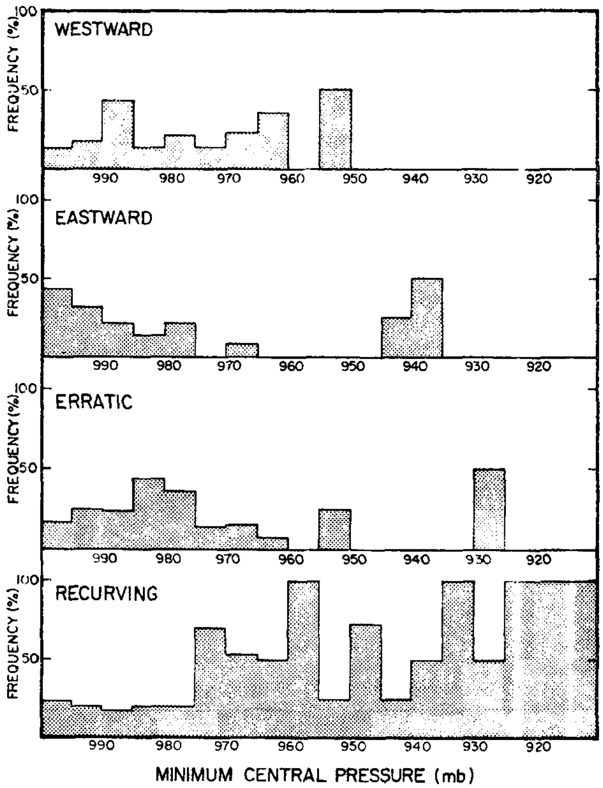

Fig. 6.7. Percent frequency of maximum intensity for tropical cyclones in the westward, eastward, erratic and recurving movement classes (see text for definitions).

study conclusions that the intensification to hurricane or major hurricane stage occurs during an interaction between the cyclone and an approaching westerly trough.

6.2.2 Rapid Intensification

Periods of extreme rapid intensification are certainly underestimated in the Australian region. This results from the almost universal use since 1966 of satellite techniques (Anderson et al., 1974; Dvorak, 1975) in which intensity change is limited as much as possible to two or three characteristic rates. Hence, using the Dvorak (1975) rapid intensification curve as a basis, we define rapid intensification as any period in which the central pressure fell by at least 6 mb in a 6 hour period and a rapid intensification cycle as the period in which the central pressure continued to fall at a minimum rate of 6 mb for subsequent 6 hour periods. The distribution of total central pressure fall during these rapid intensification cycles is shown in Fig. 6.8. A large number of single event 6 mb falls were recorded; and some of these were quite suspect, occurring at landfall or as the cyclone crossed an observation point. The largest sustained rapid pressure falls were two observations of 48 mb over periods of 36 and 42 hours; nothing even approaching the occasional northwest Pacific pressure falls of 40-90 mb in 24 hours (Holliday and Thompson, 1979) has been recorded in the Australian region.

The distributions of central pressure, latitude, and month at which rapid intensification commenced are shown in Figs. 6.9, 6.10 and 6.11. Rapid intensification typically started around 995 mb for both single and multiple period cycles and in 75% of cases ended within 12 hours of maximum intensity. A secondary peak may be seen at the 970-975 mb central pressure band and almost no rapid intensification cycles began below 970 mb. The mean latitude of commencement is near 15°S and the distribution is skewed towards higher latitudes. All of the low latitude observations occurred in the early or late part of the season, but the general distribution is normally distributed throughout the season.

The mean and median cyclone speeds at the start of rapid intensification were 4.1 and 3.6 m s^{-1} respectively; these are slightly slower than the mean speed of all hurricanes. With regard to direction of motion: 41% recurved within 24 hours of the rapid intensification cycle; 10% displayed evidence of a missed recurvature; 16% moved continuously westward; 21% moved eastward, the majority of which

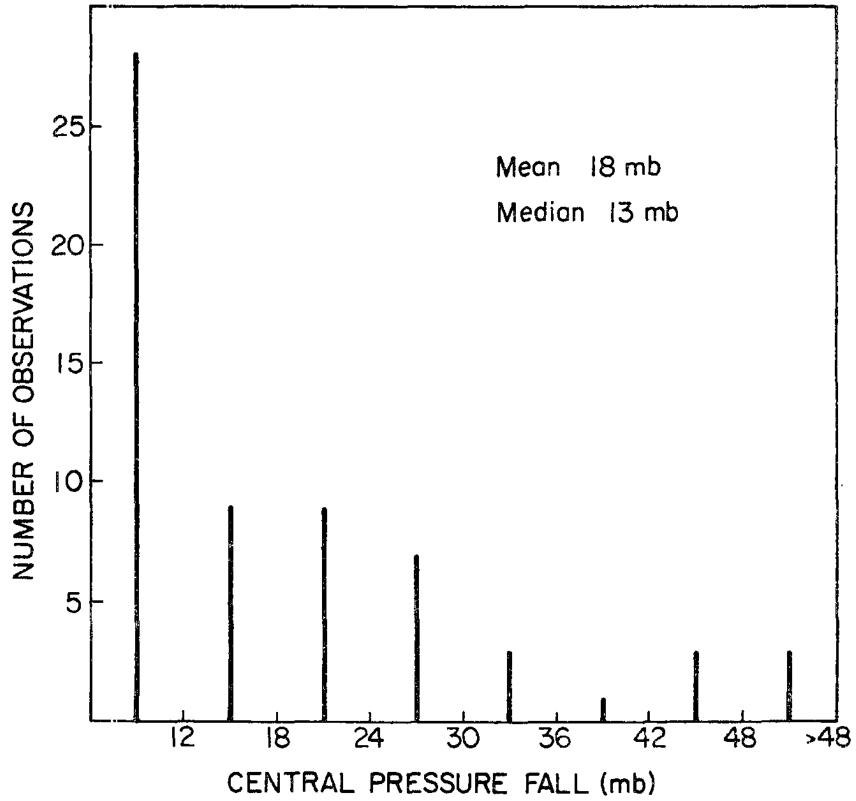

Fig. 6.8. Distribution, in 6 mb classes, of total falls in central pressure during rapid intensification cycles for Australian region hurricanes.

accelerated by more than 5 m s^{-1} within 24 hours of the rapid intensification cycle; 6% moved continuously southward; and 6% were distinctly erratic. These proportions are quite similar to the hurricane distribution in Fig. 6.1, an expected result since most hurricanes experience a period of rapid intensification.

6.3 The Physics of Cyclone/Environment Interaction

The manner in which a cyclone will respond to a given environmental (or internal) forcing is believed to be dictated by its basic structure, with the dominant features being the ratio of inertial to static stability and, to a lesser extent, the baroclinity.

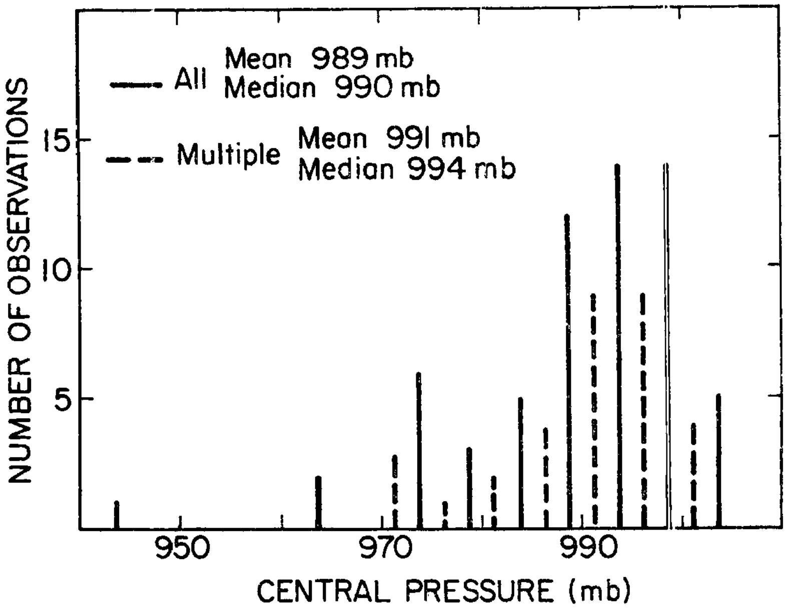

Fig. 6.9. Distribution, in 5 mb classes, of central pressure at which rapid intensification commenced and for: 1) all occurrences, 2) multiple period occurrences in which rapid intensification was maintained for at least 12 hours.

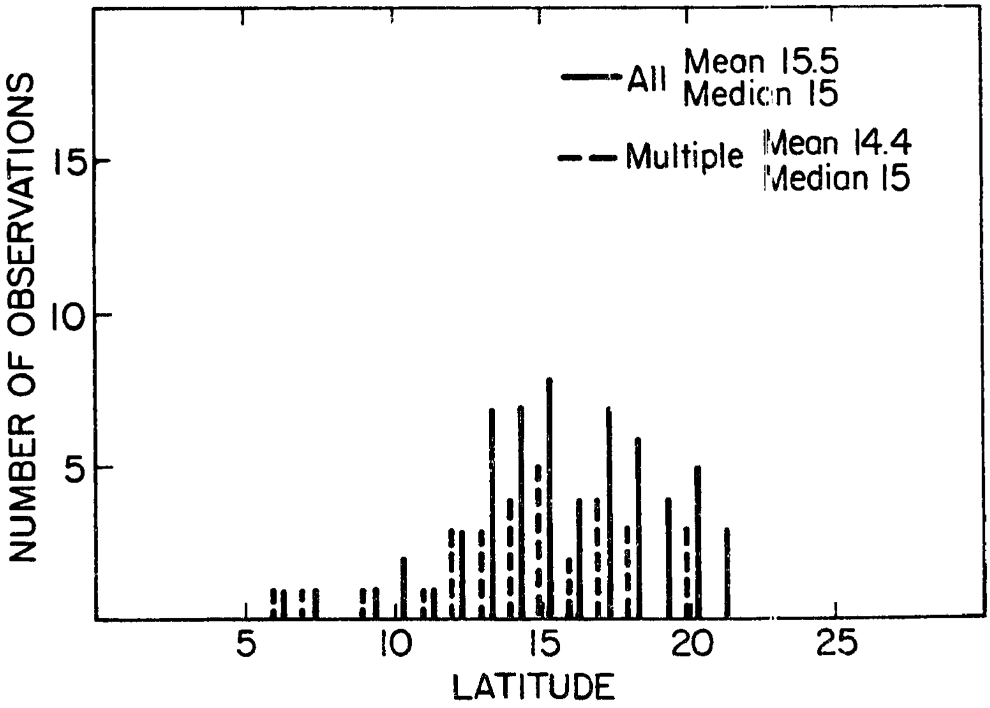

Fig. 6.10. Distribution, in one degree classes of the latitude at which rapid intensification commenced and for: 1) all occurrences, 2) multiple period occurrences in which rapid intensification was maintained for at least 12 hours.

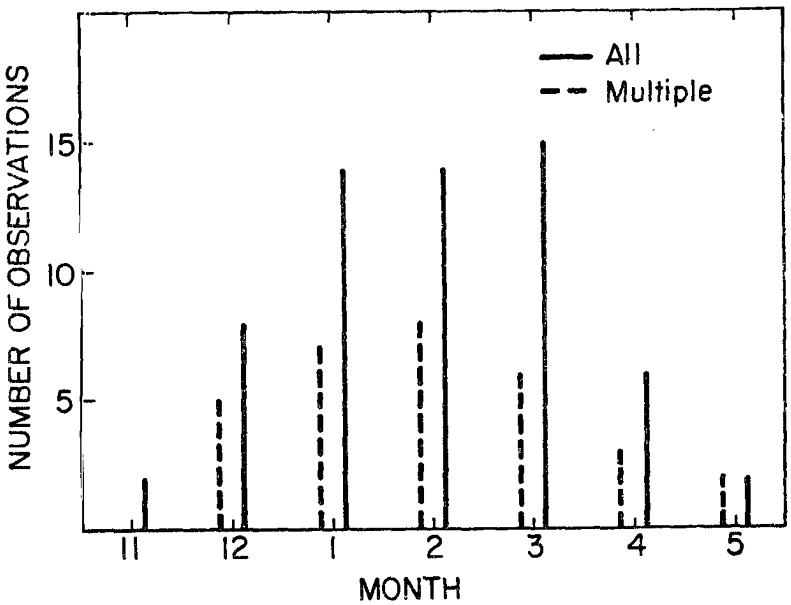

Fig. 6.11. Seasonal distribution, in one month classes, of the month in which rapidly intensifying cyclones occurred and for: 1) all rapidly intensifying cyclones, 2) those cyclones in which rapid intensification continued over more than one 6 hour period.

Physically, if we have an axisymmetric system, parcels leaving a constant forcing region (Fig. 6.12) are able to move horizontally or vertically depending on the inertial and static stabilities. For horizontal motion the radial gradient of angular momentum will cause an acceleration in the azimuthal wind speed, an increase in the cyclostrophic and Coriolis forces and a resistance to further horizontal motion (we neglect for simplicity the transient features of the geostrophic adjustment problem). The vertical density stratification in a statically stable atmosphere will also resist vertical motion. Mass continuity, however, requires that a circulation be completed. Then, as shown in Fig. 6.12, the induced circulation is determined by the relative effects of the inertial and static stabilities. For a relatively weak inertial stability a long horizontal circulation will occur and the effects will be felt some distance from the forcing

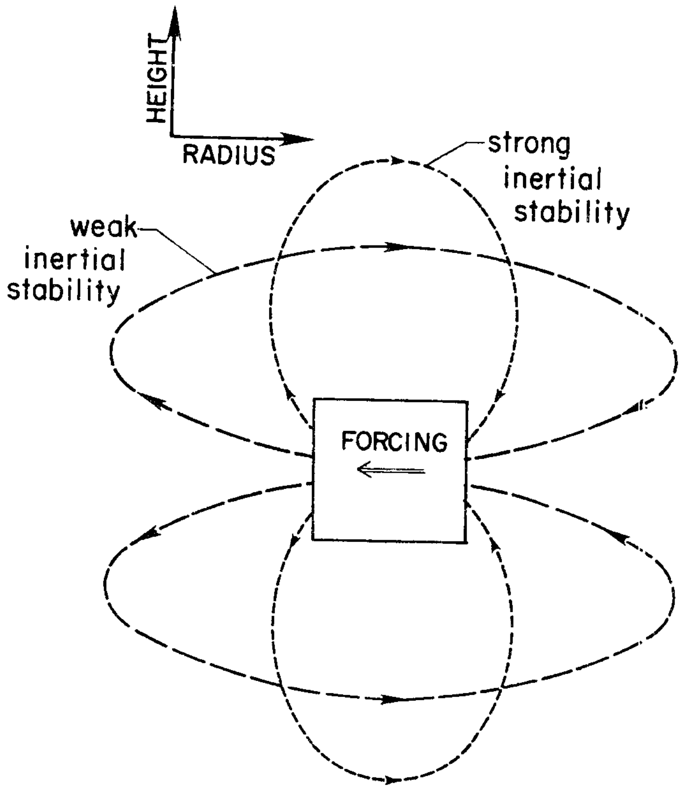

Fig. 6.12. A schematic of the secondary circulations arising from a specified forcing in a region of weak and strong inertial stability compared to the static stability.

regions. A relatively strong inertial stability, however, will constrain the circulation to the near vicinity of the forcing. A similar result to that shown in Fig. 6.12 will occur for a vertical forcing, such as a heat source. As has been shown by Eliassen (1951), baroclinity will also tilt the circulation axes in Fig. 6.12 as parcels tend to follow the sloping isentropic surfaces. Boundary conditions will further distort the circulations, as may be seen in the work of in Willoughby (1979), Schubert and Hack (1982a) and Shapiro and Willoughby (1982).

As an example let us consider the Large Northwest Pacific Typhoon in Fig. 6.13 (Merrill, 1982). This is almost identical to the oceanic hurricane described in Chapter 5, and has a basic structure which is

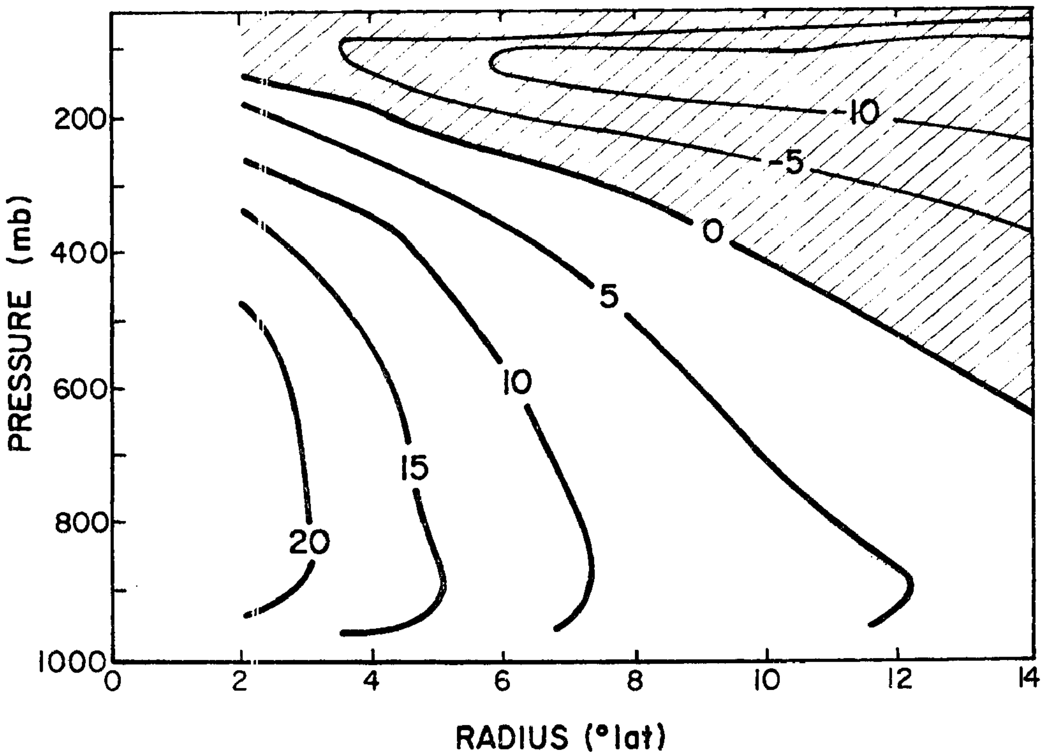

Fig. 6.13. Axisymmetric vertical cross-section of azimuthal winds ($m\ s^{-1}$) in the Large Northwest Pacific Typhoon.

typical of all hurricanes (eg. Gray, 1979). Core region winds were added to the axisymmetric cross section in Fig. 6.13 by presuming a maximum wind speed of 40 m s^{-1} at 50 km radius and 850 mb. The azimuthal winds were then interpolated to a 10 km by 30 mb grid using a 5 node bicubic spline.

The resulting inertial stability cross-section (obtained from Eq. A3.15 of Appendix 3) is shown in Fig. 6.14. Note how the lower levels are remarkably stable out to a large radius, whereas the upper levels are only weakly stable. Since the static stability (not shown) is essentially constant up to the stratospheric 'lid', this varying inertial stability characteristic provides a definite constraint on the secondary circulations which can arise from any imposed forcing. For

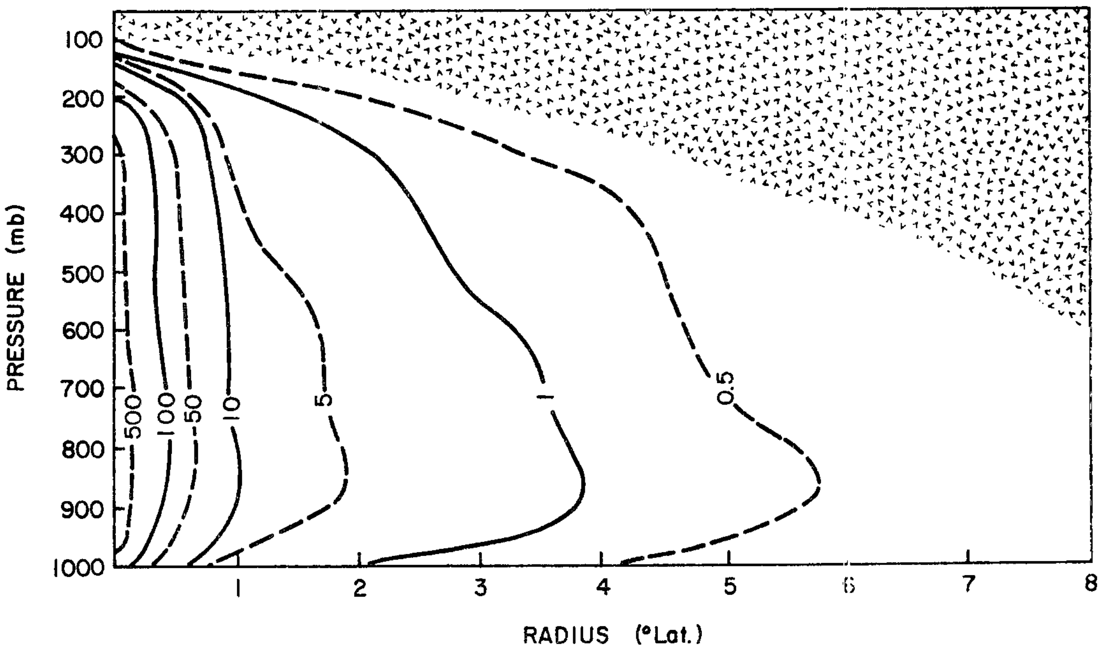

Fig. 6.14. Axisymmetric vertical cross-section of inertial stability (I^2, $10^{-8}s^{-2}$) in the Large Northwest Pacific Typhoon. The stippled region is less than f_o^2.

example, we would expect a low level environmental forcing at, say, 8° latitude radius to effect only the outer circulation. A similar upper level forcing may produce an effect in the central region.

A semi-quantitative indication of the likely response to such a forcing may be obtained from a diagnostic solution of Eliassen's (1951) balanced vortex equations as described in Appendix 3. These equations form the basis of early balanced hurricane models (Ooyama, 1969; Sundqvist, 1970) and have been used by Willoughby (1979), Challa and Pfeffer (1980), Smith (1981), Schubert and Hack (1982a), and Shapiro and Willoughby (1982) to examine secondary circulations and balanced response to sources of heat and momentum. We say semi-quantitative because the results are strictly applicable only to a balanced, perfectly axisymmetric system. Willoughby (1979) has shown that the lower level inner circulation is axisymmetric to a first approximation. But the upper levels, and in many cases the outer circulation, are often highly asymmetric. We shall consider the effects of these asymmetries presently, but at this stage will confine our discussion to the response of an axisymmetric vortex to a core region heat source, and to outer region upper and lower momentum sources.

<u>Core Region Heat Source</u>. The secondary circulation response to an imposed heat source of maximum 10K/day and distributed as shown in Fig. 6.15 is given in Fig. 6.16a. In agreeement with earlier work by Willoughby (1979), we see that two gyres are formed: with subsidence in the eye region, ascent in the heated region, and subsidence outside. As we have intimated in our previous discussion of moist convective interactions, a deep low level inflow layer and shallower, more intense upper outflow layer is established. Of most interest, however, is the horizontal constraint on the outer circulation by the high inertial stability. Strong subsidence occurs just outside the heated region and the radial circulation becomes negligible beyond 2-3^{o} latitude radius. Similar results have been obtained by Smith (1981).

<u>Environmental Forcing</u>: The response to an environmental imposition of an upper level outflow is simulated by the upper momentum forcing profile in Fig. 6.15. The maximum amplitude was chosen so that a radial outflow of 1-2 m s^{-1} was generated at 190 mb and 6^{o} latitude radius. The resulting secondary circulation is shown in Fig. 6.16b. Notable features are the long shallow outflow layer, the deep inflow layer, and the inflow in the stratosphere. This environmental forcing has a substantial effect on the core region, even to the extent of generating upper tropospheric and lower stratospheric subsidence in the eye region.

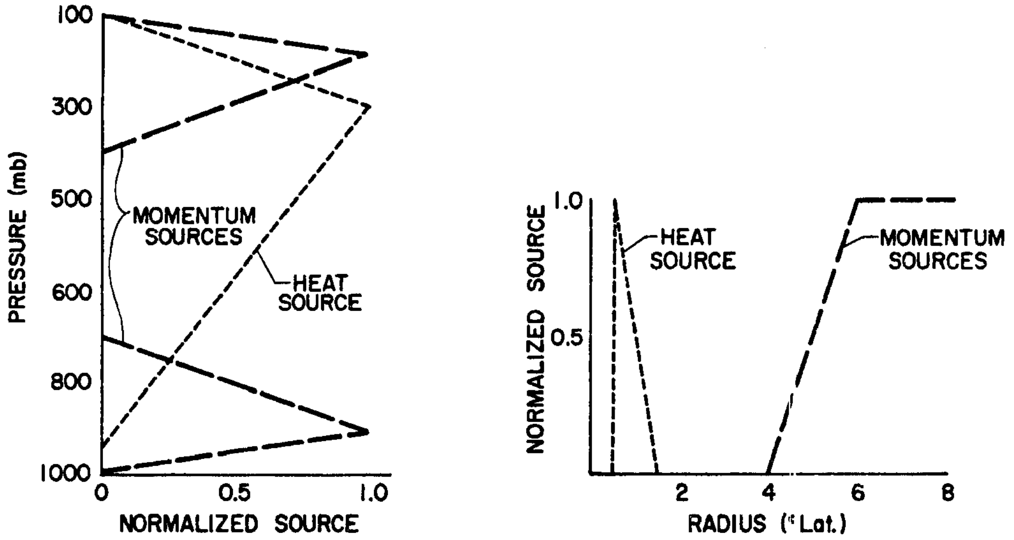

Fig. 6.15. Distributions of heat and momentum sources used in diagnosing the hurricane responses shown in Fig. 6.16.

By comparison, a lower level forcing with the same distribution (Fig. 6.15) produces a different response. As may be seen in Fig. 6.16c, a stronger radial flow occurs at 6^{o} radius. But the high inertial stability in the lower troposphere (Fig. 6.14) restricts the extent of the environmental forcing and its direct influence on the core is relatively small. If moist processes were included in a conditionally unstable atmosphere, this extent would probably be less.

6.4 Synthesis: The Intensity Change Process

6.4.1 Axisymmetric Effects

As we have discussed in section 6.1, moist convection is the primary driving mechanism in hurricane intensification. But there is substantial and convincing evidence that the rate of intensification, and ultimate intensity, are largely controlled by the environment.

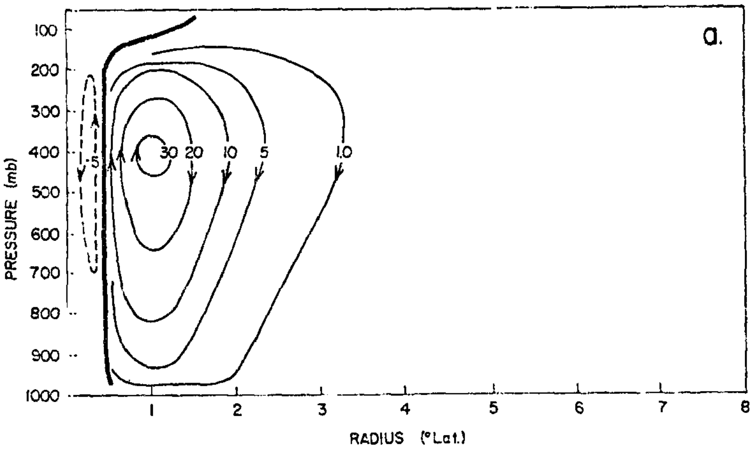

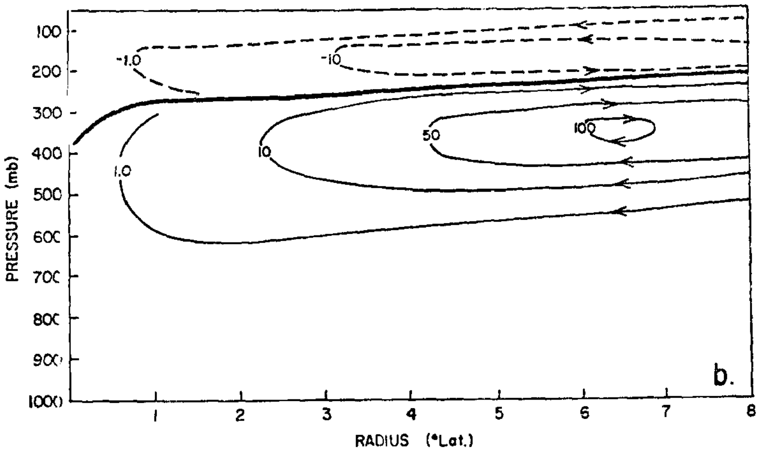

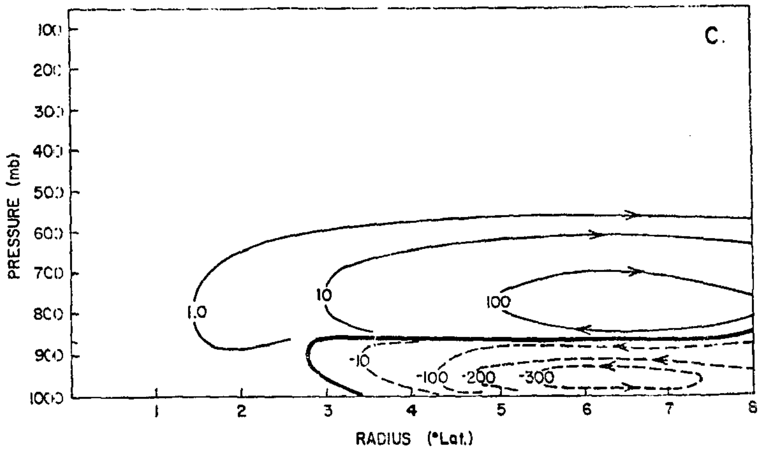

Fig. 6.16. Streamfunction fields showing secondary circulation responses to the heat and moment source distributions in Fig. 6.15: a) core region heating response; b) upper level environmental momentum forcing response; c) lower level environmental momentum forcing response.

Previous studies, including those of hurricane-like subtropical and polar low systems, together with our Australian region climatology, composite study of developing and major hurricanes and model diagnosis, indicate that for intensification the most effective cyclone/environmental interaction occurs in the upper tropospheric outflow layer. By comparison, these observations, plus the preliminary investigation by Merrill (1982), indicate that size change results from interactions in the lower troposphere.

The diagnosed secondary circulations from our application of Eliassen's balanced vortex equations are summarized in Fig. 6.17, and Fig. 6.18 also contains a schematic summary of the major secondary circulation features in intensifying systems over the Australian/southwest Pacific region. Taken together, these secondary circulations indicate that the above synoptic conclusions may be physically valid, at least insofar as linear environmental interactions with the axisymmetric component of the hurricane circulation is concerned.

As we have shown in Fig. 6.17, the strong lower level inertial stability inside 200-300 km constrains the horizontal extent of the secondary circulation response to a core region heating. By specifying a heated region of 50-150 km radial extent we produced a secondary circulation which was negligible beyond 250-300 km. A narrower heat source in the eyewall region would produce a much more constrained circulation. Thus, even though the observed inner region outflow maximum in Fig. 6.18 may be convectively driven, the long sustained outflow and secondary outer region maximum cannot be so explained.

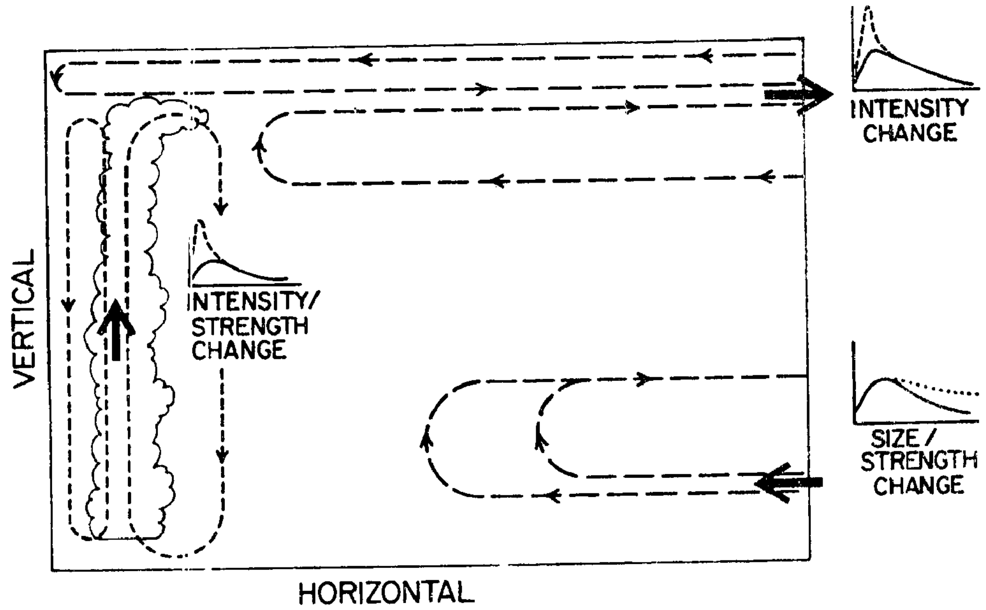

Fig. 6.17. Schematic summary of the secondary circulations resulting from inner core convective heating and outer region momentum forcing.

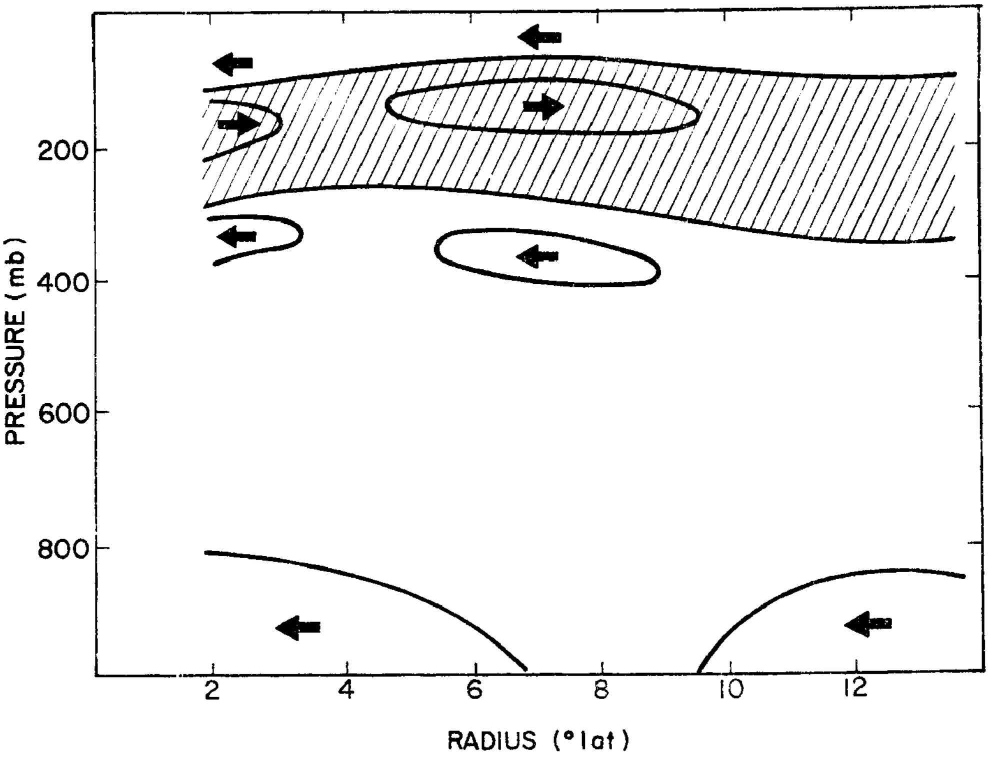

Fig. 6.18. Schematic summary of the observed axisymmetric secondary circulation in intensifying Australian/southwest Pacific region tropical cyclones.

We also believe that this constrained circulation response causes the donut shaped subsidence région which surrounds the eyewall at the end of the intensification stage of many intense hurricanes.

Since the inertial stability in a hurricane decreases with height and the static stability increases at the tropopause, the hurricane response to an upper level environmental forcing is quite different from that at lower levels. As we show schematically in Fig. 6.17, the upper level forcing extends a secondary circulation into the inner region of the cyclone. It thus may affect the core region directly by providing a long outflow channel, a mid to upper tropospheric inflow, and possibly by warming due to lower stratospheric inflow and enhanced subsidence in the eye. If the forcing is increasing with time a sustained upper level divergence may be also maintained over the hurricane core. Further, if we combine the secondary circulations arising from this upper level forcing and the core region heating a close approximation to the observed mid to upper tropospheric circulation in Fig. 6.18 is achieved. The subsiding branch is then well removed from the core region and spread over a wide area. Then long wave radiational cooling can effectively balance the subsidence warming, and the debilitating effect of excess subsidence drying near the eye is removed. Differential angular momentum transports between the outflow layer and the radial inflow response near 400 mb (Fig. 6.18) will also generate the observed strong upper tropospheric vertical wind shear (e.g., Fig. 5.10). This helps maintain and increase the observed warm core maximum near 300 mb.

By comparison our model results and observations in Figs. 6.17 and 6.18 indicate that a low level environmental forcing does not directly affect the core region. Rather, it provides an import of the substantial amount of angular momentum needed to provide the quite large (by other ocean basin standards) size and strength of the intensifying Australian/southwest Pacific region tropical storm and hurricane. A linear combination of this low level environmental forcing and the core region convection produces little, if any, extra effect. However, following the work of Schubert and Hack (1982a,b), the concomitant increase in inertial stability helps to organize the inner region moist convection. It also increases the efficiency of primary circulation ajustment to the convective heating. Thus, the outer region size change may lead indirectly to a strengthening and intensification of the tropical cyclone.

Recent numerical modeling results by Challa and Pfeffer (1980) provide some confirmation of these diagnostic results. They used Sundqvist's (1970) axisymmetric model (which is based on Eliassen's balanced equations) to examine tropical cyclone intensification under different imposed environmental forcing profiles. Though their discussion centered on asymmetric effects, their modelling results really were a response to an axisymmetric forcing. An upper level axisymmetric forcing, then, produced an intensity change with very little size change. In contrast a low level axisymmetric forcing produced a substantial size change, consequential intensity change, and development of a much stronger system. Compared to a reference run without forcing, Challa and Pfeffer found that the environment forcing produced a more rapid intensification and more intense systems. They also noted that even with subcritical sea surface temperatures (and presumably weaker convection) intensification could be maintained by the environmental forcing.

6.4.2 Environmental Forcing and Asymmetric Effects

Since the observed secondary circulations in intensifying tropical cyclones require some form of upper tropospheric, outer region forcing, we proceed naturally to the question of how this can be achieved. Other important questions involve the validity of our linear, axisymmetric diagnosis, the effects of asymmetries, and the mechanisms whereby the core region and environment become coupled. A complete answer to these questions requires far more research than we have done in this study, together with better outflow layer observations. However, our present knowledge does enable us to speculate on some of the more likely processes.

Low Level Forcing: Let us first consider the low level inflow into the outer regions of the intensifying storm (Fig. 6.18). We have shown in Chapters 4 and 5 that this is maintained by a combined equatorial influx from the monsoonal westerlies and a subtropical influx from the trade wind easterlies.

Love (1982) has examined the role of the equatorial surge in the establishment and development of pre-tropical storm depressions. He proposed, and produced convincing supporting evidence, that this resulted from a surge originating in the winter hemisphere. The basic argument is that the cold winter hemisphere surge creates a high pressure region over the equator. In these low latitudes, an unbalanced, down the pressure gradient surge is then developed which extends into the vicinity of the incipient depression. Subsequent pressure falls in the developing disturbance could also help maintain or enhance such a process.

The initiation of the subtropical trade wind surge has long been a forecasting rule for tropical depression intensification in the Australian region (e.g., Wilkie, 1964). It is a quite transient effect associated with strong anticyclogenesis poleward of the depression.

Both inflow mechanisms seem to be operating equally in our composite tropical storm of Chapter 4. But this is probably an artifact of the compositing process. It is more likely that the equatorial surge will be more important in low latitude systems and the trade wind surge will predominate at higher latitudes.

Upper Level Forcing: A number of forcing mechanisms may operate in the outflow layer of tropical cyclones and thus contribute to the observed variety of outflow configurations around the world (Chen, 1983). We shall only consider three. The first is the subtropical jet/cyclone outflow interaction, which we have shown to be the predominant mechanism in the Australian/southwest Pacific region. The second is the development of regions of inertial instability, which seems to be the main mechanism in numerical models. And the third is the weaker equatorial outflow, which we have also observed in our composite study

A plausible explanation for the development of the poleward outflow jet lies in the reduction of inertial stability and the divergence fields associated with the subtropical jet. The high speed westerlies moving into near proximity with the cyclone core develop a strong anticyclonic shear and substantially reduce the already weak inertial stability on the cyclone's poleward side. They may even produce transient regions of instability, though these have never been observed.

Following our observations of Hurricane Kerry in Figs. 5.37, 5.38, a possible interaction scenario might follow the schematic depiction in Fig. 6.19. Substantial divergence will develop in the hatched region when an anticyclonically curved jet streak lies southeast of the incipient hurricane (McRae, 1956). Should there be a concomitant amplification of the upstream trough and movement towards the cyclone, this divergence will be further enhanced (Ramage 1959, 1974). In the statically stable, low inertial stability atmosphere which the juxtapositioning of the cyclone outflow and subtropical westerlies has developed, this divergence can be partially compensated by horizontal as well as vertical motion. Thus, the cyclone outflow turns, accelerates, and forms a strong outflow channel into the divergent region. The initialization of this outflow channel may be aided by a transient establishment of an inertially unstable region between the cyclone and subtropical jet. But once the channel is established the inertial stability actually increases slightly.

As we show in Fig. 6.20, the compensating return flow tends to occur immediately above and below this shallow outflow channel.

Thus, even though the cyclone/environment interaction is quite asymmetric, our simple axisymmetric diagnosis in the previous section appears to be physically valid. Note, however, that much of the compensating motion for the divergence region in Fig. 6.19 is actually provided by the westerly winds and nearby vertical motion. But, there is also a large volume reduction from the interaction region to the cyclone core. Hence, only a very small proportion of the interaction region mass flow is required to produce a substantial core region response. From an axisymmetric viewpoint, an otherwise uncompensated

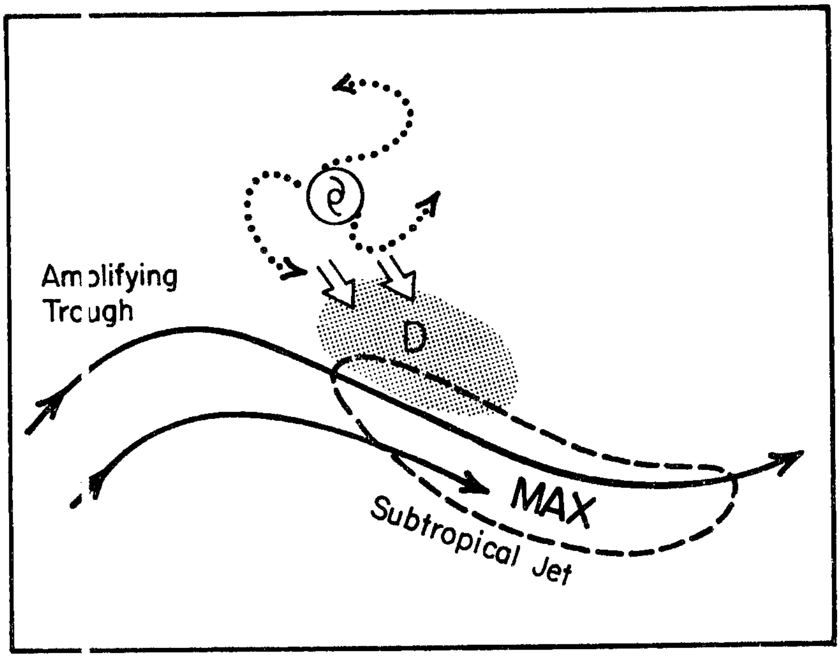

Fig. 6.19. An illustration of the manner in which the subtropical westerlies and cyclone may interact to produce an extended poleward outflow channel.

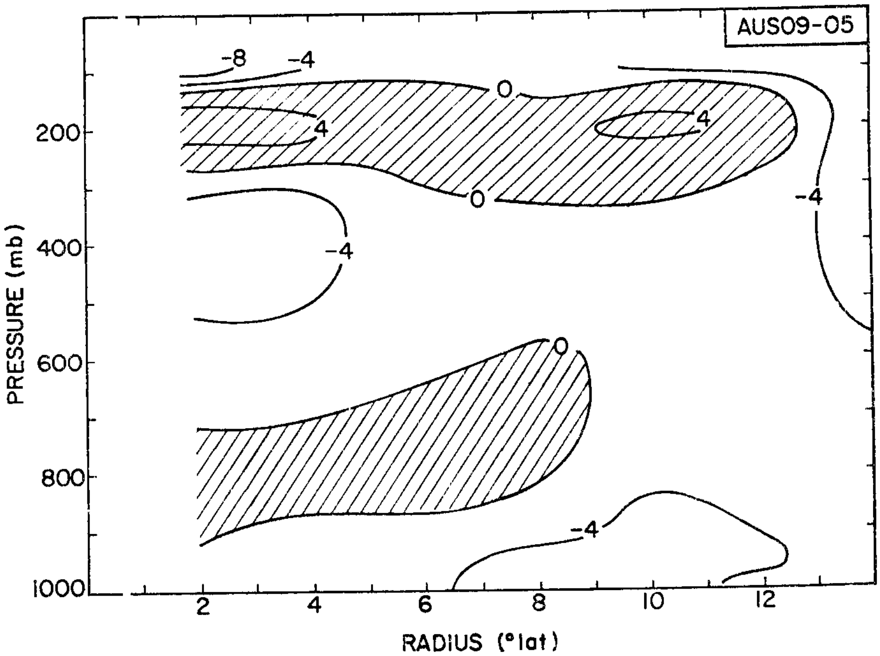

Fig. 6.20. Meridional cross-section poleward of the Pre-hurricane Tropical Storm showing the marked lower stratospheric and 400 mb return flows above and below the divergent flow at 200 mb.

1 m s^{-1} variation in radial wind at an interaction radius of 6^{o} latitude would induce a 10-12 m s^{-1} radial wind at the maximum wind radius. Hence, almost undetectable axisymmetric outflow variations in the outer circulation could still be responsible for large eye region changes.

There are, further, probably non-linear interactions which could not possibly be discerned in an axisymmetric model. Because of the scales involved, the initial coupling must occur by a chance interaction between initially independent systems. But once the coupling occurs the subtropical and cyclone systems may interact to their mutual enhancement. For example once the outflow forms it will provide strong warm air advection ahead of the trough, which, together with the warm cyclone core, can enhance the baroclinicity of the cold upper level trough. Confluence between the cyclone outflow and westerlies may also provide a strong frontogenetic influence. Thus, baroclinic, or barotropic, processes may amplify the upstream trough, which increases the downstream divergence, which further enhances the outflow channel, and so on. It is also possible that the warm cyclone outflow could initiate a perturbation in the nearby upper level subtropical westerly flow.

Studies of intensity change by advanced numerical models have relied almost entirely on internal processes and have certainly produced intense hurricanes. As has been shown by Anthes (1972), these hurricane models develop an asymmetric outflow, with strong jets, by generating regions of inertial instability. Kitade (1980, Fig 14) shows that large areas become unstable and DeMaria (1983) finds that the local anticyclonic vorticity may approach twice the magnitude of the Coriolis vorticity. Yet, even though the outflow region is only weakly stable in nature, there has been no proof that large areas of instability develop: Alaka (1962) presented a detailed analysis of the outflow layer of the developing hurricane Carla and could find at best very small, and presumably transient, instability regions; Black and Anthes (1971) found none. It is possible that the strong outflow near 2° latitude radius in Fig. 6.18 is partially due to inertial instability in the unresolved core region. This possibility is supported by the associated strong inflow maxima near 400 mb and in the lower stratosphere which would be the expected response to a forced outflow at 150-200 mb. But it is highly unlikely that the observed outer region outflow arises from sustained inertial instability. The logical conclusion, then, is that without any environmental interaction, numerical models must take the alternative, and presumably more difficult, path of developing large regions of instability.

In addition to the major poleward outflow channel, our Australian/southwest Pacific region composites also display a weaker, high level equatorward outflow. This seems to be a consistent feature of most tropical cyclones in all ocean basins. Chen (1983) has shown that for the FGGE year at least 50% of all tropical cyclones had some form of equatorward outflow channel.

Taken alone, this is a physically reasonable result. Other things being equal the inertial stability should be weaker on the equatorward side. Thus weaker environmental features, such as an equatorial easterly jet, may induce a strong response. However, the convective feeder band emanating from lower latitudes will also contribute to the maintenance of this equatorward outflow jet. Lee (1982) has shown that the total convective effect in tropical cyclones is a downgradient rearrangement of angular momentum. Essentially, lower level cyclonic angular momentum is deposit in the upper outflow layer. Lee also presented a trajectory analysis of the outflow regions of a composite northwest Pacific typhoon and showed a southwesterly 'jet' with air flowing across absolute angular momentum surfaces. Since this jet also lies over the general position of the major equatorial feeder band, Lee arrived at the reasonable conclusion that the convective cells maintain an infusion of more cyclonic air from below. This continuous source then allows the air to flow across the absolute angular momentum surfaces.

Both our observations and the modelling results of DeMaria (1983) provide confirmation of these conclusions. DeMaria conducted two parallel experiments, one with and one without momentum transports in his cumulus parameterization scheme. With momentum transports a strong equatorward jet developed over the major feeder band. Without such transports a weaker and more constrained outflow resulted. Observationally, it is notable that our composites show a weak equatorward outflow concentrated near the tropopause where the deep convective detrainment is largest. It is also strongest over the mean convective region (as indicated by the 500 mb moisture fields) and weakens rapidly on leaving that region.

6.5 Summary

In this chapter we have investigated the major mechanisms associated with the intensification and decay of tropical cyclones in the Australian/southwest Pacific region.

Following Merrill (1982) we have separated tropical cyclone intensification into three modes: an acceleration of the maximum winds with no change in outer circulation, which we refer to as intensification; an acceleration of the outer circulation with no change in maximum winds, which we refer to as size change; and an overall increase of relative angular momentum in the core region, which we refer to as strength change. We have shown diagnostically and observationally that size, strength and intensity change arise from different environmental processes. Specifically: inner core convection and upper tropospheric couplings with the environment can directly affect intensity change lower level couplings can produce an initial size change followed by a non-linear feedback and eventual strength and intensity change The dominant parameter in producing these differential responses is the variations of inertial stability within the cyclone.

In our observations for the Australian/southwest Pacific region, we find agreement with recent work by Love (1982) and earlier forecasting rules (e.g. Wilkie, 1964), that the early intensification period follows a size change from low level cyclone/environment interactions; specifically by surges from the monsoonal westerlies and trade wind easterlies. Intensification past the tropical storm stage, and particularly the development of major hurricanes, seems to require a favorable coupling with the subtropical jet stream. This coupling is similar to that described by McRae (1956) and produces a long sustained outflow channel to the southeast. The observed coupling requires a precise juxtapositioning of the cyclone and subtropical jet. Should they be too far apart, a coupling will not occur. Should they approach too closely, the cyclone will be destroyed.

By comparison, we have noted that numerical models, which do not have the above environmental interactions, tend to create outflow jets by the development of large regions of inertial instability. Except, perhaps, for the inner core region, such inertially unstable regions have not been observed in nature.

Substantial questions still remain on the linkages and highly non-linear and asymmetric processes which accompany these cyclone/moist convection/environment interactions. These are the topic of ongoing research.

7. TROPICAL CYCLONE MOTION

> "Some will be found to be relatively simple systems moving straight away under a definite wind and pressure pattern that is not changing. These are easy, but there are others so complicated, so buffeted by changing currents or opposing forces, that forecasting is very uncertain and trying' : Norton (1947)

Tropical cyclone motion is a complex, non-linear geostrophic adjustment process which results from an interaction between the cyclone circulation, the environmental wind field, the earth's vorticity field, the underlying surface and the fields of moist convection. Though the detailed physics, and particularly the non-linear interactions, are poorly understood at this stage, we have recently indicated (Holland, 1982, 1983b) that the dominant mechanisms appear to be the interactions with the environmental wind field (including asymmetries) and with the earth's vorticity field. In this chapter we shall summarize and extend this preliminary theoretical work and discuss the results in terms of tropical cyclone observations in the Australian/southwest Pacific region. No attempt is made to completely survey the considerable literature on this topic. For the interested reader, excellent surveys may be found in George and Gray (1976), Bureau of Meteorology (1978), WMO (1979) and Chan (1982).

7.1 Background and Theory

7.1.1 Isolated, Axisymmetric, Barotropic Vortex on a β Plane With no Friction

The frictionless horizontal equations of motion in cylindrical coordinates are given by

$$\frac{du}{dt} - \frac{v^2}{r} - fv = -\alpha\frac{\partial p}{\partial r} \qquad (7.1)$$

$$\frac{dv}{dt} + \frac{uv}{r} + fu = -\frac{\alpha}{r}\frac{\partial p}{\partial \theta} \qquad (7.2)$$

where u, v are the radial and azimuthal wind components and the other symbols have their usual meaning (c.f. Appendix 1).

Let us first consider an isolate vortex which has both axisymmetric wind and pressure fields. Since the Coriolis force f varies with latitude this vortex cannot be in gradient wind balance. If we let gradient wind balance be satisfied due east and west of the center, then from Eq. (7.1), if we let f_o be evaluated at the cyclone center and assume a constant $\beta = \beta_o$.

$$\begin{aligned}\frac{du}{dt} &= \frac{v^2}{r} + (f_o + \beta_o r\cos\theta)v - \alpha\frac{\partial p}{\partial r} \\ &= v\beta_o r\cos\theta \qquad (7.3)\end{aligned}$$

Then, the vortex will experience an outward radial acceleration in its poleward sector and an inward radial acceleration in its equatorward sector from the unbalanced Coriolis force. The net result is a poleward acceleration of the vortex. If we integrate Eq. (7.3) over the vortex domain we get a poleward acceleration per unit mass given by

$$a = \frac{\beta_o}{\pi R^2} \int_o^R v r^2 dr \tag{7.4}$$

where R is the racial extent of the vortex. This is the result obtained by Rossby (1948), and which has been used for many years to explain the observed poleward drift of cyclonic vortices and equatorward drift of anticyclonic vortices. However, the result is merely a geostrophic adjustment to an initially unbalanced vortex and there appears to be no evidence that atmospheric vortices actually exist in such a continuous state of imbalance.

Let us therefore consider an axisymmetric vortex that is in gradient balance. From Eq. (7.1) this implies that the radial pressure gradient varies azimuthally according to

$$\alpha \frac{\partial p}{\partial r} = \frac{v^2}{r} + f_o v + v\beta_o r\cos\theta \tag{7.5}$$

hence if we assume no horizontal density variations and take an azimuthal derivative, and a radial integration:

$$\left(\alpha \frac{\partial p}{\partial \theta}\right)_{r=R} = -\beta_o \sin\theta \int_o^R r\ v\ dr \tag{7.6}$$

substituting Eq. (7.6) into (7.2) and noting u = o we have

$$\frac{dv}{dt} = \beta_o \frac{\sin\theta}{R} \int_o^R r\ v\ dr \tag{7.7}$$

and since there are no advective terms (u, $\partial v/\partial\theta = 0$) the LHS is equal to the local time derivative. We can see from the sin θ term on the RHS that the acceleration is cyclonic to the west and anticyclonic to the east. Thus, the initial effect on the vortex in this case is to move it westward.

If we presume that the vortex remains in a balanced state the beta plane effect can be more easily seen from the vorticity equation. We start with the frictionless, divergent barotropic vorticity equation in cylindrical coordinates

$$\frac{\partial \zeta}{\partial t} = -u\frac{\partial \zeta}{\partial r} - \frac{v}{r}\frac{\partial \zeta}{\partial \theta} - v_n\beta - \frac{\zeta+f}{r}\left(\frac{\partial ru}{\partial r} - \frac{\partial v}{\partial \theta}\right) \quad (7.8)$$

where ζ is the relative vorticity and v_n the meridional component of wind speed. Then, for a symmetric vortex on a beta plane we have zero u, $\partial\zeta/\partial\theta$ and divergence $(\partial ru/\partial r + \partial v/\partial\theta)$, and

$$\begin{aligned}\frac{\partial \zeta}{\partial t} &= - v_n\beta_o \\ &= + v\beta_o \sin\theta \qquad (7.9)\end{aligned}$$

The sin θ term provides a cyclonic vorticity change to the west and anticyclonic to the east. Thus, the vortex initially drifts westward and we have the same result as for Eq. (7.7). The equivalence between Eqs. (7.7) and (7.9) may be seen by first noting that, for our axisymmetric vortex $\zeta = \frac{1}{r}\frac{\partial rv}{\partial r}$. Then, from Eq. (7.9)

$$\frac{\partial}{\partial t}\frac{1}{r}\frac{\partial rv}{\partial r} = v\,\beta_o \sin\theta$$

or

$$\frac{\partial}{\partial r}\left(\frac{\partial rv}{\partial t}\right) = v\,r\,\beta_o \sin\theta$$

and hence

$$\frac{\partial v}{\partial t} = \beta_o \frac{\sin\theta}{R}\int_o^R r\,v\,dr$$

which is the same as Eq. (7.7).

The advantage of using the vorticity equation is that following the approach suggested by Holland (1983b) we can explicitly calculate the initial speed and direction of motion of the vortex (non-linear effects will be considered later). To do this we assume that the vortex will move toward the region of maximum vorticity change. The direction and speed of motion will then be given by the solutions to

$$\frac{\partial}{\partial\theta}\left(\frac{\partial\xi}{\partial t}\right)' = 0 \tag{7.10}$$

$$V_c = -\left[\left(\frac{\partial\xi}{\partial t}\right)'/\left(\frac{\partial\xi_s}{\partial r}\right)\right]_{\theta_m} \tag{7.11}$$

where θ_m is the solution to Eq. (7.10), ξ_s is the vorticity associated with the symmetric vortex, and the prime indicates that any azimuthally symmetric terms, which can alter the size, strength or intensity but not the initial motion tendency, have been neglected.

We next assume that the tropical cyclone may be approximated by a modified Rankine vortex. (A justification for using the Rankine vortex may be found in Appendix 4.) Then:

$$v_s = c/r^x \qquad r>r_m, \qquad 0 < x < 0.8 \tag{7.12}$$

$$u_s = -\gamma v_s \qquad \begin{array}{l}\gamma > 0 \text{ Northern Hemisphere}\\ \gamma < 0 \text{ Southern Hemisphere}\end{array} \tag{7.13}$$

where u_s and v_s are the radial and azimuthal wind components of the symmetric cyclone; c, x and γ are constants which define the intensity, radial profile shape and divergence for the cyclone; and r_m is the radius of maximum winds. If we substitute Eqs. (7.12) and (7.13) in the

For a uniform basic current the radial dependence arises solely from the interaction between the vortex and the gradient of earth vorticity. Hence we can also simplify our discussion, without loss of generality, by only considering an isolated axisymmetric vortex on a beta plane.

For a vortex we use the axisymmetric portion of the AUS05 oceanic hurricane (Appendix 2) shown in Fig. 7.2. The 800-300 mb azimuthal wind profile is approximated by

$$v = c_1 r^{-x} - c_2 r^{y} \tag{7.22}$$

where $x = 0.5$, $c_1 = -7{,}218$, $y = 2.0$, $c_2 = -4.4 \times 10^{-12}$, and a maximum wind of 40 m s^{-1} at a radius of 32.6 km is assumed. This profile is almost exactly a modified Rankine vortex inside 200-400 km. Outside this region the $c_2 r^y$ term compensates for the tendency of the modified Rankine vortex to overestimate the actual winds. As we show in Appendix 4, Eq. (7.22) can approximate the actual wind profiles very well.

Outer Region Distortion and Induced Poleward Motion: Figure 7.3 shows the local vorticity changes resulting from applying Eq. (7.9) to the axisymmetric portion of AUS05 on a beta plane valid at 18.2°S (the mean latitude of the composite hurricane). We can see that there is no beta effect due north/south of the center, where the winds are zonal. The vorticity changes are largest due east/west where the meridional wind component is maximum, and decrease with increasing radius.

The resulting radial deformation of the vortex obtained by applying Eq. (7.11) at all Θ, is shown in Fig. 7.4. There is obviously a tendency for considerable distortion. The vortex elongates on the western side and compresses on the eastern side, and the effect is maximum at about 6° latitude radius. The reasons for this distortion are more clearly seen in the zonal cross-section of Fig. 7.5. At point

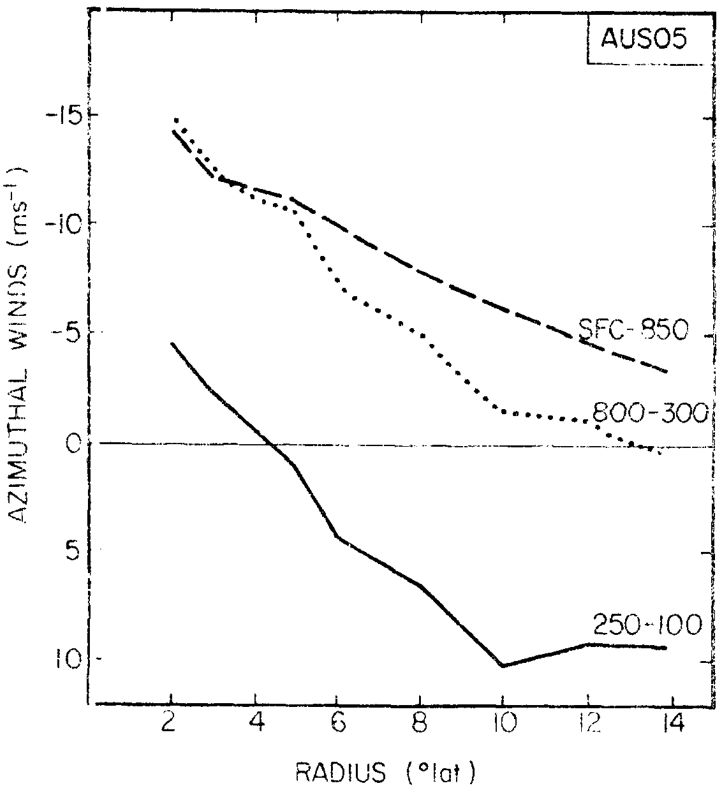

Fig. 7.2. **Axisymmetric radial profiles of pressure weighted average azimuthal winds over three levels in the AUS05 hurricane composite.**

A the vorticity change is quite large, but, because of the strong vorticity gradient there, only a very small compensating vortex motion occurs. At point B, the vorticity change is smaller than at point A, but, because of the weaker vorticity gradient, a much larger compensating vortex motion is required.

If we next assume that the inner region does not distort and moves exactly with the 2° latitude radius vortex ring (more on this later), the net distortion of the outer regions will be as shown by the stippled area in Fig. 7.5. The vortex becomes more cyclonic to the west and less cyclonic, and possibly anticyclonic to the east.

DeMaria (1983) provides an equivalent, but alternative explanation for this distortion in terms of Rossby wave separation. If we consider

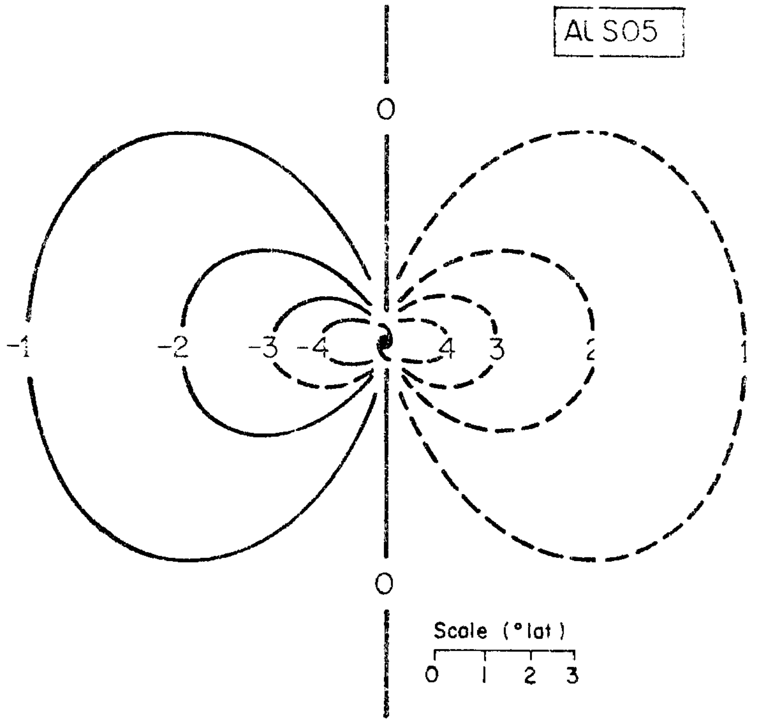

Fig. 7.3. Local change of relative vorticity ($10^{-10} s^{-2}$) resulting from the beta effect on the oceanic hurricane, AUS05

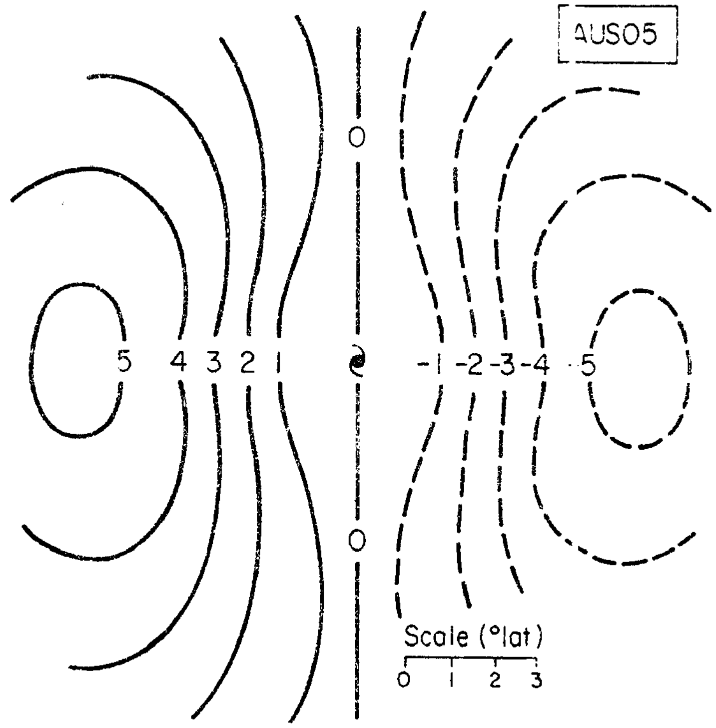

Fig. 7.4. Deformation (in units of m s^{-1} radial speed) resulting from the beta effect on the oceanic hurricane, AUS05.

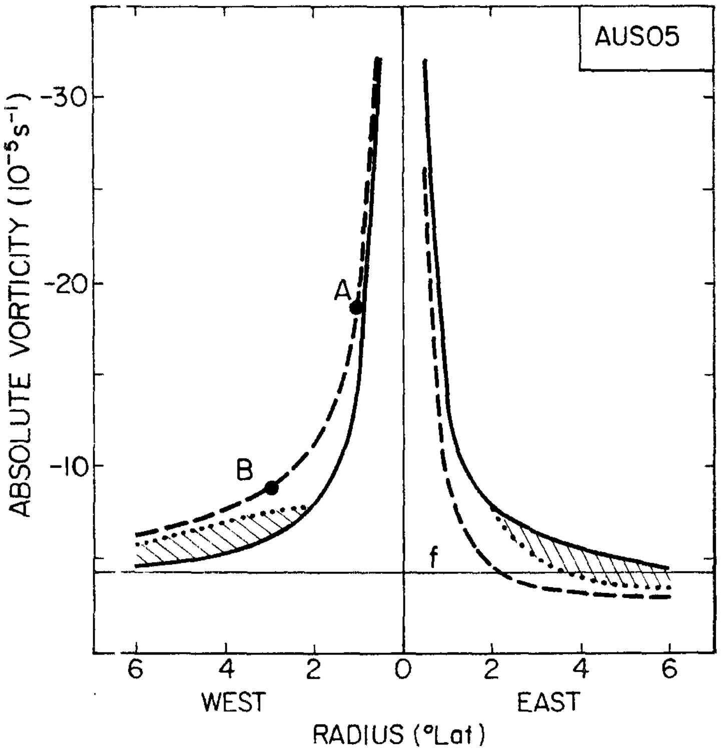

Fig. 7.5. Zonal cross section through the oceanic hurricane, AUS05 showing: the initial vorticity profile (——); the vorticity profile after 1 day of uncompensated distortion (- -); and the outer region vorticity changes on the assumption that no inner region distortion occurs (hatched).

the initial vortex to be made up of a package of Rossby waves, then the beta effect will cause the longer waves to move westward more quickly than the shorter waves. Thus, a wave separation will occur. The longer waves will congregate to the west of the vortex and cause an elongation of the vortex there. The shorter waves will congregate to the east, causing a vortex compression and possibly anticyclogenesis there.

Now we know that the circulation around a given area, A, is equal to the integrated vorticity over that area:

$$C = \int_A \zeta \, dA \tag{7.23}$$

Hence the vortex distortions shown in Fig. 7.5 will introduce a cyclonic gyre to the west and anticyclonic gyre to the east. As has been noted by Anthes (1982, p. 107), these gyres introduce a poleward steering current over the cyclone center. Then, the cyclone, which was initially moving due westward, turns and accelerates poleward.

Thus, the poleward drift of tropical cyclones is caused by the development of a poleward steering current, not by maintaining the vortex in a continuously unbalanced state, as was suggested by Rossby (1948).

Of course these distortions do not continue unabated, for they would soon destroy the cyclone. Rather, any distortion immediately activates the advection and divergence terms in Eq. (7.8). These then begin to compensate for such distortion. Numerical modelling experience (c.f., Holland, 1983b; DeMaria, 1983; or Fig. 7.7) indicates that the cyclone quickly gains a steady state with the advection and divergence cancelling the beta effect distortion. The motion then reduces to a quasi-linear combination of the westward, beta effect, and a poleward advection by the induced steering current. Actual tropical cyclones (Fig. 7.6) also tend to move along smooth, consistent tracks with no evidence of any domination by uncompensated non-linear processes.

Non-linear processes may become important during a period of changing environment, such as at recurvature, but, as we shall show in section 7.2.2, recurvature can certainly be explained from linear processes alone. There are, however, a number of erratically moving cyclones, such as Edith (#2) and Cynthia (#8) in Fig. 7.6, which may be dominated by uncompensated, evolving non-linear processes. We shall not consider these types of motion further in this chapter.

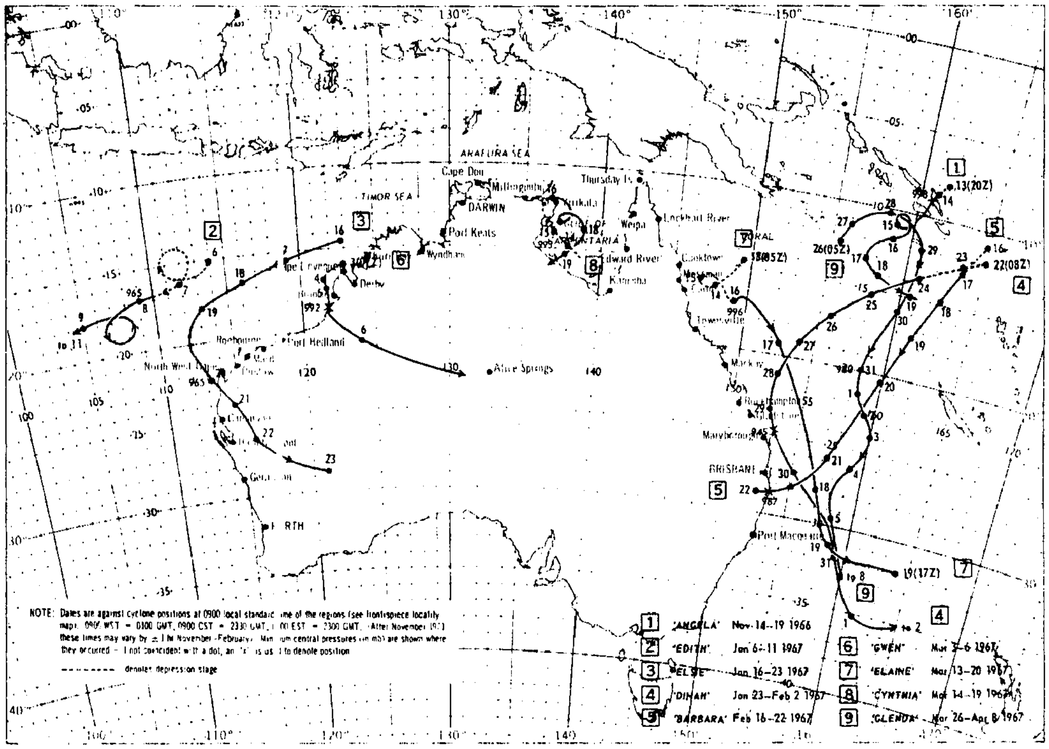

Fig. 7.6. Australian region tropical cyclone tracks for July 1966 to June 1967 (from Lourensz, 1981).

The net distorting effect on the vortex may be seen quite clearly in Fig. 7.7. This figure contains the results of f and β plane integrations of a nondivergent barotropic model from an initially axisymmetric vortex by DeMaria (1983). Also shown is the AUS05 850 mb wind field. We can see that no distortion occurs during the f plane integration. On the β plane, however, the cyclone elongates to the west and compresses to the east, with anticyclogenesis farther to the east. Similar modelling results have been presented by Anthes (1972) and Anthes and Hoke (1975), who also showed that introducing divergence tends to accentuate the beta effect distortion.

The actual wind field for AUS05 is strikingly similar to the β plane vortex, as indeed are all composites presented throughout this study. This implies that the asymmetries are largely induced by the

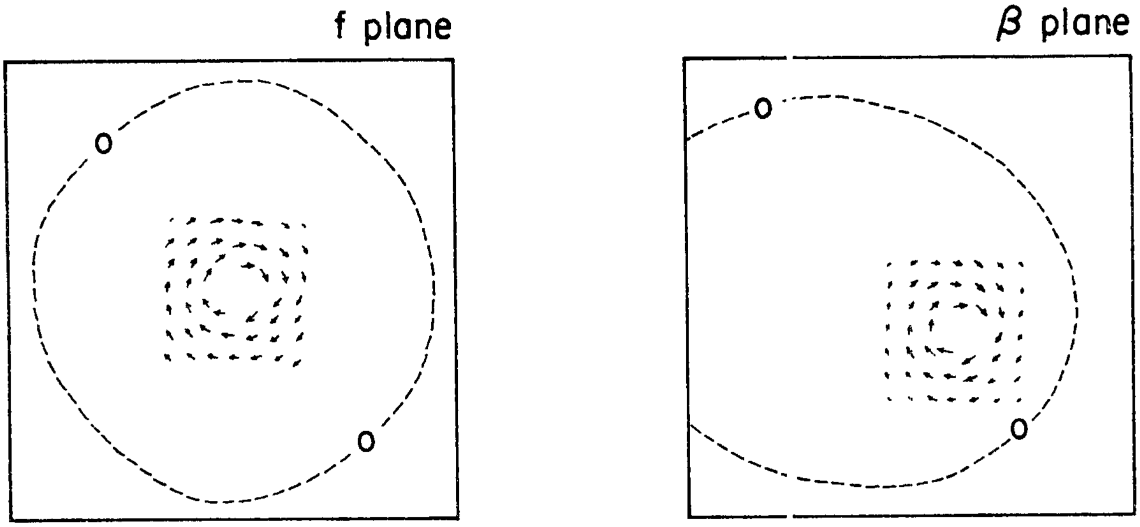

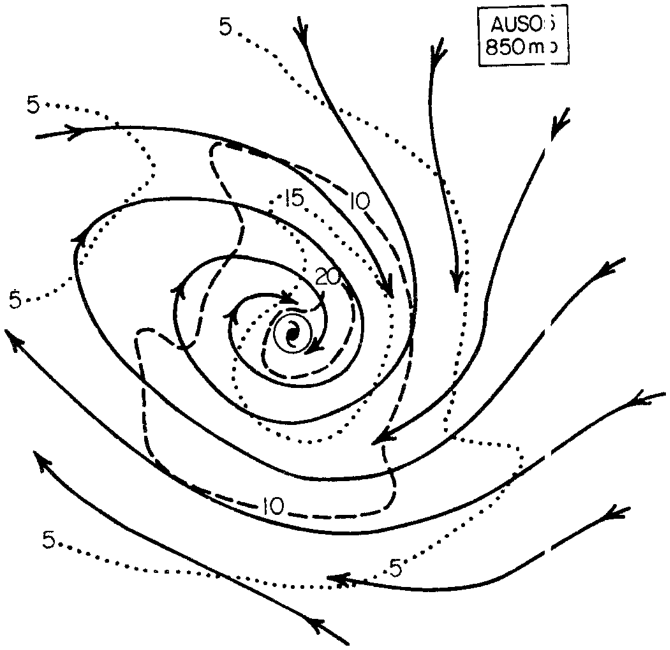

Fig. 7.7. Vortices resulting from integrations of a nondivergent barotropic model from an initially axisymmetric vortex on f and β planes (upper) (after De Maria, 1983) together with the AUS05 850 mb wind field (lower).

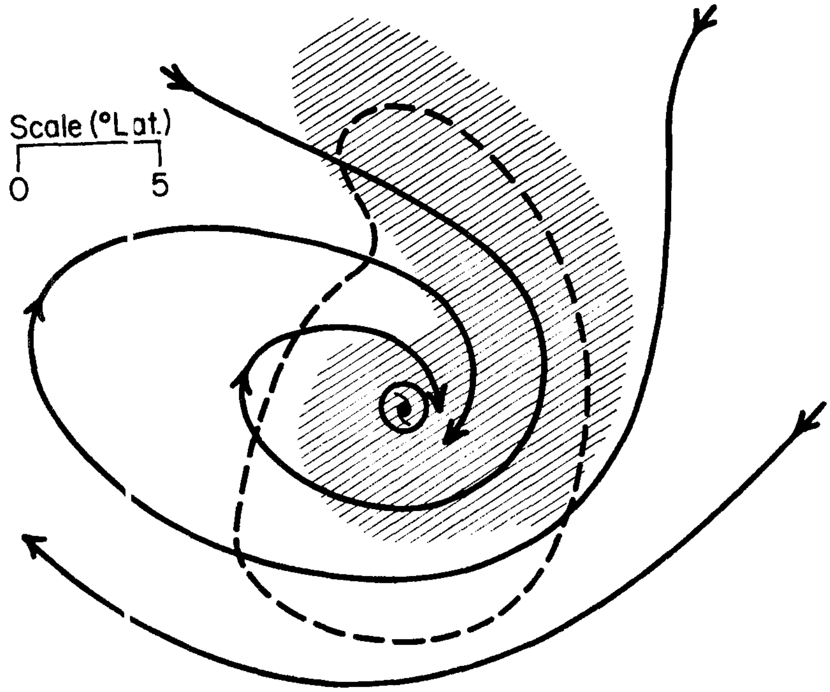

Fig. 7.8. An illustration in support of the discussion on observed cyclone distortion. Cross-hatching indicates typical regions of deep moist convection.

beta effect distortion. However, recent work by other authors indicates that additional processes act to reinforce this distortion. In a detailed case study of the boundary layer characteristics of hurricane Kerry, Holland and Black (1983) and Black _et al_. (1983) suggested that the convergence on the eastern side was driven equally by surface frictional dissipation, and by vertical recycling of high momentum air aloft and low momentum air downwards by deep convection and boundary layer roll vortices. By comparison, the region to the west of the hurricane was virtually free of convection. The divergent flow in this western sector was partially supported by subsidence of higher momentum air into the boundary layer, partially by transient high speed surges from the impinging trade wind regime and partially by a boundary layer decoupling from cold upwelled oceanic water. Lajoie (personal communication, 1982) further considers that asymmetric upper level convergence regions (such as the observed confluence between the hurricane outflow and subtropical westerlies in Chapters 4 and 5) also have an important effect. He has suggested that the subsidence and lower level divergence underneath such upper convergence regions may introduce additional vortex distortion.

An illustration of the total process is then given in Fig. 7.8. An interaction between the cyclone and the gradient of earth vorticity produces the characteristic distorted shape. But, to the north and east, advection of moist tropical air, together with enhanced boundary layer convergence from the beta effect, generates considerable moist convection (c.f. our structure discussion in Chapters 4 and 5). Inside 300-400 km radius, this moist convection, together with the development of horizontal roll vortices, then removes momentum from the boundary layer to further enhance the convergent flow (Holland and Black, 1983; Black et al., 1983). On the western side, the drier subtropical air, together with subsidence from conservation of potential vorticity, effectively suppress convective activity. These, and transient surges from the trade wind regime act to reinforce the observed low level divergent flow.

The Effective Radius and Core Movement: In describing the outer region distortion and subsequent cyclone motion under a combined beta effect and non-linear generation of a poleward steering current, we implicitly assumed that the inner 200-300 km retained a quasi-symmetric shape with little distortion. This assumption is consistent with observations that the inner few hundred kilometers of a tropical cyclone maintains an axisymmetric identity even under quite adverse conditions (c.f. Willoughby, 1979).

The conservative processes which maintain this identity are perhaps most simply viewed in terms of the high core region inertial stability in tropical cyclones (c.f. Appendix 3 and the discussion in section 6.3). The radial profile of inertial stability for AUS05 (which is typical of all hurricanes) is shown in Fig. 7.9, together with some other dynamic parameters for comparison. We can see that there is a sharp increase in stability 200-300 km from the center. Inside this radial band the inertial stability is typically one to two orders of magnitude larger than the earth vorticity. Thus, horizontal deformations are very strongly resisted. Outside this radial band the inertial stability and earth vorticity have the same magnitude. Thus, considerable distortion may (and, as we have shown, does) occur.

When we take Eqs. (7.20) and (7.21) and solve for radius using observations and a known cyclone motion, we also find that a single radial band dominates for each cyclone. This band typically lies in the range 200-400 km (Holland, 1983b). Hence, the cyclone/environment interactions which lead to motion are maximized at a radial band approximately coincident with the rapid change in gradient of inertial stability. As we show in Fig. 7.10, the motion may then be conceptually viewed as a moving envelope at what we have described as the effective radius of interaction (Holland, 1983b). At this effective radius the cyclone/environmental interactions dominate in determining the subsequent motion. Inside, the high rotational stiffness prevents any

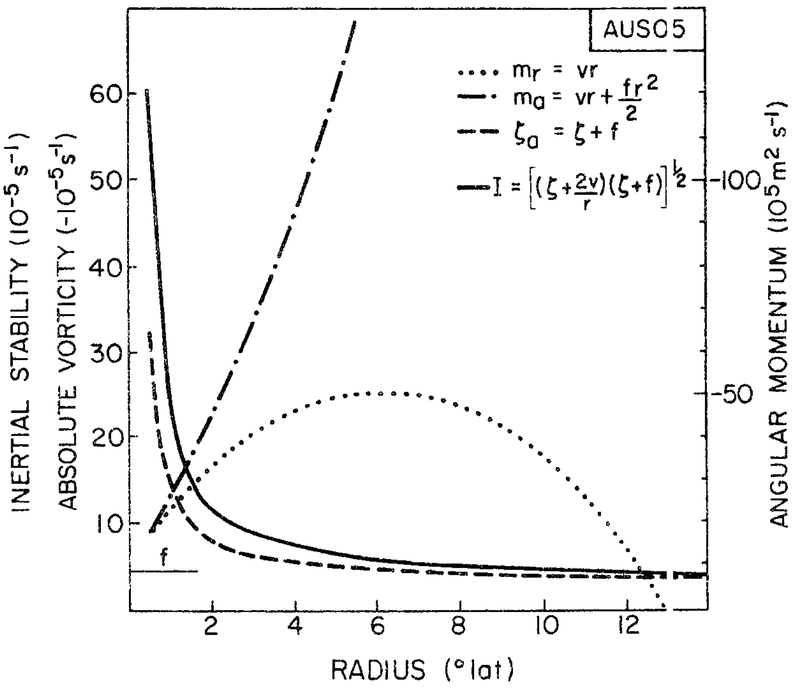

Fig. 7.9. Radial profiles of relative angular momentum (M_r), absolute angular momentum (M_a), absolute vorticity (ζ_a), and inertial stability (I) for the 800-300 mb layer in the oceanic hurricane AUS05.

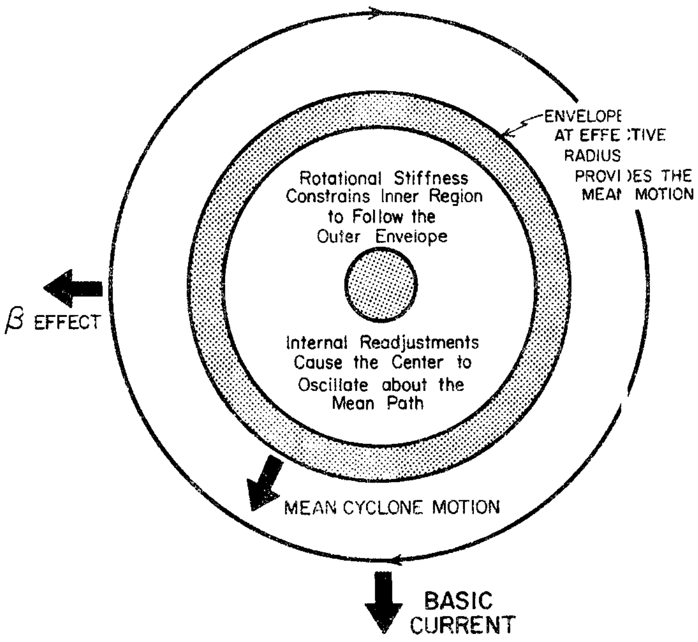

Fig. 7.10. A simple schematic of cyclone motion on a beta plane under a basic current (after Holland, 1983b).

significant distortion and the center slavishly follows the outer envelope.

Of course, the contact between the center and envelope is not a rigid one. Rather, the center has a limited degree of freedom to move within the envelope constraints. Thus, as we have suggested in Holland (1983b), internal perturbations, and subsequent oscillations of the center may provide the observed oscillatory track of many tropical cyclones.

This concept of steering by cyclone/environmental interaction at an envelope defined by the region of rapid increase in inertial stability predicts that: 1) intensity variations will not affect the motion; and 2) vortex size and strength changes will affect the motion by changing the effective radius. These predictions are consistent with general observations that no track changes accompany oscillations in central pressure or maximum winds in hurricanes. Confirmation has also been provided in recent modelling experiments by DeMaria (1983). DeMaria made a control, nondivergent barotropic integration of an initially axisymmetric vortex on a beta plane. He then repeated the experiment with two new vortices. In the first experiment the intensity was changed by doubling the maximum winds and keeping the outer circulation unchanged. In the second experiment the size was changed by a 20% increase of winds outside the maximum wind belt with almost no intensity change.

The resulting trajectories are shown in Fig. 7.11, together with insets showing the three initial azimuthal wind profiles and the position differences from the control experiment. We can see that the substantial intensity change made almost no trajectory difference. But

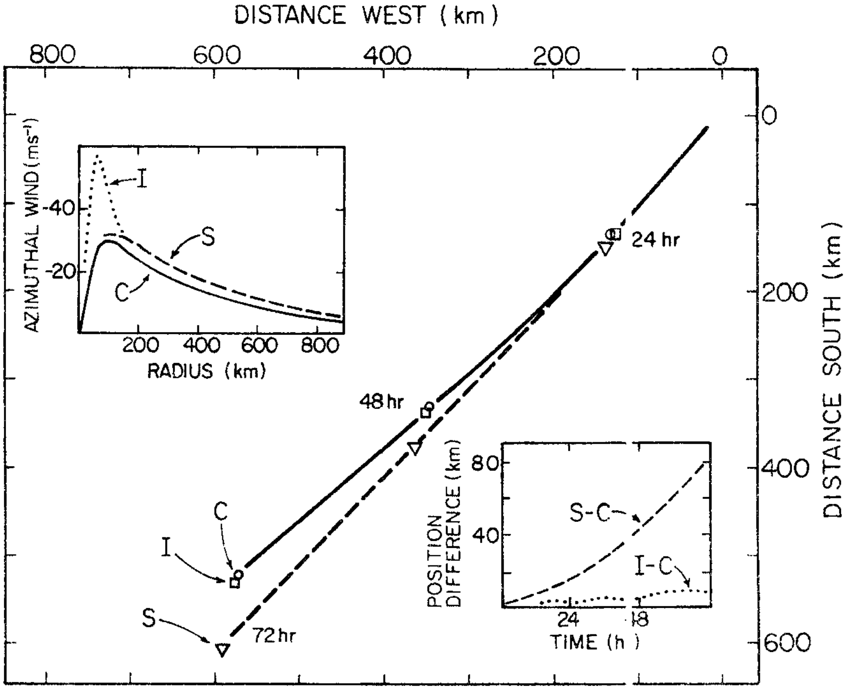

Fig. 7.11 Beta plane trajectories for a control experiment (C), an intensity change experiment (I) and a size/strength change experiment (S). Insets show the initial azimuthal wind profiles and the position separation with time (after DeMaria, 1983).

the modest size/strength change caused the larger vortex to move westward and poleward faster than the reference vortex. The increase in westward motion arose from the stronger beta effect on a larger effective radius. And the extra poleward motion arose from a stronger (in absolute terms) outer region distortion, and thus generation of a meridional steering current.

The Geostrophic Adjustment Problem: Throughout our discussion in this and other sections we have completely neglected the transient geostrophic adjustment aspects, and, in using the vorticity equation approach, implicitly assumed an instantaneous 100% adjustment of the mass to the wind fields. However, Schubert and Hack (1982a,b) and

Schubert (much personal communication, 1981, 1982) have shown that the decreasing Rossby radius of deformation (a ratio of the speed of gravity waves to the system vorticity, which indicates the degree of partitioning of perturbations to inertial and gravity wave modes) in mature hurricanes considerably reduces the efficiency of mass adjustment to wind field changes. If we neglect the beta effect, presume a barotropic vortex and introduce a uniform basic current, Eqs. (7.16) and (7.17) indicate that the vortex mass and circulation move together with no adjustment requirements. But non-linear effects, such as the westward beta drift, horizontal or vertical basic current or vortex asymmetries, and asymmetric fields of moist convection, involve wind field accelerations and subsequent mass adjustments (or vice versa).

Intuitively, the imperfect mass adjustment, with some energy being lost to gravity waves, should reduce the non-linear effects. But further couplings or feedbacks could conceivably cause larger changes. Any complete understanding of cyclone motion must include an assessment of these adjustment effects. However, such work is beyond the scope of our present study and we simply presume a perfect adjustment throughout.

7.1.4 The Effects of Basic Current Asymmetries

Following Holland (1983b), if we introduce basic current asymmetries defined by any combination of constant vorticity and divergence and use Eqs. (7.8) to (7.13) the linear cyclone motion tendency will be given by solutions to

$$r^3\beta_o[\xi_1\cos\theta_m + (2\delta_o + \delta_1)\sin\theta_m]$$

$$+ r^2\beta_o v_s[\cos\theta_m - \gamma(2-x)\sin\theta_m]$$

$$+ r(1-x^2)v_s[(\xi_o - \xi_1)\cos 2\theta_m + (\delta_1 - \delta_o)\sin 2\theta_m]$$

$$- \bar{V}_B(1-x^2)v_s\sin(\theta_m-\alpha) \;=\; 0 \tag{7.24}$$

$$V_c = \bar{V}_B\cos(\theta_m - \alpha) + \frac{\beta_o r^2}{(1-x^2)}[\gamma(2-x)\cos\theta_m + \sin\theta_m]$$

$$+ \frac{\beta_o r^3}{v_s(1-x^2)}[\xi_1\sin\theta_m - (2\delta_o + \delta_1)\cos\theta_m] \tag{7.25}$$

where ξ_o, ξ_1 and δ_o, δ_1 are the constant meridional and zonal components of vorticity and divergence respectively, and $\bar{V}_B$ is the symmetric component of the basic current. Complete details on the derivation of these equations, and their solution procedures, are given in Holland (1983b). In essence, Eq. (7.24) is solved iteratively for the direction of cyclone motion, θ_m; Eq. (7.25) is then solved directly for the cyclone speed, V_c.

These equations enable us to examine some of the effects that basic current asymmetries will have on tropical cyclone motion. A number of these effects are illustrated in Fig. 7.12, which is based on the quantitative results given in Holland (1983b, Fig. 6 and Table 4). The first two compartments illustrate the effect of increasing or decreasing the basic current speed while holding the direction constant. The last six compartments illustrate the effects of introducing various basic current asymmetries without changing the azimuthal average.

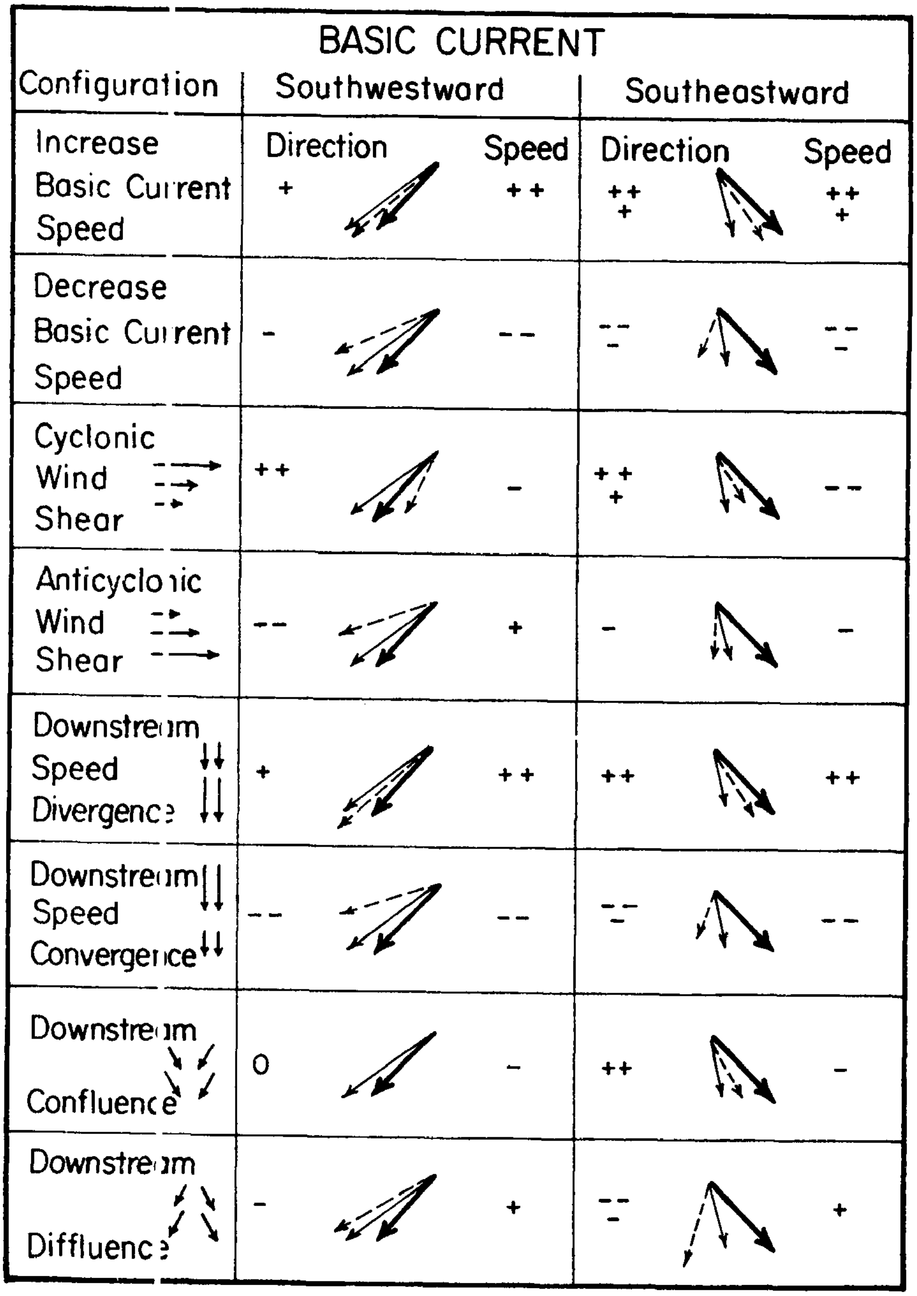

Fig. 7.12. An illustration of the tropical cyclone motion changes resulting from varying the basic current speed or from introducing asymmetries without changing the mean basic current. The heavy arrow indicates the basic current velocity; the thin arrow indicates the cyclone velocity for a uniform basic current; and the dashed line indicates the new cyclone velocity arising from the imposed asymmetries.

We must emphasize that these are linear, initial motion tendencies only and in some cases non-linear effects may significantly alter the longer term motion. Nevertheless, some very interesting physics may be seen in Fig. 7.12.

As we have already seen in Fig. 7.1, since the westward beta drift is essentially a constant for a given vortex size and effective radius, increasing the speed of a uniform basic current will not only increase the cyclone speed but reduce the angular deviation. Similarly, decreasing the basic current increases the angular deviation. And the effects are more pronounced for a southeastward moving cyclone.

Introducing a cyclonic wind shear increases the advection of vortex vorticity on the left side and also slightly increases the beta effect (since there are weaker poleward basic current winds on the western side). However, for both southeastward and southwestward mean basic currents the additional vorticity advection dominates over the beta effect and the cyclone backs and slows down. Introducing an anticyclonic wind shear has the opposite effect and the cyclone veers; though we note that the concomitant weakening of the beta effect reduces the veering considerably on the southeastward basic current situation.

Introducing downstream speed divergence increases the vorticity advection ahead of the cyclone, increases its speed and causes it to back in direction as the relative beta effect is reduced. Downstream speed convergence has the opposite effect. These linear results are, however, probably an overestimate since they also contain a concomitant cyclone distortion. Non-linear effects associated with this distortion may also cause the cyclone to move more rapidly poleward by the processes described in section 7.1.3.

A downstream confluence in the basic current will weaken the beta effect slightly for the southwestward situation and increase it for the southeastward situation. It will also concentrate the vorticity advection along the mean basic current direction. As a result very little change occurs in the motion under a southwestward basic current, but under a southeastward basic current the cyclone backs and slows down. A downstream diffluence has the opposite effect and produces a notably large veering in the southeastward moving cyclone.

We shall show in section 7.2 that these basic current asymmetry effects can have a substantial impact on the observed movement of tropical cyclones.

7.1.5 The Sensitivity of Cyclone Motion

In Holland (1983b) we defined the motion of a cyclone to be insensitive when it reacts in a damped manner to basic current variations or short lived asymmetries. Cyclones which overreact to such variations were said to be sensitive. We then showed that the imposition of the beta effect and asymmetries in the basic flow could result in different degrees of sensitivity depending on the direction and speed of the basic current.

This study revealed an important difference in the sensitivity of westward and eastward moving cyclones. Westward moving cyclones were shown to be quite insensitive to either random perturbations or basic current changes. But eastward moving cyclones were shown to be quite sensitive and prone to overreacting to such changes.

For example, the theory predicts that cyclones moving on a west/southwestward trajectory will respond by only a fraction (around half) of any changes in basic current direction. Their direction of motion is also only marginally affected by changes in basic current speed. By comparison, cyclones moving in an east/southeastward direction will deviate by up to twice the change in basic current direction. They are also very sensitive to changes in basic current speed. We have already seen an indication of these differences in Fig. 7.12. Notice how the direction and speed changes arising from introduced basic current asymmetries tend to be larger for the southeastward case.

The physics behind these different responses are quite simple and may be seen in the schematic in Fig. 7.1. A (non-divergent) cyclone under a northwestward basic current will deviate to the left from the beta effect. If we change the basic current to a southwestward direction, the beta effect deviation will be to the right. Thus, a 90° backing of the basic current only induces around 45° backing in cyclone direction. The opposite occurs in going from a southeastward to northeastward basic current. In this case a 90° backing can induce a 180° change in cyclone direction.

We have also shown in Holland (1983b) that eastward and slow moving cyclones are much more sensitive to random perturbations than those moving westward or rapidly. This may be seen in Fig. 7.13. which shows the azimuthal variation of vorticity change for a convergent Southern Hemisphere cyclone under different basic currents. A cyclone with a relatively flat vorticity change maximum will be quite sensitive to imposed perturbations and thus may undergo large changes in the direction of motion. As the vorticity change maximum becomes stronger

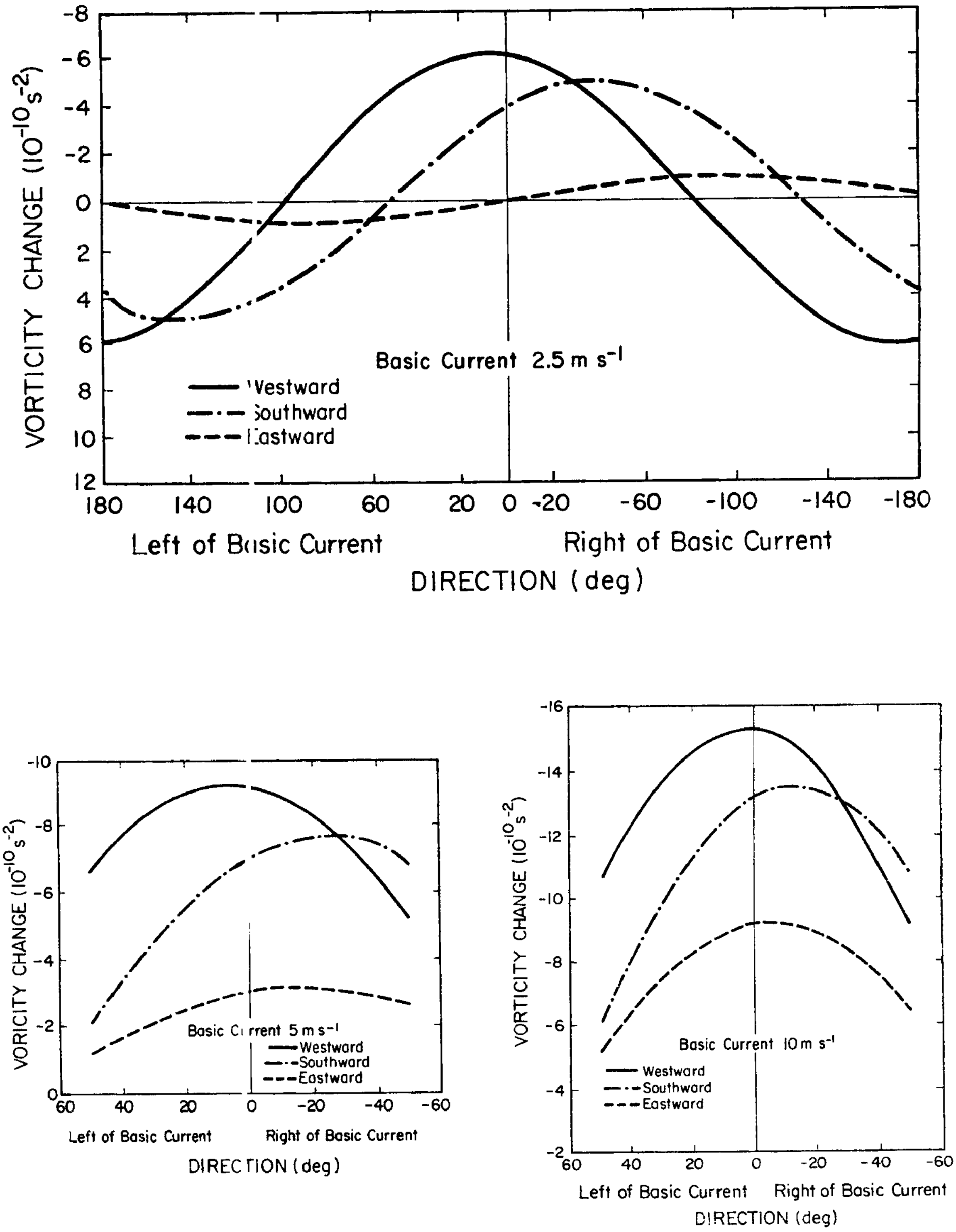

Fig. 7.13. Azimuthal variation of vorticity changes at an effective radois of 300 km for a typical, convergent Southern Hemisphere tropical cyclone under basic currents of 2.5, 5 and 10 m s^{-1} (after Holland, 1983b).

and sharper this sensitivity will decrease. Figure 7.13, then, indicates that westward moving cyclones are less sensitive than southward or eastward moving cyclones, and that the sensitivity decreases in all cases as the basic current increases. For low wind speeds, eastward moving cyclones are highly sensitive to minor perturbations in any direction, whereas those moving westward will only respond to perturbations very close to the direction of motion.

Notice also in Fig. 7.13 that the addition of the beta effect results in a different response to perturbations on either side of the storm motion. Westward moving Southern Hemisphere cyclones will respond more to a given perturbation on the left hand than on the right hand side of the direction of storm motion. Southward and eastward moving storms will respond more to perturbations on the right hand side.

These linear theory results are in good qualitative agreement with our general observations that westward moving cyclones tend to follow smoother and more consistent tracks than those moving eastward. We shall also provide quantitative observational confirmation in section 7.2.

7.1.6 The Effect of Surface Friction

Throughout our discussion in previous sections we have neglected any effects of surface friction. This is because friction is a difficult, if not impossible, mechanism to incorporate into our analytical treatment. An analytic study by Kuo (1969) and numerical, f plane modelling experiments by Jones (1977) indicate that surface friction will cause the cyclone to move a few degrees (~ 5) to the left of the basic current in the Southern Hemisphere and to the right in the Northern Hemisphere.

The frictionally induced deviation is therefore generally smaller than the beta effect and the effect of significant asymmetries in the basic current. It is within the noise level of our data and our inability to precisely determine an effective radius. Thus, its neglect should have very little impact on our discussion or conclusions.

7.2 A Comparison of Theory and Observations

7.2.1 On Determining a Steering Current

> "It is better to use points outside the immediate vicinity of the storm; 200 or more miles ahead are usually best": Norton (1947)

We have shown in section 7.1.5 that the azimuthally averaged winds around a cyclone may not be sufficient to accurately describe its motion; the horizontal asymmetries may also be important. We must next address the question of what horizontal and vertical domain should be used. That the answer is not obvious may be seen in the proliferation of domains used in the literature. For example: in the horizontal George and Gray (1976) used a domain 1-7° latitude radius from the center, Brand et al. (1981) used 200-300 km, and Chan and Gray (1982) used a radial band at 5-7° latitude radius; in the vertical Riehl and Shafer (1944) used 700, 500 mb, Simpson (1946) used the "top of the vertical circulation", Sanders and Burpee (1968) used a surface to 100 mb deep layer mean, and other authors have used almost every possible combination of levels or layers in between (c.f. George and Gray, 1976, for a complete survey).

In the horizontal, a basic current defined by the wind field over a radial band centered on the effective radius, say 200-300km, would be ideal; since we have shown that this is the region in which the cyclone interacts with the environment to produce an overall motion. But there are normally very few observations in this region. Fortunately, however, as may be seen in Fig. 7.14, the radial variations in the normal and parallel components of the mean basic current are generally quite small. Hence, we shall use the wind field averaged over a 5-7° latitude radius band. This is consistent with the work of Chan and Gray (1982), and agrees with the above conclusion by Grady Norton. It also ensures sufficient observations for an accurate determination of the wind asymmetries, which should be relatively independent of the choice of mean vortex. When applying the model in Eqs. (7.24) and (7.25) we then simply interpolate to the effective radius.

In the vertical, two parameters need to be considered: the vertical structure of the mean vortex and the vertical shear of the basic current. As may be seen in Fig. 7.2 or Appendix 4, even though the absolute values differ, the low, middle, or upper level gradients in azimuthal winds, and also in vorticity, are very similar. Thus, the vorticity advection by a vertically uniform basic current will cause little, if any, tilting of the cyclone. This differential motion is relatively small and may easily be compensated by vertical transports in deep cumulus clouds (Lee, 1982).

A moderate vertical shear in the basic current may similarly be compensated by cumulus transports. Since the radial gradient of vorticity is nearly uniform with height, the cyclone should then move with the mass-weighted vertical average of the basic current. Of course, if the vertical wind shear becomes too large, the convection can no longer "integrate" to remove the motion differential and the cyclone will be destroyed. Huntley and Diercks (1981) show some interesting examples of this tilting effect. They observed that weak tropical cyclones, with little convection near the center, generally tilt in the direction of the vertical wind shear and towards the major convective region. Such a tilt can exceed 100 km between the surface and 700 mb. As the cyclones intensify, and convection becomes well established around the center, the tilt tends to disappear.

Unfortunately, we cannot directly incorporate the data rich boundary and outflow layers into this vertically integrated estimate of the basic current. This is because the asymmetric inflow/outflow jets, which do not contribute to the motion, can significantly distort the basic current evaluations.

That a distortion of the basic current occurs may be seen in Fig. 7.14, and in Fig. 7.15, which shows the mean parallel and normal wind components averaged over 5-7^{o} latitude radius for the five motion composites (AUS12 to AUS16) discussed in the next section. We can see that the basic current in the 800-300 mb layer is reasonably consistent and linear with height and radius, even when there is considerable vertical shear. However, large, and as George and Gray (1976) show, occasionally erratic, changes can occur in the surface-850 mb and 250-100 mb layers (at 100 mb we can also see the effect of the stratospheric easterlies). Numerical modeling experience (DeMaria, 1983) is that these boundary and outflow layer asymmetries have an insignificant effect on the cyclone motion. Hence, their inclusion in the basic current evaluation will merely introduce unwanted noise.

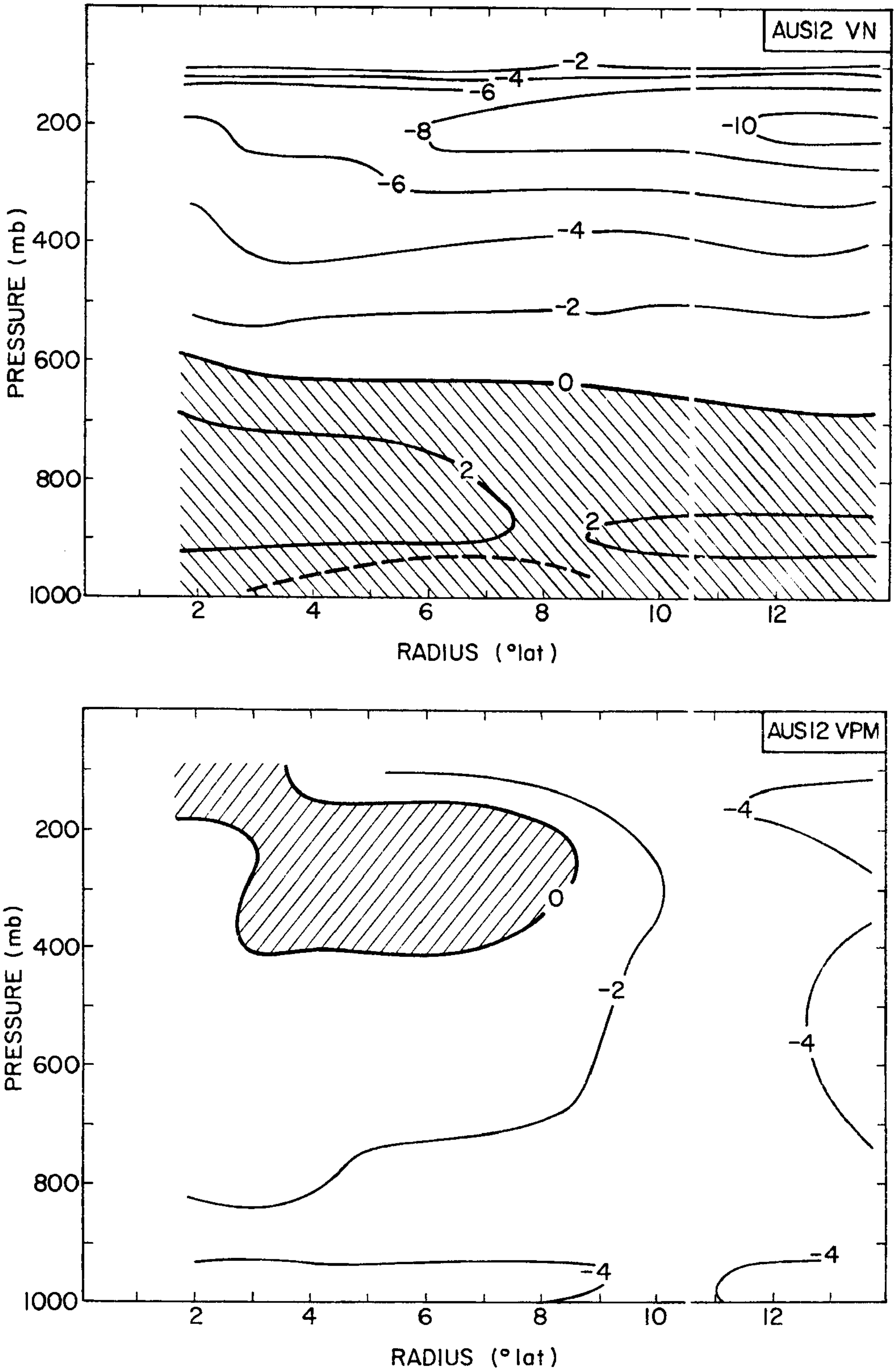

Fig. 7.14. Axisymmetric cross-sections showing the environmental wind components normal (VN) and parallel (VPM) to the southward moving tropical cyclone AUS12. Hatching indicates regions where the cyclone is moving to the left of and slower than the environmental wind.

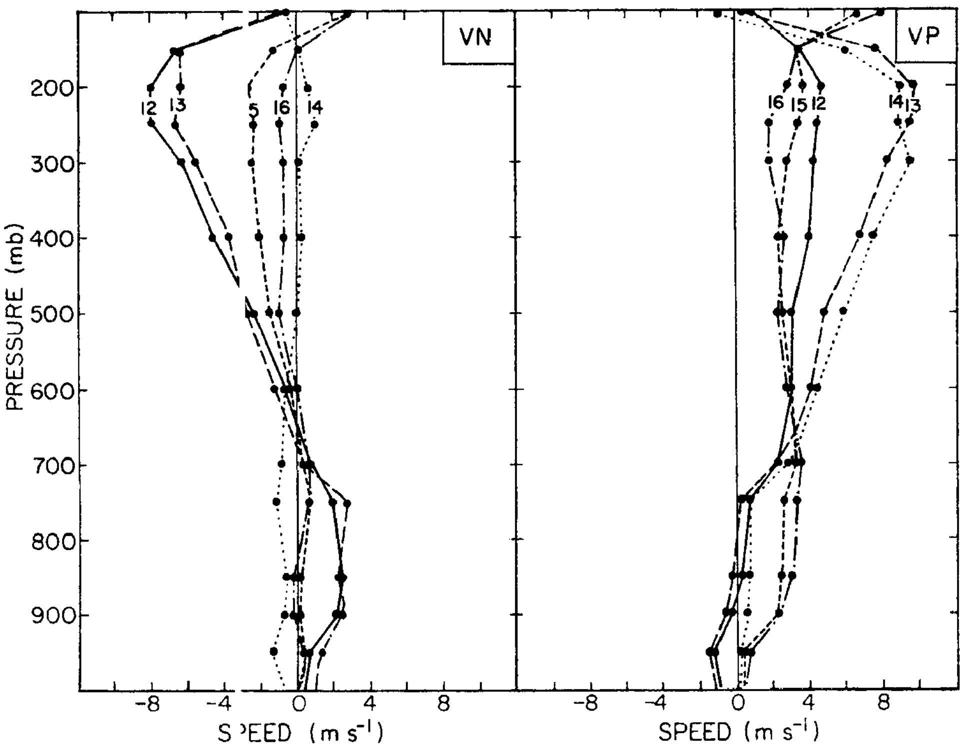

Fig. 7.15. Vertical profile of environmental wind components normal (VN) and parallel (VP) to the direction of motion of the AUS12 to AUS16 composite cyclones at a nominal radius of 6° latitude. A positive VN or VP indicates an environmental flow to the right of or faster than the cyclone velocity.

To illustrate this point, let us assume that the observed wind at some point (after we have removed the mean vortex) consists of an asymmetric inflow jet component $\underset{\sim}{V}_{IN}$ and a basic current component $\underset{\sim}{V}_B$. Then, from the vorticity equation, if we neglect tilting and frictional effects on the basic current

$$\frac{\partial \zeta}{\partial t} = - \underset{\sim}{V}_B \cdot \nabla(\zeta + f) - (\zeta + f)\nabla \cdot \underset{\sim}{V}_B \tag{A}$$

$$- \underset{\sim}{V}_{IN} \cdot \nabla(\zeta + f) - (\zeta + f)\nabla \cdot \underset{\sim}{V}_{IN} + \underset{\sim}{k} \cdot \left(\frac{\partial \underset{\sim}{V}_{IN}}{\partial p} \times \nabla\omega\right) + k \cdot (\nabla \times \underset{\sim}{F}) \tag{B}$$

Where ω is the vertical motion and $\underset{\sim}{F}$ is the frictional dissipation at the surface. Term A , the advection and divergence of vorticity by the basic current, provides the major component of $\partial\zeta/\partial t$ and hence cyclone motion. The inflow jet, however, is flowing into the cyclone in such a way that the anticyclonic vorticity advection is largely compensated by convergence, tilting and friction. Thus, there is little, if any, vorticity change and Term B is nearly zero. A similar explanation may be applied to the outflow jets. When we incorporate inflow/outflow asymmetries into the basic current for use in Eqs (7.24) and (7.25) we neglect these compensating effects, and thus introduce unnecessary noise into our data.

The orientation and strength of the inflow or outflow jets are determined by boundary layer interactions with the moving cyclone (Shapiro, 1983); the distribution of convection (section 7.1.3); and, as we have discussed in Chapter 6, the surrounding environmental flow patterns which provide enhanced outflow channels. It is therefore possible that techniques could be derived to remove these asymmetries and allow better use of the data rich boundary and outflow layers. However, at this stage we shall simply use a mass-weighted 800–300 mb average to define the basic current.

7.2.2 Observations

We shall use the AUS12 to AUS16 motion composites and the AUS01 to AUS03 major recurving hurricane composites to compare the observed cyclone motions under different basic currents with those predicted by the theory. A complete description of these composites is contained in Appendix 2. All cyclones have central pressures less than 1000 mb and those in AUS12 to 16 move with speeds less than 7.5 m s^{-1}. Further: AUS15 and AUS16 contain tropical cyclones which moved continuously towards the west, of which those moving between northwest and southwest comprise AUS16 and those moving between west and south comprise AUS15; AUS12 contains cyclones moving continuously between southwest and southeast; AUS13 and AUS14 contain cyclones which moved continuously eastward, of which those moving between south and east comprise AUS13 and those moving between southeast and northeast comprise AUS14. The speed and direction distributions of the cyclones in each of these composite categories are shown in Fig. 7.16.

We have already described the AUS01 to 03 composites in Chapter 5. They are made up of a single set of major hurricanes which recurved at or near maximum intensity. Of these: AUS01 is the tropical storm stage moving between west and south; AUS02 is the hurricane stage at or just before recurvature; and AUS03 is the filling stage, after recurvature but still at hurricane intensity.

Since our theory and the numerical modeling work discussed in section 7.1.3 indicated that intensity or intensity change have no significant effect on motion, no account was taken of intensity in AUS12 to AUS16 (aside from removing the early tropical depression stages). One concern is that we have also not taken account of size in these composites. We have previously shown that strength or size changes may alter the beta effect component of cyclone motion, however, the present lack of information on these parameters in the Australian/southwest Pacific region does not allow us to quantify these effects at this stage.

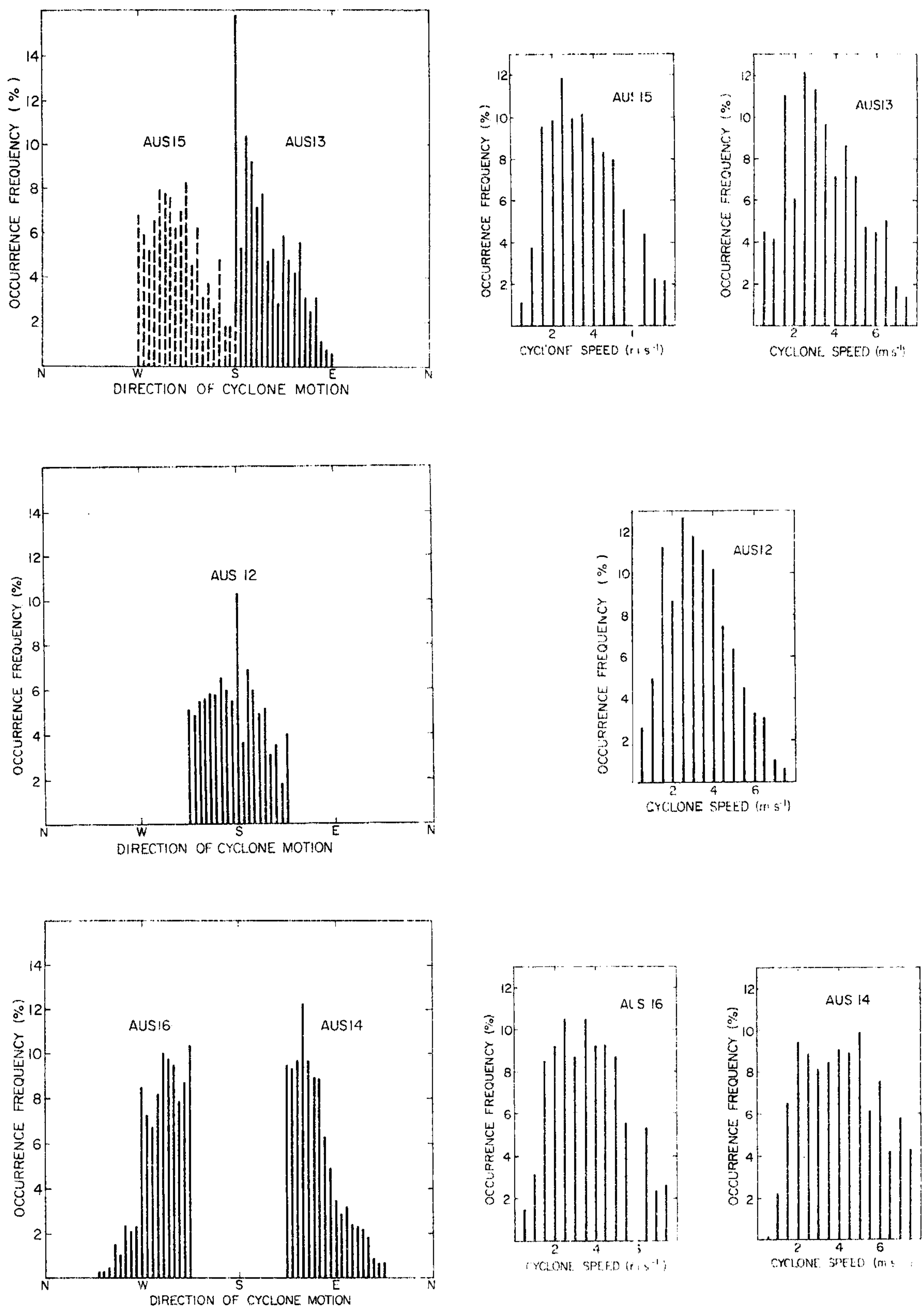

Fig. 7.16. Direction and speed distributions of the cyclones that comprise the AUS12 to AUS16 composites.

Table 7.1 contains the mean basic current and cyclone parameters for these motion composites, together with observed and predicted cyclone deviations from the basic current. Note that the observed deviations for for the AUS12 to AUS16 composites are calculated from the separately composited V_P and V_N components. Hence they may differ slightly from an algebraic subtraction of the cyclone and basic current velocities. Since V_P and V_N were not composited for AUS01 to AUS03 we estimated the deviations using the mean direction and mean absolute speed of the cyclones. For the predicted deviations in Table 7.1 we used the mean latitude of each cyclone and assumed constant cyclone parameters of $\gamma = -0.03$, $x = 0.5$, effective radius of 250 km and cyclone size and strength defined by a 6 m s^{-1} cyclonic azimuthal wind at 6^o latitude radius. We also provide a comparison between the motion predicted by the azimuthally averaged basic current and beta effect alone (column A) and that predicted by the complete current including asymmetries (column B). These asymmetries may be seen in Figs. 7.17 and 7.18.

We can, of course, produce an exact agreement between observations and theory by selecting the appropriate effective radius for each case. However, as may be seen in Table 7.1, simply using a standard cyclone introduces very few errors. In fact the excellent agreement indicates that the major mechanisms responsible for moving these steady cyclones are contained in Eqs. (7.24) and (7.25). The dominant mechanism is the advection of cyclone vorticity by the basic current. The largest consistent deviation from this dominant motion is provided by the beta effect (column A) Except for AUS14 and AUS02, AUS03, basic current asymmetries were weak (Figs. 7.17 and 7.18) and their inclusion produced

TABLE 7.1

Vital statistics on the AUS12-16 and AUS01-03 motion composites. The table gives: the 800-300 mb mean direction (α) and speed (V_B) of the basic current and its components parallel (V_P) and normal (V_N) to the direction of cyclone motion (V_P, V_N components were not composited for AUS01-AUS03); the 800-300 mb mean radial wind (u), azimuthal wind (v) and convergence (γ) into the cyclone at 6^{o} latitude radius; the mean direction (θ_m) and speed (V_c) of the cyclone; and the observed and predicted deviations of the cyclone from the basic current. Column A is the predicted deviations using the mean basic current only, column B incorporates the basic current asymmetries shown in Figs. 7.17 and 7.18.

Composite	Lat. (°S)	Basic Current				Cyclone					Dir. Deviation			Spd. Deviation		
		α	V_B	VP	VN	u	v	γ	θ_m	V_c	Obs.	A	B	Obs.	A	B
(a)																
AUS16 Westward	16.2	117	2.7	2.7	-0.2	-0.2	-6.1	-0.03	108	3.8	-4	-9	-9	1.3	1.5	1.5
AUS15 Southwestward	16.7	137	2.5	2.7	-0.9	-0.2	-6.3	-0.03	121	3.5	-18	-18	-19	1.1	1.0	1.4
AUS12 Southward	19.1	220	3.5	3.0	-1.9	-0.4	-5.4	-0.07	175	3.1	-32	-29	-33	-0.5	-0.9	-0.8
AUS13 Southeastward	19.7	233	4.9	4.7	-2.0	-0.2	-5.0	-0.04	208	3.2	-23	-16	-20	-1.1	-1.3	-1.4
AUS14 Eastward	17.5	257	5.4	5.3	-0.3	-0.2	-4.3	-0.05	252	3.9	-3	-6	-3	-1.2	-1.7	-1.7
(b)																
AUS01 TS before recurvature	15.2	135	2.4	*	*	-0.2	-6.0	-0.03	123	3.5	-13	-7	-15	1.1	1.0	1.3
AUS02 Hurricane near recurvature	17.3	193	3.2	*	*	-0.2	-5.7	-0.04	167	3.7	-26	-32	-12	0.5	0.0	0.2
AUS03 Hurricane after recurvature	22.5	200	5.5	*	*	-0.1	-5.1	-0.02	202	5.0	-2	-26	-14	-0.5	-0.5	-0.6

only a slight improvement in accuracy. Moderate asymmetries were present in AUS14 (Fig. 7.17), but they were zonally orientated and had little effect.

By comparison, the recurving AUS02 and AUS03 composites provide an excellent example of the importance basic current asymmetries can have. Almost no change in basic current direction or beta effect occurred between AUS02 and AUS03. Rather, recurvature was accomplished entirely by an increase in wind speed and the development of asymmetries, with

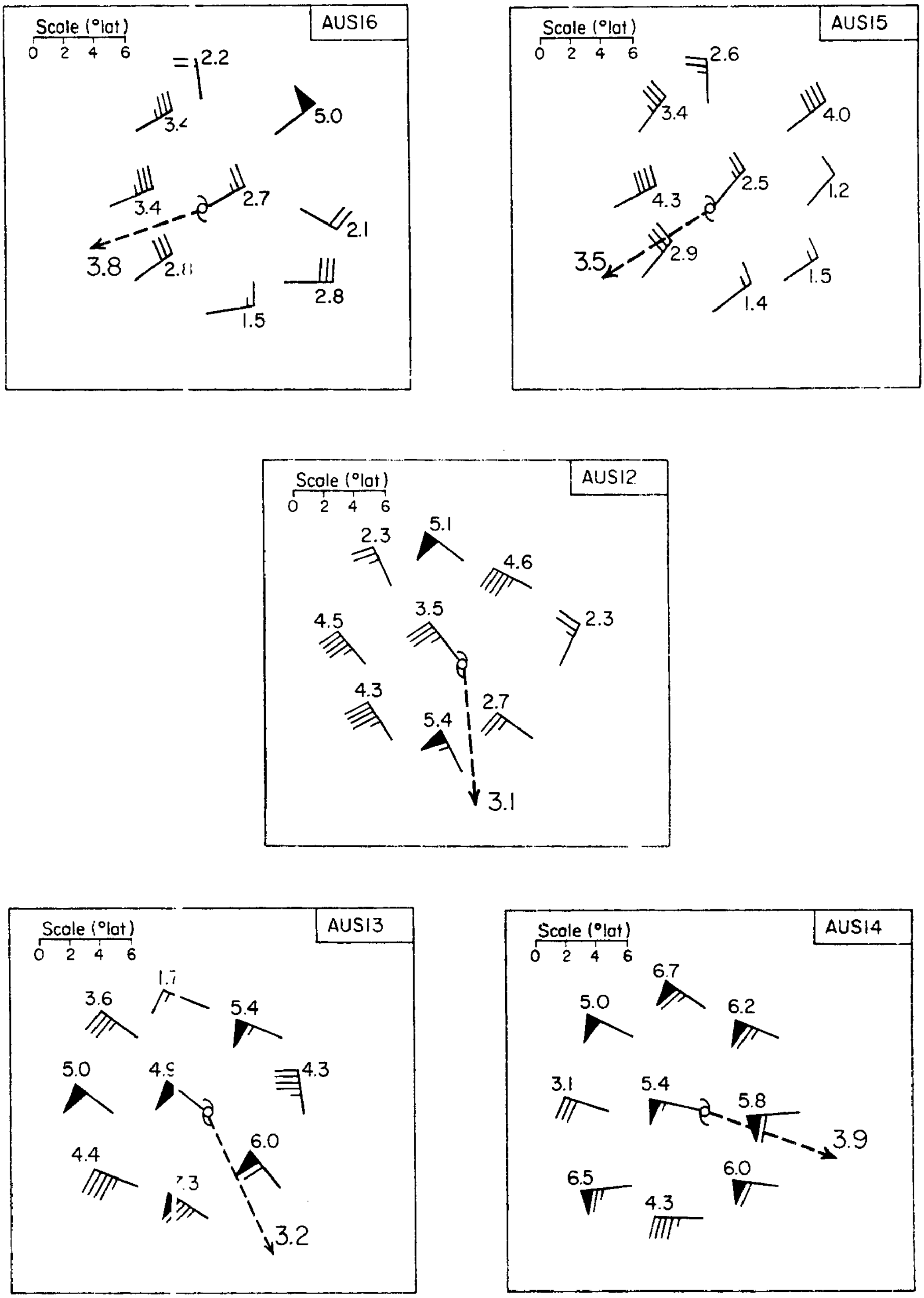

Fig. 7.17. Basic currents and cyclone motion for AUS12 to AUS16. Each inset contains the 800-300 mb mass-weighted mean current at eight octants and a nominal radius of 6° latitude; the azimuthally averaged basic current is shown at the cyclone center; and the direction of cyclone motion is indicated by the dashed arrow. Speed convention is one barb = 1 m s^{-1} and actual speeds are also shown.

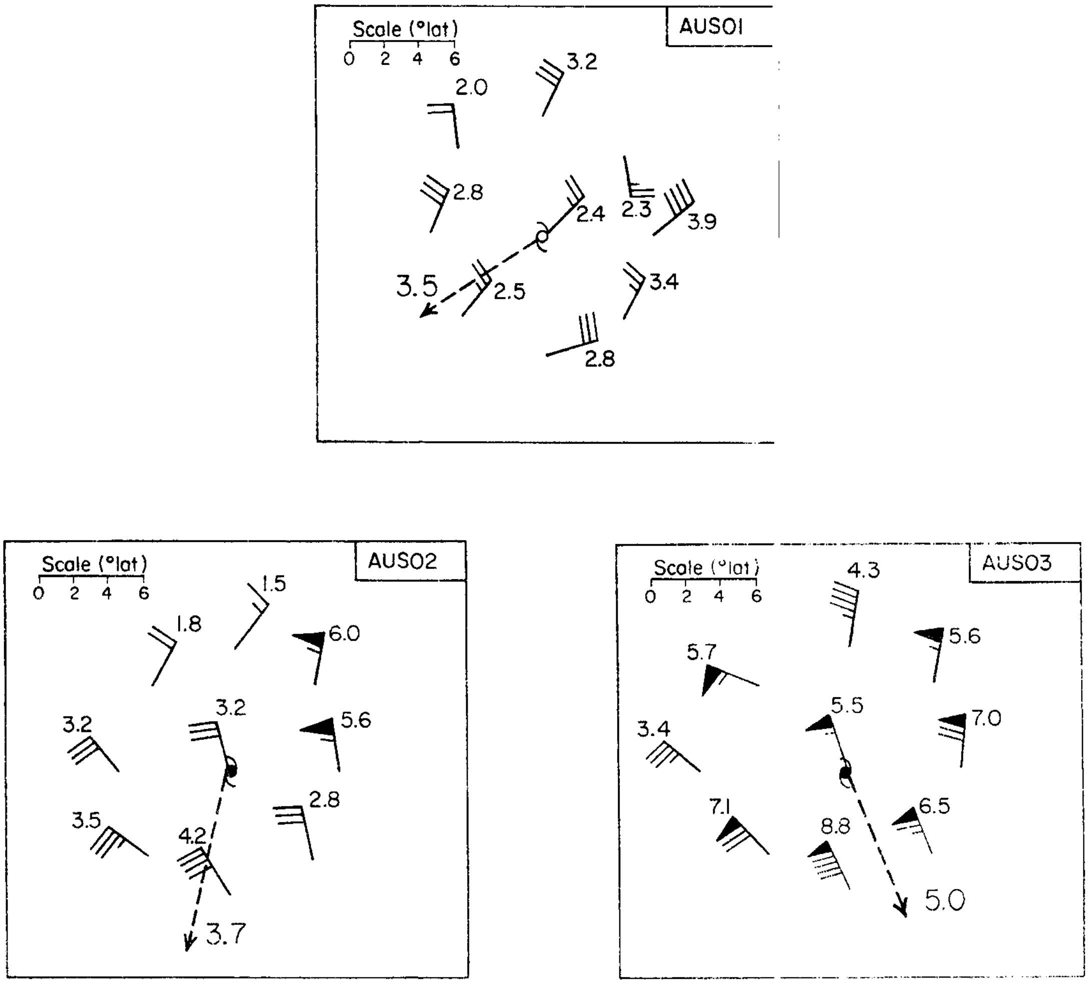

Fig. 7.18. Basic currents and cyclone motion for AUS01 to AUS03. Each inset contains the 800-300 mb mass-weighted mean current at eight octants and a nominal radius of 6° latitude; the azimuthally averaged basic current is shown at the cyclone center; and the direction of cyclone motion is indicated by the dashed arrow. Speed convention is one barb = 1 m s^{-1} and actual speeds are also shown.

the major turning being due to the strong confluence and downstream divergence (compare Fig. 7.13 with the AUS02 and AUS03 plan views in Fig. 7.18).

7.3 Summary

In this chapter we have examined the mechanics of tropical cyclone motion from a theoretical and observational viewpoint to expand the preliminary work by Holland (1982, 1983b). By utilizing linear analytic solutions to the frictionless, divergent, barotropic vorticity equation on a beta plane, we have shown that the major linear components of cyclone motion are an advection by the (asymmetric) basic current, together with a westward deviation arising from an interaction between the cyclone and the earth's vorticity field. This motion is provided by interactions in a radial band some 200-300 km from the center, just outside the high inertial stability core region. It appears that the cyclone center slavishly follows this outer envelope, presumably due to a strong inertial coupling, though the precise mechanisms are not known.

Possible non-linear and surface frictional effects have also been discussed. However, the close agreement between the linear theory and observations indicates that cyclone motion is largely a linear process.

We have further shown that the combination of a basic current advection and beta effect makes westward and rapidly moving cyclones quite insensitive to environmental perturbations. But eastward and slowly moving cyclones are quite sensitive and will tend to overreact to imposed perturbations.

A detailed summary of these results may be found in section 8.4.

8. SUMMARY

In this paper we have documented the completed first stage of a collaborative project between Colorado State University and the Australian Bureau of Meteorology to study tropical cyclones in the Australian/ southwest Pacific region. We have used a variety of sources to gather all available cyclone and environmental data for the period 1958-1979. Further, we have adopted Professor Gray's compositing routines to a Southern Hemispheric perspective, and have incorporated new statistical and climatological techniques. These new techniques have been very useful in the stratification and analyses stages.

Using these data and new routines, we have provided a comprehensive description of the major climatological and structural features of tropical storms and hurricanes throughout the region. We have further documented some interesting environmental effects, and examined the mechanisms associated with intensity change and motion.

8.1 Climatology

The tropical cyclone season extends primarily from November to May, though unseasonal cyclones occasionally occur in other months. Within the season, tropical storms rise to a mid-season maximum followed by a secondary, late season peak. Hurricanes, however, exhibit an early season maximum and those in the northwest Australian region have a mid-season minimum. We have attributed this mid-season minimum (which does not appear in the tropical storm distribution) mainly to the detrimental effect of the Australian continent. As the monsoonal trough extends poleward over northern Australia, most cyclones form very close to the coast and in the Gulf of Carpentaria. They thus often suffer a premature demise. However, changing environmental flow fields, with many cyclones forming under a strong upper level easterly flow, may also have an effect.

The Australian continent also contributes to distinctive variations in the spatial distributions of tropical storms and hurricanes. Tropical cyclones have been observed throughout the region from 105°E to 150°W but the occurrence peaks, and relative hurricane/tropical storm proportions, vary considerably. The highest tropical storm frequency occurs in the land-locked Gulf of Carpentaria, with secondary maxima in the Coral Sea and off the northwest Australian coast. By comparison, hurricanes have a very high frequency off the northwest Australian coast, occur only occasionally in the Gulf of Carpentaria, and are spread more widely throughout the southwest Pacific. The relative proportions of hurricane to tropical storm occurrence are 70/30 off the northwest Australian coast, 20/80 in the Gulf of Carpentaria, and 50/50 in the southwest Pacific. These proportions reflect both the number of systems and their lifetime.

We have thus observed a unique situation in that both the highest frequency and proportion of intense systems occurs off the west coast of a major continent. Indeed, around 40% of all major hurricanes in the entire region occur just off, and make landfall on, the northwest Australian coast. Contributing factors to this behavior include: the warm ocean temperatures there; the interaction with hot continental air, which helps steer cyclones along and just off the Australian coast (section 8.2); and the prevailing flow fields, in which the cyclone is embedded in a deep low level tropical environment but can still interact with the subtropical westerly flow in the upper troposphere (section 8.3).

The overall proportions of major hurricanes, all hurricanes, and tropical storms in the Australian region is 15/45/55 respectively. Insufficient information was available to enable us to distinguish major hurricanes east of 165°E, but Revelle (1981) found similar proportions there for the period 1969-1979. The most intense hurricanes came from the recurving motion category. They typically originated near 10°S in the Coral Sea region and near 15-18°S in the northwest Australian region; but many weaker tropical cyclones also form at these latitudes. The more intense systems generally intensify at a faster rate and take longer to reach maximum intensity; but this trend is less obvious for the very intense major hurricanes. Overall, then, tropical storms often form and decay over tropical waters, or over Australia; hurricanes tend to intensify while moving polewards to 20-25°S then decay rapidly by crossing the coast, by becoming entangled in the strongly sheared subtropical westerlies or by moving over a cold ocean surface.

Rapid intensification is certainly underestimated throughout the region. But those cyclones which follow the Dvorak (1975) rapid intensification curve typically come from the recurving motion category. Their rapid intensification cycle also starts either near 990-995, or 970 mb and ceases within 12 hours of maximum intensity. The seasonal and latitudinal distribution of rapid intensification events is similar to that for tropical cyclones generally.

Tropical cyclones in the southwest Pacific region also move very differently to the classical pattern in other ocean basins. That is, the largest proportion tend to move eastward, or erratically; and, indeed, tropical storms move almost exclusively eastward. This peculiar motion is a response to the low latitude, upper tropospheric westerlies and strongly sheared environment in this region. The Gulf of Carpentaria also has a majority of erratic and eastward moving systems. But most tropical cyclones off the northwest Australian coast move along the classical westward track or recurving parabola. This west coast movement is partially due to the prevailing flow there and partially due to interactions between the cyclone and the hot, dry air mass over northern Australia (section 8.2).

8.2 Structure

We have separately examined the structure of developing and non-developing oceanic tropical storms; of intensifying and decaying oceanic hurricanes; of hurricanes just off the east and west Australian coasts; and of recurving major hurricanes and supertyphoons.

These cyclones have many similar features to those of the well documented northwest Pacific and North Atlantic systems. They are moist and warm cored, with a maximum temperature anomaly near 300 mb. An upper tropospheric anticyclone overlies a low and mid-level cyclonic circulation which extends beyond 1500 km radius. The vertical wind shear is concentrated near 300 mb in developing systems and spreads to lower levels as the cyclones decay. The secondary circulation displays the classical boundary layer inflow and upper tropospheric outflow regimes. Secondary inflow maxima occur in the lower stratosphere and near 400 mb, especially in developing cyclones, and there is evidence of a weak outflow near 600 mb in some cyclones.

The low level circulation also exhibits a distinctive distortion, with a cyclonic extension to the west and convergence/anticyclogenesis to the east. We have surmized that this is the result of an interaction between the cyclone and the earth's vorticity field which is reinforced by the concomitant development of a moist tropical feeder band on the equatorward and eastward side. Holland and Black (1983) and Black *et al*. (1983) provide a more quantitative discussion of these features.

There are further, a number of regional peculiarities which arise from the monsoonal environment, the close proximity of subtropical jet westerlies, and the effects of the Australian continent.

In the low levels, a distinct outer region inflow maximum is observed at the tropical storm stage. This inflow maximum arises from the development of surges in the monsoonal westerlies, as has been previously discussed by Love (1982), and/or trade wind easterlies. It leads to the characteristic large size of these systems, and, we believe, provides an optimum environment for development through the tropical storm stage.

The prevailing low latitude subtropical jet westerlies in this region, and especially over the southwest Pacific, provide very characteristic upper tropospheric structures. Developing tropical storms and intensifying hurricanes are typically close to, but not under, this westerly flow and are located between upstream trough and downstream ridge axes. Thus, in our mean composites we observe a marked confluence zone between the hurricane outflow and impinging westerlies some 600 km to the west and southwest of the center. We also observe a long, intense outflow jet to the southeast. By comparison, decaying hurricanes, and especially non-developing tropical storms, over the southwest Pacific lie under the upper level westerlies. They are strongly sheared with convective activity displaced to the east and strong subsidence to the west. Indeed, in the southwest Pacific they will often appear as a low level exposed circulation just west of a large convective region.

Cyclones just off the east and west Australian coast are also distinctly affected by the continent. In east coast hurricanes the low level winds are funneled along the Great Dividing Range. Hence, there is little inland penetration of moist tropical maritime air below 850 mb. Rather, dry continental air, which is advected off the continent and around the equatorward perimeter, tends to cut off the hurricane's tropical moisture supply. During the peak of the cyclone season a semi-permanent upper level anticyclone is also located over central northern Australia by the monsoonal convection. The concomitant downstream trough over the Coral Sea then maintains an adverse, strongly sheared environment for most east coast storms. It also tends to steer them away from the coast.

West coast hurricanes are not so adversely affected. Rather, they are embedded in a deep tropical environment, moisture extends well inland over northwestern Australia, and the core is protected from the dry continental air. An unusual interaction does occur, however, as the hot continental air is advected off the coast on the cyclone's poleward side. Firstly, this produces a distinctly cold-cored structure below 700 mb. Secondly it introduces an equatorward directed temperature gradient, which, from thermal wind considerations (and observations), maintains a deep easterly flow over the cyclone core. Thus the cyclone/continental interaction helps maintain a long westerly trajectory, just off the northwest coast.

8.3 Intensity Change Mechanisms

We have adopted the suggestion by Gray (personal communication, 1982) and Merrill (1982) and separated tropical cyclone "intensification" into three modes: an intensity change, which is an increase in maximum winds; a size change, which is an increase in outer circulation alone; and a strengthening, which is an overall increase in core region winds.

After an extensive literature survey, we concluded that the current state of the science is that virtually no specific work has been done on strengthening or size change mechanisms. (Though some of the work on "intensification" may be more readily applicable to these two modes.) The general concensus on intensity change is that it requires a benevolant environment (conditionally unstable atmosphere, warm ocean, etc; see, eg., Gray, 1968). Intensification then proceeds by both a cooperative interaction between the moist convection and cyclone scales (the CISK process) and a cooperative interaction between the cyclone and synoptic scales of motion. The CISK process has been the subject of extensive observational and, especially, numerical modeling research. But work on the cyclone/ environment interaction has been largely limited to documentation of different observations.

We have made a simple examination of the ways in which a cyclone can interact with its environment by using observations and a linear diagnostic version of Eliassen's balanced vortex equations. This has lead us to the conclusions that: 1) upper tropospheric interactions can directly affect intensity change; 2) lower tropospheric interactions will directly produce a size change which, by subsequent nonlinear interactions, may indirectly affect intensity change, or strengthening. The inertial stability dominates in determining these different responses. In the low levels, the cyclone is very stable out to large radii, thus horizontal motion is constrained and large accelerations may result from an imposed forcing. By comparison, the outflow layer has a quite low inertial stability, thus long radial trajectories are possible and an outer region forcing may directly affect the core region.

We have also shown that inner core convective heating may directly affect intensity change. But the constrained secondary circulation is unlike that typically observed for intensifying hurricanes. Numerical models, which rely on the convective processes alone, tend to generate large inertially unstable regions followed by a sustained outflow. Such large regions of inertial instability have not been observe in nature.

We thus believe that intensification from the tropical storm to minimal hurricane may be, and in many cases probably is, accomplished by CISK type processes alone. However, the initial development, intensification past the minimal hurricane stage, and rapid intensification, normally require some form of beneficial dynamical interaction between the cyclone and its environment.

We have therefore proposed that tropical cyclone development and subsequent intensification in the Australian region typically proceeds as follows. Angular momentum transports by an initial surge in the monsoonal westerlies and/or trade wind easterlies generates a large, inertially stable monsoonal depression or shear zone. Provided this depression is in the benevolent environment described by Gray (1968), it can then loosely organize the fields of moist convection. This convection may in turn help intensify the depression by core heating and surface pressure falls (initially very weak), by an inward contraction of the maximum wind region, and by a vertical recycling of heat and momentum and enhanced oceanic evaporation. The more intense depression is then able to better organize the convective fields, and so on. Though this cooperative interaction is initially very inefficient, the efficiency increases exponentially as the system strengthens or intensifies. Thus, a strong monsoonal depression which has developed over northern Australia may rapidly intensify on moving over the ocean.

Of course, this development and intensification may be prematurely aborted by adverse environmental factors. The cyclone may move over land; or it may be sheared off by impinging strong upper tropospheric westerly winds (as we have documented in the southwest Pacific), or by easterly winds (as occasionally happens in the northern Australian region).

An equatorward outflow channel will normally develop during the early formation stage. This will be located just under the tropopause and will be maintained by vertical cyclonic momentum transports in the monsoonal "feeder band".

Further intensification past the minimal hurricane stage in the Australian/southwest Pacific region then usually occurs as a result of a cooperative interaction between the cyclone and environment in the outflow layer. We believe that this interaction starts during the tropical storm stage and proceeds as follows. A chance passage of a subtropical jet streak 600-800 km poleward of the cyclone and/or development of a westerly trough 800-1000 km upstream of the cyclone reduces the already low inertial stability in the outflow regime. It also generates a divergent area poleward and eastward of the cyclone center. The initially constrained anticyclonic flow over the cyclone then turns and accelerates southeastward to develop a long intense outflow channel. Core region inertial instability, created by active convection in the nascent eye region, with possible transient inertial instabilities associated with the passage of the jet streak, may aid this initial coupling.

Once established, this enhanced outflow may invigorate the core region convection, provide an inward contraction of the maximum wind region, and thus intensification. The outflow is also partially compensated by an inflow below the jet and in the lower stratosphere. Differential angular momentum transports by the outflow and lower inflow generate a strong vertical wind shear between 400 and 150 mb and enhance the warm core development near 300 mb. The stratospheric inflow and concomitant eye region subsidence may further enhance the warm core development and provide further intensification (especially past the hurricane stage where wind to mass field adjustment becomes quite efficient).

The long outflow channel also allows compensating subsidence to occur over a large area. This reduces the debilitating subsidence heating and drying just outside the eyewall region that would result from the constrained circulation response to an increase in eyewall convection alone.

Of course, the cooperation is almost certainly mutual. The cyclone outflow ahead of the westerly trough provides a strong warm advection.

The temperature gradients may be further enhanced by the frontogenetic effect of the confluent outflow and westerly wind regimes. Thus, baroclinic or even barotropic processes may intensify the trough/subtropical jet couplet. It is even possible that the cyclone could initiate a perturbation in an initially zonal subtropical westerly flow.

This coupling is usually of short duration, say one to two days. It ceases when the trough moves past and cuts off the outflow channel to leave a slowly decaying cyclone (as happened with Hurricane Kerry); or more typically when the westerlies move over the cyclone center and strong shearing followed by rapid decay occurs.

8.4 Motion Mechanisms

In Chapter 7 and Holland (1983b) we used a combined theoretical and observational study to examine the major mechanisms of tropical cyclone motion.

In essence, we have shown that cyclones move by an interaction between the cyclone, the basic current, and the earth's vorticity field; and, to a lesser extent, by an interaction between the cyclone and the earth's surface. The precise details of these interactions are not well understood, but the dominant mechanisms appear to be: 1) an advection of the tropical cyclone vorticity field by the uniform component of the basic current: 2) a differential advection and divergence of earth vorticity by the cyclone circulation, which cause a west/southwestward deviation from the basic current in the Southern Hemisphere; and 3) differential effects of basic current asymmetries which may on occasion cause large motion changes.

An initially symmetric vortex on a f plane with no friction will remain symmetric and simply be advected in a balanced state with the basic current.

The cyclonic rotation across a gradient in earth vorticity, or β, will distort the cyclone by causing an increase in cyclonic vorticity to the west and anticyclonic vorticity to the east. We believe that this beta effect is also enhanced by the convective activity resulting from a concomitant advection of moisture into the convergent eastern and equatorward quadrant. However, the distortion is not unbounded; nor is it uniform. Rather, our observations from nature and numerical model experiments indicate that tropical cyclones generally maintain a consistent, or slowly varying shape, suffer very little core region distortion, and move along relatively straight tracks. We consider that any tendency for core region distortion is inhibited by the strong inertial stability there. Outside 300 km, or so, the much lower inertial stability allows more distortion to occur; but this distortion normally maintains a quasi-steady state with the compensating effects of relative vorticity advection and divergence.

The beta effect then provides two components of motion: westward and poleward. The differential advection of earth vorticity, which distorts the cyclone, also moves it westward. The zonally orientated cyclone/anticyclone couplet associated with the distortion further introduce a poleward steering current over the cyclone core. However, in an observational study this extra poleward component is merely part of the derived basic current. Thus, the only observed beta effect is a westward deviation.

Of course, even though we have concentrated on the beta effect in this study, a gradient of relative vorticity will have a similar effect; though additional asymmetric advective processes must then be taken into account.

We have also described the linear motion response to a number of current asymmetries and shown that they may be very important. We have also shown that basic current changes and random perturbations may affect some cyclones more than others. Specifically: our linear results indicate that westward and rapidly moving cyclones are quite insensitive to such effects; eastward and slowly moving cyclones are quite sensitive and large changes may result from relative minor perturbations. We consider that this provides a partial explanation for the observed steady motion of westward moving cyclones, and for the high proportion of erratically moving cyclones over the Gulf of Carpentaria and southwest Pacific Ocean.

We have suggested that the cyclone motion resulting from these (and other) mechanisms is determined by the interactions in a radial band between the inertially stable inner region and distorted outer region. We call this band the effective radius of interaction, and have provided numerical modelling evidence that it is a function of size and strength but not of intensity. Further research is required to see whether this finding is consistent with observations.

As a corollary to this effective radius concept we have also speculated that the often observed trochoidal motion of hurricanes is due to random perturbations, and subsequent oscillations of the center within the constraint of the slowly moving outer envelope.

In relating these theoretical results to observational studies we have given careful consideration to the determination of a steering current. We first determined the environmental winds by extracting the axisymmetric cyclone from all observations. Since in an axisymmetric sense there then appears to be little horizontal variation of these winds out to 6° latitude radius, we followed the recommendation of Chan and Gray (1982) and used the average of all observations in a $5-7^{\circ}$ latitude band. This provides more observations and a better definition than regions closer to the cyclone center. In the vertical, we have shown that the azimuthal wind and vorticity gradients are surprisingly consistent. Thus, under a vertically uniform basic current only minor differential motion will occur. We have assumed that this differential, together with that arising from a moderate vertical basic current shear, can be compensated by cumulus transports. Then the cyclone can be expected to move with the mass-weighted deep layer mean basic current. Unfortunately, however, we have also shown that additional asymmetries are present in the boundary layer inflow and upper tropospheric outflow layer regimes. These asymmetries are not a part of the advecting current and hence merely introduce unwanted noise.

Hence, we remove the axisymmetric cyclone from the 800-300 mb mass-weighted mean of the average winds over $5-7^{\circ}$ latitude radius to define a basic current. Linear interpolation is then used to determine the current at the effective radius of interaction.

After calculating this steering current in a number of carefully stratified composites we have shown that there is good agreement between our simple theory and the observed motion of tropical cyclones. We have also shown that the current asymmetries cannot always be neglected. In one example, recurvature was accomplished by a combined increase in basic current speed and development of asymmetries without any change in its direction. Much more research is needed before the complete effects of different basic current asymmetries (vertical as well as horizontal) will be fully understood.

8.5 Further Research and Forecast Implications

We have described a number of interesting features of tropical cyclones in the Australian/southwest Pacific region, and of the ways in which these cyclones intensify and move. But this work is by no means complete: the energetics and diurnal modulation of these cyclones have yet to be documented; and more research is required on the specific mechanisms responsible for cyclone formation, intensity, size and strength change, and movement.

We also hope that the information presented in this paper will lead to an improvement in the overall understanding that forecasters have on tropical cyclones in the Australian/southwest Pacific region; and especially of the ways in which these systems intensify and move. But history has shown that there is a long, and often unachievable, step between improved understanding and better forecasts. Further, in some cases we have merely filled in details on events that were already known to occur as a logical consequence. For example, forecasters have known for years that cyclone formation often follows a trade wind surge; we have only provided some physics of why this should be so.

Nevertheless, we believe that these results, and future research based on them, hold some promise for forecast improvement. We also believe that this forecast improvement will occur mainly in the 'difficult' situations of recurvature, rapid intensification, etc.

Structure and Enegetics. We have provided a comprehensive description of the gross structural features of tropical cyclones throughout the Australian/southwest Pacific region. The logical next steps are to compare these cyclones to those in other ocean basins, and to examine their energetics and diurnal modulation. A comparison with other regions could provide valuable information on the relative effects of different environments. The energetics examination was originally a component of this first stage; but it was deleted to keep the report to a reasonable length. Further work and publications on this energetics component are planned. Most of our upper wind observations are taken four times daily and extend across a major continental area as well as an uninterrupted ocean. Hence, our basic data set, and compositing routines, are well suited to a detailed examination of the diurnal modulation of oceanic and continental weather systems of different intensities and levels of organization. We envisage that this will become a major area of research on this project.

Intensity Change. In Chapters 4, 5, and 6 we have documented a consistent upper tropospheric coupling between the cyclone outflow and subtropical jet during intensification. This interaction is especially apparent during the development of intense systems.

Though the linkage is an observed fact, our present understanding of the underlying mechanisms is somewhat tentative. Further research towards delineating these mechanisms, and their relative importance, is needed and recommended. Such research should incorporate both observational and numerical modelling approaches. Observational research, incorporating wherever possible all cyclone regions around the globe, should attempt to discern the modes of interaction, obtain statistics of their occurrence, describe their lifecycle and energetics. A combine numerical modelling and observational study could then examine the physical linkages in each mode.

It is also possible that a quantitative intensity forecasting scheme could be developed for use with upper tropospheric cloud winds. Unpublished real time calculations by the author during the 1981 Atlantic hurricane season indicated that outward, jet-like surges in the outflow layer often preceded intensification bursts by around 12 hours. Similarly, a sudden reduction in these jets often preceded decay. Since there are usually sufficient upper cloud wind observations to detect such variations, further applications orientated research could lead to the development of a good, objective intensity change forecast technique.

These upper tropospheric interactions might also provide the basis for a hurricane modification program. Should further work confirm that such interactions are indeed necessary for the development of intense hurricanes, an examination of possible ways in which the interactions could be aborted would be desirable. Such methods might involve the carbon black approach suggested by Gray (1973), or they might require hitherto unthought of procedures. This is a longer term project, but one with intriguing and potentially beneficial possibilities.

<u>Size and Strength Change</u>. It is likely that a better understanding of the concepts of size and strength will lead to an improved quality of cyclone warnings. We also believe that size and strength changes are important components of the formation and early development stages.

This and previous studies suggest that size change is a result of lower tropospheric environmental interactions. We have also intimated that strength change results from an internal rearrangement of angular momentum following size change. But the actual physical processes have barely been touched upon. A similar modus operani to that suggested for intensity change is therefore recommended here.

<u>Motion</u>. Forecasting motion has been described as the most important meteorological decision facing any tropical cyclone forecaster (Simpson, 1971). Errors in forecasting intensity, strength or size are not nearly so critical as placing the cyclone in the wrong place. As such this topic has also been subject to intense applied research culminating in a number of forecast techniques (WMO, 1979; Neumann and Pelissier, 1981; Keenan, 1981).

Can the results presented in Chapter 7 then be of any use in forecasting cyclone motion? Possibly. We are attempting to extend this basic approach to learn more about the mechanisms of cyclone motion. We are also experimenting with the use of Eqs. (7.24 and 7.25) in a forecast mode. However, potentially more profitable lines of operational research would be to use our current findings in the development of statistical techniques; as a differentiator of "difficult" forecast situations; or as an input to the information required by advanced numerical models.

Some very sophisticated statistical forecasting techniques have been developed for tropical cyclone forecasting. Yet they all have less skill than simple persistence and climatological techniques equatorward of 25^{o} latitude (Neumann and Pelissier, 1981; Keenan, 1981). One contributing factor to this lack of skill might lie in our finding that

REFERENCES

Alaka, M. A., 1962: On the occurrence of dynamic instability in incipient and developing hurricanes. Mon. Wea. Rev., 90, 49-58.

Anderson, R. K., J. P. Ashman, F. Bittner, G. R. Farr, E. W. Ferguson, V J. Oliver and A. H. Smith, 1974: Applications of meteorological satellite data in analyses and forecasting. ESSA Tech. Rept., NESC 51, 338 pp.

Anthes, R. A., 1972: The development of asymmetries in a three-dimensional numerical model of the tropical cyclone. Mon. Wea. Rev., 100, 461-476.

Anthes, R. A., 1982 Tropical cyclones: their evolution, structure and effects. Meteor. Monographs, Vol. 19, No. 41, AMS, Boston, MA, ISBN 0-933876-54-8, 208 pp.

Anthes, R. A. and J. E. Hoke, 1975: The effect of horizontal divergence and latitudinal variation of the Coriolis parameter on the drift of a model hurricane. Mon. Wea. Rev., 103, 757-763.

Atkinson, G. D., 1971: Forecasters' guide to tropical meteorology. Tech. Rept. 240, Air Weather Service (MAC), United States Air Force, 360 pp.

Barclay, P. A., 1972: Radar observations of tropical cyclones Althea and Ada: estimation of maximum wind speed from radar echo motion. Proc. of 15th Radar Met. Conf., Champagne, IL, USA, October 1972, Amer. Meteor. Soc., Boston, MA, USA, 107-110.

Bath, A. T., 1957: The Mackay cyclone of 21 January 1918. Aust. Met. Mag., No. 19, 46-59.

Bell, G. J., 1981: Operational forecasting of tropical cyclones: Past, present, future. Aust. Met. Mag., 27, 249-258.

Bjerknes, J., 1966: A possible response of the atmospheric Hadley circulation to equatorial anomalies of ocean temperature. Tellus, 18, 820-829.

Black, P. G. and R. A. Anthes, 1971: On the asymmetric structure of the tropical cyclone outflow layer. J. Atmos. Sci., 28, 1348-1366.

Black, P. G., G. J. Holland and M. D. Powell, 1983: Boundary layer dynamics in hurricane Kerry, II: Heat and moisture budgets. Submitted to J. Atmos. Sci.

Bond, H. G. and A. T. Rainbird, 1956: Surface structure of tropical cyclones, with particular reference to those of 1955-1956 in the Australian region. Proc. of the Trop. Cyclone Symp., Brisbane, Bureau of Meteorology, P.O. Box 1289K, Melbourne, Vic 3001, Australia, 159-170.

Brand, S., C. A. Buenafe and H. D. Hamilton, 1981: Comparison of tropical cyclone movement and environmental steering. Mon. Wea. Rev., 109, 908-909.

Broadbridge, L., 1981: The 1978-1979 Australian region tropical cyclone season. Aust. Met. Mag., 27, 131-146.

Brunt, A. T., 1958a: The Crohamhurst storm of 1893. Proc. of Conf. on Estimation of Extreme Precipitation, Melbourne, 22-24 April, 1958, Bureau of Meteorology, P.O. Box 1289K, Melbourne, Vic 3001, Australia, 191-228.

Brunt, A. T., 1958b: Notes on the Mackay storm of February 1958. Ibid., 229-244.

Brunt, A. T., 1966: Rainfall associated with tropical cyclones in the northeast Australian region. Aust. Met. Mag., 14, 85-109.

Brunt, A. T., 1968: Space-time relations of cyclonic rainfall in the northeast Australian region. Civ. Eng. Trans. Instn. Eng. Aust., April 1968, 40-45.

Brunt, A. T., 1969: Low latitude cyclones. Aust. Met. Mag., 17, 67-90.

Brunt, A. T. and J. Hogan, 1956: The occurrence of tropical cyclones in the Australian region. Proc. of the Trop. Cycl. Symp., Brisbane, December 1956, Bureau of Meteorology, P.O. Box 1289K, Melbourne, Vic 3001, Australia, 5-18.

Bureau of Meteorology, 1956: Proc. of Tropical Cyclone Symposium, Brisbane, 1956. Bureau of Meteorology, P.O. Box 1289K, Melbourne, Vic 3001, Australia, 5-18.

Bureau of Meteorology, 1978: The Australian Tropical Cyclone Forecasting Manual. Bureau of Meteorology, P.O. Box 1289K, Melbourne, Vic 3001, Australia, 274 pp.

Challa, M. and R. Pfeffer, 1980: Effects of eddy fluxes of angular momentum on model hurricane development. J. Atmos. Sci., 37, 1603-1618.

Chan, J. C. L., 1982: On the physical mechanisms responsible for tropical cyclone motion. Dept. of Atmos. Sci. Paper No. 358, Colo. State Univ., Ft. Collins, CO, 200 pp.

Chan, J. C. L. and W. M. Gray, 1982: Tropical cyclone movement and surrounding flow relationships. Mon. Wea. Rev., 110, 1354-1374.

Chen, Lian-shou, 1983: Global view of the upper level flow patterns associated with tropical cyclone intensity change during FGGE. Dept. of Atmos. Sci. Paper (in preparation), Colo. State Univ., Ft. Collins, CO, 80523.

Chong, K. L., J. T. Steiner and J. W. Hutchings, 1980: Regression prediction of tropical cyclone motion in the southwest Pacific. Aust. Met. Mag., 28, 7-18.

Coleman, F., 1972: Frequencies, tracks and intensities of tropical cyclones in the Australian region, 1909-1969 Met. Summary, Bureau of Meteorology, P.O. Box 1289K, Melbourne, Vic 3001, Australia, 42 pp. plus 44 figs.

Crutcher, H. L. and L. R. Hoxit, 1974: Southwest Pacific and Australian area tropical cyclone strike probabilities. USA Naval Weather Service Command, US Dept. of Commerce, 208 pp.

Crutcher, H. L. and R. G. Quale, 1974: Mariners' world wide climate guide to tropical storms at sea. NAVAIR 50-1C-61, US Naval Weather Service, Environmental Detachment, Asheville, NC, 114 pp. plus 312 charts.

DeMaria, M., 1983: Experiments with a spectral tropical cyclone model. Dept. of Atmos. Sci. Report, Colo. State Univ., Ft. Collins, CO. (In preparation).

Depperman, C. E., 1947: Notes on the origin and structure of Philippine typhoons. Bull. Amer. Meteor. Soc., 28, 399-404.

Dexter, P. E., 1981: Optimum instrument spacing for cyclone interception in the Australian tropics. Aust. Met. Mag., 29, 31-38.

Dexter, P. E. and K. B. Watson, 1975: Extreme wave heights in the Australian tropics. Tech. Rept. 17, Bureau of Meteorology, P.O. Box 1289K Melbourne, Vic 3001, Australia, 12 pp. plus appendices.

Director of Meteorology, 1970: Report by Director of Meteorology on Cyclone Ada. Bureau of Meteorology, P.O. Box 1289K, Melbourne, Vic 3001, Australia, 38 pp.

Director of Meteorology, 1972: Report by Director of Meteorology on Cyclone Althea. Australian Government Publishing Service, Canberra, Australia, 61 pp.

Director of Meteorology, 1977: Report on Cyclone Tracy December 1974. Australian Government Publishing Service, Canberra, Australia, 82 pp.

Director of Meteorology, 1979: Cyclone Joan, December 1975. Bureau of Meteorology, P.O. Box 1289K, Melbourne, Vic 3001, Australia, 40 pp.

Dobson, T., 1853: Australasian cyclonology. William Pratt and Son, Hobart, 103 pp

Dobson, A. J. and J. Stewart, 1974: Frequencies of tropical cyclones in the northeastern Australian area. Aust. Met. Mag., 22, 27-36.

Dropco, K. M., 1981: Tropical cyclone intensity change - A quantitative forecasting scheme. Dept. of Atmos. Sci. Paper No. 333, Colo. State Univ., Ft. Collins, CO, 89 pp.

Dvorak, V. F., 1975: Tropical cyclone intensity analysis and forecasting from satellite imagery. Mon. Wea. Rev., 103, 420-430.

Eliassen, A., 1951: Slow thermally or frictionally controlled meridional circulation in a circular vortex. Astrophys. Norv., 5, 19-60.

Erickson, C. D., 1967: Some aspects of the development of Hurricane Dorothy. Mon. Wea. Rev., 95, 121-130.

Falls, R., 1970: On the formation, structure and decay of an intense monsoon depression. Synoptic Analysis and Forecasting in the Tropics of Asia and the Southwest Pacific. Proc. of the Regional Training Seminar, Singapore, December 1970, WMO No. 321, 403-420.

Fitz Roy, Admiral R., 1863: The weather book: A manual of practical meteorology. Longman, Green, Roberts and Green, London, 464 pp.

Frank, W. M., 1976: The structure and energetics of the tropical cyclone. Dept. of Atmos. Sci. Paper No. 258, Colo. State Univ., Ft. Collins, CO, 180 pp.

Frank, W. M., 1977a The structure and energetics of the tropical cyclone, I: Storm structure. Mon. Wea. Rev., 105, 1119-1135.

Frank, W. M., 1977b The structure and energetics of the tropical cyclone, II: Dynamics and energetics. Mon. Wea. Rev., 105, 1136-1150.

Gabites, J. F., 1956: A survey of tropical cyclones in the South Pacific. Proc. of the Trop. Cycl. Symposium, Brisbane, December 1956, Bureau of Meteorology, P.O. Box 1289K, Melbourne, Vic 3001, Australia, 19-24.

Gentilli, J., 1971: Dynamics of the Australian troposphere. Climates of Australia and New Zealand. Ed. J. Gentilli, Elsevier Publishing Co., Amsterdam-London-New York, 53-117.

George, J. E. and W. M. Gray, 1976: Tropical cyclone motion and surrounding parameter relationships. J. Appl. Meteor., 15, 1252-1264.

Gibbs, W. J., 1955: Theory of formation, deepening and filling of tropical cyclones. Working Paper 5, in Rept. of Tropical Cyclone Conf., Brisbane, 1955, Bureau of Meteorology, P.O. Box 1289K, Melbourne, Vic 3001, Australia, 94-106

Gibbs, W. J., 1956: Two cases of cyclogenesis in tropical latitudes. Proc. of Tropical Cyclone Symposium, Brisbane, December 1956, Bureau of Meteorology, P.O. Box 1289K, Melbourne, Vic 3001, Australia, 275-288.

Giovannelli, J., 1952: Les cyclones tropicaux en Nouvelle-Caledonie au cours d'un siecle (1852-1951). Nouvelle-Caledonie et ependences Service Meteorologique, 25 pp.

Giovannelli, J. and J. Robert, 1964: Quelques aspects es depressions et cyclones tropicaux dans le Pacifique sud-oest. Monographie de la Meteorologie Nationale, 33, Paris, 24 pp.

Gomes, L. and B. J. Vickery, 1976: On the prediction of tropical cyclone gust speeds along the northern Australian coast. University of Sydney School of Civil Engineering Research Rept. R278, 44 pp. plus appendices.

Gorshkov, S. G. (Ed.), 1976: World Ocean Atlas: Vol. 1, Pacific Ocean. Library of Congress Cat. Card No. 76-375, 350 pp.

Gourlay, R. J., 1970: Microseismic storm of 17 January 1970 recorded at Cairns. Met. Note, 37, Bureau of Meteorology, P.O. Box 1289K, Melbourne, Vic 3001, Australia, 9 pp.

Gray, W. M., 1968: Global view of the origin of tropical disturbances and storms. Mon. Wea. Rev., 96, 669-700.

Gray, W. M., 1973: Feasibility of beneficial hurricane modification by carbon dust seeding. Dept. of Atmos. Sci. Paper No. 196, Colo. State Univ., Ft. Collins, CO, 130 pp.

Gray, W. M. 1975: Tropical cyclone genesis. Dept. of Atmos. Sci. Paper No. 234, Colo. State Univ., Ft. Collins, CO, 121 pp.

Gray, W. M., 1979: Hurricanes: their formation, structure and likely role in the tropical circulation. Meteorology Over the Tropical Oceans. Royal Meteorological Society, James Glaisher House, Grenville Place, Bracknell, Berkshire, RG12 1BX, 155-218.

Gray, W. M., 1982: Tropical cyclone genesis and intensification. Intense Atmospheric Vortices, (Ed. L. Bengtsson and J. Lighthill), Springer Verlag (ISPN 3-540-11657-5), 3-20.

Gray, W. M., E. Buzzell, G. Burton and Other Project Personnell, 1982: Tropical cyclone and related meteorological data sets available at CSU and their utilization. Dept. of Atmos. Sci. Paper, Colo. State Univ., Ft. Collins, CO, 186 pp.

Gray, W. M. and D. S Shea, 1973: The hurricanes inner core region, II: Thermal stability and dynamic characteristics. J. Atmos. Sci., 30, 1565-1576.

Hawkins, H. F. and D. T. Rubsam, 1968: Hurricane Hilda, 1964: II, The Structure and budgets of the hurricane on October 1, 1964. Mon. Wea. Rev., 99, 427-434.

Hebert, P. J. and K. O. Poteat, 1975: A satellite classification technique for subtropical cyclones. NOAA Tech. Memo. NWS SR-83, US National Weather Service, Washington, DC, 25 pp.

Holland, G. J., 1978: Observations of a vortex embedded in a monsoonal flow. Aust. Met. Mag., 26, 19-24.

Holland, G. J., 1980: An analytic model of the wind and pressure profiles in hurricanes. Mon. Wea. Rev., 108, 1212-1218.

Holland, G. J., 1981: On the quality of the Australian tropical cyclone data base. Aust. Met. Mag., 29, 169-181.

Holland, G. J., 1982: Tropical cyclone motion: Environmental interaction plus a beta effect. Dept. of Atmos. Sci. Paper No. 348, Colo. State Univ., Ft. Collins, CO, 47 pp.

Holland, G. J., 1983a: Angular momentum transports in tropical cyclones. Quart. J. Roy. Meteor. Soc., 109, 187-209.

Holland, G. J., 1983b: Tropical cyclone motion: Environmental interaction plus a beta affect. J. Atmos. Sci., (February issue).

Holland, G. J. and I. G. Black, 1983: Boundary layer dynamics in Hurricane Kerry, I: Mesoscale structure. Submitted to J. Atmos. Sci.

Holland, G. J. and T. D. Keenan, 1980: Diurnal variations of convection over the Maritime Continent. Mon. Wea. Rev., 108, 223-225.

Holland, G. J. and C. S. Pan, 1981: On the broadscale features of tropical cyclone movement in the Australian region. Tech. Rept. 38, Bureau of Meteorology, P.O. Box 1289K, Melbourne, Vic 3001, Australia, 25 pp.

Holland, G. J., T. D. Keenan and G. D. Crane, 1983: The black hole in Hurricane Kerry. Submitted to Mon. Wea. Rev.

Holliday, C. R. and A. H. Thompson, 1979: Climatological characteristics of rapidly intensifying typhoons. Mon. Wea. Rev., 107, 1022-1034.

H. M. Hydrographic Department, 1938: Admiralty Weather Manual 1938. HMSO, London, 496 pp.

Huntley, J. E. and J. W. Diercks, 1981: The occurrence of vertical tilt in tropical cyclones. Mon. Wea. Rev., 109, 1689-1700.

Hutchings, J. W., 1953: Tropical cyclones in the southwest Pacific. N. Z. Geogr., 9, 37 pp. (Also published as NZ Met. Service Met. Office Note 37).

James Cook University of North Queensland, 1972: Cyclone Althea - Part II - Storm Surges and Coastal Effects. James Cook University of North Queensland, Townsville, Qld, Australia, 215 pp.

Jones, R. W., 1977: Vortex motion in a tropical cyclone model. J. Atmos. Sci., 34, 1518-1527.

Keenan, T. D., 1981: An error analysis of objective tropical cyclone forecasting schemes used in Australia. Aust. Met. Mag., 29, 133-141.

Kerr, T. S., 1976: Tropical storms and hurricanes in the southwest Pacific: November 1939 to April 1969. Misc. Pub. 148, New Zealand Meteorological Service, Wellington, NZ.

Kitade, T., 1980: Numerical experiments of tropical cyclones on a plane with variable Coriolis parameter. J. Meteor. Soc. Japan, 58, 471-488.

Kleinschmidt, E., 1951: Grundlagen einere theorie der tropischen zyklanen. Arch. Met. Geophys. Bioklim., A, 4, 53-72.

Kuo, H. L., 1969: Motions of vortices and circulating cylinder in shear flow with friction. J. Atmos. Sci., 26, 390-398.

Kurihara, Y., 1975: Budget analysis of a tropical cyclone simulated in an axisymmetric numerical model. J. Atmos. Sci., 32, 25-29.

Lajoie, F. A., 1976a: On the direction of movement of tropical cyclones. Aust. Met. Mag., 24, 95-104.

Lajoie, F. A., 1976b: On the speed of movement of tropical cyclones. Aust. Met. Mag., 24, 105-110.

Lajoie, F. A., 1977: On the direction of motion of tropical cyclone Tracy. Tech. Rept. 24, Bureau of Meteorology, P.O. Box 1289K, Melbourne, Vic 3001, Australia, 15 pp.

Lajoie, F. A., 1981: Cloudtop equivalent black-body temperatures and tropical cyclone forecasting in the Australian region. Aust. Met. Mag., 29, 73-88.

Lajoie, F. A. and I. J. Butterworth, 1982: Location of tropical cylones from digital IR satellite data. Tech. Rept., Bureau of Meteorology, P.O. Box 1289K, Melbourne, Vic 3001, Australia, (in press).

Lajoie, F. A. and N. Nicholls, 1974: A relationship between the direction of movement of tropical cyclones and the structure of their cloud systems. Tech. Rept. 11, Bureau of Meteorology, P.O. Box 1289K, Melbourne, Vic 3001, Australia, 22 pp.

Lee, C. S., 1982: Cumulus momentum transports in tropical cyclones. Dept. of Atmos Sci. Paper No. 341, Colo. State Univ., Ft. Collins, CO, 73 pp.

Leigh, R. M., 1969: A meteorological satellite study of a double vortex system over the western Pacific Ocean. Aust. Met. Mag., 17, 48-62.

Lourensz, R. S., 1977: Tropical cyclones in the Australian region July 1909 to June 1975. Met. Summary, Bureau of Meteorology, P.O. Box 1289K, Melbourne, Vic 3001, Australia, 111 pp.

Lourensz, R. S., 1981: Tropical cyclones in the Australian region July 1909 to June 1981. Ibid., 94 pp.

Love, G. B., 1982: The role of the general circulation in western Pacific tropical cyclone genesis. Dept. of Atmos. Sci. Paper No. 340, Colo. State Univ., Ft. Collins, CO, 215 pp.

Mackey, C. W. and H. F. Wittingham, 1956: Sea and swell in tropical cyclones. Proc. Trop. Cyclone Symposium, Brisbane, Bureau of Meteorology, P.O. Box 1289K, Melbourne, Vic 3001, Australia, 413-430.

Maher, J. V. and D. M. Lee, 1977: Upper air statistics, Australia, surface to 5 mb, 1957 to 1975. Met. Summary, Bureau of Meteorology, P.O. Box 1289K, Melbourne, Vic 3001, Australia, 202 pp.

Maragos, J. E., G. B. K. Baines and P. J. Beveridge, 1973: Tropical cyclone Bebe creates a new land formation on Funafuti Atoll. Science, 181, 1161-1164.

McBride, J. and R. Zehr, 1981: Observational analysis of tropical cyclone formation, Part II: Comparison of non-developing versus developing systems. J. Atmos. Sci., 38, 1132-1151.

McBride, J. and T. D. Keenan, 1982: Climatology of tropical cyclone genesis in the Australian region. J. Climat., 2, 13-33.

McRae, J. N., 1956: The formation and development of tropical cyclones during the 1955-1956 summer in Australia. Proc. of Trop. Cycl. Symp., Brisbane, December 1955, Bureau of Meteorology, P.O. Box 1289K, Melbourne, Vic 3001, Australia, 233-261.

Merrill, R. T., 1982: A comparison of large and small tropical cyclones. Dept. of Atmos. Sci. Paper No. 352, Colo. State Univ., Ft. Collins, CO, 75 pp.

Meteorologisch Instituut, 1949: Seas around Australia oceanographic and meteorologial data. Koninkklijk Nederlands Meteorologisch Instituut, 124, 79 pp.

Mielke, P. W., K. J. Berry an E. S. Johnson, 1976: Multi-response permutation procedures for a priori classification. Commun. Statist.-Theor. Meth., A5, 1409-1424.

Miller, B. I., 1958: On the maximum intensity of hurricanes. J. Meteor., 15, 184-195.

Milton, D., 1978: The rainfall from tropical cyclones in western Australia. Geowest, 13, Department of Geography, Univ. of Western Australia ISBNO 909678, 15 4, 61 pp.

Neal, A. B. and W. R. Wilkie, 1970: Features of tropical cyclones in the northeastern Australian region as revealed by satellite cloud photographs. Working Paper 126, Bureau of Meteorology, P.O. Box 1289K, Melbourne, Vic 3001, Australia, 15 pp.

Neumann, C. J. and J. M. Pelissier, 1981: Models for the prediction of tropical cyclone motion over the north Atlantic: An operational evaluation. Mon. Wea. Rev., 109, 522-538.

Neumann, B. W. and P. S. Upton, 1958: Microseisms associated with cyclones over northeast Australian waters. Aust. Met. Mag., 22, 24-35.

Newell, R. E., J. W. Kidson, D. G. Vincent and G. J. Boer, 1972: The general circulation of the tropical atmosphere and interactions with extratropical latitudes The MIT Press, MA: Vol. 1 (ISBN 0-262- 14012-8), 258 pp.; Vol. 2 (ISBN 0-262-14020-9), 370 pp.

Norton, G., 1947: Hurricane forecasting (a soliloquy). Unpublished manuscript, Copy Available from G. Holland, 12 pp.

Oliver, J., 1974: Tropical cyclones as natural hazards: An evaluation of Queensland experience in its meteorological context. Aust. Met Mag., 22, 49-52.

Ooyama, K. V., 1969: Numerical simulation of the life cycle of tropical cyclones. J. Atmos. Sci., 26, 3-40.

Ooyama, K. V., 1982: Conceptual evolution of the theory and modeling of the tropical cyclone. J. Meteor. Soc. Japan, 60, 369-380.

Palmen, E. and C. W. Newton, 1969: Atmospheric circulation systems, their structure and physical interpretations. Int. Geoph. Series, Vol. 13, Academic Press, NY, 603 pp.

Pearce, R. P., 1981: A dynamical analysis of hurricane intensification. Contributions to Atmospheric Physics, 54, 19-41.

Perlroth, I., 1967: Hurricane behavior as relate to oceanographic environmental conditions. Tellus, 19, 258-268.

Perlroth, I., 1969: Effects of oceanographic media on equatorial Atlantic hurricanes. Tellus, 21, 230-244.

Piddington, H., 185 : The sailor's horn-book for the law of storms. Williams and Norgate, London, (2nd edition), 360 pp.

Pisharoty, P. R. and S. B. Kulkarni, 1956: Interaction between tropical revolving storms on either side of the equator. Proc. of Trop. Cycl. Symp., Brisbane, December 1956, Bureau of Meteorology, P.O. Box 1289K, Melbourne, Vic 3001, Australia, 289-294.

Ramage, C. S., 1959 Hurricane development. J. Meteor., 16, 227-237.

Ramage, C. S., 1968 Role of tropical Maritime Continent in the atmospheric circulation. Mon. Wea. Rev., 96, 365-370.

Ramage, C. S., 1970 Meteorology of the South Pacific tropical and middle latitudes. Scientific Explorations of the South Pacific, Nat. Acad. of Sciences, Washington, DC, 16-29.

Ramage, C. S., 1971: Monsoon meteorology. International Geophysics Series, Vol. 15, Academic Press, London and New York, 296 pp.

Ramage, C. S., 1974: The typhoons of October 1970 in the South China Seas: Intensification, decay and ocean interaction. J. Appl. Meteor., 13, 739-751.

Rasmussen, E., 1979: The polar low as an extratropical CISK disturbance. Quart. J. Roy. Meteor. Soc., 105, 531-549.

Reid, W., 1838: An attempt to develop the law of storms by means of facts, arranged according to place and time; and hence to point out a cause for the variable winds with the view to practical use in Navigation. John Weale, London, 436 pp.

Revelle, C. G., 1981: Tropical cyclones in the southwest Pacific November 1969 to April 1979. Misc. Pub. 170, New Zealand Meteorlogical Service, Wellington, NZ, (ISSN 0110-6937), 53 pp.

Riehl, H., 1954: Tropical meteorology. McGraw Hill 392 pp.

Riehl, H., 1959: On production of kinetic energy from condensation heating. The Atmosphere and the Sea in Motion, (B. Bolin, Ed.), Rockefeller, Institute Press, 381-399.

Riehl, H., 1979: Climate and weather in the tropics. Academic Press, (ISBN 0-12-588180-0), 611 pp.

Riehl, H. and R. J. Shafer, 1944: The recurvature of tropical storms. J. Meteor., 1, 42-54.

Rooney, W., 1981: The Australian tropical cyclone season 1980-81. Aust. Met. Mag., 29, 143-153.

Rossby, C. G. and Collaborators, 1939: Relation between the intensity of the zonal circulation and displacements of the semi-permanent centers of action. J. Marine Res., 2, 38-55.

Rossby, C. G., 1948: On displacements and intensity changes of atmospheric vortices. J. Marine Res., 7, 175-187.

Sadler, J. C., 1967: The tropical tropospheric trough as a secondary source of typhoons and a primary source of trade wind disturbances. Rept. HIG67-12, Cambridge Research Laboratory, 44 pp.

Sadler, J. C., 1975: The upper tropospheric circulation over the global tropics. UHMET-75-05, Dept. Meteor., Univ. of Hawaii, 35 pp.

Sadler, J. C., 1978: A role of the tropical upper tropospheric trough in early season typhoon development. Mon. Wea. Rev., 104, 1266-1278.

Sanders, F. and R. H. Burpee, 1968: Experiments in barotropic hurricane track forecasting. J. Appl. Meteor., 7, 313-323.

Sanders, F. and J. R. Gyakum, 1980: Synoptic-dynamic climatology of the 'bomb'. Mon. Wea. Rev., 108, 1589-1606.

Sawyer, J. S., 1947: Notes on the theory of tropical cyclones. Quart. J. Roy. Meteor. Soc., 73, 101-126.

Schubert, W. H. and J. J. Hack, 1982a: Inertial stability and tropical cyclone development. J. Atmos. Sci., 39, 1687-1697.

Schubert, W. H. and J. J. Hack, 1982b: Transformed Eliassen balanced vortex model. To appear in J. Atmos. Sci.

Schubert, W. H., J. J. Hack, P. L. Silva Dias and S. R. Fulton, 1980: Geostrophic adjustment in an axisymmetric vortex. J. Atmos. Sci., 37, 1464-1484.

Shapiro, L. J., 1983: The asymmetric boundary layer flow under a translating hurricane. Submitted to J. Atmos. Sci.

Shapiro, L. J. and H. E. Willoughby, 1982: The response of balanced hurricanes to local sources of heat and momentum. J. Atmos. Sci., 39, 378-394.

Shea, D. J. and W. M. Gray, 1973: The hurricane's inner core region: I, Symmetric and asymmetric structure. J. Atmos. Sci., 30, 1544-1564.

Sheets, R. C. and G. J. Holland, 1981: Australian tropical cyclones Kerry and Rosa, February-March 1979. NOAA Tech. Memo ERL AOML-46, National Hurricane Research Laboratory, Gables No. 1 Tower, 1320 S. Dixie Highway, Coral Gables, FL, 33146, USA, 138 pp.

Simpson, R. H., 1946: On the movement of tropical cyclones. Trans. Amer. Geophys. Union, 27, 641-655.

Simpson, R. H., 1971: The decision process in hurricane forecasting. NOAA Tech. Memo., NWS SR-53, National Atmospheric and Oceanic Administration, Dept. of Commerce, Washington, DC, 35 pp.

Simpson, R. H., 1974: The hurricane disaster potential scale, Weatherwise, 27, 169-186.

Smith, R. K., 1981: The cyclostrophic adjustment of vortices with application to tropical cyclone modification. J. Atmos. Sci., 38, 2021-2030.

Southern, R. L., 1981: The global socio-economic impact of tropical cyclones. Aust. Met. Mag., 27, 175-196.

Southern, R. L. and A. N. Scott, 1976: The genesis and characteristics of tropical cyclones. Proc. Symp. on the Impact of Tropical Cyclones on Oil and Mineral Development in Northwest Australia, Perth, 1975, Australian Government Publishing Service, Canberra, Australia, 1-32.

Spillane, K. T. and P. E. Dexter, 1976: Design waves and wind in the Australian tropics. Aust. Met. Mag., 24, 37-58.

Staff Members of the Bureau of Meteorology, 1975: Cyclone Tracy: An interim report. Tech. Rept. 14, Bureau of Meteorology, P.O. Box 1289K, Melbourne, Vic 3001, Australia, 55 pp.

Streten, N. A., 1970: A note on the climatology of :he satellite observed zone of high cloudiness in the centra South Pacific. Aust. Met. Mag., 18, 31-38.

Sundqvist, H., 1970: Numerical simulation of the de'elopment of tropical cyclones with a ten-level model, I. Tellus, 22, 359-390.

Tsui, K. S., G. J. Bell and P. C. W. Fung, 1977: Ch.nge in intensity of typhoons which develop cloud-plume outflow alo.'t. Quart. J. Roy. Meteor. Soc., 103, 151-156.

Visher, S. S., 1925: Tropical cyclones of the Pacific. Bulletin 20, Bernice P. Bishop Museum, Hawaii, 163 pp.

Visher, S. S. and D. Hodge, 1925: Australian hurria.ies and related storms. Bulletin, 16, Bureau of Meteorology, P.O. Box 1289K, Melbourne, Vic 3001, Australia, 54 pp.

Whittingham, H. E., 1958: The Bathurst Bay hurrican: associate storm surge. Aust. Met. Mag., 23, 14-36.

Whittingham, H. E., 1959: Storm surges along the Qu:ensland coast. Aust. Met. Mag., 27, 40-41.

Whittingham, H. E., 1960: Tropical cyclones of the northeast Australian region 1959-60 season. Aust. Met. Mag., 30, 1-38.

Whittingham, H. E., 1963: The Bathurst Bay hurrican:. Aust. Met. Mag., 42, 37 pp.

Whittingham, H. E., 1964: Cyclone passage over Weipa. Aust. Met. Mag., 44, 45-46.

Whittingham, H. E. and B. Swan, 1960: Location of a tropical cyclone by aircraft reconnaissance. Aust. Met. Mag., 31, 13-31.

Whittingham, H. E. and B. R. Aubrey, 1967: Radar watch on cyclone Barbara. Working Paper 101, Bureau of Meteorology, P.O. Box 1289K, Melbourne, Vic 3001, Australia, 13 pp.

Wilkie, W. R., 1960: The application of radar to the detection of rain in tropical cyclones. Seminar on Rain, Vol. 4, Session 6, Paper 5, Bureau of Meteorology, P.O. Box 1289K, Melbourne, Vic 3001, Australia.

Wilkie, W. R., 1964: Evaluation of methods of forecasting development and movement of cyclones in the northeast Australia region: 1962-63 season. Proc. Symp. on Tropical Meteorology, Rotarua, NZ, (Ed. J. W. Hutchings), New Zealand Met. Serivce, Wellington, NZ, 715-729.

Wilkie, W. R. and R J. Gourlay, 1971: Surface wind speeds near the centre of cyclone Ada. Working Paper 137, Bureau of Meteorology, P.O. Box 1289K, Melbourne, Vic 3001, Australia, 16 pp.

Williams, K. T. and W. M. Gray, 1973: A statistical analysis of satellite observed trade wind cloud clusters in the western north Pacific. Tellus, 21, 313-336.

Willoughby, H. E., 1979: Forced secondary circulations in hurricanes. J. Geophys. Res., 84, 3173-3183.

Willoughby, H. E., J. A. Clos and M. G. Shoreibah, 1982: Concentric eye walls, secondary wind maxima, and the evolution of the hurricane vortex. J. Atmos. Sci., 39, 395-411.

WMO, 1979: Operational techniques for forecasting tropical cyclone intensity and movement. WMO-528, World Meteorological Organization, Geneva, Switzerland, 138 pp.

Xu, Jianmin and W. M. Gray, 1982: Environmental circulations associated with tropical cyclones experiencing fast, slow and looping motion. Dept. of Atmos. Sci. Paper No. 341, Colo. State Univ., Ft. Collins, CO, 273 pp.

Yanai, M., 1964: Formation of tropical cyclones. Rev. Geophys., 2, 367-414.

APPENDIX 1 - LIST OF SYMBOLS AND ACRONYMS

A	1. Area 2. Static stability in Appendix 3
B	Baroclinity
c	Constant which defines the cyclone intensity
C_p	Specific heat of dry air at constant pressure
C	Inertial stability in Appenix 3
E	Thermal Forcing
f	Coriolis parameter
F	1. Frictional dissipation 2. Momentum forcing in Appendix 3
I	Internal stability
k	Unit vector in the local vertical
K	Ratio of gas constant to specific heat at constant pressure
m	Absolute angular momentum in Appendix 3
m_a	Absolute angular momentum
m_r	Relative angular momentum
p	Pressure, pressure coordinate
p_B	Component of the pressure field needed to balance the basic current.
Q	1. Moisture mixing ratio 2. Heat source in Appendix 3
r	Radius
r_E	Effective radius
r_m	Radius of maximum winds

t	Time
T	Temperature
u	$= dr/dt$, Radial wind component
u_B	Radial component of basic current
u_s	Axisymmetric radial wind component
v	$= r\, d\theta/dt$, Aximuthal wind component
v_s	Axisymmetric azimuthal wind component
v_B	Azimuthal component of basic current
v_n	$= dy/dt$, Northward component of the total wind
$\underset{\sim}{V}$	Wind velocity
V_B	Basic current speed
V_β	Beta effect component of cyclone speed
V_c	Cyclone speed of motion
V_E	Eastward component of the basic current
V_N	1. Northward component of the basic current 2. Component of the basic current normal to the cyclone motion
V_p	Component of the basic current parallel to the direction of cyclone motion
x	1. Eastward ordinate 2. Constant which defines the shape of the azimuthal wind profile
y	1. Northward ordinate 2. Constant which defines the shape of the azimuthal wind profile
α	1. Angle the basic current tenders with due north 2. Specific volume
β	$= \partial f/\partial y$, Meridional variation of Coriolis parameter
γ	Tangent of the constant inflow angle
δ_o	$= \partial V_N/\partial y$, Meridional component of divergence
δ_1	$= \partial V_E/\partial x$, Zonal component of divergence

θ	1. Azimuth, measured counterclockwise from due north 2. Potential temperature
θ_E	Equivalent potential temperature
θ_m	Direction towards which cyclone is moving
ζ	Vertical component of relative vorticity
ζ_a	Vertical component of absolute vorticity
ζ_s	Axisymmetric component of relative vorticity
ζ_o	$= -\partial V_E/\partial y$, Meridional component of relative vorticity
ζ_1	$= -\partial V_N/\partial x$, Zonal component of relative vorticity
ψ	Streamfunction
ϕ	Geopotential
Φ	$\phi + r^2f^2/g$ in Appendix 3
χ	Momentum source in Appendix 3
ω	$= dp/dt$, Vertical motion in pressure coordinates
SER	Subequatorial Ridge
STR	Subtropical Ridge
TUTT	Tropical Upper Tropospheric Trough

APPENDIX 2 - THE COMPOSITE STRATIFICATIONS

A2.1 Preamble

The purpose of this appendix is to provide salient details on the composites used in this study. Table A2.1 contains an abbreviated summary of all composites, and section A2.2 gives the rationale behind each stratification.

Complete information on these composites are held on file with Professor Gray's project at CSU and with the author at the Australian Bureau of Meteorology. In addition to the actual composite information described in Chapter 3, these files contain: 1) a listing of all cyclones in the stratification, together with position, intensity, motion, etc.; 2) a climatology of these cyclones, containing distributions of all related parameters; 3) a composite of the latitude, longitude, Julian day number and their covariances for those cyclones which contribute data to each grid point; 4) basic statistics on the composite parameters.

We again emphasize the point made in Chapter 3 that these composites are not generic. They have been derived for very specific purposes. A careful examination of the above files should be made before they are used for any other than their designated purpose.

NAME	PURPOSE STR	INT	MOT	TMP	WND	INTENSITY	LAT	LONG	MOTION TOWARDS (MS^{-1})	NO. OBS WITHIN 6° LAT	MASS BALANCE CORRECTION AT 6° LAT (MS^{-1})	QUALITY
AUS01	*	*	*		*	TS	15°S	125°E	237/2.9	64	-0.13	Good
AUS02	*	*	*		*	Hurr	17°S	127°E	193/2.6	373	-0.22	Good
AUS03	*	*	*		*	Hurr	23°S	142°E	157/4.1	338	-0.32	Good
AUS04	*			*	*	--	21°S	154°E	167/2.9	541	0.08	Fair
AUS05	*			*	*	Hurr	18°S	172°E	157/2.7	306	0.34	Exc
AUS06	*	*		*	*	Hurr	17°S	172°E	156/2.6	180	0.47	Exc
AUS07	*	*		*	*	Hurr	20°S	173°E	161/3.2	111	-1.81	Exc
AUS08	*	*		*	*	TS	16°S	173°E	136/3.8	200	0.29	Exc
AUS09	*	*		*	*	TS	14°S	170°E	159/1.9	179	0.13	Good
AUS10	*			*	*	--	18°S	117°E	216/2.8	951	-0.22	Fair
AUS12			*		*	--	19°S	144°E	185/3.1	832	-0.23	Exc
AUS13			*		*	--	20°S	154°E	152/3.2	462	0.32	Exc
AUS14			*		*	--	17°S	161°E	107/3.9	704	-0.37	Exc
AUS15			*		*	--	17°S	130°E	231/3.5	1,334	-0.06	Exc
AUS16			*		*	--	16°S	129°E	253/3.8	1,108	0.40	Exc
NWPR11	*	*	*	*	*	TS	16°N	143°E	292/4.4	115	1.54	Good
NWPR12	*	*	*	*	*	Typh	18°N	139°E	300/4.2	91	1.13	Fair
NWPR13	*	*	*	*	*	Typh	19°N	137°E	312/5.3	131	0.23	Good
NWPRF	*	*	*	*	*	Typh	25°N	135°E	001/4.7	257	0.18	Good

Fig. A2.1. A listing of the salient details of the composites used in this study. Under the purpose column: STR indicates a structure composite; INT an intensity and/or intensification stratification; MOT a motion stratification; TMP indicates that thermal composites were possible; WND indicates that wind composites were made. The quality column gives a subjective estimate based on our analysis of each composite.

A2.2 Rationale for Each Composite

<u>AUS01, AUS02, AUS03</u>: Each of these composites represents sequential intensity and motion stages of major recurving hurricanes in the Australian region. In deriving them, we selected all recurving hurricanes in the Australian region for which the minimum central pressure was less than 960 mb and occurred at, or within one day before, recurvature. Tropical cyclones which attained maximum intensity at landfall were excluded. The tracks were then truncated at the first observation of a 995 mb central pressure, and either two days after maximum intensity or the first observation of 980 mb during decay (whichever came sooner). These cyclones were then separated into the

westward moving tropical storm stage (AUS01), the intensifying hurricane near recurvature phase (AUS02), and the decaying hurricane after recurvature phase (AUS03).

The decay period cut off was to stop any undue bias by sheared off, but nonetheless long lived and gradually weakening systems. We have also assumed that the strict selection criteria imply a consistent environment and thus minimize any windfield bias. However, since these cyclones occur on both sides of the Australian continent we cannot also produce acceptable thermal composites.

We have used these composites for structural comparisons and motion. But because of their homogeneity, time rates of change can be explicitly calculated. Thus, these composites will be of value in future budget studies.

<u>AUS04</u>: This composite was derived in an attempt to delineate the continental effects on cyclones off the east Australian coast. It contains all cyclones within about 500 km of the east coast, between 15 and 25^{o}S, and with central pressures of less than 990 mb. As such, AUS04 is quite asymmetric; there are many observations in the western semicircle, but few, and occasionally no, observations to the east. It delineates the broad continental influences very well, but has no other use.

<u>AUS05, AUS06, AUS07, AUS09</u>: These are the oceanic cyclone composites which were derived to provide good thermal as well as wind information on tropical cyclones in the southwest Pacific region. To do this we selected all hurricanes in the southwest Pacific which were at least 1000 km from Australia, and in which the intensifying hurricane phase occurred between 10 and 20^{o}S. Early and late season hurricanes,

together with a couple at the eastern extremity of the region, were also deleted. Four separate composites were then made: the Steady State Oceanic Hurricane (AUS05) contains all deepening and decaying observations at hurricane intensity; the Developing Oceanic Hurricane (AUS06) contains the deepening hurricane observations; the Decaying Oceanic Hurricane (AUS07) contains the decaying observations; and the Pre-hurricane Tropical Storm (AUS09) contains the developing tropical storm observations.

The above precautions were taken in an attempt to ensure a stable thermal composite despite the strong latitudinal gradients in this region and the low level effects of the Australian continent. As we have seen in Chapter 4 and 5, the result was some excellent thermal composites with quite fine details. Since AUS09, AUS06, and AUS07 all contain the same cyclones, we are also able to calculate time rates of change for future budget calculations. However, the lack of definitive intensity information in this region, especially from earlier years (see Chapter 2), meant that not all observations could be incorporated. There is also some uncertainty about the exact points of transition to tropical storm, intensifying, and decaying hurricane. We do not believe that this uncertainty has significantly affected the resulting composites.

<u>AUS08</u>: This Non-developing Tropical Storm composite was derived for comparison with the AUS09 Pre-hurricane Tropical Storm. It contains the intensifying phase of tropical storms in the southwest Pacific which did not reach hurricane intensity. The same spatial and temporal constraints as for AUS09 were applied. AUS08 is also subject to the

same intensity uncertainty and may contain some minimal hurricanes; again, we do not believe this has had a significant impact.

AUS10: This is a counterpoint to AUS04 and delineates the continental effects on cyclones off the northwestern Australian coast. It contains cyclones within about 500 km of the coast, between 15 and 25°S, and with central pressures less than 990 mb. AUS10 is also quite asymmetric, with almost no observations in the western sector. Thus, as with AUS04, it delineates the broad continental influences very well, but has no other use.

AUS12, AUS13, AUS14, AUS15, AUS16: These are our first purely motion composites. They were derived from steadily moving cyclones which suffered no major perturbations or change of direction. The tropical depression stages were deleted, as were all cyclones moving faster than 7.5 m s^{-1}. AUS15 and AUS16 are made up from tropical cyclones which moved continuously westward, of which those moving between northwest and southwest comprise AUS16 and those between west and south comprise AUS15. AUS12 is made up from cyclones which moved continuously between southwest and southeast. AUS13 and AUS14 are made up from cyclones which moved continuously westward, of which those moving between south and east comprise AUS13 and those between southeast and northeast comprise AUS14.

We have presumed that the consistent long term tracks imply a consistent environmental wind field and thus minimize any bias problems. We have also taken no account of intensity, strength or size variations. We have shown in Chapter 7 that intensity variations should be of no consequence. Size or strength fluctuations in individual cyclones may have introduced some noise, but the total effect seems to be small. In any case, we cannot at present differentiate size and strength change in the Australian/southwest Pacific region.

APPENDIX 3 - THE BALANCED VORTEX MODEL

We begin with the Eliassen (1951) balanced vortex equations in the form:

$$\frac{m^2}{r^3} = \frac{\partial \Phi}{\partial r} \tag{A3.1}$$

$$\frac{\partial \Phi}{\partial p} = -\alpha \tag{A3.2}$$

$$\Theta = \frac{p\alpha}{R} \left(\frac{p_o}{p}\right)^K \tag{A3.3}$$

$$\frac{dm^2}{dt} = 2m\chi \tag{A3.4}$$

$$\frac{\partial ru}{r\partial r} + \frac{\partial \omega}{\partial p} = 0 \tag{A3.5}$$

$$C_p \frac{d}{dt}(\ln\Theta) = \frac{Q}{T} \tag{A3.6}$$

where $m = rv + f\,r^2/2$ is the absolute angular momentum per unit mass, $\Phi = \phi + f^2\,r^2/g$, χ and Q are the momentum and heat sources, $d/dt = \frac{\partial}{\partial t} + u\frac{\partial}{\partial r} + \omega\frac{\partial}{\partial p}$ and the other terms have their usual meaning.

The hydrostatic Eq. (A3.2) and the gas law yield

$$-\frac{\partial}{\partial p}\frac{\partial \Phi}{\partial t} = \alpha \frac{\partial}{\partial t}(\ln \Theta) \qquad (A3.7)$$

and the gradient wind Eq. (A3.1) yields

$$\frac{\partial}{\partial r}\frac{\partial \Phi}{\partial t} = \frac{1}{r^3}\frac{\partial m^2}{\partial t} \qquad (A3.8)$$

Substituting Eqs. (A3.7), (A3.8) into Eqs. (A3 2), (A3.6) and (A3.4) we have

$$-\frac{\partial}{\partial p}\frac{\partial \Phi}{\partial t} + \alpha\,\omega \frac{\partial}{\partial p}(\ln \Theta) + \alpha\, u \frac{\partial}{\partial r}(\ln \Theta) = \frac{\alpha Q}{C_p T} \qquad (A3.9)$$

$$\frac{\partial}{\partial r}\frac{\partial \Phi}{\partial t} + \frac{\omega}{r^3}\frac{\partial m^2}{\partial p} + \frac{u}{r^2}\frac{\partial m^2}{\partial r} = \frac{2m\mathcal{F}}{r^3} \qquad (A3.10)$$

We next define a streamfunction ψ such that

$$u = \frac{\partial \psi}{\partial p}, \quad \omega = \frac{\partial r\psi}{r\partial r} \qquad (A3.11)$$

The continuity Eq. (A3.5) is then satisfied. Substituting Eq. (A3.11) into Eqs. (A3.9), (A3.10) and eliminating time derivatives then gives the diagnostic equation in ψ

$$\frac{\partial}{\partial r}\left(A \frac{\partial r\psi}{r\partial r} + B \frac{\partial \psi}{\partial p}\right) + \frac{\partial}{\partial p}\left(B \frac{\partial r\psi}{r\partial r} + C \frac{\partial \psi}{\partial p}\right) = \frac{\partial E}{\partial r} + \frac{\partial F}{\partial p} \qquad (A3.12)$$

where

$$A = -\alpha \frac{\partial}{\partial p} (\ln \theta) \quad \text{(Static Stability)} \tag{A3.13}$$

$$B = \alpha \frac{\partial}{\partial r} (\ln \theta) = -\frac{\partial m^2}{r^3 \partial p} \quad \text{(Baroclinity)} \tag{A3.14}$$

$$C = \frac{\partial m^2}{r^3 \partial r} = (f + \frac{\partial rv}{r \partial r})(f + \frac{2v}{r}) \text{(Inertial Stability)} \tag{A3.15}$$

$$E = \frac{\alpha Q}{C_p T} \quad \text{(Thermal Forcing)} \tag{A3.16}$$

$$F = \frac{2m\chi}{r^3} \text{(Momentum Forcing)} \tag{A3.17}$$

Equation (A3.12) was then solved in finite difference form using successive over-relaxation on a 33 x 151 grid with spacing of 30 mb in the vertical and 10 km in the horizontal. Boundary conditions were ψ = 0 at the origin and upper and lower boundaries, and $\partial\psi/\partial r$ constant at the outer boundary (which was sufficiently well removed to have no effect on the calculations).

APPENDIX 4 - AN ALTERNATE AXISYMMETRIC AZIMUTHAL WIND PROFILE FOR TROPICAL CYCLONES

A correction is applied to the well known modified Rankine vortex to provide an accurate description of the azimuthal wind profile outside the inner core region. The effects on vorticity, angular momentum, inertial stability and kinetic energy are described

A4.1. Description

The commonly used modified Rankine vortex

$$vr^x = C_1 \quad r > r_m \tag{A4.1}$$

$$\frac{v}{r} = C_2 \quad r < r_m \tag{A4.2}$$

is based on the the assumption of constant relative angular momentum due to efficient horizontal transports in the inner region of tropical cyclones, with some modification due to frictional losses which increase as the square of the wind speed. This profile, with the shape typically defined by $0.4 \leq x \leq 0.6$, can very well simulate actual wind profiles in the inner core regions of tropical cyclones (Holland, 1980). But it becomes quite unrealistic in the outer regions where it considerably overestimates the observed wind speeds.

An alternative is therefore proposed in which the quasi-conservative parameter is still relative angular momentum in the inner core but this is modified at larger radii. The suggested equation is

$$V = C_1 r^{-x} - C_2 r^{y} \qquad (A4.3)$$

where C_1, x define the intensity and shape of the inner core region and C_2, y define the deviation from the modified Rankine vortex in outer regions.

A4.2 Method of Solution

We require data at two points in the core region, r_1, v_1, r_2, v_2 and at two points in the outer region r_3, v_3, r_4, v_4. Then from Eq. A4.1, since C_1 is constant

$$x = \ln (v_2/v_1)/\ln (r_1/r_2) \qquad (A4.4)$$

$$C_1 = v_1 r_1^{x} \qquad (A4.5)$$

For the outer region, defining

$$\begin{aligned} \Delta_3 &= C_1 r_3^{-x} - v_3 \\ \Delta_4 &= C_1 r_4^{-x} - v_4 \end{aligned} \qquad (A4.6)$$

we have similarly from Eq. A4.3

$$y = \ln (\Delta_3/\Delta_4)/\ln (r_3/r_4) \qquad (A4.7)$$

$$C_2 = \Delta_3 r_3^{-y} \qquad (A4.8)$$

A4.3 Pacific Typhoon Examples

The pressure weighted average tangential wind profiles for the WPD3d (Developing Tropical Storm), WPD4 (Steady State Typhoon), and WPD5 (supertyphoon) data sets (c.f. Gray et al., 1982) for SFC-850 mb, SFC-300 mb, and 250-150 mb are given in Fig. A4.1. Notice that the upper outflow layer has the same shape as the inflow layers and can be

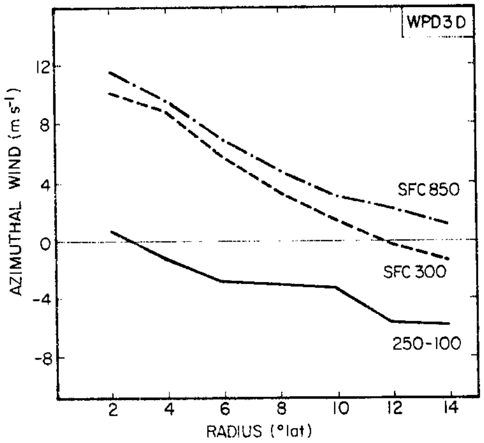

Fig. A4.1. Azimuthal wind profiles for the northwest Pacific developing tropical storm (WPD3D), steady state typhoon (WPD4) and supertyphoon (WPD5).

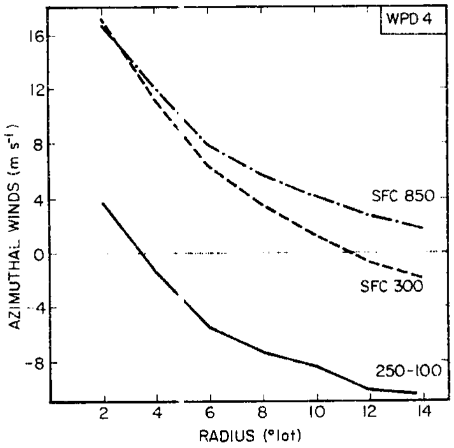

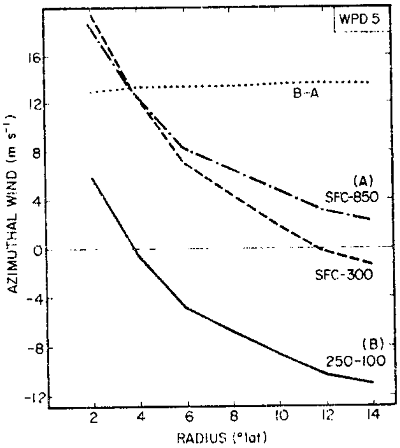

described by Eq. A4.3 with suitably reduced empirical constants C_1 and C_2.

Using typical parameters for the inner core region the rough best fit parameters in Eq. A4.3 to the profiles for each cyclone are given in Table A4.1, together with mean error, standard deviation, and RMS error. (The standard deviation is presented purely as a measure of variance).

TABLE A4.1

Profile parameters and errors from the application of Eq. A4.3 to northwest Pacific tropical cyclones.

Cyclone	Level	v_m	r_m	x	c_1	y	c_2	Error Mean	Error SD	Error RMS
	SFC-850	60	40	0.6	34,625	1.000	3.053×10^{-6}	0.2	0.9	0.8
WPD5	SFC-300	60	40	0.6	34,625	1.171	5.213×10^{-7}	−0.1	0.7	0.4
	250-300	20	40	0.6	11,542	0.892	4.332×10^{-5}	0.3	1.1	1.1
	SFC-850	40	40	0.5	8,000	1.26	8.293×10^{-8}	−0.3	0.5	0.7
WPD4	SFC-300	40	40	0.5	8,000	1.14	6.911×10^{-7}	0.2	1.0	0.8
	250-300	15	50	0.5	3,354	0.69	7.965×10^{-4}	−0.4	1.1	1.2
	SFC-850	25	40	0.4	1,733	1.95	4.917×10^{-12}	0.0	0.7	0.5
WPD3D	SFC-300	20	50	0.4	1,516	1.917	1.031×10^{-11}	−0.1	0.7	0.5
	250-300	5	100	0.4	500	0.283	0.098	0.7	0.9	1.2

A4.4 Discussion

We saw in section A4.1 that Eq. A4.3, with suitably chosen parameters could accurately describe the axisymmetric wind profiles of Pacific typhoons at large radii. In this section we briefly present and compare the profiles of azimuthal winds, vorticity, angular momentum inertial stability and kinetic energy for the WPD4 typhoon using Eq. A4.3, and the normal Rankine vortex Eq. A4.1 with x = 0.5 and x = 1.

The modified Rankine vortex, with $x = 0.5$, has often been used to describe inner core winds and many people have used the full Rankine vortex, with $x = 1$, in analytic work and in defining a symmetric storm.

Azimuthal Winds: The azimuthal winds for the three different profiles are shown in Fig. A4.2. We see that Eq. A4 1 with $x = 0.5$ provides a fair description out to about 4^{o} latitude radius but begins to diverge after that. The Rankine vortex, $x = 1$, is a very poor fit to the observed data at all radii.

Relative Vorticity: Relative vorticity in an axisymmetric vortex is given by

$$\zeta = \frac{1}{r}\frac{\partial rV}{\partial r} \tag{A4.9}$$

which on substituting Eq. A4.3 becomes

$$\zeta = \frac{1}{r}\left((1-x)C_1 r^{-x} - (1+y)C_2 r^{y}\right) \tag{A4.10}$$

or from the modified Rankine vortex Eq. A4.1

$$\zeta = \frac{1-x}{r} C_1 r^{-x} \tag{A4.11}$$

The radial profiles of relative vorticity from these two equations are shown in Fig. A4.3. Surprisingly, Eq. A4.1 with $x = 0.5$ is a fair approximation, except that the observed anticyclonic vorticity outside 6^{o} latitude radius is not duplicated. The cyclonic values given by Eq. A4.11 at these radii arise from the reduction in anticyclonic shear and higher cyclonic winds in Eq. A4.1 compared to Eq. A4.3.

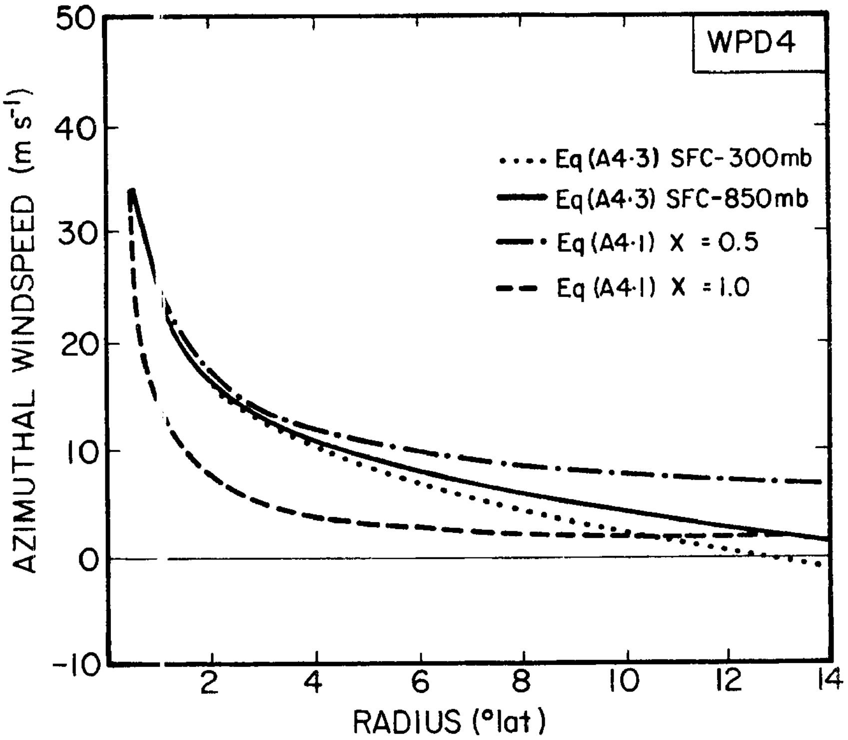

Fig. A4.2. Azimuthal wind profiles described by the three techniques of Eq. A4.3, Eq. A4.1 with x = 0.5 (modified Rankine vortex), Eq. A4.1 with x = 1 (full Rankine vortex).

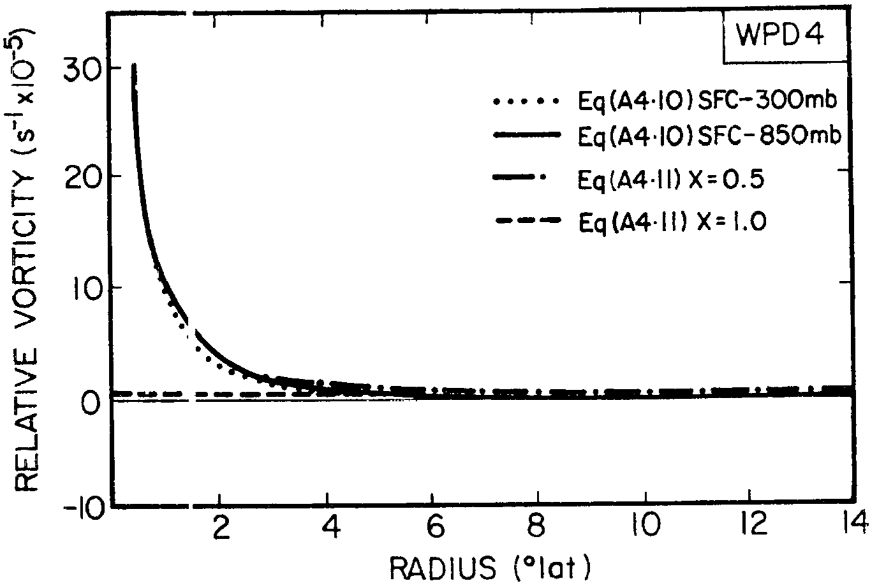

Fig. A4.3. As Fig. A4.2 but for relative vorticity.

The Rankine vortex ($x = 1$) has zero relative vorticity everywhere and provides no information on the actual vorticities.

Inertial Stability: The inertial stability parameter is given by

$$I^2 = (\zeta + \frac{2V}{r})\ (\zeta + f) \qquad \text{(A4.12)}$$

The resulting profiles of inertial stability using either Eqs. A4.1 and A4.11, or Eqs. A4.3 and A4.10 are shown in Fig. A4.4. Once again, the $x = 0.5$ profile is a quite good approximation to the actual profile. However, the $x = 1$ Rankine vortex is quite poor and given a constant static stability and radial wind forcing, would allow air to flow in much closer to the center than would be possible for the observed profile.

Relative Angular Momentum: The relative angular momentum is given by

$$M_r = Vr \qquad \text{(A4.13)}$$

and the resulting profiles are shown in Fig. A4.5. The $x = 0.5$ profile is a quite poor approximation outside 2-4^o latitude radius and the $x = 1$ profile, which has constant relative angular momentum everywhere, provides no useful information.

Kinetic Energy: The radial profiles of kinetic energy/unit mass are shown in Fig. A4.6. The $x = 0.5$ profile is a poor approximation outside 4^o latitude radius and the $x = 1$ profile is a very poor fit at all radii.

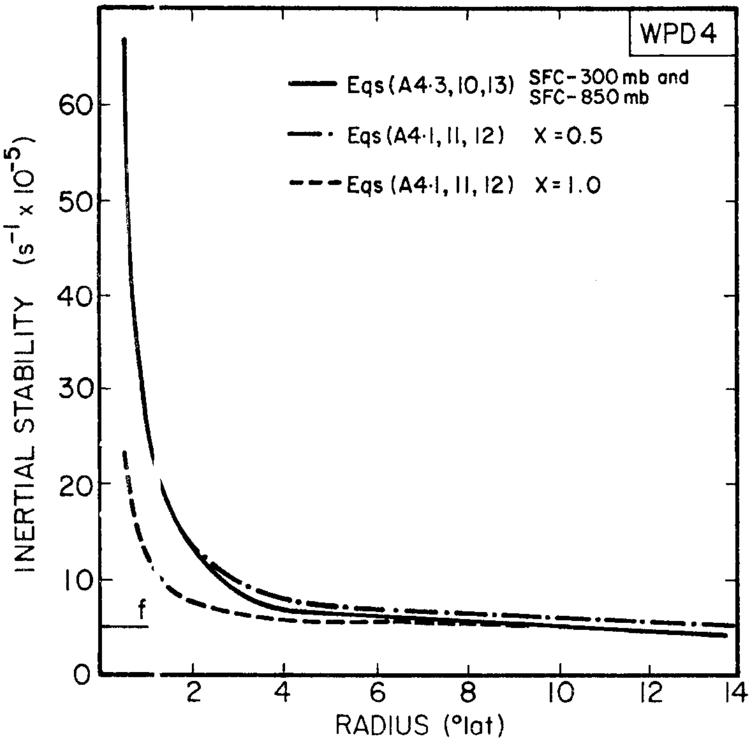

Fig. A4.4. As Fig. A4.2 but for the inertial stability.

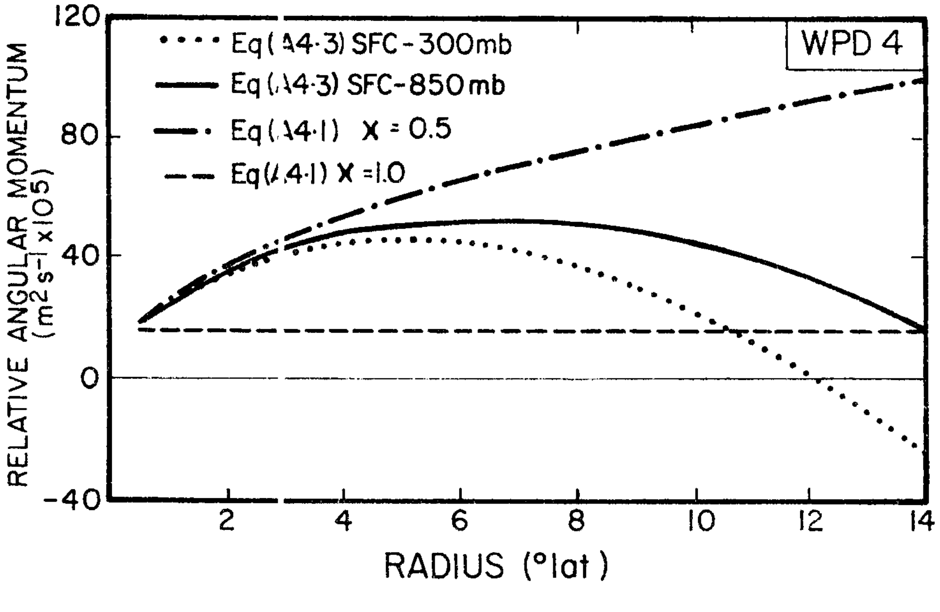

Fig. A4.5. As Fig. A4.2 but for relative angular momentum.

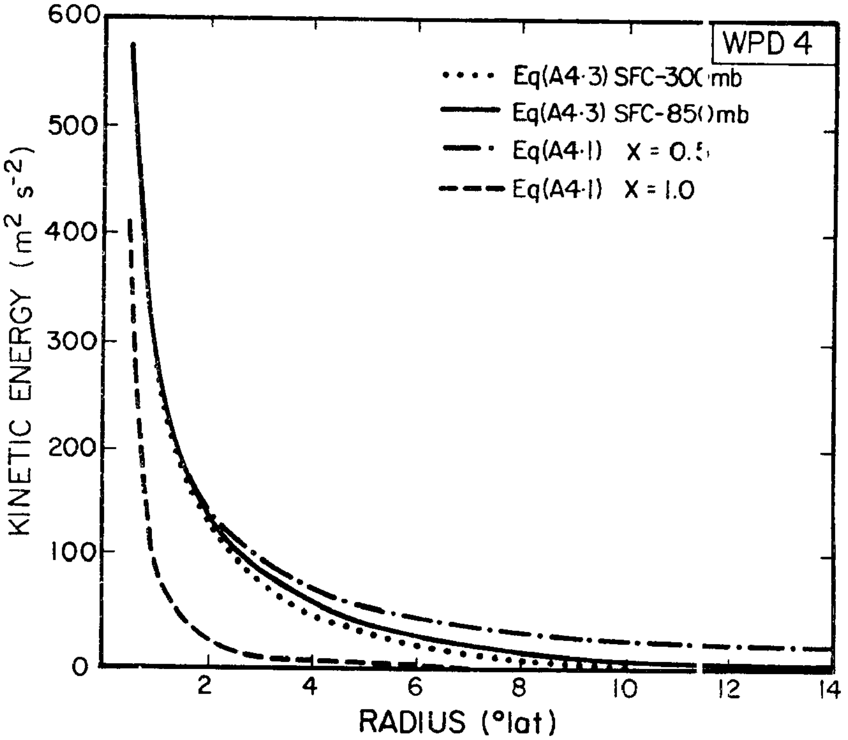

Fig. A4.6. As Fig. A4.2 but for kinetic energy.

A4.5 Conclusion

The suggested correction to the modified Rankine vortex at large radii allows a very good fit to be made to the observed axisymmetric wind profiles in tropical cyclones. The modified Rankine vortex with x = 0.5 or thereabouts can describe the wind and dynamic profiles out to 4-6° latitude radius with reasonable accuracy but rapidly becomes inaccurate at larger radii. The full Rankine vortex is a quite poor description of the observed momentum and dynamic fields at all radii.

W. M. GRAY'S FEDERALLY SUPPORTED RESEARCH PROJECT REPORTS SINCE 1967

CSU Dept. of Atmos. Sci. Report No.	Report Title, Author, Date, Agency Support
104	The Mutual Variation of Wind, Shear and Baroclinicity in the Cumulus Convective Atmosphere of the Hurricane (69 pp.). W. M. Gray. February 1967. NSF Support.
114	Global View of the Origin of Tropical Disturbances and Storms (105 pp.). W. M. Gray. October 1967. NSF Support.
116	A Statistical Study of the Frictional Wind Veering in the Planetary Boundary Layer (57 pp.). B. Mendenhall. December 1967. NSF and ESSA Support.
124	Investigation of the Importance of Cumulus Convection and Ventilation in Early Tropical Storm Development (88 pp.). R. Lopez. June 1968. ESSA Satellite Lab. Support.
Unnumbered	Role of Angular Momentum Transports in Tropical Storm Dissipation over Tropical Oceans (46 pp.). R. F. Wachtmann. December 1968. NSF and ESSA Support.
Unnumbered	Monthly Climatological Wind Fields Associated with Tropical Storm Genesis in the West Indies (34 pp.). J. W. Sartor. December 1968. NSF Support.
140	Characteristics of the Tornado Environment as Deduced from Proximity Soundings (55 pp.). T. G. Wills. June 1969. NOAA and NSF Support.
161	Statistical Analysis of Trade Wind Cloud Clusters in the Western North Pacific (80 pp.). K. Williams. June 1970. ESSA Satellite Lab. Support.
---	A Climatology of Tropical Cyclones and Disturbances of the Western Pacific with a Suggested Theory for Their Genesis/Maintenance (225 pp.). W. M. Gray. NAVWEARSCHFAC Tech. Paper No. 19-70. November 1970. (Available from US Navy, Monterey, CA). US Navy Support.
179	A diagnostic Study of the Planetary Boundary Layer over the Oceans (95 pp.). W. M. Gray. February 1972. Navy and NSF Support.
182	The Structure and Dynamics of the Hurricane's Inner Core Area (105 pp.). D. J. Shea. April 1972. NOAA and NSF Support.

CSU Dept. of Atmos. Sci. Report No.	Report Title, Author, Date, Agency Support
188	Cumulus Convection and Larger-scale Circulations, Part I: A Parametric Model of Cumulus Convection (100 pp.). R. E. Lopez. June 1972. NSF Support.
189	Cumulus Convection and Larger-scale Circulations, Part II: Cumulus and Meso-scale Interactions (63 pp.). R. E. Lopez. June 1972. NSF Support.
190	Cumulus Convection and Larger-scale Circulations, Part III: Broadscale and Meso-scale Considerations (80 pp.). W. M. Gray. July 1972. NOAA-NESS Support
195	Characteristics of Carbon Black Dust as a Tropospheric Heat Source for Weather Modification (55 pp.). W. M. Frank. January 1973. NSF Support.
196	Feasibility of Beneficial Hurricane Modification by Carbon Black Seeding (130 pp.). W. M. Gray April 1973. NOAA Support.
199	Variability of Planetary Boundary Layer Winds (157 pp.). L. R. Hoxit. May 1973. NSF Support
200	Hurricane Spawned Tornadoes (57 pp.). D. J. Novlan. May 1973. NOAA and NSF Support.
212	A Study of Tornado Proximity Data and an Observationally Derived Model of Tornado Genesis (101 pp.). R. Maddox. November 1973. NOAA Support.
219	Analysis of Satellite Observed Tropical Cloud Clusters (91 pp.). E. Ruprecht and W. M. Gray. May 1974. NOAA/NESS Support.
224	Precipitation Characteristics in the Northeast Brazil Dry Region (56 pp.). R. P. L. Ramos. May 1974. NSF Support.
225	Weather Modification through Carbon Dust Absorption of Solar Energy (190 pp.). W. M. Gray, W. M. Frank, M. L. Corrin, and C. A. Stokes. July 1974.
234	Tropical Cyclone Genesis (121 pp.). W. M. Gray. March 1975. NSF Support.

CSU Dept. of Atmos. Sci. Report No.	Report Title, Author, Date, Agency Support
---	Tropical Cyclone Genesis in the Western North Pacific (66 pp.). W. M. Gray. March 1975. US Navy Environmental Prediction Research Facility Report. Tech. Paper No. 16-75. (Available from the US Navy, Monterey, CA). Navy Support.
241	Tropical Cyclone Motion and Surrounding Parameter Relationships (105 pp.). J. E. George. December 1975. NOAA Support.
243	Diurnal Variation of Oceanic Deep Cumulus Convection. Paper I: Observational Evidence, Paper II: Physical Hypothesis (106 pp.). R. W. Jacobson, Jr. and W. M. Gray. February 1976. NOAA-NESS Support.
257	Data Summary of NOAA's Hurricanes Inner-Core Radial Leg Flight Penetrations 1957-1967, and 1969 (245 pp.). W. M. Gray and D. J. Shea. October 1976. NSF and NOAA Support.
258	The Structure and Energetics of the Tropical Cyclone (180 pp.). W. M. Frank. October 1976. NOAA-NHEML, NOAA-NESS and NSF Support.
259	Typhoon Genesis and Pre-typhoon Cloud Clusters (79 pp.). R. M. Zehr. November 1976. NSF Support.
Unnumbered	Severe Thunderstorm Wind Gusts (81 pp.). G. W. Walters. December 1976. NSF Support.
262	Diurnal Variation of the Tropospheric Energy Budget (141 pp.). G. S. Foltz. November 1976. NSF Support.
274	Comparison of Developing and Non-developing Tropical Disturbances (81 pp.). S. L. Erickson. July 1977. US Army Support.
---	Tropical Cyclone Research by Data Compositing (79 pp.). W. M. Gray and W. M. Frank. July 1977. US Navy Environmental Prediction Research Facility Report. Tech. Paper No. 77-01. (Available from the US Navy, Monterey, CA). Navy Support.
277	Tropical Cyclone Cloud and Intensity Relationships (154 pp.). C. P. Arnold. November 1977. US Army and NHEML Support.
297	Diagnostic Analyses of the GATE A/B-scale Area at Individual Time Periods (102 pp.). W. M. Frank. November 1978. NSF Support.

CSU Dept. of Atmos. Sci. Report No.	Report Title, Author, Date, Agency Support
298	Diurnal Variability in the GATE Region (80 pp.). J. M. Dewart. November 1978. NSF Support.
299	Mass Divergence in Tropical Weather Systems, Paper I: Diurnal Variation; Paper II: Large-scale Controls on Convection (109 pp.). J. L. McBride and W. M. Gray. November 1978. NOAA-NHEML Support.
---	New Results of Tropical Cyclone Research from Observational Analysis (108 pp.). W. M. Gray and W. M. Frank. June 1978. US Navy Environmental Prediction Research Facility Report. Tech. Paper No. 78-01. (Available from the US Navy, Monterey CA). Navy Support.
305	Convection Induced Temperature Change in GATE (128 pp.). P. G. Grube. February 1979. NSF Support.
308	Observational Analysis of Tropical Cyclone Formation (230 pp.). J. L. McBride. April 1979. NOAA-NHEML, NSF and NEPRF Support.
333	Tropical Cyclone Intensity Change - A Quantitative Forecasting Scheme. K. M. Dropco. May 1981. NOAA Support.
340	The Role of the General Circulation in Tropical Cyclone Genesis (230 pp.). G. Love. April 1982. NSF Support.
341	Cumulus Momentum Transports in Tropical Cyclones (78 pp.). C. S. Lee. May 1982. ONR Support.
343	Tropical Cyclone Movement and Surrounding Flow Relationships (68 pp.). J. C. L. Chan and W. M. Gray. May 1982. ONR Support.
346	Environmental Circulations Associated with Tropical Cyclones Experiencing Fast, Slow and Looping Motions (273 pp.). J. Xu and W. M. Gray. May 1982. ONR Support.
348	Tropical Cyclone Motion: Environmental Interaction Plus a Beta Effect (47 pp.). G. J. Holland May 1982. ONR Support.
---	Tropical Cyclone and Related Meteorological Data Sets Available at CSU and Their Utilization (186 pp.). W. M. Gray, E. Buzzell, G. Burton and Other Project Personnel. February 1982. NSF, ONR, NOAA, and NEPRF Support.

CSU Dept. of Atmos. Sci. Report No.	Report Title, Author, Date, Agency Support
352	A Comparison of Large and Small Tropical Cyclones (75 pp.). R. T. Merrill. July 1982. NOAA and NSF Support.
358	On the Physical Processes Responsible for Tropical Cyclone Motion (200 pp.). Johnny C. L. Chan. November 1982. NSF, NOAA/NHRL and NEPRF Support.
363	Tropical Cyclones in the Australian/Southwest Pacific Region (264 pp.). Greg J. Holland. March 1983. NSF, NOAA/NHRL and Australian Government Support.

17b. Identifiers/Open-Ended Terms

17c. COSATI Field/Group

18. Availability Statement	19. Security Class (This Report) UNCLASSIFIED	21. No. of Pages 264
	20. Security Class (This Page) UNCLASSIFIED	22. Price

FORM NTIS-35 (Rev. 3-72)

CSU Dept. of Atmos. Sci. Report No.	Report Title, Author, Date, Agency Support
352	A Comparison of Large and Small Tropical Cyclones (75 pp.). R. T. Merrill. July 1982. NOAA and NSF Support.
358	On the Physical Processes Responsible for Tropical Cyclone Motion (200 pp.). Johnny C. L. Chan. November 1982. NSF, NOAA/NHRL and NEPRF Support.
363	Tropical Cyclones in the Australian/Southwest Pacific Region (264 pp.). Greg J. Holland. March 1983. NSF, NOAA/NHRL and Australian Government Support.

BIBLIOGRAPHIC DATA SHEET	1. Report No. CSU ATS-363	2.	3. Recipient's Accession No.
4. Title and Subtitle TROPICAL CYCLONES IN THE AUSTRALIAN/SOUTHWEST PACIFIC REGION			5. Report Date March, 1983
			6.
7. Author(s) Greg J. Holland (P.I. William M. Gray)			8. Performing Organization Rept. No. CSU ATS-363
9. Performing Organization Name and Address Department of Atmospheric Science Colorado State University Fort Collins, CO 80523			10. Project/Task/Work Unit No.
			11. Contract/Grant No. ATM-7923591;NA81RAH00001
12. Sponsoring Organization Name and Address NSF 18th and G. Street, N.W. Washington, DC 20550	NOAA/NHRL Gables No. 1 Tower, 1320 S. Dixie Hwy. Coral Gables, FL 33146		13. Type of Report & Period Covered Project
			14.

15. Supplementary Notes

16. Abstracts

Some results are presented from the completed first stage of a collaborative Colorado State University/Australian Bureau of Meteorology project to investigate various aspects of tropical cyclones in the Australian/southwest Pacific region. We begin with a brief description of the major environmental and geographical features of this region, together with an overview of previous research work. We then discuss the distinguishing climatological and structural features of tropical storms, hurricanes and major hurricanes throughout the region, and highlight the effects of the prevailing flow patterns and the Australian continent. Finally, we present a theoretical and observational examination of the mechanisms leading to development, intensification and motion of these cyclones.

17. Key Words and Document Analysis. 17a. Descriptors

Tropical cyclones
Australian/southwest Pacific

17b. Identifiers/Open-Ended Terms

17c. COSATI Field/Group

18. Availability Statement	19. Security Class (This Report) UNCLASSIFIED	21. No. of Pages 264
	20. Security Class (This Page) UNCLASSIFIED	22. Price

FORM NTIS-35 (Rev. 3-72)

CSU Dept. of Atmos. Sci. Report No.	Report Title, Author, Date, Agency Support
352	A Comparison of Large and Small Tropical Cyclones (75 pp.). R. T Merrill. July 1982. NOAA and NSF Support.
358	On the Physical Processes Responsible for Tropical Cyclone Motion (200 pp.). Johnny C. L. Chan. November 1982. NSF, NOAA/NHRL and NEPRF Support.
363	Tropical Cyclones in the Australian/Southwest Pacific Region (264 pp.). Greg J. Holland. March 1983. NSF, NOAA/NHRL and Australian Government Support.

BIBLIOGRAPHIC DATA SHEET	1. Report No. CSU ATS-363	2.	3. Recipient's Accession No.
4. Title and Subtitle TROPICAL CYCLONES IN THE AUSTRALIAN/SOUTHWEST PACIFIC REGION			5. Report Date March, 1983
			6.
7. Author(s) Greg J. Holland (P.I. William M. Gray)			8. Performing Organization Rept. No. CSU ATS-363
9. Performing Organization Name and Address Department of Atmospheric Science Colorado State University Fort Collins, CO 80523			10. Project/Task/Work Unit No.
			11. Contract/Grant No. ATM-7923591;NA81RAH00001
12. Sponsoring Organization Name and Address NSF 18th and G. Street, N.W. Washington, DC 20550	NOAA/NHRL Gables No. 1 Tower, 1320 S. Dixie Hwy. Coral Gables, FL 33146		13. Type of Report & Period Covered Project
			14.

15. Supplementary Notes

16. Abstracts

Some results are presented from the completed first stage of a collaborative Colorado State University/Australian Bureau of Meteorology project to investigate various aspects of tropical cyclones in the Australian/southwest Pacific region. We begin with a brief description of the major environmental and geographical features of this region, together with an overview of previous research work. We then discuss the distinguishing climatological and structural features of tropical storms, hurricanes and major hurricanes throughout the region, and highlight the effects of the prevailing flow patterns and the Australian continent. Finally, we present a theoretical and observational examination of the mechanisms leading to development, intensification and motion of these cyclones.

17. Key Words and Document Analysis. 17a. Descriptors

Tropical cyclones
Australian/southwest Pacific

17b. Identifiers/Open-Ended Terms

17c. COSATI Field/Group

18. Availability Statement	19. Security Class (This Report) UNCLASSIFIED	21. No. of Pages 264
	20. Security Class (This Page) UNCLASSIFIED	22. Price

FORM NTIS-35 (Rev. 3-72)